2806045677

The Posterior Lobe of the Monkey Cerebellum: Anatomical Connections and their Functional Implications.

Catherine Swales

Department of Anatomy, University College London

Submitted in partial

fulfilment for the degree of Doctor of Philosophy

22nd April 1998

ProQuest Number: U641880

All rights reserved

INFORMATION TO ALL USERS
The quality of this reproduction is dependent upon the quality of the copy submitted.

In the unlikely event that the author did not send a complete manuscript
and there are missing pages, these will be noted. Also, if material had to be removed,
a note will indicate the deletion.

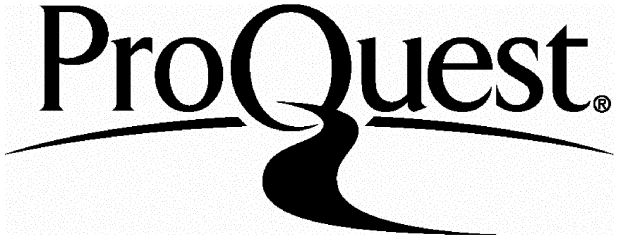

ProQuest U641880

Published by ProQuest LLC(2015). Copyright of the Dissertation is held by the Author.

All rights reserved.
This work is protected against unauthorized copying under Title 17, United States Code.
Microform Edition © ProQuest LLC.

ProQuest LLC
789 East Eisenhower Parkway
P.O. Box 1346
Ann Arbor, MI 48106-1346

ABSTRACT

The cerebellum links visual and motor structures in the brain and plays a critical role in visuo-motor co-ordination.

Mossy fibre-mediated visual information is transmitted to the posterior lobe of the cerebellum via the dorsolateral pons (dlpn). Anterograde tracing studies have demonstrated that the dlpn projects heavily to the dorsal paraflocculus (dpf), and moderately to the posterior vermis and hemispheres. The projection to the flocculus is virtually non-existent, but it receives climbing fibre-mediated visual information via the dorsal cap of the inferior olive.

Sixteen monkeys received injections of the bi-directional tracer WGA-HRP into cerebellar cortical areas receiving mossy or climbing-fibre mediated visual information. The following questions were addressed:

i) Do retrograde studies confirm the absence of floccular projections from the dlpn?

ii) How is the olivo-cortico-nuclear parasagittal zonation represented in the monkey?

iii) Do cerebellar cortical projections overlap in the deep cerebellar nuclei?

The results suggest that the flocculus only receives a sparse collateral input from the dlpn. The olivo-cortico-nuclear system in the monkey is shown to diverge beyond the strict parasagittal zonation seen in non-primates, allowing cross-talk between functional modules. In addition, cortico-nuclear projections from different cortical regions overlap. Indeed, hemispheric eye-movement related areas (dpf, flocculus and crus II) all project to the ventrocaudal posterior interposed nucleus, a discrete eye movement region involved in the control of vertical saccades and the far-response in vergence and accommodation (Van Kan et al., '93; Zhang and Gamlin, '94; Robinson et al., '96). Vermal lobule VII projects to the fastigial oculomotor region of Noda et al. ('88), which controls horizontal saccades and the near-response (Robinson et al., '93; Zhang and Gamlin, '96).

Finally, additional observations on cortico-nuclear topography demonstrate how multiple somatotopies in the cortex (e.g. multiple eye movement areas) are reduced onto a single representation of the body in each of the deep cerebellar nuclei.

ACKNOWLEDGEMENTS

I owe a huge amount to many people.

I would like to thank my supervisor Mitch Glickstein and everyone in the lab for their enthusiasm, encouragement and confidence - and especially Ned and Ines for all their help, support and laughter. In addition, many thanks to Fred and Jenny Miles and everyone at the National Eye Institute who made me feel so welcome.

The greatest debt is to my family and friends for putting up with all my nonsense.

And finally to Chris for being such a rare find. I still can't believe my luck, nor thank him enough.

TABLE OF CONTENTS

LIST OF FIGURES AND PHOTOS

CHAPTER 1

CHAPTER 2

CHAPTER 3

CHAPTER 4

1. INTRODUCTION

1.1 VISUOMOTOR CO-ORDINATION

Humans and non-human primates possess a wide repertoire of skilled movements. The accuracy, and therefore the success, of these movements is critically dependent on visuo-motor co-ordination. Without this skill even the most simple task, such as reaching for a target, becomes unmanageable.

The question of how we use our visual system to control voluntary movements is complex and difficult to approach, but from it we can derive the simpler anatomical question of how the visual and motor areas of the brain are linked. One such connection has been found in the cerebellum, a huge subcortical structure which, through a series of electrophysiological and clinical studies, has been heavily implicated in visuomotor control. The cerebellum receives visual information from cortical and subcortical structures and, via its nuclei, projects to all of the great descending motor systems of the brain. One of the diagnostic signs of cerebellar disease is an impairment in the visual guidance of movement.

This thesis will focus on the anatomical connections of those areas of the macaque cerebellum known to receive visual input and hence most likely to be involved in the visual guidance of voluntary movement. I shall compare my anatomical data to what is already known in other species with simpler visual systems and motor capacities, and will also relate my results to electrophysiological and behavioural studies performed on these pathways in the macaque. I shall pay particular attention to eye movement studies, since oculomotor control is the undoubtedly the most powerful example of the visual guidance of voluntary movement.

This introduction is divided into six parts, covering detail on the gross structure and subdivisions of the cerebellum, its cellular architecture, connectivity, and its afferent and efferent connections with the rest of the brain. Details on the tracer and cytochemical techniques used will be given in the materials and methods section.

1.2 GROSS CEREBELLAR ANATOMY

The cerebellum lies immediately dorsal to the IVth ventricle and the brainstem in the posterior cranial fossa. It straddles the midline and consists of an intricately convoluted cortex covering a mass of white matter, within which lie three bilaterally paired nuclei. The relative size of the cerebellum has grown massively in evolution, but the basic wiring of the structure has remained unchanged. Due to the close packing of its constituent cells, the cerebellum contains a larger number of cells than the rest of the brain in total, and yet constitutes only 10% of the total mass. In addition, the Purkinje cells, the sole output of the cerebellar cortex, are the largest neuronal elements in the brain with respect to the number of synapses they receive and probably with regard to the complexity of their integrative properties. It is clear that in spite of the simplicity of the cortical afferent and efferent circuitry, the cerebellum is designed to integrate a massive amount of information and has huge computational power.

1.2.1 Basic circuitry

Information from a wide range of sources is received by the cerebellum and is distributed in a highly stereotyped manner onto the Purkinje cells of its cortex. Cerebellar afferents are distributed via two very disparate systems called the *climbing* and *mossy* fibre systems. These differ in terms of their origins within the brain, their method of termination on Purkinje cells and the Purkinje cells' physiological response to their inputs. The Purkinje cells project via monosynaptic, inhibitory contacts onto the cells of the deep cerebellar nuclei or the vestibular nuclei in the brainstem. The exact arrangement of cortico-nuclear projections depends on the position of the Purkinje cells in the cerebellar cortex. The deep cerebellar nuclei, which will be the focus of this thesis, are the fastigial (medial), the interposed (which in primates can be separated into the anterior and posterior interposed, corresponding to the globose and emboliform nuclei in Man), and the dentate (lateral) nucleus. The cells within these nuclei additionally receive collaterals from mossy and climbing fibres, which are the sources of information to the Purkinje cells. Thus the nuclei integrate information from both the cerebellar cortex and its afferent systems and they project to a wide range of areas in the brainstem or thalamus.

The afferent and efferent fibres of the cerebellum travel via three cerebellar peduncles either side of the midline, which connect the cerebellum to the brainstem.

1.2.2 Cerebellar subdivisions

1.2.2.1 Whole cerebellum

a) Gross Subdivisions - The nomenclature of the cortical areas:

The cerebellum has been subdivided according to anatomical, electrophysiological and functional criteria. The most salient of the anatomical divisions arises as a result of the midline cortex bulging out from the remainder, forming the vermis. Immediately lateral to the vermis lies the pars intermedia and beyond that, the lateral hemispheres. There are no obvious landmarks that separate the pars intermedia from the hemispheres, although in some animals, a faint depression may demarcate the paravermal region. In Man, the hemispheres are so overdeveloped that they fold over and cover the vermis almost completely.

Superimposed upon the basic longitudinal organisation of vermis versus hemispheres, there are a number of transverse fissures of varying depths which further divide the cerebellar cortex into lobes and sublobules, and smaller ones dividing the sublobules into individual folia. The deepest of the fissures, the primary fissure, separates the anterior lobe from the posterior lobe, which in turn is separated from the flocculo-nodular lobe by the posterolateral fissure. Additional gross anatomical subdivisions are described using nomenclature derived from Larsell (1934) and Bolk's (1906) independent studies of the cerebellum. Larsell's nomenclature is based on roman numerals listing the separate sublobules of the vermis heading rostrocaudally. The anterior lobe therefore contains sublobules I to V, and the posterior vermis lobules VI to IX. Lobule X is the nodulus. Larsell described the hemispheric components as extensions of the vermis, and denoted them accordingly as, for example, "hemispheric" VI (or HVI).

Bolk, however, concentrated on the fact that the cerebellar cortex is a continuous sheet, such that throughout the anterior lobe, and in the region just behind the primary fissure (which he called the simple lobule), the vermis is continuous with the hemispheres. In the remainder of the posterior lobe the continuity between the vermis and hemispheres

is broken in places, as the cortical sheet forms a chain that loops mediolaterally. Bolk's nomenclature for the hemispheric divisions of the posterior lobe is based upon his names for the laterally and medially-directed portions of this chain.

The loop originates in the hemispheric cortex just behind the simple lobule, next to lobule VI. Initially it bends laterally, forming crus I, and medially again to produce crus II. The next division of the hemisphere lies parallel to the vermis, and hence is called the paramedian lobule. The hemispheric chain then bends out laterally and medially again. Bolk referred to this entire loop as the formatico vermicularis. Larsell, however, defined the laterally directed portion of the chain as the dorsal paraflocculus, and the medial part as the ventral paraflocculus. This thesis will employ the terms dorsal and ventral paraflocculus for the different parts of this cerebellar loop. The very last part of the chain, nestled against vermal lobule X is known as the flocculus. Crus I and II are therefore associated with the vermal lobule VII, the paramedian lobule with lobule VIII, the dorsal and ventral paraflocculus with VIII and IX, and the flocculus with X. Due to the folial chain twisting as it forms the paraflocculi and flocculus, the medial edge of the ventral paraflocculus and flocculus corresponds to the lateral edge of the hemisphere (see figure 1).

The dorsal and ventral paraflocculus are formed by the hemispheric chain bending laterally and medially and through a rostrally directed loop, the petrosal lobule, so called because it is encased within the petrous bone. There are no objective criteria for separating the dorsal from the ventral paraflocculus within the petrosal lobule, so the border between them is arbitrarily located at the base of one of the intervening fissures. There has also been some difficulty in forming a consensus on the borders of the flocculus and ventral paraflocculus. The border between the two is formed by the lateral extension of the posterolateral fissure. In the adult cerebellum, the posterolateral fissure is easily visualised in the vermis, but in the hemisphere the path of the fissure is directed almost parasagittally. Larsell's 1953 monograph placed the posterolateral fissure too far laterally, thereby including much of the ventral paraflocculus into the flocculus. Madigan and Carpenter's atlas of the cerebellum of the Rhesus monkey (1971) reflects Larsell's original division, thus perpetuating the confusion. As a result, a number of authors studying the anatomy and physiology of the so-called "flocculus" have recorded

from the ventral paraflocculus and not the flocculus proper (see Langer, '85; Lisberger and Fuchs, '78). Gerrits and Voogd (1982) re-examined the problem in the cat, and, using their anatomical criteria, the borders of the flocculus have been more clearly established. The ventral paraflocculus lies lateral to the posterolateral fissure and the flocculus medial to it, such that, when seen in coronal section, the caudal six folia of the "floccular complex" are the flocculus proper. The remaining four rostral folia, lying beneath the anterior lobe, belong to the ventral paraflocculus.

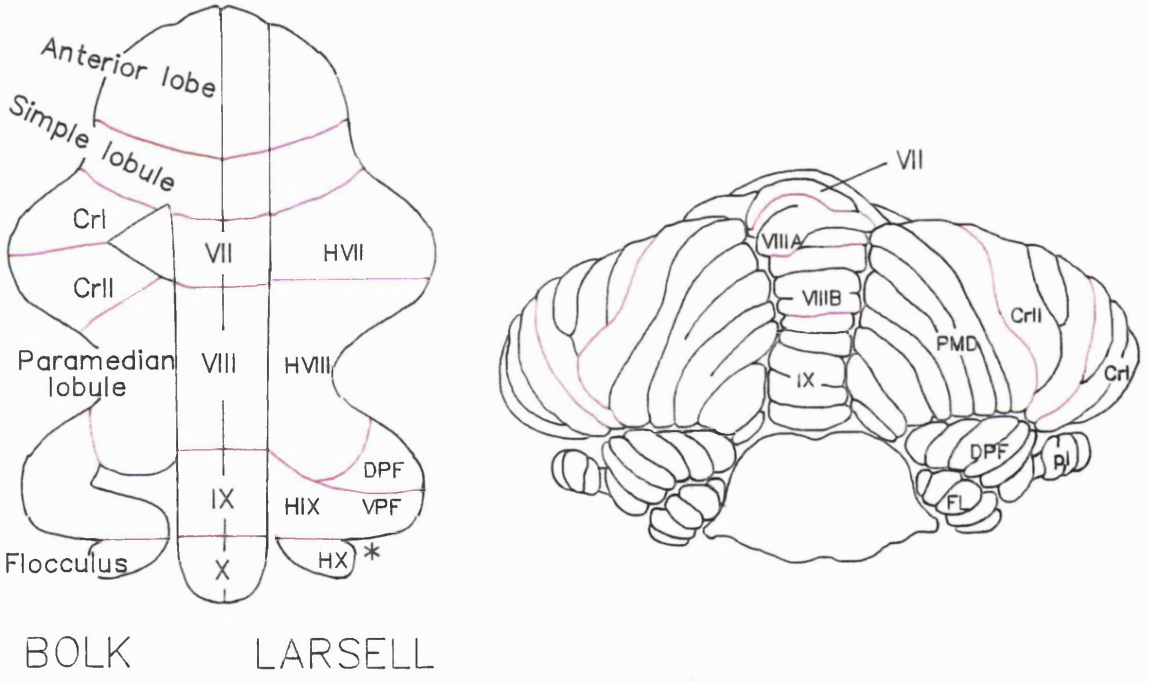

Figure 1: a) A comparison of Bolk (1906) and Larsell's (1970) nomenclature for cerebellar subdivisions. Note the continuity of the cortical chain in Bolk's nomenclature.

* denotes the position of the posterolateral fissure

(Adapted from Glickstein and Voogd, '95)

b) Posterior view of the macaque cerebellum.

PMD - Paramedian lobule
DPF - Dorsal paraflocculus
FL - Flocculus
PT - Petrosal lobule
CrI - Crus I
CrII - Crus II

b) Connectional Subdivisions - Functional Modules

The original divisions of the cerebellar cortex into different functional areas depended upon the afferent and efferent connections its constituent parts. Herrick (1924) and Larsell (1937) separated the cerebellum into the three functional divisions, the boundaries of which roughly corresponded with gross anatomical features. The *spinocerebellum* consisted of the anterior lobe, simple lobule and vermal lobule VIII. It was known to receive somatosensory information from the spinal cord, and was believed to be involved in guiding limb movement and the maintenance of posture. The *cerebrocerebellum*, which comprised vermal lobules VII and IX and the lateral hemispheres of the anterior and posterior lobes received input from the cerebral cortex via the pontine nuclei and participated in the planning of movement. The *vestibulocerebellum*, corresponding to the flocculonodular lobe received input from the vestibular labyrinth and was presumed to function in the maintenance of balance and the control of eye and head movements. These functional subdivisions also corresponded approximately to subdivisions based on phylogenetic age (Larsell, '35). The cerebrocerebellum is phylogenetically the youngest part of the cerebellum and for this reason was also named the neocerebellum. The flocculonodular lobe, on the other hand, is the oldest cerebellar subdivision and was thus termed the archicerebellum. Remaining portions were collectively termed the paleocerebellum.

The functional subdivisions were gross approximations, but they took into account the routes by which the various cerebellar subdivisions projected out of the cerebellum via the deep nuclei. This consideration proved to be central to a clearer understanding of cerebellar function. In studies of degenerating fibres following cortical lesions in the monkey, Jansen and Brodal (1942) demonstrated that the midline cortex projected to the fastigial (medial) nucleus, the intermediate to the interposed and the lateral hemispheres to the dentate (lateral). This cortico-nuclear segregation has been carefully correlated with the inputs to the cerebellar cortex and afferent/efferent system compartmentation in the white matter (Voogd, '64, '69; Voogd and Bigare, '80; Hess and Voogd, '86; Buisseret-Delmas, '88) for the different cortical areas. The cerebellum is now conceived as a series of functional modules - longitudinal strips each comprised of a specific pattern of afferent and efferent projections. This anatomical organisation in the

cerebellum is known as parasagittal zonation. It is central to its function and will be returned to in more detail later, as it forms the focus of the experimental work in this thesis.

1.2.2.2 The cerebellar cortex

The smallest of the transversely orientated fissures in the cerebellum produce folds of cortex called folia, and the elements of the cortex are arranged in axes either parallel or orthogonal to the long axis of the folia. The Purkinje cells of the cerebellar cortex are arranged in a single layer, thereby dividing the cortex into the molecular layer above and the granular layer below. Deep to the granular layer is the mass of white matter, containing the afferent and efferent compartments and the deep cerebellar nuclei. The arrangement of cells within the layers is very uniform across the cerebellar cortex such that the differences in functions between different areas is due to the different afferent and efferent connections of that particular area. As a result, the study of the anatomical connections of the cerebellar cortex provide some indication of the physiology and functions of a particular subdivision.

a) Layers and constituent elements:
Each of the cortical layers has its own characteristic population of cells or fibres.

i) The superficial *molecular layer* contains the dendritic fields of the Purkinje cells. These dendritic trees are flattened and orientated orthogonal to the long axis of the folium, such that they look like stacks of leaves. The axons of the cortical input elements run through and around these trees. In addition, there are two types of interneurons located in this layer - the basket and stellate cells.

ii) Deep to the molecular layer is the *Purkinje cell* monolayer. [See photo 1] Purkinje cell bodies have a very distinctive tear-drop shape and measure approximately 60μm vertically by 30μm horizontally. One or occasionally two primary dendrites arise from the superficial pole of the Purkinje cell - they arborise extensively to form the flattened dendritic trees in the molecular layer. The axon of the Purkinje cell emanates from its base, travels through the granular layer, becomes myelinated and enters the white matter. The Purkinje cell is the sole output of the cerebellar cortex, and their axons terminate on the cells of either the deep cerebellar nuclei or the vestibular nuclei

in the brainstem. Purkinje cell axons give off collaterals as they project through the white matter which contact Purkinje cells (recurrent collaterals) or the basket and Golgi interneurons (see below).

iii) Between the Purkinje cell layer and the white matter lies the *granular layer*. This is formed by the dense packing of its constituent granule cells, which receive the

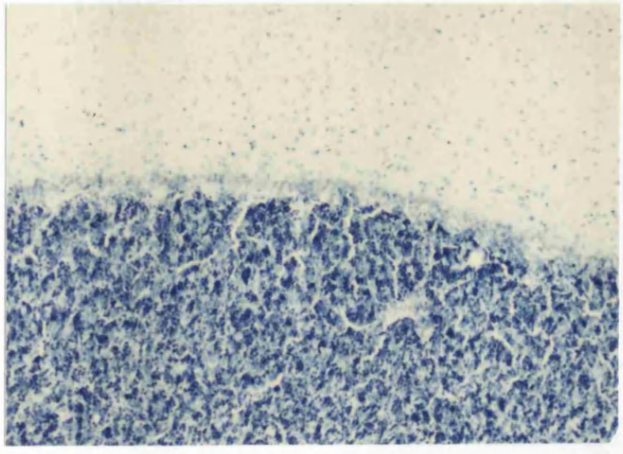

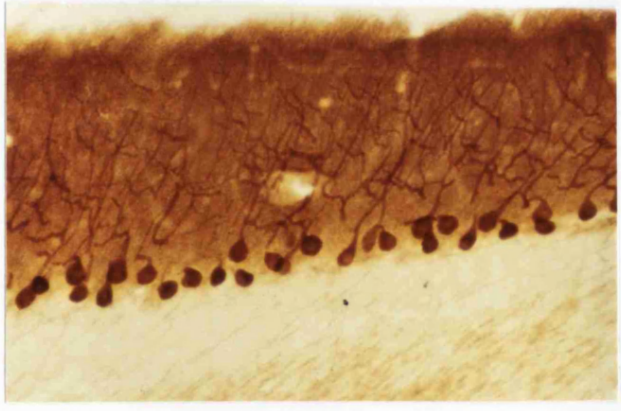

Photomicrograph 1: The cerebellar cortex

A: Cresyl violet-stained section through the cerebellar cortex, showing the densely packed granular layer, and the Purkinje cell monolayer above.

B: Height-matched section through the cerebellar cortex, following reaction with the Purkinje cell-specific marker zebrin II. The Purkinje cells, dendritic trees and axons are strongly zebrin positive. The molecular layer is more weakly immunopositive, whilst the granular layer is immunonegative.

Magnification x60.

mossy fibre input to the cortex. Each granule cell measures approximately 7μm, and generally produces three to five dendrites and a fine axon which passes up through the Purkinje cell layer above, into the molecular layer. Here the axons bifurcates into T-shaped parallel fibres - so-called because they are arranged parallel to the long axis of the folium, but orthogonal to the planes of the dendritic fields of the Purkinje cells. Parallel fibres run for up to 6mm along the length of a folium (Mugnaini, '83), and are found throughout the depth of the molecular layer, although those in superficial molecular layer are longer than those in the deeper areas. The granular layer also includes a population of large interneurons called the Golgi cells. Unlike Purkinje cells, the dendrites of Golgi cells are arranged in a spherical rather than flattened form.

All of the interneurons in the cerebellar cortex receive input from the granule cells' parallel fibres - basket and stellate cells subsequently act on Purkinje cells, whilst the Golgi cells inhibit the granule cells. The net result of the inhibitory interneurons interaction during Purkinje cell activation by parallel fibres is that a sharply defined beam of Purkinje cells fires upon the deep nuclei very briefly.

b) Cortical input elements:

The cerebellar cortex receives afferent input via climbing and mossy fibres. These two systems differ in their sites of origin, their method of termination (monosynaptic versus disynaptic), and the response they elicit in the Purkinje cells upon stimulation.

The *climbing fibres* arise solely from the inferior olivary nucleus in the brainstem, which contains information from a wide range of brain areas, such as the spinal cord, the brainstem, the cerebellar nuclei and the motor cortex. The olivo-cerebellar fibres are long and myelinated - they decussate at the olivary rostrocaudal level from which they originate, and course rostrally to enter the cerebellum through the inferior cerebellar peduncle. While travelling through the white matter to the cortex, they give off collaterals to the deep nuclei, and branch into several fine fibres. They travel through the granular and Purkinje cell layer, and, having entered the molecular layer, each fine fibre wraps repeatedly round the proximal parts of the Purkinje cell's dendritic tree. This monosynaptic input to the Purkinje cell is excitatory and one of the most powerful synapses in the entire nervous system - although each Purkinje cell receives input from only one climbing fibre, the fibre may make as many as 200 contacts with the Purkinje

cell's dendritic field. Stimulation of the inferior olive produces a powerful burst of excitation in its Purkinje cell, which is characterised by an all-or-nothing burst of spikes called "complex" spikes.

The *mossy fibres* distribute information onto the cerebellar cortex from a wide range of areas in the CNS, such as the spinal cord, the vestibular nuclei, the reticular formation, the cerebellar nuclei and the cerebral cortex via the massive cortico-ponto-cerebellar pathway. These fibres enter the cerebellum through the middle and superior cerebellar peduncles. Certain populations of mossy fibres send collaterals to the deep nuclei, depending on their original source, but all forms branch up through the white matter to synapse onto the granule cells of the granular layer. As described above, the granule cell axon projects upward and bifurcates in the molecular layer to form the parallel fibres. As the parallel fibre runs across the molecular layer it makes contacts with a great many of Purkinje cells dendritic trees, which are arranged orthogonal to the direction taken by the parallel fibres. The parallel fibre input focuses at the terminal portions of the dendritic trees, such that the Purkinje cell dendrites can be subdivided into a central area receiving climbing fibre input and more peripheral parts receiving parallel fibre inputs. Activation of the parallel fibres cause the Purkinje cell to fire with a volley of characteristic "simple spikes".

1.2.2.3 Deep cerebellar nuclei

Embedded within the white matter of the cerebellum lie the bilaterally paired deep nuclei. Moving from medial to lateral, these are the fastigial, the interposed (anterior and posterior divisions) and the dentate. The cells within these nuclei receive a topographically organised input from the Purkinje cell axons and project out of the cerebellum to a range of brainstem and thalamic areas. The deep cerebellar nuclei are not simple relay stations, however. Cells within the nuclei are arranged into complex synaptic patterns, combining Purkinje cell axons with collaterals from a sub-set of mossy fibre afferents, all climbing fibres and recurrent collaterals from the nuclear projecting cells. The synaptic integration that this arrangement allows is central to cerebellar function.

The nuclear cells are not uniform in size - populations of small (15-20 μm diameter), medium (20-30 μm) and large (30-40 μm) neurons can be recognised in differing ratios in each of the nuclei. Each nucleus contains minor subdivisions that can be distinguished on a cytoarchitectonic basis. In the monkey (Courville and Cooper, '70), the most consistent intra-nuclear difference is restricted to the dentate. Cells within caudal levels of this nucleus are generally smaller than those located more rostrally, with the result that the caudal areas have also been referred to as the parvicellular dentate.

The vast majority of nuclear cells are multipolar, and give rise to about 10-12 dendrites (about 400 μm long) that radiate to encompass a sphere, with the result that there is extensive overlap of the dendritic trees of separate cells within the nucleus. Purkinje cell axons enter a particular nucleus, and their 2 or 3 terminal branches arborise extensively to form a cone. GABAergic synapses between the Purkinje cell and the nuclear cell are usually formed on the dendritic thorns or spines of nuclear cells, although axosomatic synapses have also been encountered. Collaterals from mossy and climbing fibre afferents synapse on the proximal and distal dendrites of the nuclear cells.

The majority of nuclear cells have long axons that leave the nuclei via the superior cerebellar peduncle, the uncinate fasciculus or the juxtarestiform body. Prior to leaving the cerebellum, these projecting axons give rise to collaterals that terminate in the cerebellar cortex as mossy fibres, in the contralateral inferior olivary nucleus or recurrent collaterals to the nucleus from which they arose.

The nuclei differ in their extracerebellar targets. The fastigial projects caudally to the pons, medulla, vestibular nuclei and the spinal cord, and sparsely to the ventral thalamic nuclei. The interposed and dentate nuclei project rostrally to the red nucleus and the ventral thalamic nuclei. I shall describe the nuclear efferents in more detail in section 1.5.2.

The question of whether the nuclei contain a population of local interneurons has not been completely resolved.

Nuclear cells have a high resting discharge rate, which modulates over a large range before or at the onset of movement (Evarts and Thach, '69). Cells responsive to movements of different parts of the body are arranged such that each cerebellar nucleus

contains a "motor map" of the body (Thach, '78; Asanuma et al., '83a-c; Thach et al., '92, '93; Van Kan et al., '93). The head is represented caudally, the hindlimb rostrally, the limbs medially and the trunk laterally. This somatotopy is maintained in the efferent projections of each of the cerebellar nuclei to the thalamus and red nucleus (Asanuma et al., '83a and b), and in its inputs via climbing fibre collaterals (Gibson et al., '87).
Each nucleus controls a different type or "mode" of movement. The fastigial nucleus controls muscles only during sitting, standing and walking, the interposed controls stretch and other somatosensory reflexes and may help damp the inherent mechanical reflex oscillation of body parts (Thach et al., '92). It may also preferentially control self-paced rapid alternating movements, and has been strongly implicated in the control of reach-to-grasp movements (Gibson et al., '94). The dentate helps to initiate (via thalamus and motor cortex) those movements that are triggered by mental or arbitrary sensory cues and are therefore called volitional movements. It has also been heavily implicated in the control of multi-jointed movements (Thach et al., '93). More details on the somtatotopy of the deep nuclei can be found in section 1.5.1 of the introduction.

The cortico-nuclear projection will be the focus of the experimental work in this thesis. As was described in the section on functional modules, the projection from the cerebellar cortex to the deep nuclei is topographically organised - the vermis projects to the fastigial nucleus, the intermediate cortex to the interposed and the lateral hemispheres to the dentate. There is a wealth of literature on the details of this pathway in various species such as the rat and cat, but details on the efferents of the posterior cortex of the macaque cerebellum are still very unclear - the most recent study dealing with the entire system in the primate was performed in 1942 by Jansen and Brodal, using a Marchi degeneration technique. The major limitation of this technique is that it relies on the presence and identification of degenerating myelin and thus favours the detection of large calibre fibres. Fibre projections with smaller diameters may be overlooked. Since that time, however, a variety of new tracing techniques have been developed, the cortico-nuclear projection in other animals has been correlated with the climbing fibre input into discrete zones (Groenewegen and Voogd, '77; Groenewegen et al., '79; Voogd and Bigare, '80; Bernard, '87; Yamada and Noda, '87; Buisseret-Delmas, '88; Noda et al., 90), and much more is known about the electrophysiology and

functions of the deep nuclei in the primate (Thach, '78; Thach et al., '92, '93; Gibson et al., '87, '96; van Kan et al., '93). Hence, I decided to re-assess this pathway in particular, as it is central to cerebellar function in an animal with a high degree of visual and motor sophistication.

1.3 CEREBELLAR CORTEX - AFFERENTS

The cerebellar cortex receives inputs from the rest of the brain via the mossy and climbing fibre systems. This section will describe particular details of these systems, focusing on the visual afferents from each of them.

1.3.1 The Climbing Fibre System

1.3.1.1 The Inferior Olive

The inferior olivary nucleus is the sole source of climbing fibres to the cerebellar cortex, and the inferior olive is central to cerebellar function. Damage to the olive is indistinguishable from that to the cerebellum itself.

The inferior olive is located in the ventral medulla, immediately caudal to the pontine nuclei and dorsal to the pyramids. It has been divided into three subnuclei (Bowman and Sladek, '73), which are named according to their relative positions. The cells within these nuclei are predominantly medium-sized and there are no major cytoarchitectonic differences between the these nuclei.

The principal olive is the largest of the olivary subdivisions. It appears towards the rostral end of the caudal third of the complex, and extends to its rostral pole, spanning approximately 5mm. Caudally, it consists of a ventrolaterally-directed band of grey matter, but at more rostral levels it forms a well-developed hairpin shape consisting of dorsal, ventral and lateral lamellae. These lamellae can be distinguished by their patterns of invaginations, but the locations of the borders between lamellae are somewhat arbitrary. The dorsal lamella is the first to invaginate and typically has one major and two minor invaginations, while the lateral lamella into which it leads typically has two major invaginations. The ventral lamella has a different pattern of invaginations - all of them are minor and the lamella has a distinctly linear appearance. It is also characterised by its discontinuity.

The medial accessory olive has a rostro-caudal length of about 7mm, and consists of seven individual cell groups. In the cat (Walberg, '56; Taber, '61), these are named groups a-g. In the monkey, the nomenclature is somewhat different. Groups a and b

coalesce to form the main body of the caudal MAO, group c is known as the nucleus β, groups d and e form the dorsal cap (of Kooy), while group g is approximately equivalent to the dorsomedial cell column, which fuses with the medial tip of the ventral lamella of the principal olive.

The dorsal accessory olive lies dorsal to the principal olive, spanning approximately 6mm rostrocaudally. Rostrally, the DAO moves into a distinctive comma-shape, which reflects an actual increase in size rather than a mere shift in position, and at the very rostral pole, it becomes contiguous with the ventral lamella. [See figure 2]

The inferior olive itself receives inputs from a wide range of brain and brainstem areas, and, although it receives visual information, the bulk of its input is somatosensory in origin, and thus the olive is primarily involved in transmitting both cutaneous and deep somatosensory input to the cerebellum. The spinal inputs to the olive ensure that the climbing fibre system is more concerned with egocentric details, representing information about the body, rather than exteroceptive information, the bulk of which seems to be carried by the mossy fibre system (Baker et al., '76; Mower et al., '80). Somatosensory information destined for the olive arises from the spinal cord and dorsal column nuclei, which project in an appropriate overlapping topography onto different subdivisions of the olivary complex (Boesten and Voogd, '75; Berkely and Hand, '78; Molinaris, '84). For example, projections from the upper cervical spinal segments and cuneate nucleus overlap to produce discrete forelimb regions of the olive, and lumbar spinal input converges with those from the gracile onto hindlimb regions. This arrangement is most apparent in the rostral DAO, which contains a complete somatotopic representation of the body surface across its mediolateral dimension (Gellman et al., '83). Cells in this olivary subnucleus have small, discrete receptive fields and respond optimally to cutaneous stimuli. More caudal levels of the DAO display a broader somatotopy than rostral areas, since cells in these areas possess larger receptive fields and respond optimally to deep somatosensory information, such as muscle squeeze, which is more "blunt" and more difficult to localise. The remaining olivary subnuclei do not seem to display a discrete somatotopy since they are also sensitive to deep somatosensory information and have larger, overlapping receptive fields. However, topographical inputs from areas such as the deep cerebellar nuclei

(Graybiel et al., '73; Berkely and Worden, '78; Chan-Palay, '78; Dietrichs and Walberg, '81, '85, '86; Angaut and Cicirata, '82; Ruigrok and Voogd, '90), which do contain clear somatotopic representations (Thach, '78; Asanuma et al., 83a-c; Thach et al., '92, '93; van Kan et al., '93; Gibson et al., '96) suggests that some degree of somatotopic representation is likely to be present within all olivary subnuclei.

In addition to spinal inputs to the olive, there is a powerful projection from the parvicellular division of the red nucleus and from the deep cerebellar nuclei, both directly and indirectly via the Nucleus of Darkschewitsch and the tegmental tracts, which provide signals on the motor output of the system. Rubrospinal projections from the magnocellular division of the red nucleus also provide collateral inputs to the inferior olive (Robinson et al., '87) and this projection has important functional consequences for olivary output to the cerebellar cortex. This will be described in detail in section 1.5.1(b).

The deep cerebellar nuclei, which receive collaterals from climbing fibres as they approach the cortex also project strongly onto the inferior olive via an efferent collateral system (Tolbert, '76a; McCrea et al., '78; Dietrichs and Walberg, '81; Legendre and Courville, '87). The nucleo-olivary pathway is largely reciprocal to that of the olivo-nuclear (Brodal, '81; Dietrichs and Walberg, '87; Ikeda et al., '89), although there are some notable differences. The presence of a fastigio-olivary projection is disputed (Batton et al., '77; Kalil, '79; Asanuma et al., '79; Dietrichs and Walberg, '87; Ikeda et al., '89) and the nucleo-olivary projection shows some degree of divergence and overlap, with neighbouring nuclear zones projecting to a particular olivary region (Dietrichs and Walberg, '81).

In addition, the nucleo-olivary pathway has a unique topography that has not been reported for the olivo-nuclear pathway. Asanuma et al. ('83) examined the efferents of the dentate nucleus and found that the collaterals projecting to the olive (in this case, the principal olive) terminated in patches, separated by areas which did not seem to receive an input from the dentate. The rubro-olivary pathway is also striated (Strominger et al., '79). It is not known whether the olivary patches from these two sources interdigitate or overlap.

Additional inputs to the inferior olive arise from the superior colliculus (Frankfurter, '77; Kyuhou and Matsuzaki, '91), providing auditory and visual information (Saint-Cyr and Courville, '82), from the vestibular nuclei (Saint-Cyr and Courville, '79), cerebral cortex - chiefly from the motor cortex (Sousa-Pinto and Brodal, '69; Berkely and Worden, '78), and smaller projections from the Edinger-Westphal nucleus, pretectal area, nucleus of the solitary tract and the lateral cervical nucleus.

Fibres from the olivary subnuclei decussate and enter the cerebellum through the contralateral inferior cerebellar peduncle to reach the Purkinje cells of the cerebellar cortex, upon which they terminate. The topography of the projection from the inferior olive to the cerebellar cortex has been extensively studied in a wide range of mammals (Rat: Bernard, '87; Buisseret-Delmas, '88; Ruigrok and Voogd, '90; Cat: Groenewegen and Voogd, '77; Groenewegen et al., '79; Walberg et al., '79, '87; Rosina and Provini, '82, '83, '87; Kanda et al., '89; Dietrichs and Walberg, '90; Monkey: Brodal and Kawamura, '80; Brodal and Brodal, '80 and '81), and provides the basis for much of the comparative anatomical and physiological studies (Ekerot and Larson, '79; Oscarsson, '80) that have been performed on the cerebellum.

As a result of its close association with the cerebellum, and the fact that it receives and transmits information on the consequences of an animal's movement, the olive has been described as a "comparator" between desired motor action and the actual outcome of a particular movement. Where necessary, it provides an error signal which is used to modify cerebellar output in order to correct motor performance. However, olivary neurons fire at spectacularly low rates, in the order of one per second, and thus would be limited in their ability to transmit sophisticated details on motor error. New details on olivary physiology have indicated that the olive is better defined as a "somatic event detector" (Houk and Gibson, '87), providing information about disturbances to the body resulting from external events, rather than quantitative information about stimulus parameters or motor inaccuracy. For example, olivary neurons do not respond during self-produced movement, and those proprioceptive neurons that fire during passive displacement of a limb do not code for amplitude or rate of displacement (Rushmer et al., '76). During the step cycle of the cat, olivary neurons are silent during the actual

movement of the paw. Equally, they do not respond to the cutaneous stimulation elicited when the paw is placed down (Gellman et al., '85). If the course of the paw is disturbed by some external force, or the platform onto which the paw is placed is moved, the previously silent olivary neurons generate short-latency complex spikes to signal the occurrence, but not the detail, of the unanticipated event (Bauswein et al., '83; Anderson and Armstrong, '85, '87; Gibson and Gellman, '86; Lou and Bloedel, '86).

1.3.1.2 The olivocerebellar system - parasagittal zonation of the cerebellar cortex

Brodal made lesions in the cerebellar cortex and mapped retrograde degeneration of cells in the inferior olive (1940). These classic studies indicated that individual subregions of the inferior olive projected onto distinct subregions of the cerebellar cortex in a topographically ordered fashion. Voogd's studies in 1964 and 1969 subsequently showed that the climbing fibres from individual olivary subnuclei bound for the cerebellar cortex travelled through anatomically distinct compartments in the white matter, and that the climbing fibre terminations in the cortex were arranged into narrow parasagittal strips (or zones) running orthogonal to the long axis of the folia. Courville et al's 1974 autoradiographic study additionally supported the principle of parasagittal climbing fibre terminations in the cerebellar cortex. The anatomical compartments through which the separate olivocerebellar zones run can be visualised on the basis of differing fibre diameters using anticholinesterase and myelin stains (Hess and Voogd, '86; Voogd et al., '86). These anatomical compartments are also employed by the cortico-nuclear projection, such that the parasagittal zones in the cerebellum consist of an olivary subnucleus, a longitudinal strip of cerebellar cortex, and a deep cerebellar nucleus or portion thereof. There is now a wealth of literature supporting this detailed olivo-cortico-nuclear parasagittal zonation of the cerebellum (Voogd, '64, '69, '89; Haines, '76, '84, '89; Chan-Palay et al., '77; Groenewegen and Voogd, '77; Brodal and Walberg, '79, '80; Groenewegen et al., '79; Oscarsson, '80; Walberg, '80; Brodal and Brodal , '81, '82; Dietrichs, '81a, b, '83; Eisenman, '81; Haines et al., '82; Beyerl, '82; Rosina and Provini, '83, '87; Bernard, '87; Trott and Armstrong, '87a, b, c; Buisseret-Delmas, '88; Trott, '89; Buisseret-Delmas and Angaut, '93; Buisseret-Delmas et al., '93. For reviews see Bigare and Voogd, '80; Brodal and Kawamura, '80). In

addition to the zonation within the cortical afferent and efferent pathways, the climbing fibres projecting to the cortex give rise to topographically organised collaterals which terminate in the appropriate deep cerebellar nucleus receiving input from Purkinje cells in the cortical areas to which the parent climbing fibre axon projects (Brodal, '40; Matsushita and Ikeda, '70; Brodal, '75; Beitz, '76; Eller and Chan-Palay, '76; Hoddevik, '76; Chan-Palay, '77; Courville, '77; Groenewegen and Voogd, '77; Kitai, '77; Ruggerio, '77; Groenewegen, '79; Courville and Faraco-Cantin, '80; Carpenter and Batton, '82; Wiklund, '84; Gibson et al., '87; van der Want and Voogd, '87; Buisseret-Delmas, '88; van der Want et al., '89).

Andersson and Oscarsson ('78) showed that in the lateral vestibular nucleus of Deiter's, identical neurons are excited by climbing fibre collaterals and indirectly inhibited by the same climbing fibre via the cortex. It is assumed that a parallel situation exists within the deep cerebellar nuclei, although direct evidence for this is not yet available.

Although there are interspecies differences in both the width and the length of individual olivocerebellar zones (see Voogd and Bigare, '80), and the extent to which they deviate from the midline (Voogd, '69; Groenewegen et al., '79; Buisseret-Delmas, '88, '93), the olivo-cortico-nuclear projection is a fundamental principle in the cerebellum, and is regarded as its functional module. Much of this thesis will be based on this system.

The following description of cortical zones will be largely confined to the olivocerebellar system. Details of the cortico-nuclear parasagittal zonation will be described in part 1.4.1.

a) Anatomical nomenclature

Each zone of the cerebellar cortex which receives a distinct olivary input has been assigned a letter - A (divisible into A1-3), B, x, C1-3, Cx and D1-2, moving from the vermis laterally into the hemispheres (see figure 3). Four of these zones receive climbing fibres from separate olivary regions - A, B, C2 and D1 and 2. C1 and C3 receive input from the identical olivary subnucleus. In the cat, the remaining zones form pairs: x and Cx (also known as lateral C1), medial C1 and medial C3, each pair being innervated by branches from a common group of olivo-cerebellar fibres (Ekerot and Larson, '83; Campbell and Armstrong, '85; Trott and Armstrong, '86).

The vermis contains zone A, the bulk of which receives input from the caudal division of the medial accessory olive, and projects to the fastigial nucleus.

Zone A has been subdivided into A1-3 subzones, but not all zones can be accounted for in the entire length of the vermis. Zones A1 and A2 are both supplied by the cMAO, and it appears that olivary efferents to the A1 zone sit medial to those destined for the A2 zone (Groenewegen and Voogd, '77).

The width of zone A varies across the species, and may show lateral deviation from the midline vermis, or encroachment by other cortical zones in the pars intermedia, but it generally fills the mediolateral extent of the vermis in the posterior lobe in all mammals studied thus far (Rat: Bernard, '87; Buisseret-Delmas, '88; Buisseret-Delmas and Angaut, '88; Paallysaho et al., '90; Cat: Groenewegen and Voogd, '77; Dietrichs, '83; Monkey: Haines et al., '82; Yamada and Noda, '87).

There is an additional vermal zone, zone B, which is present at its greatest width in the anterior lobe. It receives olivary fibres from the caudal half of the DAO, and unlike the rest of the cortical zones, does not send its major projection to a cerebellar nucleus, but to the lateral vestibular nucleus of Deiters in the brainstem. Zone B is also unusual in that it only extends caudally as far as lobule VI .

A few reports have indicated that the B zone may additionally project into the medialmost edge of the anterior (Dietrichs and Walberg, '81 in the cat) or posterior (Haines et al., '76 in the Galago) interposed nucleus. However, the cortico-nuclear projection from the B zone is still disputed due to the proximity of the cortical B zone to its neighbouring x zone, which is known to project to the deep nuclei (see below).

The A and B zones in the vermis are separated by zone x which projects to the interface between the fastigial and the posterior interposed (Rat: Yatim et al., '95; Cat: Voogd, '83; Trott and Armstrong, '87b), or the medial edge of the PIP (Monkey: Haines and Dietrichs, '91). This zone is only evident from lobules IV to VI in the squirrel monkey, but may have a greater extent in the Galago (II/III to VI) and the rat (IV-VI and VIII-X) (Haines et al., '82; Yatim et al., '95). It receives input from the mid-to-rostral levels of the MAO in all animals studied so far (Voogd, '83; Campbell and Armstrong, '85; Voogd et al., '87a; Voogd and Hess, '89). Although the olivary input to cortical zone

C2 also arises from this area, there is no evidence to suggest that x and C2 zones are supplied by the bifurcating fibres of individual olivary neurons, as is the case in the C1 and C3 zones.

The areas of the hemispheres adjacent to the vermis (pars intermedia) are filled by the olivary C zones. C1 and C3 are supplied by bifurcating fibres (Rosina and Provini, '83, '87; Trott, '87) from the rostral half of the DAO, and project with only partial overlap onto the anterior interposed nucleus (Garwicz and Ekerot, '94; Rosina and Provini, '96). The rDAO receives a powerful and topographically organised input from the spinal cord and dorsal column nuclei, and the somatotopy that this arrangement confers is maintained even at the level of the bifurcating olivary fibres supplying C1 and C3. The climbing fibre branching originates in sets of inferior olive neurons that connect different pairs of somatotopically homologous cerebellar cortical areas (Rosina and Provini, '83 and '87).

Olivary input to the C1 and C3 zones in the cat are complicated by the fact that they are divisible into medial and lateral halves for each (Trott, '87). The medial C1 and medial C3 form a pair receiving input from bifurcating olivary projections arising in the rostral DAO, whilst C1 is paired with the vermal x zone (and, as a result is sometimes described as Cx), and receives olivary input from middle levels of the MAO. In the cat, the lateral C3 zone is paired with a Y zone in the extreme lateral hemispheres, and they share an input from the rostral DAO.

No such Y zone has been documented in the monkey, nor have there been reports of a cortical C zone receiving input from the MAO, as in the cat.

The C2 zone is intercalated between C1 and C3. It receives input from the rostral MAO and projects to the posterior interposed nucleus. The C2 zone is unpaired, although a link with the B zone has been suggested by anatomical (Voogd, '64) and developmental (Voogd, unpublished observations) studies.

The projections of the x and C2 zones into the posterior interposed do not overlap. The x zone projects to the most medial edge, while the C2 zone projects into more central and lateral areas (Haines and Dietrichs, '91).

The lateral hemispheres are filled by the cortical D zones, which receive olivary input from the principal olive and project into the dentate nucleus. There is still some debate as to which lamella projects to the D1 and which to the D2 zone. Brodal and Walberg ('77b and '79) and Brodal and Kawamura ('80) performed HRP studies in the cat, and showed that the lateralmost parts of the paramedian lobule, which they anticipated as belonging to the D2 zone, received olivary input from the ventral lamella, while the dorsal lamella projected to zone D1. However, Voogd and Bigare's autoradiographic studies (1980) and Rosina and Provini's ('83, '87) studies in the cat indicated that the ventral lamella projects to the cortical D1 zone, and the dorsal lamella to the D2 zone. In the monkey, Brodal and Brodal's extensive HRP study on olivocerebellar projections ('81, '82), demonstrated that the dorsal lamella and lateral bend supply cortical zone D1 while the ventral lamella projects to zone D2.

The situation becomes somewhat more complex in the "floccular complex", due to the twisting and folding of the folial chain. As the folial chain is followed round through the paramedian lobule, it bends sharply out laterally and becomes the dorsal paraflocculus. The dorsal paraflocculus continues laterally into the petrosal lobule and here the folial chain heads rostrally to become the ventral paraflocculus. In the dorsal and ventral paraflocculus, the C1 and C3 zones vanish from the folial chain, and only C2 and the D zones are in evidence. Beyond the four folia of the ventral paraflocculus, the chain bends caudally again - it heads medially, ventral to the dorsal paraflocculus and medial to the posterolateral fissure, from which point it is known as the flocculus. The flocculus continues medially and finishes adjacent to the vermal lobule X or nodule.

The flocculus contains an extension of the C2 zone described previously, but the D zones are replaced by the floccular zones FZ1-4, which receive input from different parts of the dorsal cap, ventrolateral outgrowth and vestibular nuclei, and have different efferent targets (Dow, '36, '38a, b; Jansen and Brodal, '40; Yamamoto and Shimoyama, '77; Balaban et al., '81; Sato et al., '82a, b; Carpenter and Cowie, '85; Langer, '85; Tan et al., '95). The caudal dorsal cap projects to FZII and IV, whilst the rostral dorsal cap and the ventrolateral outgrowth terminate in the interleaving FZI and III.

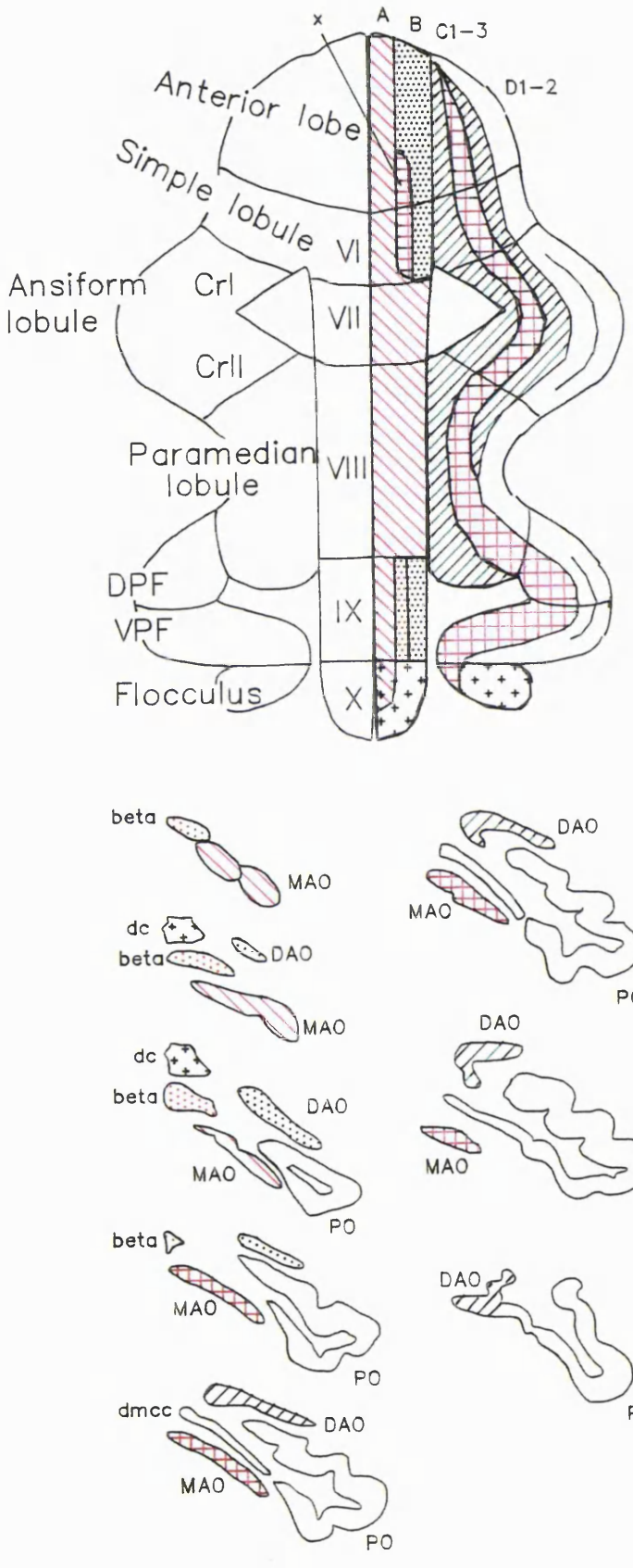

CrI - Crus I

CrII - Crus II

DPF - Dorsal paraflocculus

VPF - Ventral paraflocculus

dmcc - dorsomedial cell colum

beta - subnucleus beta

dc - dorsal cap

DAO - dorsal accessory olive

MAO - medial accessory olive

PO - principal olive

Figure 2: The parasagittal zonation of the cerebellar cortex as determined by olivary input.

(Adapted from Groenewegen et al., '79).

b) Physiological criteria

Electrophysiological investigation of the olivo-cerebellar complexes (Oscarsson, '69; Ekerot and Larson, '79; Oscarsson, '80) have shown that each parasagittal zone receives a characteristically different climbing fibre input from the spinal cord. The majority of the zones receive spinal information only from the ipsilateral side of the body, but the B and C2 zones receive information from both sides.

The anatomically-defined zones can be further subdivided into electrophysiologically-defined microzones. Each microzone is approximately 200 μm wide, and receives spinal information concerning a different body part to that of its neighbouring microzone. For example, in the B zone, the microzones are arranged in such a way that as you move from medial to lateral across the cortex, there is a gradual shift of bilateral inputs from face to forelimbs, to trunk to hindlimbs and to tail (Andersson and Eriksson, '81). Indeed, the B zone is not the only zone to contain a detailed somatotopic representation of the whole ipsilateral body surface - the C1 and C3 zones also share this characteristic. The C2 zone that separates them, however, is unusual in that most Purkinje cells have large receptive fields often including all four limbs and the head.

1.3.1.3 Visual climbing fibre afferents

The pathway providing visual information via the climbing fibre system has been most clearly elucidated by Maekawa and Simpson ('72 and '73) in the rabbit. The pathway begins in the directionally selective ganglion cells in the retina, which are responsive to slow target speeds (Oyster et al., '67 and '68). The axons of these cells project via the accessory optic tract to the lateral edge of the brain stem (Oyster, '80) where they terminate on three nuclei - the lateral, medial and dorsal terminal nuclei, all of which can be activated by the appropriate directional visual stimulation. These three nuclei project to the dorsal cap and the ventrolateral outgrowth of the inferior olive, which supply the flocculus, nodulus, caudal folia of the uvula and the ventral paraflocculus. Indeed, recent double label retrograde tracing studies have demonstrated that olivary neurons in the dorsal cap bifurcate to supply the flocculus and nodule, and the nodule and the uvula (Takeda et al., '89).

In monkeys, there is a set of neurons that line the brachium of the superior colliculus, partially contained in the nucleus of the optic tract and the lateral terminal nucleus, that

are reputed to contain directionally-selective visual neurons that project to the inferior olive (Mustari and Fuchs, '89, '90; Ilg and Hoffmann, '91; Buttner-Ennever et al., '96). Visual units in the NOT respond during both full-field visual stimulation and smooth pursuit eye movements, although any particular unit will respond more vigorously to one form of stimulation than the other (Mustari and Fuchs, '90). LTN units form a continuum of types ranging from purely visual to purely oculomotor (Mustari and Fuchs, '89).

In addition to its cerebellar input via the climbing fibre system, the accessory optic system also contributes to mossy fibre-mediated cerebellar input via projections to precerebellar nuclei in the pontine nuclei and NRTP (Torigoe et al., '86; Mustari et al., '90).

Visual and oculomotor information from the superior colliculus is also transmitted to vermal lobules VI and VII of the cerebellum via the caudal division of the medial accessory olive (Kyuho and Matsushita, '91). The colliculus contains a rostro-caudal topographical organisation with respect to visual field representation and saccadic amplitude. The rostral superior colliculus contains units representing the perifoveal visual field and which, upon stimulation, generate small saccades. The collicular projection to the vermis via the cMAO is arranged into sagittal strips. Olivary regions receiving input from rostral superior colliculus project more medially in the vermis than those receiving projections from more caudal levels. Thus, medial vermal areas receive input from collicular areas which generate small saccades and contain representations of the perifoveal visual field; lateral areas receive input from collicular areas generating larger saccades and containing representations of the peripheral visual field.

1.3.1.4 Response properties of visual climbing fibres

In the rabbit, neurons in the dorsal cap of the inferior olive respond best to the slow rotation of large fields of random dot stimuli. Rotation in one direction about a preferred axis elicits maximal excitation, whereas rotation in the other causes inhibition (Maekawa and Simpson, '72, '73). Neurons fall into three main types, which are classified according to the preferred orientation of these axes - vertical, anterior horizontal and posterior horizontal, which correspond to the axes in the semicircular

canals. Furthermore, electrical stimulation of the dorsal cap in rabbits produces smooth pursuit eye movements.

The data on the monkey system is less complete. However, recent studies have shown that the nucleus of the optic tract, which provides a major input to the dorsal cap (Buttner-Ennever, '96), contains directionally selective cells which respond to a moving visual scene with very short latencies of 40-60 msecs, and that cells in the dorsal cap itself increase their activity during contraversive or upward movements of the visual field (Kawano et al., '96).

The majority of the work performed on the role of visual climbing fibre afferents in cerebellar function has focused on its role in smooth pursuit eye movements and the vestibulo-ocular reflex.

During pursuit of a sinusoidally moving target, complex spike firing in the flocculus indicates the occurrence of small-amplitude retinal slip (Miles and Lisberger, '81; Watanabe, '85; Stone and Lisberger, '86, 90). This transient firing is used by the smooth pursuit system to correct for the tracking errors and to fine-tune pursuit.

The vestibulo-ocular reflex, on the other hand, is responsible for stabilisation of gaze, and its gain is normally close to unity. This can be forcibly modified by wearing inverting prisms. During adaptation of the VOR gain, complex spikes firing rates increase until the reflex is appropriately adjusted and the retinal slip is abolished (Watanabe, '84).

1.3.2 The Mossy Fibre System

The mossy fibre system is quantitatively the most powerful route to the cerebellum. Within that, the pontine nuclei in the brainstem are the greatest source of mossy fibre afferents to the cerebellar cortex. Cortical and subcortical efferents terminate on pontine cells. The majority of the pontocerebellar fibres decussate in the basal pons and project through the contralateral middle cerebellar peduncle to terminate on the granule cells of the cerebellar cortex. Those pontocerebellar fibres that do not decussate travel through the adjacent ipsilateral middle cerebellar peduncle. The cortico-ponto-cerebellar pathway is the largest subcortical pathway in the brain.

Other areas contributing to the mossy fibre system include the vestibular nuclei, the lateral reticular nucleus, the spinal trigeminal nucleus, the dorsal column nuclei, and the reticular formation, including the nucleus reticularis tegmenti pontis (NRTP).

The reticular formation as a whole provides a widespread afferent system to the cerebellar cortex, and the NRTP is the most defined nucleus within it. This nucleus lies directly dorsal to the pontine nuclei, and although it should be considered as a separate nuclear system, and not simply an extension of the pontine nuclei, the two areas have some similar anatomical connections and responses and thus will be considered together in the following section.

A number of these cerebellar cortical afferent systems provide collaterals to the deep nuclei. This will be described in more detail in later sections.

1.3.2.1 The cortico-ponto/NRTP-cerebellar pathway

a) The anatomy of the pontine nuclei and NRTP

The macaque pontine nuclei have been divided into eight subdivisions (Nyby and Jansen, '51): the dorsolateral, lateral, peduncular, ventral, paramedian, dorsal and medial nuclei. In this thesis, I shall describe pontine connections using this nomenclature. It should be noted, however, that although it facilitates comparative conclusions on terminal fields or efferent cell groups of the pons, the borders of these subdivisions are not precisely defined, but based only on their position relative to the fascicles of the corticospinal tract which runs through the basal pons. Immediately dorsal to the pontine nuclei, and separated from them by the medial lemniscus, lies the nucleus reticularis tegmenti pontis (NRTP). This triangular-shaped group of reticular cells spans much of the rostro-caudal length of the pontine nuclei, and reaches its maximum breadth caudally. At more rostral levels, it separates into numerous cell groups that are connected to the pontine nuclei by cellular bridges. More rostrally still, it merges totally with the dorsal pons, but can still be differentiated from it, since it is strictly a reticular nucleus, and contains larger cells than any in the pontine nuclei. Within the NRTP large and medium-sized cells collect centrally; small cells collect ventrally and laterally (Gerrits et al., '84). See figure 3.

The pathway from the cerebral cortex to the pontine nuclei and the NRTP is predominantly ipsilateral and arises from layer Vb pyramidal cells (Jones and Wise, '77; Kawamura and Chiba, '79; Glickstein et al., '80, '85; Albus et al., '81; Legg et al., '89; Mercier et al., '90) in a wide range of cerebral cortical areas. Early light microscopy studies showed that over 90% of the cortical efferent fibres within the cerebral peduncles project to the pontine nuclei. Moreover, there is evidence that all or nearly all of the pyramidal tract fibres give off collaterals as they traverse the pontine nuclei (Cajal, 1911). No direct evidence for collateral input from the pyramidal tract to the NRTP exists, but cortical areas giving rise to projections to the NRTP correspond closely to those sending fibres to the spinal cord in the monkey (Kuypers, '60; Russle and DeMyer, '61; Coulter et al., '76; Jones and Wise, '77).

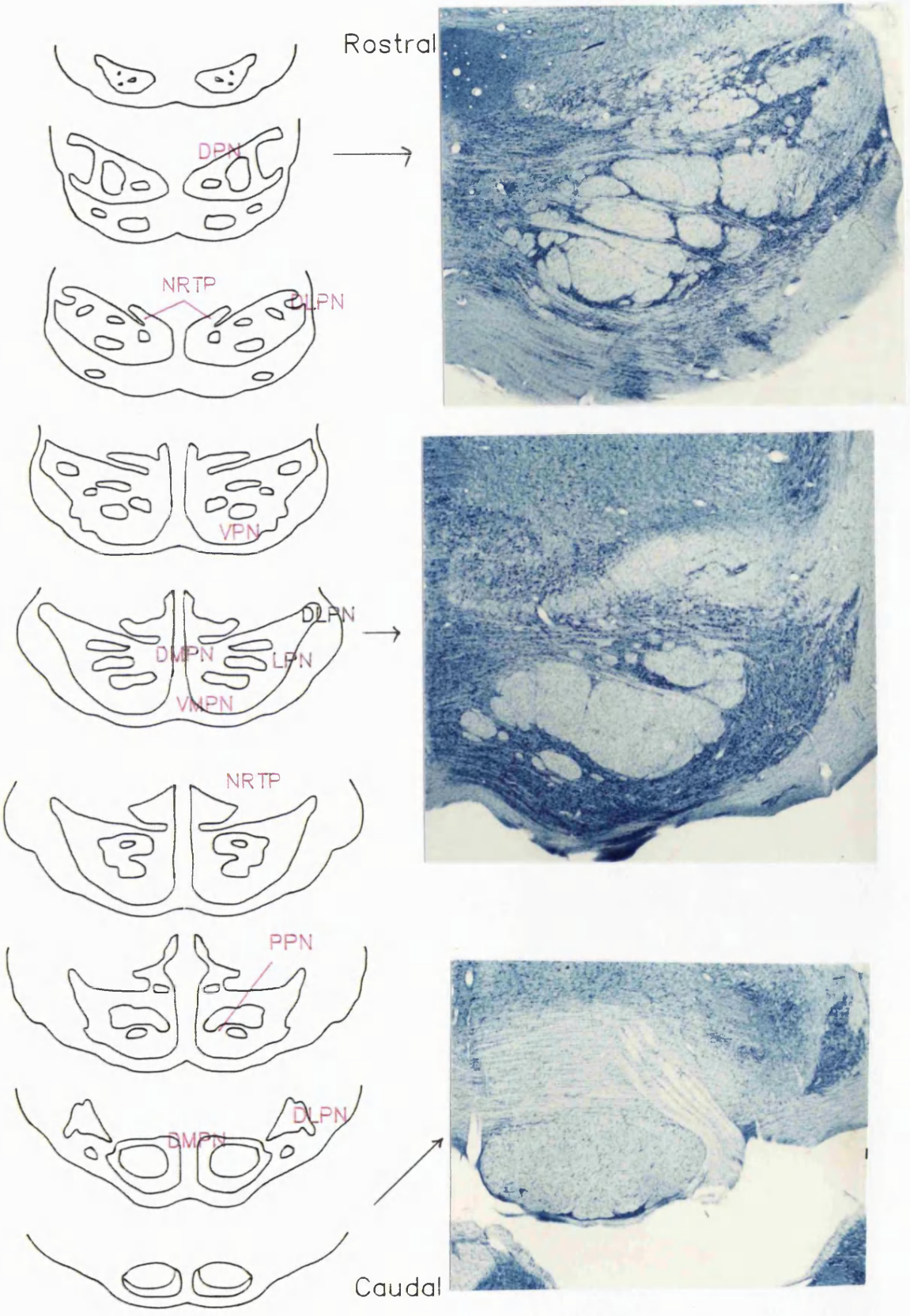

Figure 3: Standard coronal sections through the macaque NRTP and pontine nuclei (600μm apart). Photomicrographs are height matched to the diagrams.

NRTP - Nucleus reticularis tegmenti pontis
DLPN - Dorsolateral pontine nucleus
VPN - Ventral pontine nucleus
DPN - Dorsal pontine nucleus
VMPN - Ventromedial pontine nucleus
DMPN - Dorsomedial pontine nucleus

A far larger percentage of the cerebral cortex projects to the pontine nuclei than the NRTP, which is dominated by subcortical afferents, particularly from the deep cerebellar nuclei (Carpenter and Nova, '60; Brodal and Szikla, '72; Walberg et al., '72; Chan-Palay, '77; McCrea et al., '78). Cerebellar inputs to the NRTP terminate in almost all parts of the nucleus, except lateral areas, and with the highest density centrally throughout its rostrocaudal extent.

The great majority of cortical inputs to the pons arise from areas in the cingulate cortex medially to the sylvian fissure laterally; and from the superior temporal fissure caudally to the medial part of the frontal granular cortex rostrally (Brodal, '78; Glickstein et al., '85).

Cerebral inputs to the NRTP, however, are restricted to more central areas of the hemispheres - indeed the prefrontal, temporal, occipital and cingulate regions do not project to the NRTP at all (Brodal, '80). The cortical efferents that the NRTP and the pontine nuclei do share are those associated with the visual guidance of movement, namely certain motor and visual cortices. The more moderate projections to the pontine nuclei, such as from the cingulate, auditory, inferior temporal and frontal association areas are not shared by the NRTP, although some somatosensory areas (Brodmann's areas 3, 1 and 2) may project to both (Brodal, '80; Glickstein et al., '85).

Studies on the topography of the cortico-pontine projection have indicated a rough topography of projections across the cerebral cortex (Nyby and Jansen, '51; Brodal, '78; Glickstein et al., '80). The most anterior regions of cortex project predominantly to areas that lie most ventral and medial within the pontine nuclei. Caudal areas and some divisions of the temporal lobe project to the most dorsolateral pontine regions, while intermediate areas of cortex adjacent to the central sulcus project centrally in the pons.

The cortico-NRTP projection has a different topography to that of the cortico-pontine system. The anterior cortical areas project medially and posterior ones more laterally in the NRTP, although there is extensive overlap in the terminal fields from different cortical areas (Brodal, '80).

The cortico-pontine projection has a precise but divergent terminal pattern. Cortical neurons project onto discrete patches of cells in widespread parts of the pontine nuclei. When viewed three dimensionally, these terminal fields have been described as

columns, slabs or lamellae, and in single sections they appear clustered as multiple small patches or bands (Brodal and Bjaalie, '92). This high degree of divergence in the cortico-pontine projection ensures that the same information is delivered to pontocerebellar neurons with quite different cerebellar targets. Consequently, the outputs of individual cortical areas are distributed over widely separated parts of the cerebellar cortex.

The cortico-pontine projection is not purely divergent, however. Studies employing double anterograde tracing have shown that there is a mixture of overlapping and segregated cerebral cortical input to the pons (Aas and Brodal, '89; Bjaalie and Brodal, '89; Brodal et al., '91). Physiological studies have shown that pontocerebellar neurons are activated from more than one cortical site (Ruegg and Wiesendanger, '75; Ruegg et al., '77), and that the visual receptive fields of pontine cells are invariably larger than those of the cortical neurons supplying them (Baker et al., '76; Cohen et al., '81). Thus in addition to marked divergence, the cortico-pontine projection undergoes convergence both from within a single cortical area and between neighbouring cortical regions.

The projection from the cerebral cortex to the NRTP is more diffuse than that to the pons. There is no tendency for cortical terminals in the NRTP to cluster into well-defined groups, as is the case for the pontine input (Brodal, '80). However, there seems to be a large amount of convergence in the cortico-NRTP pathway, since larger lesions in the cortex simply produce denser degeneration in the NRTP, rather than a wider distribution (Brodal, '80).

The presence of pontine interneurons has been debated for some time, but recent immunocytochemical studies have described a population of GAD-positive cells which do not project to the cerebellum (Border and Mihailoff, '85; Thier and Koehler, '87; Brodal et al., '88), but may act to limit the rate of pontine cell firing. The percentage of interneurons in the pontine nuclei increases in higher animals, such that they form approximately 5% of the population in the monkey (Thier and Koehler, '87; Brodal et al., '88). The larger population of inhibitory interneurons in the monkey probably reflects the increasing sophistication of the information processing occurring within the pontine nuclei in this animal; for example, by providing lateral inhibition to increase the

precision of cerebro-cerebellar transmission. In addition, pontine interneurons have very long straight dendrites which may serve to distribute inhibition over long distances in the pontine nuclei, thereby interconnecting cell groups with different cortical inputs. Indeed, the GABA-ergic interneurons seen in the monkey pontine nuclei tend to cluster together, in a pattern reminiscent of the terminal projection of cortico-pontine fibres. No direct evidence for the existence of NRTP interneurons is available. However, following small injections of HRP into the rat NRTP, Torigoe et al. ('86) observed a large number of labelled neurons beyond the injection sites. Although the possibility that the label may have been the result of direct spread from the injection site cannot be excluded, they suggested that these populations are indicative of interneuron cell groups.

The clarity of the somatotopic maps inherent in the cortical areas is lost in the transmission to the pons or the NRTP, presumably as a result of the simultaneous divergence and convergence in the pathways. Although there is no evidence of a somatotopic organisation in the cortico-pontine projection from the primary motor cortex, the NRTP does maintain a very basic somatotopy, such that the primary motor cortex (M1) arm projection to NRTP lies dorsal to the projection from areas representing the leg (Brodal, '80).

There is a gradient in the strength of projections across those cortical areas that are connected with the pons or NRTP (Glickstein et al., '85).

The densest projection to the pontine nuclei and the NRTP and thence to the cerebellum is from Brodmann (1905) areas 4 (primary motor cortex), 6 (pre-motor cortex) and the supplementary motor area, all of which project centrally in the pons and medially in the NRTP, although it is not known whether the projections to pons and NRTP arise from separate cells in interdigitating populations or collaterals from the same cells (Brodal, '80; Glickstein et al., '85).

The extrastriate visual cortices provide a moderately dense input to the pons and NRTP. Since this thesis is concerned with the anatomy underlying visuomotor co-ordination via the cerebellum, the rest of this section will concentrate on the visual cortical afferents to the pons and the NRTP. For simplicity, and since the pontine nuclei receive more

extrastriate cortical input than the NRTP, the cortico-pontine projection will be described first. Inputs to the NRTP will be detailed at the end of the section.

b) The visual cortical areas

Visual information passes from the retinal ganglion cells via the optic nerve, chiasm and tract into the lateral geniculate nucleus of the thalamus. From here, the information is projected to the striate cortex in the calcarine fissure, prestriate cortices in surrounding areas and subsequently to a wide range of interconnected visual cortical areas.

Functional segregation is a fundamental feature of the visual pathway. The two classes of retinal ganglion cell, Pα and Pβ (Leventhal et al., '81; Perry et al., '84), project onto the M and P layers of the geniculate nucleus, the cells of which have different physiological characteristics. The anatomical and physiological segregation is maintained in the geniculo-cortical projection. The P cells of the geniculate project onto the blobs and interblobs of layers 2 and 3 of the striate cortex (Lund and Boothe, '75) which are concerned primarily with processing colour and form respectively. The M layers of the geniculate terminate in layer 4B of the striate cortex. Orientation and direction selectivity are generated in this area.

Both the M and P pathways arising in the striate cortex project to the extrastriate visual areas directly. However, there is an additional relay via V2, a cortical area lying within the lunate and inferior occipital sulci (see figure 4), and the precision of this projection ensures that the retinal representation produced in V1 is maintained in V2, albeit more crudely (Desimone and Ungerleider, '86).

On the basis of the anatomical connections and physiology of these constituent areas, the projections from striate cortex and V2 into the extrastriate cortices have been divided into two broad streams (see figure 4a). One stream is directed ventrally from the striate cortex into nearby regions around the lunate and inferior occipital sulcus (containing cortical areas V2, V3 and V4). It is primarily concerned with form analysis and pattern recognition, and is therefore frequently referred to as the "what" stream. The other is directed dorsally from its origin in the striate cortex to both banks of the superior temporal sulcus (cortical areas V5 and V5a), and visual areas within the

parietal cortex and the intraparietal sulcus. This stream is concerned with spatial organisation in the visual fields and the analysis of motion, and is frequently referred to as the "where" pathway (Ungerleider and Mishkin, '79, '82; Desimone and Ungerleider, '86; Broussard et al., '90). Although this division into two streams is a huge oversimplification - there are many interconnections between areas residing in the different streams - it is useful in the examination of the cerebellar role in visuomotor co-ordination. The dorsal "where" pathway projects heavily to the cerebellum via the pontine nuclei. The ventral "what" pathway does not (Glickstein et al., '80; Glickstein and May, '82). This seem intuitively correct, since any system concerned with motor control and the visual guidance of voluntary movement would require information on spatial and directional aspects of the hand/eye and target. The precise form or colour of the target would be of less significance. Indeed, massive lesions of the "what" pathway produce no detectable deficit in visually guided movement (Buchbinder et al., '80).

The marked convergence and divergence inherent to the cortico-pontine pathway as a whole is also evident in projections from the monkey extrastriate visual areas. Projections from these cortical areas focus in the lateral and dorsolateral nuclei of the pons, and provide additional smaller projections to other divisions (Brodal, '78; Glickstein et al. '80, '85, '90; Galletti et al., '82; Ungerleider et al., '84; May and Andersen, '86; Stanton et al., '88b; Schmamann and Pandya, '89; Fries, '90; Boussaoud et al., '92; Brodal and Bjaalie, '92).

Although all of the cortical visual areas in the "where" stream project to the cerebellum via the dorsolateral pontine nuclei, there is a definite gradient between the strengths of these projections from different visual areas within this stream (Glickstein et al., '85).

The pontine projection is densest from the more rostral of these areas, such as the anterior (dorsal) bank of the medial part of the superior temporal sulcus (MST or V5a) (Boussard et al, '92), the adjacent area 7 of the parietal lobe (posterior parietal cortex), and from the rostral bank of the parieto-occipital sulcus on the medial face of the hemisphere. The projection from area MT or V5 at the base of the superior temporal sulcus is more moderate (Glickstein et al., '80; '85; Galletti et al., '82; Ungerleider et al., '84). The striate cortex itself only projects sparsely to the pontine nuclei, and only from the rostral portion of the upper bank of the calcarine fissure, in a region

representing the lower periphery of the visual field (Brodal, '72; Glickstein and Whitteridge, '76; Glickstein et al., '85; Fries, '90).

c) The visual cortical areas projecting to the cerebellum via the dorsolateral pons

The anatomical connections and characteristics of the cortical areas in the dorsal stream define the type of visual information that reaches the cerebellum and is used by it for visuomotor control. A number of the areas projecting to the cerebellum are not only visually sensitive, but also have oculomotor characteristics and are fundamentally involved in the generation of eye movements. The areas vary in terms of their receptive fields, motion selectivity and the type of eye movement in which they are involved. This section will describe the most salient of each of these characteristics for the major areas in the dorsal stream that project to the dorsolateral pons and thence to the cerebellum, beginning with the striate cortex itself.

The *striate cortex* in the calcarine fissure provides a sparse pontine input from its rostral region, which represents the peripheral visual field (Glickstein and Whitteridge, '76; Glickstein et al., '85; Fries, '90). Lesions to this area have a profound affect on saccades and smooth pursuit eye movements, and it has been proposed that the striate cortex is involved particularly in the estimation of stimulus velocity (Segraves et al., '87).

The striate cortex projects directly and indirectly via V2 in the lunate and inferior occipital sulci to the superior temporal sulcus (STS) in a topographical fashion, such that the retinotopy evident in the striate cortex is maintained in the STS visual areas, albeit more crudely (Ungerleider and Mishkin, '79; Desimone and Ungerleider, '86). Projections from the areas of the striate cortex representing the central 30 - 40 degrees of the visual field project to a heavily myelinated portion of the posterior bank of the superior temporal sulcus (STS), in an area known as the medial temporal (MT or V5) area. Projections from areas of the striate cortex representing more peripheral parts of the visual field cortex project to a more lightly myelinated area known as MTp, which lies medial to MT (Desimone and Ungerleider, '86).

The visual areas *MT and MTp* (V5) provide a far denser projection to the dorsolateral pons than the striate cortex. Both MT and MTp are required to process the full output of V1 in the superior temporal sulcus, and thus they should be regarded as two distinctive parts of a single visual area.

The MT is specialised for the analysis of visual motion, and its functional properties have been clearly mapped (Zeki, '74, '78a,b; Baker et al., '81; Maunsell and Van Essen '83a; Allbright, '84; Felleman and Kaas, '84). Cells in this area have a high degree of direction and speed selectivity, and there is marked tendency for nearby units to have a similar preferred direction and speed. Most units in the MT also show selectivity (with brief responses) for stimulus orientation when tested with stationary flashed bars. The preferred orientation is usually, but not always, perpendicular to the preferred direction of movement.

The neurons in MT which represent the fovea discharge in response to the residual motion produced by imperfect tracking as well as passive visual stimulation during fixation (Komatsu and Wurtz, '88a). Lesions in MT areas cause deficits in the generation of pursuit eye movements (Newsome et al., '85).

MT provides a strong projection to the dorsolateral pons.

The MT is the gateway to the rest of the dorsal stream. It feeds back onto V1 and V2, and has connections with the ventral stream via inputs to V4. Its strongest projection is to the medial superior temporal (MST or V5a) area in the anterior bank of the STS and the fundus of the superior temporal sulcus (FST) in its floor (Ungerleider and Desimone, '86).

The *medial superior temporal area* (area MST or V5a) receives a direct projection from the striate cortex as well as its input from MT. It contains a high proportion of directionally selective cells with large receptive fields, but nonetheless displays a crude visuotopic organisation (Desimone and Ungerleider, '86). Cells in all areas of MST are involved in visual motion analysis, but those in the dorsal regions are concerned with analysing visual motion produced by self-motion, whereas those more ventrally situated are concerned with the analysis of object movements in external space (Erickson and Thier, '91; Tanaka et al., '93). The MST is also involved in smooth pursuit, and, much like MT, lesions here produced deficits in initial tracking. Small lesions produce greater

deficits in MST than they do in MT however - due to the cruder visuotopic map in this area, greater portions of the visual field are affected by even a small lesion (Dursteler and Wurtz, '88).

The MST provides a very dense input to the dorsolateral pons.

The MST also supplies the cerebellum via its projections to the accessory optic system (Tusa and Ungerleider, '88). The AOS provides both mossy and climbing fibre input to the cerebellar cortex via both the dlpn/NRTP (Buttner-Ennever, '96; Kawano et al., '96) and the dorsal cap/ventrolateral outgrowth of the inferior olive.

The *fundus of the superior temporal sulcus* (FST), receives input from both the MT and the MST, and has similar has similar characteristics to both.

FST projects only moderately to the dorsolateral pons.

All of the visual areas within the STS project to extrastriate visual areas in the parietal sulcus and the frontal lobe (Maunsell and Van Essen, '83; Leichnetz, '89; Blatt et al., '90) .

The intraparietal sulcus contains a visual area on its lateral border (the lateral intraparietal area) and one situated more ventrally (ventral intraparietal area).

Neurons in the *lateral intraparietal area* (LIP) have activity related to both visual stimulation and saccadic eye movements (Andersen, et al., '92), and their visual receptive and motor fields generally overlay one another.

The *ventral intraparietal area* (VIP) shares many of its anatomical connections and physiological responses with the LIP. Neurons in the VIP have direction and speed selectivity, and some are selective for the distance at which a stimulus is presented (Colby et al., '93). Unlike the LIP, VIP neurons are not active in relation to saccadic eye movements, although some are active during the smooth pursuit of a target.

Both the LIP and VIP provide moderate projections to the dorsolateral pons, and send strong connections to the frontal cortex, terminating in the frontal eye fields (area 8) (Barbas and Mesulam, '81).

The *frontal eye fields* (area 8) are found on the banks of the arcuate sulcus in the frontal cortex. In combination with the superior colliculus, the FEFs are heavily involved in saccadic generation. The frontal eye fields have a topographical organisation both with

respect to the visual field representation (Suzuki and Azuma, '83) and the amplitude of saccades generated by stimulation at a given location. Stimulation of the ventrolateral areas of the FEFs elicits small saccades (Robinson and Fuchs, '69; Bruce et al., '85), whilst the dorsomedial areas elicit large saccades. Projections to the FEFs from earlier visual areas in the dorsal stream arise from MT and MST (Barabas et al., '81; Ungerleider and Desimone, '86). There is no clear topography to this projection, and the inputs are restricted to the caudal bend of the arcuate sulcus. Both areas of the frontal eye fields project back to the ventral and lateral intraparietal areas (Leichnetz, '89; Stanton et al., '95).

Recent reports indicate that the FEFs also have a role in smooth pursuit eye movements (Lynch et al., '87; MacAvoy et al., '91). The smooth pursuit and saccadic-related areas are situated very close together, but the populations do not seem to overlap, as smooth pursuit neurons respond only weakly during passive visual stimulation or during saccadic eye movements (MacAvoy et al., '91).

The FEFs project strongly to the entire rostrocaudal length of the pontine nuclei, terminating in the medial, dorsal and dorsolateral subdivisions (Stanton et al., 88).

The *posterior parietal cortex* (PPC or area 7) is the highest level for visual motion analysis, and neurons here have both visual and saccade-related activity (Andersen and Gnadt, '89). The PPC provides a powerful input to the dorsolateral pontine nuclei (May and Andersen, '86; Faugier-Grimaud and Ventre, '89; Schmahmann and Pandya, '89).

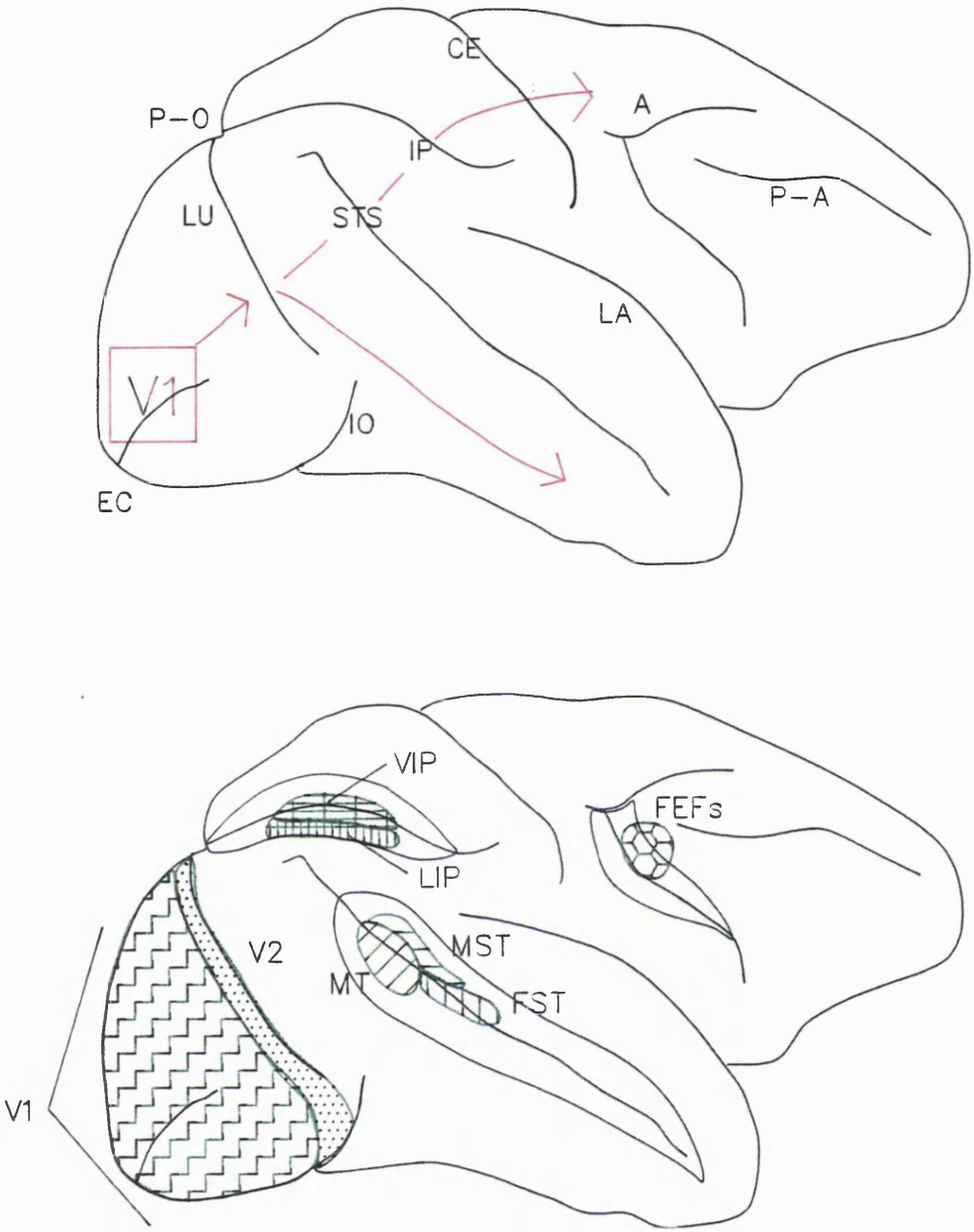

Figure 4: a) The dorsally-directed 'where' and ventrally-directed 'what' streams in the extrastriate visual cortical areas of the macaque.

b) The dorsal stream extrastriate areas that project to the dorsolateral pontine nuclei.

(Adapted from Ungerleider and Desimone, '86)

EC - external calcarine sulcus
LU - lunate sulcus
P-O - parieto-occipital sulcus
STS - superior temporal sulcus
IP - intraparietal sulcus
LA - lateral sulcus
P-A - pre-arcuate sulcus
A - arcuate sulcus
CE - central sulcus
IO - inferior occipital sulcus

MT - middle temporal area
MST - medial superior temporal area
FST - fundus of the superior temporal sulcus
FEFs - frontal eye fields
VIP - ventral intraparietal area
LIP - lateral intraparietal area

d) The visual cortical areas projecting to the cerebellum via the NRTP

The NRTP receives some cortical input, but it is dominated by subcortical afferents, particularly from the contralateral deep cerebellar nuclei. The majority of the fibres arise from the dentate and the anterior interposed, with a small contribution from the fastigial (Walberg et al., '62; Brodal and Szikla, '72; Chan-Palay, '77; McCrea et al., '78). Cerebello-NRTP projections terminate in a diffuse manner across most of the NRTP, but focus centrally in its entire rostrocaudal extent (Brodal et al., '72; Gonzalo-Ruiz et al., '88; Gonzalo-Ruiz and Leichnetz, '90).

The only visual cortical areas that project to this nucleus are the posterior parietal cortex and the frontal eye fields.

Area 7 (PPC) projects rostrolaterally in the NRTP (Schmahmann and Pandya, '89), while the frontal eye fields project to medial, dorsal and dorsolateral divisions. The projection from the FEFs to the NRTP has a specialised degree of topography: the dorsomedial FEFs which on stimulation generate large saccades project ipsilaterally, whereas the ventrolateral FEFs (producing small saccades) project bilaterally (Leichnetz et al., '84; Stanton et al., '88).

e) Subcortical visual areas projecting to the pons and NRTP

Another visual- and oculomotor-related area projecting to the dorsolateral pontine nucleus and NRTP is the superior colliculus. The colliculus is a laminated structure on the roof of the midbrain which, on the basis of anatomical and physiological studies, has been divided into the "superficial" laminae 1, 2 and 3, and the "deeper" laminae 4-7. Both the superficial and deep layers of the colliculus project to the cerebellum (Glickstein et al., '90).

The superficial laminae receive a retinotopic input via bifurcating optic tract fibres, and thus contain a map of the visual field which distributed across the rostrocaudal extent of the colliculus (Mouse: Drager and Hubel, '75; Cat: McIlwain, '83; Monkey: Wurtz and Goldberg, '72; Wurtz and Albano, '80). The perifoveal portion of the visual field is represented at the very rostral end of the colliculus, the peripheral parts of the visual

field are represented more caudally. The superficial layers are purely visual and are briskly activated by visual stimuli.

The deeper layers of the colliculus however, are polysensory (Edwards et al., '79; Killackey et al., '81; Rhoades et al., '81) and contain sensory maps which are in register with the visual map immediately above them (Drager and Hubel, '75).

In rats, the ratio of optic tract fibres to the superior colliculus compared with those terminating in the LGN is higher than in primates, where the bulk of the optic tract fibres are destined for the cortex. However, the primate superior colliculus receives input from visual cortical areas which the rat does not possess, such as the frontal eye fields, MT and MST. The FEFs project topographically to the superior colliculus (Stanton et al., '88), such that the ventrolateral (small saccade generating) FEFs project to the rostral portion of the superior colliculus (representing perifoveal vision and generating small saccades), and the dorsomedial FEFs (large saccades) project onto the more caudal levels of the colliculus (representing the entire visual field and generating large saccades).

MT and MST differ in their projections to the superior colliculus. The MT projects to the superficial and intermediate layers of the colliculus; the MST projects to deeper layers (Maioli et al., '92).

Cells in the superficial (visual) and deep (polysensory) layers of the superior colliculus both project to the pontine nuclei, but there are differences between their routes through the brainstem and terminations in the pontine nuclei. Numerous studies on the efferents of the superior colliculus differentiated between two efferent pathways (Harting, '77; Mower et al., '79; Glickstein et al., '90). One, the predorsal bundle, arises from the cells in the deep layers of the colliculus, courses medially and decussates in the midbrain to terminate a wide range of areas, including the contralateral NRTP and the spinal cord (as the tectospinal tract). Cells from the superficial layers, however, project round the edge of the brainstem to terminate in the ipsilateral dorsolateral pons. There are thus two routes by which the superior colliculus can project to the cerebellum - via the NRTP and via the dlpn.

There is some overlap in the dorsolateral pons between visual cortical and superior collicular terminal fields. The visual cortical termination zones cover most of the

rostro-caudal extent of the dlpn, but focus rostrally. The collicular termination zone is partially co-extensive with this cortical area, but focuses in its caudal portion (Glickstein et al., '90). It is unclear whether the visual input to the dorsolateral pons derived from different cortical and subcortical areas actually converge onto individual pontine cells or onto populations of interdigitating cells in the nucleus.
Collicular and frontal eye field projections overlap in the NRTP, although the collicular input focuses more caudally, as it does in the pontine nuclei. The projections from the PPC and colliculus do not overlap significantly in the NRTP.

The nucleus of the optic tract (NOT) also projects to the superior colliculus. In addition, it projects to the precerebellar nuclei, including the dorsolateral and dorsomedial pontine nuclei and the NRTP (Torigoe et al., '86; Mustari et al., '90; Buttner-Ennever et al., '96). Recent electrophysiological studies (Kawano et al., '96) on the NOT have shown that it may play a role in short-latency smooth pursuit eye movements (the ocular following response).

The supraoculomotor area of the periaqueductal grey (the mid-brain near-response area), which generates vergence eye movements, also sends a projection to the NRTP (May et al., '92).

f) Physiology of the dorsolateral pontine nucleus

The visual cortical areas that project to the cerebellum via the dorsolateral pons are involved in motion analysis, and a number of them are also involved in eye movements. As a result, the cells forming the dorsolateral nucleus of the pons are responsive to either visual stimuli alone, during eye movements with no apparent visual response or both during visual stimulation and eye movements (Suzuki and Keller, '84, '90; Smooth pursuit: May et al., '85, '88; Mustari et al., '88; Thier et al., '89; Saccades: Thier et al., '96; Ocular following: Kawano et al., '92, '96). All the cells in the dlpn are binocular, and there is no evidence of retinotopy. Local clusters of cells have strikingly similar functional characteristics, such as directional selectivity, which are also represented in the cortical areas from which they receive their input. Within the population of

dorsolateral pontine cells, all directions of motion are represented, and the tracking responses of dlpn neurons are characterised by their selectivity for the direction of smooth pursuit. For many of these tracking units in the dlpn, the response during pursuit is not purely visual, since they continue to respond when the target is briefly turned off, indicating the presence of an extra-retinal input (Mustari et al., '88). For those units that respond both during pursuit and visual stimulation, the preferred direction for tracking can either be the same or the opposite as the preferred direction during visual stimulation (Thier et al., '88).

The saccadic units recently found in the dlpn (Thier et al., '96), which are characterised by directionally-selective pre- or peri-saccadic bursts of discharge, are most likely the result of superior collicular and frontal eye fields input.

The receptive fields of cells in the dlpn are much larger than those in each of the cortical areas supplying them, suggesting that multiple neurons in a particular cortical area converge onto individual dlpn neurons (Cat: Baker et al., '76). There is, however, no data available to clarify whether cortical neurons from *different* visual areas also converge onto single dlpn neurons rather than to interdigitating populations of pontine cells.

The cortico-pontine projection compensates only incompletely for the over-representation of the central visual fields in the visual cortical areas (Bjaalie and Brodal, '83). Uniformity of velocity sensitivity of pontine neurons across their large receptive fields may also result from synaptic strength at the peripheral representation being greater (Cohen et al., '81).

g) Physiology of the NRTP

Physiological studies on the NRTP in the monkey have shown that it too is responsive to visual stimuli and/or eye movements. Cells in the caudal dorsomedial NRTP that receive input from the frontal eye fields and the superior colliculus are responsive to saccades, during focal visual stimulation or both (Keller and Crandall, '81). The saccadic responses in the NRTP differ from those in the pons, since they are not related

to saccade metrics, but rather increase their discharge when the saccade moves the eyes to a circumscribed region of the animal's visual field (movement field). Visual cells responsive to focal stimuli are maximally active when a small spot of light is presented in a particular portion of the animal's visual field, while it maintains fixation on a separate spot of light. These visual neurons do not have saccadic activity per se, but their activity increases when the spot of light is to be the target for a saccade. A larger group of neurons produce both visual and saccadic responses.

The caudal NRTP also contains a population of cells which are responsive to vergence (both far and near) eye movements (Gamlin and Clarke, '95). Vergence-related cells in the NRTP are found close to the saccade-related group but do not modulate their firing with saccadic eye movements: microstimulation of these cells only produces changes in accommodation and vergence.

Recording and microstimulation studies in the rostral NRTP, however, have recently described a population of smooth pursuit-related cells (Yamada et al., '96). There is no overlap between the caudally located saccadic/vergence-related group and the more rostral smooth pursuit-related cells.

In afoveates, the dmNRTP is the only visual/oculomotor division of this nucleus. Cells in this area respond only to optokinetic stimuli, as they have powerful connections with the NOT and accessory optic system. The equivalent optokinetic-responsive cells in the macaque are located in the dorsomedial pontine nucleus (Keller and Crandall, '83).

h) The visual pontocerebellar pathway

The neural tracer WGA-HRP travels bidirectionally from its site of injection. Cells in the vicinity of the injection site take up the tracer and it is transported to their axon terminals. Axonal terminations in the region of the injection take up the tracer and it is transported retrogradely to their cell bodies. If injected into the dorsolateral pons, it is possible to map the cerebellar cortical divisions to which the visual cortical and subcortical areas project.

The majority of fibres from the dorsolateral pons decussate in the basal pons to enter the contralateral middle cerebellar peduncle. They subsequently enter the cerebellar white

matter lateral to the deep cerebellar nuclei and turn laterally to enter the white matter of the paraflocculus or medially for the vermis. They terminate in the granular layer in mossy fibre rosettes. The ipsilateral fibres project directly through the adjacent middle cerebellar peduncle to the cerebellum. The ratio of the ipsilateral:contralateral pontocerebellar projections varies between species and between lobules in any particular species. In the monkey, about 10% of fibres to crus I and II and only about 3% of those to the paramedian lobule and the flocculus terminate ipsilaterally (Brodal, '79, '82).

The principal efferent target of the dorsolateral pons is the posterior cerebellar cortex (Rats: Burne et al., '78; Azizi et al., '81, '85; Mihailoff et al., '81; Dietrichs and Walberg, '83; Cat: Gibson et al., '77; Brodal and Hoddevik, '78; Mower et al., '80; Kawamura and Hashikawa, '81; Rabbit: Hoddevik, '77; Hoddevik and Walberg, '79; Monkey: Brodal, '79, '82; Glickstein et al., '94). The projection to the cerebellar cortex is not homogeneously distributed, however. The strongest projection is to the contralateral dorsal paraflocculus and the neighbouring petrosal lobule. There is a moderate projection to the uvula (vermal lobule IX), paramedian lobule, crus II and the more rostral vermal lobules up to and including vermal lobule VII. The projection to the ventral paraflocculus is sparse. There were virtually no fibres traced to the flocculus and adjacent ventral paraflocculus or nodulus (Glickstein et al., '94). These projections are mirrored in the ipsilateral cerebellar cortex (Rosina et al, '80, '88; Glickstein et al., '94), but at a massively reduced strength.

In rats, the primary visual cortex and superior colliculus both project to the dorsolateral pons (Burne et al., '78; '81) and thence to the posterior lobe of the cerebellum in a similar manner to monkeys.
In cats, however, the visual cortical areas project to the dorsomedial pontine nucleus. The superior colliculus terminal field is located in the dlpn, as it is in rats and monkeys. If WGA-HRP is used in cats to trace the projection from this dorsomedial pontine area, the distribution of terminals is virtually identical to that following a dorsolateral pontine injection.

Therefore, visual information from the cortex and subcortical areas is distributed over identical regions of the cerebellar cortex in rats, cats and monkeys.

h) The NRTP-cerebellar pathway

All of the studies performed on the NRTP-cerebellar projection have been based on retrograde studies. In 1974, LaFleur was the first to show that the vast majority (if not all) of NRTP efferents project to the cerebellum. Hoddevik's description of the system in the cat (1978) and Brodal's studies in the monkey ('80 and '82) agreed on the overall topography.

The strongest projection from the NRTP to the cerebellum arises from the dorsomedial and medial subnuclei and terminates in vermal lobules VII - VIIIa and the flocculus. More moderate projections arise from medial and lateral cell groups to the uvula, a central group to the anterior lobe hemispheres and the processus tegmentosus lateralis to the paramedian lobule. There are also scattered projections from the entire NRTP (excluding the processus tegmentosus lateralis) to crus I, crus II and vermal lobules VIIIB.

Brodal and Hoddevik saw no evidence of "clustering" of NRTP efferents, as they constantly encountered in the pontine nuclei. However, a recent double label study investigating NRTP projections to vermal lobules VII and IX in the monkey (Thier and Thielert, '93) demonstrated that NRTP efferents do indeed cluster to form discrete cell populations.

1.3.2.2 Cerebellar afferents from the vestibular nuclei and reticular formation.

Additional mossy fibre inputs to the cerebellum are derived from the vestibular nuclei and reticular formation. These areas were not included in this investigation, however, and therefore I shall describe their connections only very briefly.

The vestibular complex includes four major divisions: superior, lateral, medial and inferior (also called the spinal or descending vestibular nucleus). There are additional smaller cell groups, such as the interstitial nucleus of Cajal of the vestibular nerve, *x, y,*

z, l, f, Sv, and *g*. The vestibular nuclei both project to, and receive from the cerebellar cortex. All of the vestibular nuclei, except the lateral vestibular nucleus (of Deiter's) receive a direct input from the vestibular nerve. The nodule, the caudal part of the uvula, the ventral part of the anterior lobe and the bottom of the deep fissures of the vermis receive primary vestibular input. There are no primary vestibular fibres to the flocculus (Gerrits et al., '89).

Secondary vestibulo-cerebellar fibres take their origin from the superior vestibular nucleus and caudal portions of the medial and inferior vestibular nuclei. They terminate bilaterally in the same regions which receive primary vestibulo-cerebellar input, but also in the flocculus and adjoining paraflocculus, which lack a primary projection (Epema et al., '90).
The fastigial is bilaterally connected with the medial and spinal vestibular nuclei.
Collateral projections of the vestibulo-cerebellar fibres to the deep nuclei are still disputed.

Reticular afferents to the cerebellum arise from only 3 nuclei - the lateral reticular, the paramedian reticular and the NRTP, which has been described above. In addition to sending mossy fibres to the cerebellar cortex, the lateral reticular nucleus and the NRTP give rise to major collaterals to the deep cerebellar nuclei.

The *lateral reticular nucleus* is located in the lateral funiculus of the caudal medulla. It receives a somatotopic input from the spinal cord, collaterals from the rubrospinal and lateral vestibulospinal tracts and a projection from the cerebral cortex.
LRN projects bilaterally to the vermis and the hemispheres of the cerebellum: the dorsal part of the nucleus projects centrally into the ipsilateral hemisphere, while the ventral portion projects bilaterally, mainly to the vermis. Collateral projections to the deep nuclei focus on the rostral fastigial, AIP and the medial pole of the PIP.
The lateral reticular nucleus termination field on the cerebellar cortex is complementary to that of the NRTP.

The *paramedian reticular nucleus* consists of cell groups at the lateral border of the medial longitudinal fasciculus. It receives fibres from the vestibular nuclei, the interstitiospinal and tectospinal tracts, the spinal cord and the cerebral cortex. This nucleus projects to the entire cerebellum, with the possible exception of the paraflocculus.

1.3.2.3 Mossy fibre collateral systems to the deep nuclei

In spite of the massive inhibitory cortico-nuclear projection, cells in the deep cerebellar nuclei maintain a high discharge frequency (Thach, '68; '70a and b; '72), which suggests the presence of a powerful direct excitatory input to the nuclear neurons. The deep nuclei receive a direct input from the climbing fibre system via collaterals from olivary axons projecting to the Purkinje cells in the cortex. However, as inferior olivary neurons have a slow resting firing rate (approx. 1 Hz), they are unlikely to be solely responsible for the background excitability inherent to the nuclear neurons. The most likely candidate for a direct nuclear input from the mossy fibre system is the pontine nuclei. However, there is considerable inter-species variation in the evidence for such a projection. Lower animals, such as the rat, clearly possess a powerful ponto-nuclear projection (Mihailoff, '93), but in the cat, the presence of such a pathway is disputed (Dietrichs et al., '83; Chen et al., '83; Dietrichs and Walberg, '86; Gerrits and Voogd, '87; but see Shinoda et al., '93). In the monkey, HRP studies have indicated that there is no projection from the pontine nuclei to the deep cerebellar nuclei (Brodal et al., '86; Bjaalie and Brodal, '90; Glickstein, unpublished observations).

The most probable sources for facilitation of cerebellar nuclear efferents, therefore, are the spinal cord, the lateral reticular nucleus and the nucleus reticularis tegmenti pontis (NRTP). The spinal cord projects to the medial fastigial and the medialmost parts of the interposed (Matsushita and Ikeda, '70b), the lateral reticular nucleus projects to the interposed (Dietrichs, '83), and the NRTP projects strongly to the dentate and the lateral parts of the posterior interposed, and more moderately to the fastigial (Brodal et al., '86; Gerrits and Voogd, '87; Mihailoff, '93).

The remainder of the cerebellar afferent systems project weakly, if at all, to the deep nuclei. Within the vestibular system, primary vestibulo-cerebellar fibres send a modest projection to the ventral parvicellular dentate (Carleton and Carpenter, '84), whilst the

vestibular nuclei send a small projection to the fastigial (Van der Want, '87). The red nucleus (Walberg and Dietrichs, '86), paramedian and gigantocellular reticular formation, spinal trigeminal, dorsal column and external cuneate nuclei send only very modest projections, if any, to the deep cerebellar nuclei.

1.4 CEREBELLAR CORTEX - EFFERENTS

1.4.1 Cortico-nuclear projection

The Purkinje cell is the sole output of the cerebellar cortex. It has been known for many years that although specific regions of the cerebellar cortex, such as the flocculus and parts of the vermis project to the vestibular nuclei, the majority of Purkinje cells project to the deep cerebellar nuclei, thereby forming the cortico-nuclear projection.

The earliest investigations into the cortico-nuclear projection were performed a century ago (Klimoff, 1897 and 1899; Clarke and Horsley, 1905). These Marchi studies in the rabbit showed for the first time that the Purkinje cells do not project directly out of the cerebellum, but suggested that they terminated in the deep cerebellar nucleus that lay closest to them. Following lesions in the hemivermis, degeneration was only seen in the ipsilateral fastigial, whilst lesions in the hemisphere produced degeneration in the dentate and interposed nuclei. Even at this early stage of the investigations, it was clear that the cortico-nuclear projection had both a rostro-caudal and medio-lateral topography. In addition to the observation on vermal midline and hemispheric lateral projections, the anterior lobe was seen to project to the more rostral areas of the nuclei, and the posterior lobe to the caudal areas. Hohman's lesion studies (1929) provided the first clues of a more detailed mediolateral topography within these projections. In a series of studies in the cat, he showed that within a particular cortico-nuclear projection: i) cortical areas had a preference for particular portions of a deep nucleus, ii) that the lateral edges of the vermis projected to the lateral vestibular nucleus and iii) that there was no indication of contralateral projections. In 1940 and 1942, Jansen and Brodal published the seminal paper on the cerebellar cortico-nuclear projection. Their studies showed conclusively that the cortico-nuclear projection could be broken down into three mediolaterally arranged zones projecting into relatively localised portions of their respective deep nuclei in the cat, rabbit and the monkey.

This system was subsequently expanded by Voogd ('64, '69) who, on the basis of fibre diameter, was able to describe seven parasagittally arranged ipsilateral compartments in the subcortical white matter of the ferret. These compartments were named A, B, C1-3,

D1 and D2. Each compartment contained a longitudinal strip of cortex, the cortico-nuclear fibres and part or all of the respective deep nucleus in which they terminate. The exception was zone B, which was shown to bypass the deep cerebellar nuclei and terminate solely in the lateral vestibular nucleus.

On the basis of anti-cholinesterase studies, Hess and Voogd ('86) described the deep cerebellar nuclei involved in each zone in the monkey cerebellum. Zone A included the fastigial, zones C1 and C3 the anterior interposed nucleus, zones C2 the posterior interposed and the D zones contained the dentate. Unlike zones C1 and C3, whose terminals in the anterior interposed could not be separated into distinct parts of the nucleus, the D1 zone was linked with the ventrolateral parvicellular dentate, and D2 with the dorsomedial magnocellular dentate. It was also noted that the topographically organised climbing fibre inputs from the inferior olive followed this precise parasagittal zonation and travelled with the cortico-nuclear fibres within these white matter compartments (see section 1.3.1.2), and the olivo-cortico-nuclear system was regarded as the basic functional module of the cerebellum (Groenewegen and Voogd, '77, '79; Voogd and Bigare, '80; Buisseret-Delmas, '88; Buisseret-Delmas and Angaut, '93).

The cortico-nuclear projection (and the olivo-cortico-nuclear system as a whole) has been extensively studied in the last thirty years (Rats: Goodman et al., '63; Armstrong and Schild, '78; Haines and Kotelar, '79; Umetani et al., '86; Bernard, '87; Buisseret-Delmas, '88; Gayer and Faull, '88; Umetani and Tabuchi, '88; Umetani, '89, '93; Tabuchi et al., '89; Paallysaho et al., '90; Buisseret-Delmas and Angaut, '93. Cats: Dietrichs and Walberg, '79, '80; Voogd and Bigare, '80; Dietrichs, '81, '83; Garwicz and Ekerot, '94; Rosina et al., '96. Primates: Langer et al., '75; Haines, '75, '76, '77, '78, '81, '89; Courville and Diakiaw, '76; Haines et al., '76, '82; Haines and Whitworth, '78; Haines and Kotelar, '79; Haines and Pearson, '79; Haines and Rubertone, '79; Yamada and Noda, '87; Haines and Dietrichs, '91). New olivo-cortico-nuclear zones have been discovered, the system re-assessed and its topography is now reasonably well understood in a number of mammals. Figure 5 shows the fundamental details of the cortico-nuclear system. Although the basic longitudinal zonation pattern described by Voogd is still evident, the topography of the projections are more detailed than had been appreciated previously.

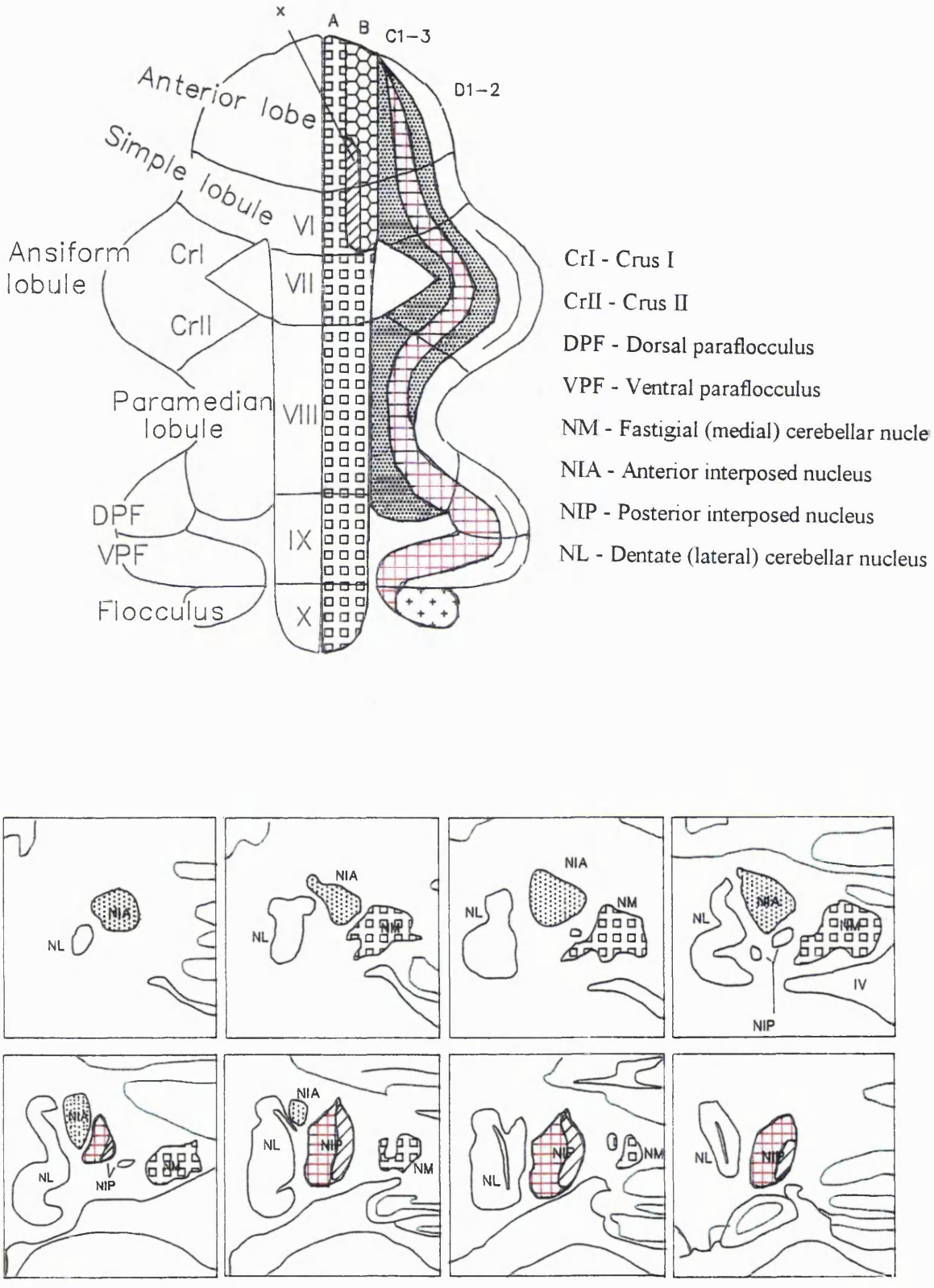

Figure 5: The cortico-nuclear projection in the macaque (adapted from Voogd and Bigare, '80). Separate olivo-cortico-nuclear modules denoted by hatching.

The vermal A zone is now divided into three sub-zones A1-3 on the basis of its olivary input from the cMAO and fibre studies (Voogd and Bigare, '80). All three zones project to the fastigial. Although a mediolateral topography was previously recognised within the vermal-fastigial projection (Armstrong and Schild, '78), there have been no studies attempting to correlate more clearly the topographies of the three vermal subzones projections into the fastigial.

The x zone is described as intercalating between the vermal zones A and B in restricted portions of the vermis (Voogd, '83; Campbell and Armstrong, '85, Voogd et al., '87a; Voogd and Hess, '89). This cortical zone receives from the middle levels of the medial accessory olive and projects to the interface between the fastigial and the posterior interposed nuclei in rat (Yatim et al., '95) and cat (Voogd, '83; Trott and Armstrong, '87b) but the medialmost edge of the posterior interposed in the squirrel monkey (Haines and Dietrichs, '91).

The B zone is still viewed as receiving from the caudal dorsal accessory olive, and projecting to the magnocellular division of the lateral vestibular nucleus (Deiter's nucleus), but recent studies have indicated that it has an additional projection out of the characteristic vermal projection zones into the medialmost edge of the anterior interposed (Dietrichs and Walberg, '79; '81). Haines et al. ('82) reported a projection from the B zone to the border of fastigial and posterior interposed, but suggested that the results were confounded by involvement of the x zone projection to this area (Haines et al., '82).

The majority of work performed on C zone efferents has been performed in the cat, which, as described previously, has complex subdivision of C1 and C3 zones into medial and lateral halves (Trott, '87).

The medial C1 and the medial C3 zones which receive from the rostral dorsal accessory olive, project into the medial and lateral anterior interposed respectively. The lateral C1 (Cx) zone, which is paired with the vermal x zone described above, receives olivary input from the middle levels of the medial accessory olive: the lateral C1 zone projects into the medial anterior interposed, whereas the x zone projects into the fastigial-PIP

border. The final C zone (lateral C3) receives input from the rostral dorsal accessory olive and terminates in the lateral portions of the anterior interposed.
In the monkey, the C1 and C3 zones both project into the anterior interposed.
The most lateral zones are the D1 and D2 zones. The medial D1 zone receives input from the dorsal leaf and lateral bend of the principal olive (Brodal, '80, '81) and projects onto the caudomedial parvicellular dentate (Hess and Voogd, '86). The more lateral D2 zone receives input from the ventral leaf and projects onto the rostromedial magnocellular dentate.

There is no data available on bifurcation of olivary afferents to paired parasagittal zones in the monkey as in the cat. A parallel system is likely to exist, although the available evidence does suggest that the parasagittal zones in these species are not identical. The x zone in the monkey appears to be more independent of the C zones than it is in the cat. Although it receives input from MAO areas that also project to the C2 zone, their projections into the posterior interposed are segregated. The x zone of the squirrel monkey projects into the medial aspect of the PIP, whilst the C2 zone projects more centrally and laterally (Haines and Dietrichs, '91).

Although parasagittal zonation is a fundamental feature of cerebellar anatomy, not all the zones are represented in each macro-division of the cerebellum.

Within the vermis, zones A1-3, x and B do not extend the entire rostrocaudal length of the cortex. Indeed, the B zone only reaches as far as lobule VI (Courville et al., '74; Bigare and Voogd, '77, '79, '80), and the x zone is only apparent in lobules V-VII (Haines and Dietrichs, '91). Although the vermis does contain zone A1 for its entire extent, A3 is missing in lobule VII, and in lobule IX, zones A1 and 2 either fuse or A2 disappears altogether. Zones C1 and C3 are only evident in those parts of the cerebellum receiving spinal input via the mossy fibre system: both these zones are wide in the anterior lobe and simple lobule (forming the "spinocerebellum"), crus I and II and the paramedian lobule, but totally absent from the paraflocculus and flocculus (Bigare and Voogd, '80).
In addition to this variation in the presence of individual zones through the cortex, there are variations in both the width and direction of the longitudinal strips. Moving up

through phylogeny, certain zones have expanded at the expense of others. This is particularly evident if primates and lower mammals are compared. Primates have larger D zones than non-primates, and the rhesus monkey has wider D zones than either the opposum or the squirrel monkey (Haines et al., '82). Olivo-cortico-nuclear paths in non-primates deviate markedly from the midline. Groenewegen et al.'s classic study on the cat ('79) showed that the C1 zone encroaches upon the vermis in lobule VIII, whilst Voogd's ('69) study on the ferret and Buisseret-Delmas and Angaut's study on the rat ('93) demonstrated that the vermal A zone extends laterally into the pars intermedia from lobules VIa to IXa. Deviation of the entire olivo-cortico-nuclear pathway from parasagittal zonation does not appear to occur in the monkey, presumably because the dominance of the D zones forces the other zones, and those of the vermis particularly into strict correspondence with parasagittal zonation.

1.4.2 Flocculo-vestibular projection

The first reports on the flocculo-vestibular projection date from 1936, when Dow performed Marchi studies on the rat, cat and monkey. More recent studies, using a variety of anatomical tracing techniques have demonstrated that the flocculus project to the superior and medial vestibular nucleus, group y and more sparsely to the descending vestibular nucleus (Jansen and Brodal, '40; Voogd, '64; Angaut and Brodal, '67; Alley, '77; Haines, '77; Yamamoto and Shimoyama, '77; Balaban et al., '81; Sato et al., '82a,b; Carpenter and Cowie, '85; Langer et al., '85; Epema, '90; De Zeeuw et al., '92 and '94b; Tan et al., '95). The flocculus contains its own system of zonation, based on input from different levels of the dorsal cap and ventrolateral outgrowth and differential projections to the vestibular nuclei, the compartments of which are visible with anticholinesterase histochemistry (Yamamoto and Shimoyama, '77; Yamamoto, '78; Balaban et al., '81; Sato et al., '82; Epema, '90; Tan et al., '95). The largest flocculo-vestibular projections are directed to the medial and superior vestibular nuclei, and the zones projecting to the different nuclei interdigitate with one another.

In the rabbit, the rostral dorsal cap/ventrolateral outgrowth project via compartments FC1 and 3 to floccular zones FZI and III which subsequently project to the superior vestibular nucleus. The caudal dorsal cap supplies (via FC2 and 4) floccular zones FZII and IV, which project onto the medial vestibular nucleus (Tan et al., '89, '95). The

rostral MAO projects onto the floccular continuation of zone C2. As yet, no anterograde studies have determined the projection of the floccular zone C2.

Langer et al. ('85) suggested that the most powerful efferent projections from the monkey flocculus are directed to the cell group y immediately ventral to the dentate nucleus, with more moderate projections to the medial and superior vestibular nucleus. However, in each of their cases, the injection sites showed spread into the overlying ventral paraflocculus, and it is likely that pure floccular efferents in the monkey parallel those demonstrated in the rabbit.

In the rabbit, cells in the dorsal cap and ventrolateral outgrowth are maximally activated by random dot visual stimuli rotated in planes equivalent to those represented in the semicircular canals (Maekawa and Simpson, '72, '73). Projections from separate subdivisions of the dc/vlo terminate on discrete floccular zones which subsequently control the activity of a different set of extraocular muscles via projections to specific vestibulo-ocular relay neurons. Indeed, stimulation in different floccular zones elicits different rotations of the eyes (Van der Steen et al., '94). The flocculus, by virtue of its anatomical connections, is ideally situated to control the vestibulo-ocular reflex employed in the stabilisation of gaze.

1.5 THE DEEP CEREBELLAR NUCLEI

1.5.1 Physiology and somatotopy

Anatomical (Strick, '76; Asanuma et al., '83a-c) and physiological studies (Thach et al., '90, '92; van Kan et al., '93a,b, '94; Gibson et al., '96) have provided evidence for a somatotopic representation of the body in each cerebellar nucleus. Within the somatotopic map, the head is represented caudally, the hindlimb rostrally, the limbs medially and the trunk laterally, although there is no clear differentiation between proximal and distal muscles within the limb-responsive population (Thach et al., '93). The somatotopy based on electrophysiological and lesion studies is maintained in the efferent projections from the deep nuclei to the ventrolateral thalamus to the motor cortex.

Each of the deep nuclei codes for a different type and context of movement, and produces a characteristic deficit in movement following inactivation (Thach et al., '90, '92). From inactivation (Kane, '88, '89; Thach et al., '90, '92) and recording studies (Van Kan et al., '93a,b, '94; Gibson et al., '96), it is suggested that the nuclei appear to control co-ordination of multiple body parts rather than single joints and are central to synergy.

The fastigial nucleus controls muscles only during sitting, standing or walking. Lesions produce an inability to maintain an upright position, with frequent falls to the side of the lesion. Under video analysis, the falls appear to result from poor co-ordination of the four limbs, such that the animal loses stability. Poor co-ordination, combined with inappropriate compensation during a fall produced profound difficulties in walking or standing unaided. The characteristic deficits following lesions in the other nuclei were not in evidence.

The interposed nucleus controls stretch and other somatosensory reflexes and may help damp the inherent mechanical oscillation of body parts. Cells within this nucleus fire at very short latencies to perturbation from a holding position, and lesions not only delay the response time to this stimulus but produce a large, low-frequency tremor at the end

of reaching or jump and pert tasks during ramps. Equally, the interpositus may be used to co-ordinate and adjust the bias and/or gain of agonist and antagonist muscles.
Precise analysis of the forelimb neurons in the interposed have demonstrated that they also discharge strongly during reach to grasp, but not during direct visual guidance of the limb (Gibson et al., '96)

The parallel phylogenetic development of the cerebral neocortex with the dentate, and the fact that its discharge leads that of motor cortex neurons and movement (Thach, '75, '78; Lamarre et al., '83) suggested that the dentate was involved in initiating voluntary movement from the motor cortex (Eccles, '67; Evarts and Thach, '69; Allen and Tsukahara, '74; Brooks and Thach, '81). The dentate discharges most profoundly to stimuli that give no information as to the nature of the movement that is to follow, and are therefore described as "volitional", and lesions of the dentate delay reaction time to these tasks. Lesions of the dentate affect multi-jointed movements much more than single-jointed ones, such that lesioned animals are unable to employ the precision pinch to remove food pellets from deep narrow food wells.

The question of whether the two divisions of the interposed each contain a separate body map has not been completely resolved (Thach, '92 and '93; Van Kan et al., '93). Anatomical data on the nuclear afferents (Groenewegen and Voogd, '77, '79; Bishop et al., '79; Bigare and Voogd, '80) and efferents (Asanuma et al., '83a-c) of the interposed nuclei have produced conflicting conclusions. The topography of the olivo-cortico-nuclear projection would suggest the presence of more than one map in the interposed, since the anterior and posterior divisions receive both different climbing fibre collateral and Purkinje cell inputs (rDAO/C1 and 3 and rMAO/C2 respectively). In addition, topographical projections from forelimb and hindlimb areas in the cerebellar cortex of the cat suggest that two separate representations exist and are maintained as mirror images to each other in the anterior and posterior interposed nuclei (Bishop et al., '79; Trott and Armstrong, '87a,b). Studies on the nuclear efferent projections (Strick, '76; Asanuma et al., '83a), however, do not support such a view, and suggest a continuum of the body representation across the entire interpositus.

Physiological investigations on the movement relations within the nuclei (Thach et al., '93; Van Kan et al., '93) have not provided conclusive evidence for multiple motor representations within the nuclei, and indeed raise the possibility of a continuum of functionally-related areas across nuclear boundaries (Van Kan et al., '93).

The possibility of a functional continuum across nuclear borders has also been postulated based on examination of the distribution and length of parallel fibres. Parallel fibres can stretch for up to 6mm across the cerebellar cortex (Mugnaini, '83) activating a beam of Purkinje cells which provide input to the somatotopic maps in the deep nuclei. This beam is long enough to not only to span the mediolateral extent of a nucleus (from which a role in co-ordination across myotomes has been suggested), but also to stretch across nuclear borders, co-ordinating the modes of control of a particular movement between separate nuclei into more complex co-ordinated acts (Thach, '92).

Oculomotor areas in the deep cerebellar nuclei have been recognised for some time. The best-known example is the fastigial oculomotor region of Noda et al. ('88). Units in the caudal fastigial fire in relation to horizontal saccades (Robinson et al., '93) and vergence/ near response eye movements (Zhang and Gamlin, '96). The caudal fastigial has been shown to have appropriate connections with the superior colliculus (Rat: Kurimoto et al., '95. Cat: Rolodan and Reinoso-Suavez, '81; Hirai et al., '82; Kawamura et al., '82; Sugimoto et al., '82. Rabbit: Uchida et al., '83; Grey squirrel: May and Hall, '86. Monkey: Gonzalo-Ruiz et al., '88; May et al., '90) and the supraoculomotor area (May et al., '92), a vergence-related midbrain region which projects to the medial rectus subdivision of the oculomotor nucleus and the abducens nucleus (Maciewicz et al., '75; Maciewicz and Spencer, '77; May et al., '87). Smooth pursuit-related neurons are also found in the fastigial oculomotor area (Fuchs et al., '93).

A second discrete eye movement region was recently described in the ventrocaudal posterior interposed and adjacent dentate nuclei (Van Kan et al., '93). Cells within these areas also show saccadic and vergence eye movement relations. However, in the posterior interposed, saccadic activity is related preferentially to *vertical* eye movements

(Robinson et al., '96) and the *far* response (Zhang and Gamlin, '94). The physiological observations on PIP units are supported by their anatomical connections with the superior colliculus and the supraoculomotor area (see above citations).

1.5.2 Anatomical connections

The main neuronal population of the deep nuclei consists of multipolar neurons of different sizes, with long ramifying dendrites and an axon that leaves the cerebellum via the superior cerebellar peduncle, uncinate tract or the juxtarestiform body. The cerebellar nuclei differ from one another in the targets of their efferent projections; indeed, to some extent, even minor parts of a single nucleus show differences in this respect. In general, however, each of the nuclei project to motor areas of the brain, either directly or by way of via relays in the thalamus. The majority of the work performed on the cerebellar efferent systems has been performed on the nucleo-thalamic projections, and details of its continuation to the motor cortex. This section on the nuclear efferents will therefore begin with what is known about this system, before moving on to the additional outputs of the nuclei to the red nucleus, brainstem and spinal cord. The following section will cover details on the collaterals arising from nuclear efferents which form feedback loops onto the precerebellar nuclei and the cerebellar cortex itself.

1.5.2.1 Extracerebellar projections

a) The nucleo-thalamic projection

The thalamus is the gateway to the neocortex, and virtually all routes to the cortex are relayed by the thalamus. The thalamus can be divided on the basis of connectivity and embryological origin into three main divisions, the dorsal thalamus, the ventral thalamus and the epithalamus. The dorsal thalamus, which is the largest division, has massive reciprocal connections with the cerebral cortex, and the output of the cerebellum is directed to subnuclei found in this tier. Neither the ventral thalamus nor the epithalamus innervate the cortex.

Within the ventral tier of the dorsal thalamus lies the ventrolateral nucleus. This nucleus is so dominated by cerebellar input that is has been termed as the "cerebellar nucleus of the thalamus". Within it, there is a cytoarchitectonically unique cell-sparse region in which fibres arising from the dentate, interposed and fastigial terminate. The cell-sparse

region consists of the subnuclei ventral posterolateral nucleus, pars oralis (VPLo), ventral lateral nucleus, caudal division (VLc), ventral lateral nucleus, pars postrema (VLps), nucleus X (Olszewski) and extensions of these between the cell clusters of nucleus ventral lateral, oral division (VLo) and the central lateral nucleus of the intralaminar complex (Olszewski, '52; Asanuma et al., '83). VPLo, Vlc and VLps project to area 4 of the motor cortex (Schell and Strick, '83; Orioli and Strick, '89). The nucleus X projects to lateral area 6, the periarcuate area. The thalamic termination zones from each of the deep cerebellar nuclei coincide within the cell-sparse region, although there are differences in the topography and strengths of their projections. The dentate and interposed nuclei have the heaviest projections (dentate stronger than the interposed) to the whole width of the contralateral cell-sparse region - the fastigial provides only a weak projection which is bilateral, restricted, and appears not to include X.

Although the dentate and interposed project to the same thalamic nuclei, double label studies (Asanuma et al., '83b) have indicated that the nucleo-thalamic projections interdigitate rather than converge onto the same cell. Indeed, the dentato-thalamic terminations are arranged as anteroposteriorly elongated rods, whilst those from the interposed form isolated patchy clusters of label which occupy distinct semilunar planes. The fastigio-thalamic projection is weaker and smaller than that from the dentate or the interposed: terminals are distributed bilaterally within a restricted region of the cell-sparse zone of the ventral lateral complex and in the central lateral nucleus of the intralaminar complex. The topography of the fastigio-thalamic projection is similar to that from the interposed, forming clusters of terminals in lamellae.

Inputs to the thalamus from the cerebellum do not converge with those from the dorsal column nuclei, pallidum or substantia nigra, and the nuclei in which these areas terminate project to different cortical regions. Spinothalamic and vestibular projections to the thalamus do, however, partially overlap with those from the cerebellum in the cell-sparse zone (Asanuma et al., '83c).

The somatotopies present in the deep cerebellar nuclei and the cerebellar thalamus are maintained through the nucleo-thalamic pathways. Within each of the deep nuclei there is a complete representation of the body: the head is found caudally, hindlimb rostrally, trunk medially and extremities laterally. The precision of the projections to the thalamus

produces one map of the body surface in the cell-sparse region, with the head medial, hindlimb lateral, trunk dorsal and extremities ventral. This is additionally supported by data on the thalamo-cortical projection (Woolsey et al., '51; Strick, '76; Asanuma et al., '83a).

b) The nucleo-rubral projection

The red nucleus lies in the midbrain, at the level of the superior colliculus and the substantia nigra. It is split into a caudally located magnocellular and rostral parvicellular divisions (Massion, '67), which have different afferent and efferent connections with the rest of the brainstem and brain. The sole projection of the parvicellular red nucleus is to the ipsilateral inferior olivary nucleus (Courville and Otabe, '74), whilst the magnocellular division projects to several brainstem sites and to interneurons in the spinal cord, thereby giving rise to the rubrospinal tract (Miller and Strominger, '73). Electrophysiological differences between these divisions support their separate anatomical connections: the parvicellular division has low frequency or no spontaneous discharge and responded weakly or not at all during a variety of sensory and motor tasks. This is in marked contrast to the responses of the magnocellular division. Neurons in this area discharge vigorously during movements of the contralateral limbs (Kennedy, '86), thereby agreeing with the presumed role of the rubrospinal tract in the control of limb movements (Ghez, '75; Ghez and Kubota, '77; Kuypers, '82).

The magnocellular red nucleus (RNm) had a clear somatotopy within it (Ghez, '71; Kuypers, '81; Gibson et al., '85a; Robinson et al., '87), such that the ventrally situated cells discharge during hindlimb movements and dorsally situated cells discharge during forelimb movements. In addition, there is also a dorsolateral column of cells, most of which are related to face movements (Kennedy, '86). Electrophysiological (Kennedy, '83; Gibson et al., '85a, b) and anatomical studies (McCurdy et al., '84; Robinson et al., '86) have shown that the RNm has an important role to play in the control of fine hand and finger movements, especially those that operate the fingers and wrist co-operatively to move the hand in a controlled fashion.

The magnocellular red nucleus also plays an important role in the ability of the inferior olive to act as a somatic event detector via a collateral system from the rubrospinal tract

to the rostral DAO (Weiss, '85; Robinson et al., '86). During an active movement, rubral neurons discharge in bursts, beginning just before the onset and ending before the offset of that movement. During that time, the rubral collateral system produces no inhibition of the olive, so that the cutaneous responsiveness of its cells are optimally sensitive. At the end of the movement, however, a powerful stimulus train which inhibits the olive and depresses its cutaneous responses ensures that they do not respond to "expected" sensory innervation such as placing the paw down (Gellman et al., '83, '85; Gibson et al., '87). A parallel form of direct olivary inhibition may occur via the nucleo-olivary pathway (see below).

The bulk of the input to the red nucleus arises from the cerebellum - strong topographical projections arise from the contralateral anterior and posterior interposed nuclei and dentate nucleus (Courville, '66; Angaut, '70; Flumerfelt et al., '73; Kalil, '82; Robinson et al, '82; Asanuma et al., '83c). The fastigial does not project to the red nucleus.

Fibres from both the dentate and interposed leave the cerebellum together via the superior cerebellar peduncle, decussate and terminate in the red nucleus. Dentato-rubral and interposito-rubral terminations are different however. The dentate nucleus projects only to the parvocellular red nucleus, whereas the interposed nuclei terminate in the magnocellular division (Asanuma et al., '83c; Walberg and Dietrichs, '86). Although Asanuma et al. did not distinguish between the anterior and posterior divisions, they commented that the caudal part of the interposed projected dorsomedially, and the rostral part ventrolaterally in the RNm. The Walberg and Dietrichs study in the cat ('86) did distinguish between the two interposed nuclei, and they found that fibres from the posterior division of the interposed actually terminate throughout the red nucleus, in both the parvocellular and magnocellular divisions. The posterior interposed-red nuclear projection does not follow a detailed topography - both rostral and caudal levels of the PIP project to the same areas at the medial edge of the red nucleus, which in the cat contains limb-related cells. The projection from the anterior interposed is restricted to the magnocellular division and shows a clearer topography: caudal AIP projects dorsomedially in the red nucleus, rostral levels ventrolaterally; medial areas project caudally and lateral areas rostrally.

The topography of the projection from the anterior interposed to the red nucleus maintains the somatotopy in each, as is the case in the nucleo-thalamic projections described previously. The sensory map in the rostral DAO (achieved via topographical projections from the spinal cord, dorsal column nuclei and trigeminal system) is in register with the motor map in the anterior interposed, which it contacts both indirectly via the cerebellar cortex and indirectly via the climbing fibre collateral system. The output of the anterior interposed onto the magnocellular red nucleus preserves this somatotopy, such that the motor maps in both the deep cerebellar nucleus and the red nucleus are also in register. Thus, limb-specific sensory regions in the DAO project upon limb-specific motor regions in the magnocellular red nucleus via the cerebellar cortex or climbing fibre collaterals to the AIP (Gellman et al., '83, '85; Robinson et al., '86; Gibson et al., '87).

c) The nucleo-collicular projection

The superior colliculus is a laminated structure in the roof of the midbrain. Although the superficial layers of the colliculus are purely visual, the deeper ones are polysensory and they differ in their anatomical routes to the cerebellum. The colliculus not only projects to the cerebellum, but its intermediate and deeper layers receive input from the deep cerebellar nuclei (Rat: Kurimoto et al., '95; Cat: Rolodan and Reinoso-Suavez, '81; Hirai et al., '82; Kawamura et al., '82; Sugimoto et al., '82; Rabbit: Uchida et al., '83; Grey squirrel: May and Hall, '86; Monkey: Gonzalo-Ruiz et al., '88; May et al., '90).
Cells in these layers of the colliculus play a role in the generation of saccades. Although following lesions of the superior colliculus, saccades are basically intact, there are subtle defects of latency and accuracy (Wurtz and Goldberg, '72), and it seems to be essential for short-latency saccades (Schiller, '87). Saccades are spatially coded across the rostrocaudal length of the superior colliculus: the amplitude and direction of the saccade depends only on the site of the stimulation, not the properties of the stimulus itself (Robinson, '72; Schiller and Stryker, '72). Stimulation at the rostral end of the colliculus, in which the perifoveal visual field is represented, elicits small saccades, whereas more caudally, where the entire visual field is represented, stimulation elicits larger saccades (Robinson, '72).

The frontal eye fields, which also have a saccade-related spatial map distributed across the banks of the arcuate sulcus project topographically to the superior colliculus, with the two maps in each being in register - the ventrolateral areas in the FEFs generating small saccades project to rostral levels of the colliculus, which contains representation of the perifoveal visual field and produces small saccades upon stimulation (Stanton et al., '88). Lesions to the superior colliculus and the frontal eye fields combined decimate saccades (Schiller et al., '80).

Fibres from the caudal fastigial terminate bilaterally in intermediate layers at the rostral edge of the colliculus. The visual map at that level represents the perifoveal visual field and stimulation there generates small saccades. It was therefore surmised that this pathway is used to control the metrics and latency of the small saccades animals must make to retain accurate foveation or during corrective saccades - eye movements made during large gaze shifts, without recomputing the target error (Becker and Fuchs, '69). Projections from the posterior interposed and dentate terminate contralaterally in the intermediate and deep layers over the entire length of the colliculus. As stimulation here elicits large saccades, the PIP/dentate-collicular pathway is regarded as controlling the larger, scanning saccades employed to foveate a new target of interest. In support of this idea on the nucleo-collicular projections, lateral-eyed animals with limited binocular vision have a sparse, if not non-existent, fastigio-tectal pathway. The PIP/dentate projection has been seen in every species studied so far.

Overlap of the two nucleo-collicular pathways occurs only at the rostral edge of the colliculus (May et al., '90). Consonant with their role in saccadic control, the PIP/dentate area do not project to the magnocellular red nucleus which contains head and limb but no eye movement-related neurons (Stanton et al., '80; Kennedy et al., '86; Gibson et al., '85a). The ventral dentate additionally projects to regions of the thalamus that are connected to the FEFs (Stanton '80; Stanton et al., '88).

The PIP/dentate input to the colliculus appears to arise as a unitary projection, leading May and his colleagues to suggest that any boundary between the two nuclei is arbitrarily imposed by passing axons, rather than a strict delimitation to the cell groups.

d) The nucleo-spinal projection

Direct projections from the deep nuclei to the spinal cord have been reported for a number of species (Cat: Fukushima et al., '77; Matsushita and Hosoya, '78; Wilson et al., '78; Tree shrew: Ware and Mufson, '79; Monkey: Batton et al., '77; Asanuma et al., '83a). Both the interposed and the fastigial project to the spinal cord. The fastigial projects directly onto motoneurons in the upper cervical segments, whereas the interposed projects onto interneurons, suggesting that the fastigiospinal and the interpositospinal pathways may have different functions. There have been no reports of the dentate nucleus projecting to the spinal cord.

e) Brainstem projections

The powerful nucleo-olivary projection is described in section1.5.2.2a.
The presence of direct projections from the deep cerebellar nuclei to the oculomotor nuclei is still being disputed. Many of the anterograde tracing studies also included the vestibular group 'y' in their dentate injections or lesions, and this portion of the vestibular complex is known to project to the oculomotor nucleus (Stanton, '80). More recent WGA-HRP studies (May et al., '92) have indicated direct projections from the deep cerebellar nuclei to the midbrain near-response regions in the macaque. The ventrolateral PIP and the fastigial project bilaterally to this region, including the supraoculomotor area, which is known to project to the medial rectus subdivision of the oculomotor nucleus and the abducens nucleus (Maciewicz et al., '75; Maciewicz and Spencer, '77; May et al., '87).
The rest of the non-olivary brainstem projections arise solely from the fastigial nucleus. The efferents of the fastigial leave via one of a number of routes: projections from caudal fastigial cross in the cerebellar midline, in part thereby passing through the opposite fastigial. They form the hook bundle of Russell (uncinate fasciculus) which loops around the superior cerebellar peduncle, and, via the inferior cerebellar peduncle, reaches the medulla oblongata. There are additional direct (uncrossed) projections to the medulla oblongata. The fastigio-brainstem projections terminate in the medial medullary reticular formation which gives rise to the reticulospinal tract. The fastigial

also influences muscles of the neck and back via connections with the medial and spinal vestibular nuclei and the medial vestibulospinal tract.

In addition, the fastigial projects to brainstem visuomotor systems, such as the superior colliculus (see above) and other saccadic brainstem areas - the paramedian reticular formation (PPRF) and the rostral interstitial nucleus of the medial longitudinal fasciculus (riMLF). The PPRF is essential for the generation of all saccades, as it contains a specific group of neurons providing the immediate premotor signals for saccades to the ipsilateral side. The riMLF is the immediate premotor structure for vertical saccades. A recent study by Gonzalo-Ruiz ('88) suggested that the fastigial also has direct connections to the extraocular motor neurons themselves.

The fastigial also projects bilaterally to the central grey, the parasolitary nucleus, the raphe nucleus and the nucleus of the locus coeruleus.

1.5.2.2 Nuclear projections to precerebellar nuclei and cerebellar cortex

All efferent fibres from the cerebellar nuclei pass to extracerebellar targets. However, many or all of these projections supply collateral projections to a number of pre-cerebellar nuclei and/or to the granular layer of the cerebellar cortex. In addition, so-called recurrent collaterals from the main axon project back into the nuclear area from which they originally arose.

a) The nucleo-olivary projection

The projection from the deep cerebellar nuclei to the inferior olive reciprocates the olivo-nuclear collaterals from climbing fibres heading for the cortex (Achenbach and Goodman, '68; Dom et al., '73; Graybiel et al., '73; Martin et al., '75, '76; King et al., '76; Beitz, '76; Brown et al., '77; Buisseret-Delmas and Batini, '78; Kalil, '79; Brodal and Kawamura, '80; Sugimoto et al., '80; Mizuno et al., '80; Dietrichs and Walberg, '81, '85, '86, '89; Dietrichs et al., '85; Ikeda et al., '89). Fibres leave the deep nuclei passing through and around the parvicellular part of the dentate in the rostral wall of the lateral recess. They ascend in the lateral angle of the IVth ventricle and enter the superior cerebellar peduncle to reach the brainstem. The main projection is predominantly contralateral. However, there are ipsilateral projections which mirror the

contralateral ones (rat: Brown et al., '77; Chan-Palay, '77; Angaut and Cicirata, '82; Swenson and Castro, '83a,b; cat: Beitz, '76; Dietrichs and Walberg, '81; monkey: Chan-Palay, '77; Kalil, '79).

The topography of the nucleo-olivary projection largely mirrors the parasagittal zonation evident in the cortico-nuclear projection (Beitz, '76; Tolbert, '76; Chan-Palay, '77; Kalil, '79; Brodal, '81; Angaut and Cicirata, '82; Courville, '83; Swenson and Castro, '83; Dietrichs and Walberg, '85, '86, '89; Dietrichs et al., '85; Billard et al., '89; Van der Want., '89). However, Dietrichs and Walberg ('79, '80, '81) have shown that in the cat, the nucleo-olivary pathway diverges somewhat from the classic reciprocal pathway, such that after an injection in a particular zone of the inferior olive, retrogradely labelled neurons often occurred not only within the corresponding cerebellar nuclear zone, but also, to some extent, within adjacent parts of the deep nuclei.

In general, the dentate nucleus projects heavily to the contralateral principal olive in a precise topographical pattern covering all lamellae in rat, cat and monkey. Likewise, the anterior interposed projects to the dorsal accessory olive and the posterior interposed to the rostral medial accessory olive. The presence of fibres from the fastigial to the olive have been disputed - a number of authors have no evidence for such a projection (Graybiel et al., '73; Tolbert et al., '76; Brown et al., '77; Buisseret-Delmas and Batini, '78; Brodal, '81; Haroian, '82), but others have observed a small bilateral fastigio-MAO pathway (Achenbach and Goodman, '68; Sugimoto et al., '80; Angaut and Circirata, '82; Dietrichs and Walberg, '81, '85, '87, '89; Ikeda et al., '89; Ruigrok and Voogd, '90).

Somatotopical representations are maintained throughout each stage of the olivo-cortico-nuclear pathway (Gibson et al., '87; Robinson et al., '87), and the precise topography of the bulk of the nucleo-olivary projections ensures congruence of the somatotopic maps in each nucleus.

Kitai ('75) stimulated the superior cerebellar peduncle, eliciting EPSPs in the inferior olive, suggesting it's an excitatory pathway. However, subsequent anatomical (Nelson, '84; Nelson and Mugnaini, '85; De Zeeuw et al., '88, '89a,b, '90) and electrophysiological (Andersson and Hesslow, '87) have indicated that the pathway is in

fact inhibitory. The olivocerebellar neurons may thus be inhibited by the cerebellar nucleo-olivary fibres, while disinhibition may occur through the Purkinje cells acting upon the nucleo-olivary fibres.

It should recalled that the inhibitory nucleo-olivary pathway is balanced out by the excitatory projections from the Nucleus of Darkschewitsch/tegmental tracts (which in turn receive input from the magnocellular red nucleus and the deep cerebellar nuclei) and the direct rubro-olivary pathway arising from the parvicellular division of the red nucleus.

b) Nucleo-pontine/NRTP

The NRTP is dominated by inputs from the deep cerebellar nuclei. The dentate and anterior interposed project heavily to the contralateral NRTP, while the projection from the fastigial is very sparse (Brodal and Szikla, '72; Brodal et al., '72; Angaut et al., '85). The areas of the NRTP which receive inputs from the deep nuclei contain relatively few neurons projecting to the cerebellar cortex, so that on the whole, the NRTP acts on other parts of the cerebellum than those whence it receives afferent fibres. This led Allen and Tsukahara ('74) to comment:

> "...rather than considering the NRTP as a relay in the cerebro-cerebellar pathway, we must consider that it is the relay in a cerebello-cerebellar loop that can be modified by the cerebral cortex...".

The fibres from the deep nuclei to the NRTP also send collaterals to the red nucleus (Kitai, '76).

Equally, the pontine nuclei receive inputs from the deep nuclei. Cerebello-pontine projections arise principally from the dentate and anterior interposed, although a smaller contribution from the fastigial has been suggested (Voogd, '64; Brodal et al., '72; Yuen et al., '74; Batton et al., '77).

c) Nucleo-cortical

The nucleo-cortical projection was first observed by Cajal in the rat (1895). The pathway has been extensively studied through a series of lesion, anterograde and retrograde tracing studies and electrophysiology, and its topography is now well understood. In the rat, cat and monkey, the substantial nucleo-cortical pathway is basically organised into three rostrocaudally orientated longitudinal zones (Tolbert et al., '76, '77; Chan-Palay, '77; Dietrichs and Walberg, '79; Gould, '79; Haines and Pearson, '79; Tolbert et al., '78b, '79; Yamada and Noda, '87) reciprocal to the vermal, pars intermedia and hemispheric cortico-nuclear projections. For the bulk of the projection in the rat and cat, there is good correspondence between the cortico-nuclear parasagittal zones and the nucleo-cortical projection. Using combined autoradiographic and HRP studies, Tolbert and Bantli ('79) showed that HRP-positive nucleo-cortical neurons lay in nuclear areas also overlain by a dense plexus of autoradiographic silver grains that resulted from the radioactive labelling of cortico-nuclear axons and their terminals. A number of other studies have additionally supported this finding (Chan-Palay, '77; Gould, '79; Haines and Pearson, '79; Dietrichs and Walberg, '79).

In spite of this strong reciprocity, the nucleo-cortical pathway is somewhat more diffuse than the cortico-nuclear projection due to the fact that the majority of nucleo-cortical fibres arise as collaterals of nucleo-fugal fibres (Tolbert et al., '76; Chan-Palay, '77; McCrea et al., '78; Dietrichs and Walberg, '79; Gould, '79; Haines and Pearson, '79; Tolbert and Bantli, '80; Tolbert, '82; Payne, '83) destined for the ventral lateral thalamus or the inferior olive. The Tolbert and Bantli study ('80) in particular indicates the presence of an intricately arranged network of bidirectionally and topographically organised cortico-nucleo-olivary feedback loops. In the monkey, this divergence of the nucleo-cortical pathway becomes even more apparent, and indeed, the majority of nucleo-cortical fibres arise from the dentate, regardless of the location of their termination (Tolbert et al., '78b). The data indicated that the organisation of macaque nucleo-cortical projections to the vermis, paravermis and lateral hemispheres arises principally from the dentate with secondary projections to the paravermis and vermis arising from the interpositus and fastigial respectively. In addition to this divergence, it appears that projections from a single injection site in the nucleus are not 'exclusive', in

that considerable overlap of terminals from neurons in different parts of the nucleus occurs in the cortex (Chan-Palay, '77). Occasionally nucleo-cortical axons project not only medially into the vermis, but also to non-specified areas of the hemispheres contralaterally (Dietrichs and Walberg, '79, '80; Dietrichs, '81). Haines ('88) double label study showed that a population of deep cerebellar nuclear cells project to spatially separated, yet possibly functionally related areas of ipsilateral cortex. Since larger and smaller somata were double-labelled it is possible that those cells with cerebellofugal processes to extracerebellar targets may simultaneously relay information to divergent cortical sites. Cells contralaterally however were small oval and fusiform, which may therefore be specifically involved in cerebelloolivary and olivocerebellar feedback loops.

In spite of small interspecies differences, it is commonly held that the nucleo-cortical pathway is comprised of "reciprocal, non-reciprocal and symmetrical" components (Buisseret-Delmas and Angaut, '88, '89). The reciprocal projections follow the zonal pattern of cortico-nuclear inputs. The symmetrical projections arise contralaterally from nuclear regions symmetrical to those giving rise to the reciprocal pathway. The non-reciprocal component is the most diffuse projection, arising from nuclear areas outside the cortico-nuclear projection.

Nucleo-cortical fibres either pass directly out of the nucleus and project individually towards the cortex or emerge from fascicles of the cerebellofugal axons travelling towards the cerebellar peduncles (McCrea et al., '78; Tolbert and Bantli, '80). The nucleo-cortical axon forms synaptic contacts within cortical glomeruli, most frequently with granule cells and more rarely with Golgi cells (Tolbert et al., '80).
Immunocytochemical studies (Chan-Palay et al., '79; Tolbert and Bantli, '80) suggest that the dentato-cortical pathway is inhibitory in nature, using GABA as a neurotransmitter. However, ultrastructural studies (Kultas-Ilinsky et al., '79; Tolbert et al., '80) indicate that in fact the nucleo-cortical synapses are of the asymmetric type and contain clear, spherical synaptic vesicles, which suggest that the contact is excitatory in nature (Uchizono, '69; Palay and Chan-Palay, '77). Lack of detail on the precise cortical termination patterns of the nucleo-cortical projection, and the affect of this input on the

target neurons naturally means that any theory on the functions of the nucleo-cortical pathway is somewhat speculative. However, a number of suggestions have arisen.

The nucleo-cortical pathway may regulate the output of the cerebellum and tend to modify any fluctuation in cerebellar nuclear activity, via an internal feedback system to the cerebellar cortex. Any increase in the cerebellar nuclei (via mossy and climbing fibre collateral input) would be reflected in an increase in activity in not only the output of the cerebellum but also in the nucleo-cortical pathway. The nucleo-cortical afferents would then act through Purkinje cell inhibition to temper the output of the cerebellar nuclei. Equally, nucleo-cortical input to the Golgi cells (which normally inhibit granule cells) would provide a source of recurrent disinhibition to the nuclear neurons.

The divergence of the nucleo-cortical pathway also allows it to be regarded as an internal path between olivo-cortico-nuclear zones and have some co-operative function, allowing cross-talk between functional modules.

However, the function of the nucleo-cortical pathway is liable to be much more complex than either of these models suggest, in view of the motor somatotopies evident in each of the deep cerebellar nuclei (Thach et al., '82; '92; '93; Van Kan et al., '93; Gibson et al., '96).

1.6 AIMS OF THE THESIS

It has been known for many years that the cerebellum is intimately involved in visuomotor coordination. Previous studies (Gibson et al., '77; Mower et al., '80; Robinson et al., '84; Glickstein et al., '94) have shown that it is only the posterior lobe of the cerebellum that receives visual information. The dorsal stream extrastriate visual cortices and the superior colliculus project to the cerebellum via mossy fibres from the dorsolateral pontine nucleus. The accessory optic system projects via the climbing fibre system from the dorsal cap and ventrolateral outgrowth of the inferior olive. The nucleus reticularis tegmenti pontis is also involved in the transmission of visual information from both cortical and subcortical visual areas to the cerebellar cortex.

This thesis is concerned with the anatomical connections of those parts of the posterior lobe of the macaque cerebellum which are known to receive to receive visual information. It will focus on the cortical projections to the deep cerebellar nuclei, each of which contains a motor map of the body. The use of the bi-directional tracer WGA-HRP allowed simultaneous examination of the functional olivo-cortico-nuclear modules, pontine/NRTP inputs and nucleo-cortical projection for each case.

To clarify the cerebellar links between visual and motor and oculomotor structures, the following questions were addressed:

i) Does the visual and oculomotor-related dorsolateral pons project to the flocculus?

ii) How is the olivo-cortico-nuclear parasagittal zonation represented in the monkey?

iii) Do cerebellar cortical projections overlap in the deep cerebellar nuclei?

iv) Is the nucleo-cortical pathway reciprocal to the cortico-nuclear projection?

2. MATERIALS AND METHODS

2.1 Principles of experimental techniques

2.1.1 The WGA-HRP method

Neurones transport material actively in both the anterograde and retrograde directions. Axonal transport forms the basis of many neuroanatomical and tracing techniques including the horseradish peroxidase method used in this series of experiments. Many macromolecules, including the plant glycohaemoprotein horseradish peroxidase (HRP) are actively endocytosed into by the axon terminal into endocytotic vesicles and transported retrogradely to the soma, as first demonstrated by Kristensson and Olsson (1971). HRP may be conjugated to the lectin wheat germ agglutinin, producing WGA-HRP (Gonatas et al., '79). The lectin has a specific affinity for n-acetyl-D-glucosamine and N-acetylneuraminic acid residues both of which are present in the neuronal plasma membrane. The lectin is thus bound to surface receptors in the neural membrane and when an endocytotic vesicle is formed at that part of the membrane, the lectin-HRP complex is bound within it. This process, which is known as adsorptive endocytosis (Gonatas et al., '79), occurs at low concentrations and appears to be relatively uninfluenced by neuronal activity (Stockel et al., '78). WGA-HRP has a number of advantages over the unconjugated form: most importantly, it is less diffusable than HRP, so injection sites are more readily confined to the area directly injected (see Staines et al., '80), and in addition, intact fibres of passage through the injection site do not take up and transport the lectin (Brodal et al., '83).

HRP and WGA-HRP can be demonstrated histochemically in all parts of the neurone. When HRP is combined with its substrate hydrogen peroxide (H_2O_2), it forms a specific complex HRP-H_2O_2. This complex has a low specificity for oxidising many compounds, including several chromogens such as tetramethylbenzidine (TMB) and diaminobenzidine (DAB). The chromogen, when oxidised, produces a dense, visible precipitate. The oxidation reaction is variable and some chromogens, such as TMB are oxidised far more readily than others, such as DAB, making them more sensitive. The

optimal hydrogen peroxide concentration was previously established in several trials, as evidence suggests that either too high or too low concentration of H_2O_2 may inhibit the reaction (Herzog and Fahimi, '73). A modification of the TMB method of Mesulam (1982) and Gibson (1984) was used throughout this study.

Labelled cells contain a varying amount of coarse and fine blue/black granules 0.5-1μm in diameter. Electron microscopy has shown that the granules are dense bodies distributed through all parts of the perikaryon, and that many of them lie in close association with the Golgi apparatus. Many positive cells are virtually filled with such granules, even to the peripheral dendrites, and their shape can be clearly recognised in sections with darkfield and/or polarised microscopy. Occasionally the peripheral part of an axon is also visualised. Fibres too are well filled and labelled, and the label extends to the terminal boutons. Caution has to be taken when studying HRP material not to confuse fibres cut in cross section with labelled terminal fields.

4% WGA-HRP was used in these experiments. There is no evidence to suggest that WGA-HRP travels retrogradely to label separate axonal projections. That is, if a neuron has collateral projections to two targets, one of which is included in the injection site, WGA-HRP will be transported back to the soma, but not down the additional collateral projection of that neuron (Mercier, '89), although this problem has been associated with the use of 3H-aspartate as a retrograde tracer (Wiklund et al., '84). In the anterograde direction, WGA-HRP will fill all axonal projections. At higher concentrations, post-labelling survival times and depending on where in the nervous system it is injected, WGA-HRP can travel trans-synaptically (Gerfen et al., '82; Itaya and Van Hoesen, '82; Martyn and Peschanski, '83; Schnyder and Kunzle, '83; Peschanski and Ralston III, '85), but this issue did not concern this particular study, due to the low concentrations used and relatively short survival time.

It has been reported that anterograde transport requires higher concentrations than retrograde, possibly because Purkinje cells are surrounded by neuroglial processes (Palay and Chan-Palay, '74) that inhibit pinocytic activity (Hedreed and McGrath, '77; Dietrichs and Walberg, '79).

2.1.2 The Zebrin method.

Studies using the retrograde-anterograde axonal transport of tracers, electrophysiological recording, somatotopic mapping and molecular mapping have all revealed a parasagittal bandlike topographical organisation of the cerebellar cortex and its efferent and afferent connections. Anti-zebrin I and II (Hawkes et al., '85; Brochu et al., '90) are two such molecular markers which are specific for, and label subsets of cerebellar Purkinje cells. The zebrin II monoclonal antibodies recognise the respiratory isoenzyme aldolase C (Ahen et al., '94; Hawkes and Herrop, '95), a single polypeptide, approximately 120 kDa in weight, which is distributed throughout the somata, dendrites and axons. Electron microscopy shows that the immunoperoxidase reaction product is intracellular and cytoplasmic, and extends throughout the axon into its collateral branches and terminal boutons.

Those Purkinje cells which are immunoreactive (the proportion of which varies from lobule to lobule) are clustered together to form a family of rostrocaudally directed parasagittal bands throughout the cerebellar cortex which are arranged symmetrically either side of the midline. Expression of the epitope is not all-or-nothing, but in the rat, at least seven major zebrin I positive (known as P+) bands have been identified in each hemisphere (Hawkes and Leclerc, '85).

Zebrin II has the same distribution as zebrin I, but has the advantage of being expressed in numerous species including fish, birds and mammals, whereas zebrin I immunoreactivity is confined to only some mammals.

Zebrin II was employed in this study.

The standard "sandwich" method of immunocytochemistry is employed in zebrin studies. The tissue section is incubated with primary antibody (anti-zebrin I or II), then a biotinylated secondary antibody which recognises the primary antibody and introduces biotin into the section at the location of the primary antibody. An avidin/biotinylated enzyme complex (in this case peroxidase) is added, introducing the enzyme into sections at the site of the antigen. Finally, the section is exposed to an appropriate substrate (DAB) for the enzyme in the complex. The resultant reaction produces an insoluble coloured reaction product at the location of the enzyme and thus the antigen

can be easily visualised in the tissue section. This technique produces a sensitive and highly specific labelling of zebrin positive Purkinje cells.

2.1.3 Material for cytoarchitectonic study

Different histological procedures produce final material of variable quality. The fixation methods necessary to preserve the enzymatic activity of WGA-HRP, for example, do not produce high quality material for routine histological examination. For this reason, some material was prepared in order to identify cell groupings and specific nuclei in the brainstem and cerebellum using a standard Nissl (cresyl violet) stain.

2.2 Surgery

Anaesthesia was identical in all cases. Each animal was premedicated by an intramuscular injection of Ketamine hydrochloride (5 mg per kg of body weight) and prepared for sterile surgery. Surgical anaesthesia was initiated (12 mg per kg of body weight) and maintained by intravenous injection of sodium pentobarbitone. The animal was held stable with a head holder. Body temperature and response to pain were monitored throughout.

The monkeys were shaved and draped for cerebellar exposure. A long mid-sagittal incision was made from the occipital protuberance to the 1/2 cervical spinal segment. Muscle and soft tissue were scraped and insertions cut to retract all soft tissue bilaterally. A bone incision was made with rongeurs, starting at the foramen magnum and extended rostrally and laterally to expose the posterior lobe of the cerebellum. Bone and tissue bleeding were controlled appropriately. Mannitol (ca. 60cc) was injected over 20 minutes and, if necessary, the cerebellum retracted on one side to expose the floccular complex beneath the paramedian lobe. Small arachnoid incisions were made to ease injection. Injections of between 70 and 200 nl of 4% WGA-HRP (see appendix) were made under visual guidance via a bevelled Hamilton syringe. Occasionally a small amount of bleeding was caused by the needle's entry into the folium.

The tissue was sutured in anatomical layers, and the animal closely monitored for 48 hours.

All surgery was performed by Prof. Mitchell Glickstein. I assisted during all cases except Pyr1, UV1, UV2, dpf1 and 696. A number of cases were performed at the National Institutes of Health in Bethesda, MD, and assistance was additionally provided by Drs. Miles and Krauzlis in these instances. Further details on the surgery and amount of WGA-HRP injected in each particular case can be found in the Appendix.

2.3 Perfusion

2.3.1 Perfusion of WGA-HRP animals

Fixation influences the sensitivity of the HRP method and prolonged exposure to aldehydes decreases the enzyme activity of HRP (Courville and Saint-Cyr, '78; Rosene and Mesulam, '78; Mesulam, '82). In the present series of experiments, aldehyde exposure was limited to 20 minutes. In addition, rather than using the glutaraldehyde/paraformaldehyde mixture (Mesulam, '82), only a 4% paraformaldehyde fix was used, which has been shown to reduce the patchiness of the fixation (Mercier, '89). The method has produced consistently good preservation of both tissue and WGA-HRP activity.

Following a 48hr post-operative survival period, the animal was terminally anaesthetised with sodium pentobarbitone (Sagatal 150mg/kg). The chest cavity was then exposed and a cannula placed in the left ventricle of the heart, guided up towards the aorta and held in place with a haemostat. The right atrium was cut to allow the escape of fluids. The animal was then perfused with 2 litres of 0.9% saline solution containing 1000 units of heparin at 37 °C, followed by 4 litres of 4% paraformaldehyde in 0.1M phosphate buffer, pH 7.4 at room temperature. The fixative was then washed out by perfusion with 2 litres of 10% sucrose followed by 2 litres of 20% sucrose in phosphate buffer, pH 7.4, both at 4°C. All fluids were perfused at a flow rate of 130 ml per minute.

The brain was removed and stored overnight in 20% buffered sucrose at 4°C.

2.3.2 Zebrin

The antigen recognised by the monoclonal antibody used in the Zebrin procedure is not susceptible to damage from particular fixation techniques. As a result, brain tissue that had been perfused with a variety of fixatives such as paraformaldehyde and buffered formalin were used. In all cases, the fixed tissue was rinsed with gentle agitation in 20% buffered sucrose overnight before it was used.

2.4 Histological techniques

2.4.1 WGA-HRP

Following 24 hours immersion in 20% buffered sucrose, the brains were prepared for histological processing. In some cases, the entire cerebellum and brainstem were embedded in gelatin before sectioning. In others, the cerebellum and brainstem were separated by cutting through the cerebellar peduncles. The cerebellar block was embedded in gelatin, the brainstem was not. Frozen sections were cut either transversely or parasagittally at 50 μm, removed with a camel hair brush and placed into 0.1M phosphate buffer chilled to 4°C. Every fifth section (i.e. every 250 μm) was processed using a modified TMB method (Mesulam, '82; Gibson, '84). A parallel set of sections were saved for cytoarchitectonic study. In addition, through the injection site, a third set of sections were collected for reaction with the DAB method.

The TMB method was modified so that all reaction solutions were chilled to 4°C. The histochemical reactions were allowed to proceed at this temperature for an interval of 40 minutes. The reaction solutions were replaced by fresh solutions every 10 minutes, thus preventing an accumulation of precipitated ferricyanide crystals on the tissue; for the same reason the nitro ferracyanide was used at a concentration of 90 mg per 100ml. These modifications resulted in material with low background artefact and high sensitivity. Following the reaction, sections were mounted onto subbed slides from 0.025M acetate buffer. Mounted sections were dehydrated quickly in alcohols of increasing concentrations, cleared in xylene and coverslipped using the DePX mounting medium. Detailed protocols of the WGA-HRP method - both TMB and DAB are given in the appendix.

2.4.2 Zebrin

The zebrin reaction consists of the standard "sandwich" technique of immunohistochemistry as previously described. All rinsing and immunoreactive solutions contain the detergent Triton in tris buffer pH7.6, at a concentration 5mls of Triton per litre of tris buffer. The detergent attacks the integrity of the neuronal plasma membrane and eases the entry of the immunoreactive fluids into the Purkinje cells,

thereby increasing sensitivity. Sections were incubated in mabQ113 at room temperature with gentle agitation for 12-24 hours, rinsed and moved into incubation in the secondary antibody, biotinylated anti-mouse, for 1-2 hours with gentle agitation. Following another rinse, the sections are reacted with an immunoperoxidase kit and then reacted according to the DAB protocol (see Appendix). The sections are rinsed, mounted onto subbed slides are allowed to dry overnight. The sections are dehydrated by passing them through a series of alcohols, cleared in xylene and the slides coverslipped using DePX mounting medium.

The monoclonal antibody mabQ113 used in these experiments was generously supplied by Dr. Richard Hawkes.

2.4.3 Cytoarchitectonic material.

A set of sections immediately adjacent to those reacted according to the TMB and DAB protocols were saved (every 250 μm), mounted onto subbed slides and allowed to dry overnight for staining with a Nissl stain. The dried sections were dewaxed in xylene, hydrated in graded alcohols and stained with cresyl violet; dehydrated, cleared in xylene and coverslipped using DePX mountant.

2.5 Analysis of data

2.5.1 WGA-HRP material plotting procedure

Sections from animals used for the study of retrograde and anterograde transport and sectioned in the coronal plane were plotted on an XY plotting system connected to a Leitz orthoplan microscope with precision potentiometers. Sections were viewed under alternately bright field (cross polarised illumination), and polarised light to confirm the presence of either labelled cells or terminals. Polarised light vibrates in a single plane. A cross polarised filter thus extinguishes polarised light. The TMB reaction product rotates the plane of polarised light and causes the TMB precipitate to reflect brightly against a dark background.

The section was outlined with point dots on the XY plotting pad, then the labelled cells were marked with a red dot, viewed under a x40 objective lens and x10 oculars. Orthogradely transported WGA-HRP was also marked on the same plots. The Nissl-stained sections and compatible plots were then transferred to a Wild M8 stereomicroscope with a drawing tube attachment. The magnification was adjusted to match the XY plots and the outline of each section filled in, together with major fibre tracts and nuclear groups as shown in the cresyl violet stained sections. Areas of terminal label were scrutinised by adjusting the level of polarisation to check for labelled cells embedded within them.

The plots with cellular and label detail were then height-matched with a group of standardised drawings of the brainstem and cerebellum, derived from the Nissl stained cases and comparison with previous studies on nuclear detail (Nyby and Jansen, '42; Courville and Cooper, '80; Madigan and Carpenter, '71). The use of closely correlated standardised drawings of the data allow for easier comparison between different cases.

There are no universally agreed criteria for determining the effective uptake area of WGA-HRP (Jones, '75). Sections through the injection site had been reacted with DAB and the more sensitive TMB chromogens - in each case, the halo of lighter TMB label extended slightly beyond the region of dark brown staining as seen with the DAB method. Sections through the primary injection site from each experiment were plotted using the drawing tube attachment on the Wild M8 stereomicroscope. For illustrating injection sites, both TMB and DAB processed sections are plotted. There is evidence

both for and against the occurrence of uptake from the region of the halo (Dursteler et al., '77; Bernard, '77). I used the clearly marked edges of the brown reaction (Jones and Hartman, '78) as the estimate of the effective injection site.

As described in the introduction, there has been some controversy on the borders of the constituent parts of the "floccular complex". In this series of studies, I used the posterolateral fissure as the division between the flocculus and ventral paraflocculus (Gerrits and Voogd, '89). Thus, the caudal six folia of the floccular complex are the flocculus proper. Those more rostrally, lying beneath the anterior lobe, are the ventral paraflocculus.

2.5.2 Reconstructions

Labelled cells and terminals were carefully transferred from the plots onto the set of standards described in section 2.4.3. The drawings of the injection sites (TMB and DAB) were carefully reconstructed to produce surface drawings of the extent of each injection site, using borders of folias, fissures and comparison with Madigan and Carpenter's atlas of the cerebellum of the Rhesus monkey (1971).

3. RESULTS

3.1 WGA-HRP studies

Extents of injection sites were derived from camera lucida drawings of TMB and DAB reacted sections of the cerebellar cortex and reconstructed to form a surface view. TMB and DAB estimations of the injection sites compare well in each case. Each injection site was focused within cortical layers, and the density of the granular layer restricted diffusion of the WGA-HRP over a large area. Purkinje cells were assumed to contribute to the injection site if they were heavily labelled and labelled axons could be seen emanating from their somata following TMB histochemistry. Purkinje cells in the lighter halo beyond the centre of the injection site could therefore be discounted. The extent of the injection site as demonstrated with DAB histochemistry correlated closely with that suggested by the dark centre of TMB-reacted sections. Surface reconstructions of injection sites were thus based upon the injection site demonstrated by the inner dark centre of the TMB reacted sections.

Anterogradely labelled terminals in the deep nuclei and retrogradely labelled cells in the inferior olive and pontine nuclei were all plotted using a microscope stage fitted with an XY potentiometer. The plots of the sections were then matched to cresyl-violet stained sections using a Wild microscope with a variable objective, and the cellular detail and important landmarks were added to the drawings.

The deep nuclei compared very well to Courville and Cooper's description (1970), and as a result, the terminal label were matched to their standard drawings of the nuclear subdivisions (500μm apart). Olivary and pontine label, however, was transferred onto our own standard drawings derived from Nissl stains from one of the cases (250μm apart). The use of standard drawings facilitated comparison between cases in the vermis, pars intermedia and hemispheres of the cerebellum.

The positions of retrogradely labelled cells in different subdivisions of the inferior olive for each case were noted, compared to previous studies on the olivocerebellar projection in the other mammals (Groenewegen and Voogd, '77, '79; Brodal and Brodal, 81, '82), and

allowed determination of the type and number of cerebellar cortical zones that had been included in each injection site.

The figures included in each experimental chapter follow the same format. For each case, figures summarising the data on the olivocorticonuclear projection are presented first. Each of these figure contains a surface reconstruction of the injection site, a coronal or sagittal section through the greatest extent of the injection site as estimated using TMB and DAB histochemistry and serial sections through the inferior olive and deep cerebellar nuclei including the position and density of labelled cells and terminals respectively.
Data on the NRTP/pontocerebellar projections are presented on figures containing a surface reconstruction and coronal/sagittal section of the injection site and serial sections through the NRTP and pontine nuclei (600 μm apart) which include the position and density of the retrogradely labelled cells.
In all figures one dot represents one cell. Strength of terminal label is demonstrated by the density of stippling.

It should be borne in mind that the surface reconstructions of injection sites do not present the most lateral edges of the hemispheres, since the edges of the cortex fold over to form the ventral surface of the cerebellum, and are covered by the folia of the dorsal and ventral paraflocculi.

3.1.1 VERMIS

3.1.1.1 Lobule VII

Case M1-96

Injection site

See figures 6 and 7.

The injection site covered vermal sublobules VIIa and b. There was very faint labelling of the white matter just lateral to the true injection site in the TMB-reacted sections. However, close scrutiny of the sections, comparison with DAB-reacted tissue and correlation with the olivary label suggested that these fibres did not contribute to the actual injection site.

The olivo-cortico-nuclear projection

The olivary label was bilateral and principally confined to the cMAO, in which labelled cells were found in its mid-mediolateral span. The label was very dense and extensive, covering the caudal 40% of the nucleus. Subnucleus β and the dorsomedial cell column both contained labelled cells at their rostral levels.

The cDAO contained a sparse, but discrete population of labelled cells.

Overall, these results indicate that the injection site covered zone A1-A3, with a smaller contribution from zone B.

Labelled fibres emanating from the injection site could be clearly seen descending ventrally to terminate as a dense band in the caudo-ventral half of the fastigial nuclei bilaterally (only right side deep cerebellar nuclei shown in figure 6). The fastigial nucleus corresponds to zone A.

At the more rostral levels of label (mid-fastigial), the terminal fields were restricted to the medial aspect of this nucleus, and more caudally, this terminal field was interrupted by an area free from terminal label. At these levels, the two patches of terminals in the ventral fastigial curved to form adjacent U-shaped fields which were closely opposed but never overlapped. The caudal areas of the fastigial label also contained a patch of labelled

terminals in the dorsal part of the nucleus. The area between the two patches of terminal label was free from WGA-HRP.
The caudo-medial area of the anterior interposed contained a faint but discrete terminal field. The anterior interposed label corresponds to the cerebellar C1 zone.

NRTP/Pontocerebellar projection

Labelled cells were found bilaterally throughout almost the entire length of the pons and NRTP. Only the most rostral and caudal levels of the pontine nuclei were devoid of label.

Labelled cells in the pontine nuclei clustered to form two main groups, although other smaller collections of cells were also recorded. The largest collection of cells was located dorsolaterally, throughout almost the entire rostrocaudal span of the pontine nuclei - only the most rostral and caudal levels contained no labelled cells. The other significant group was seen dorsomedially in the rostral half of the pontine nuclei.
The additional smaller pontine cell groups were found in the dorsopeduncular nucleus in the caudal half, beginning at the level at which the dorsomedial cell group disappeared. The rostral half of the pontine nuclei contained small collections of cells, running around the ventral surface of the pontine nuclei and in between the fascicles of the CST.
All pontine label was evident bilaterally.

The NRTP contained two distinct clusters of retrogradely labelled cells which remained discrete throughout the length of the NRTP. The larger group of cells was located in the dorsolateral corner of the NRTP; the smaller group was located in the dorsomedial division of the nucleus. Both groups were evident bilaterally throughout the rostrocaudal length of their respective nuclear areas.

The nucleo-cortical projection

Retrogradely labelled cells in the deep cerebellar nuclei were encountered bilaterally in the fastigial nucleus. The majority of labelled cells in the deep nuclei were found rostrally within this nucleus, and indeed, approximately half of the labelled cells were located considerably rostral to the first levels of terminal label. At rostrocaudal levels of the

fastigial that contained terminal label, some cells were located within the terminal fields, although an equal number were situated dorsal to the anterograde label.

A few cells were found scattered randomly in the ventral portion of the rostral posterior interposed and medially in the mid-levels of the dentate. These cells were only found unilaterally on the left hand side.

There were no consistent differences in cell sizes between reciprocal and non-reciprocal cortical afferents.

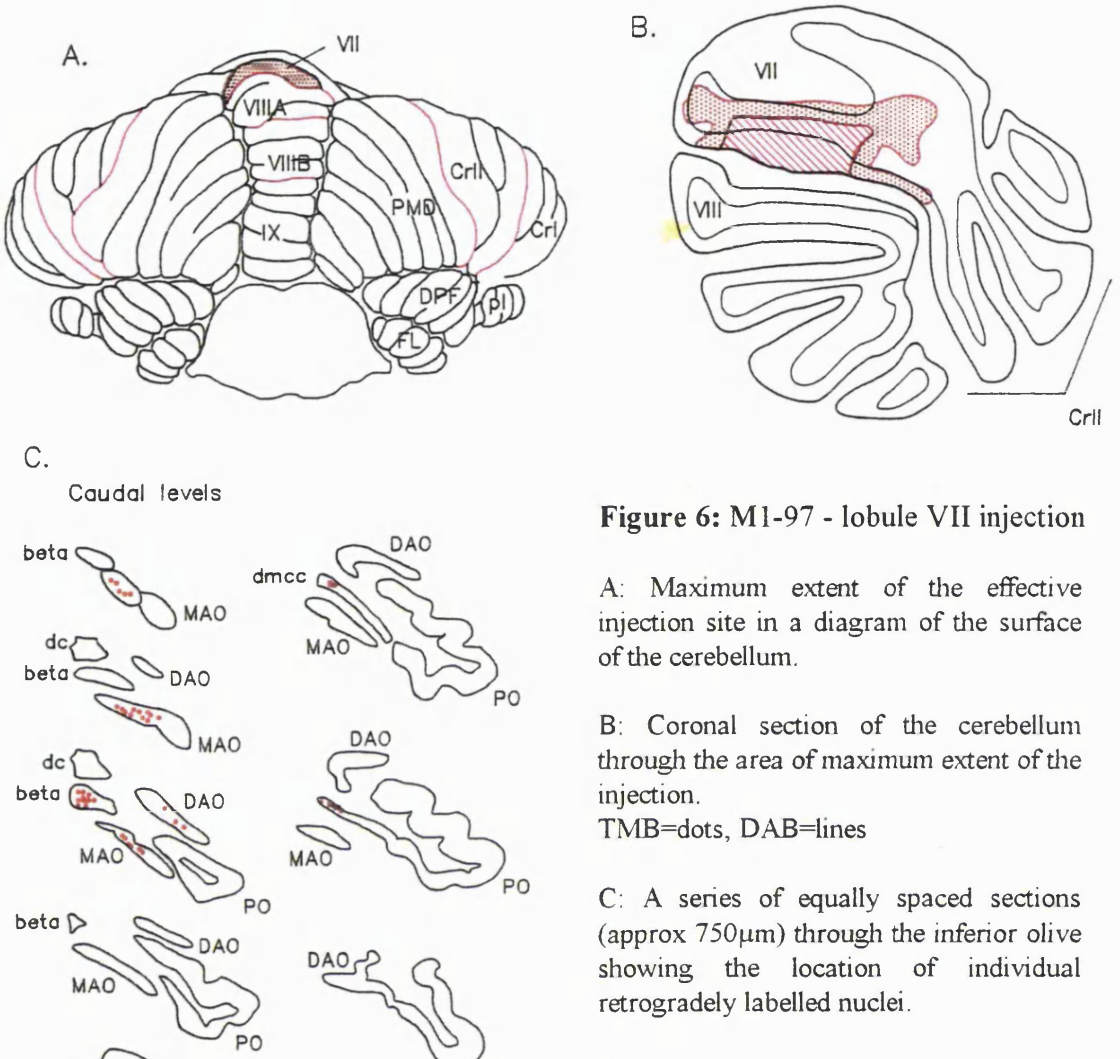

Figure 6: M1-97 - lobule VII injection

A: Maximum extent of the effective injection site in a diagram of the surface of the cerebellum.

B: Coronal section of the cerebellum through the area of maximum extent of the injection.
TMB=dots, DAB=lines

C: A series of equally spaced sections (approx 750μm) through the inferior olive showing the location of individual retrogradely labelled nuclei.

D: A series of equally spaced (500μm) coronal sections through the deep cerebellar nuclei showing position and density of anterogradely labelled terminals and retrogradely labelled cells.

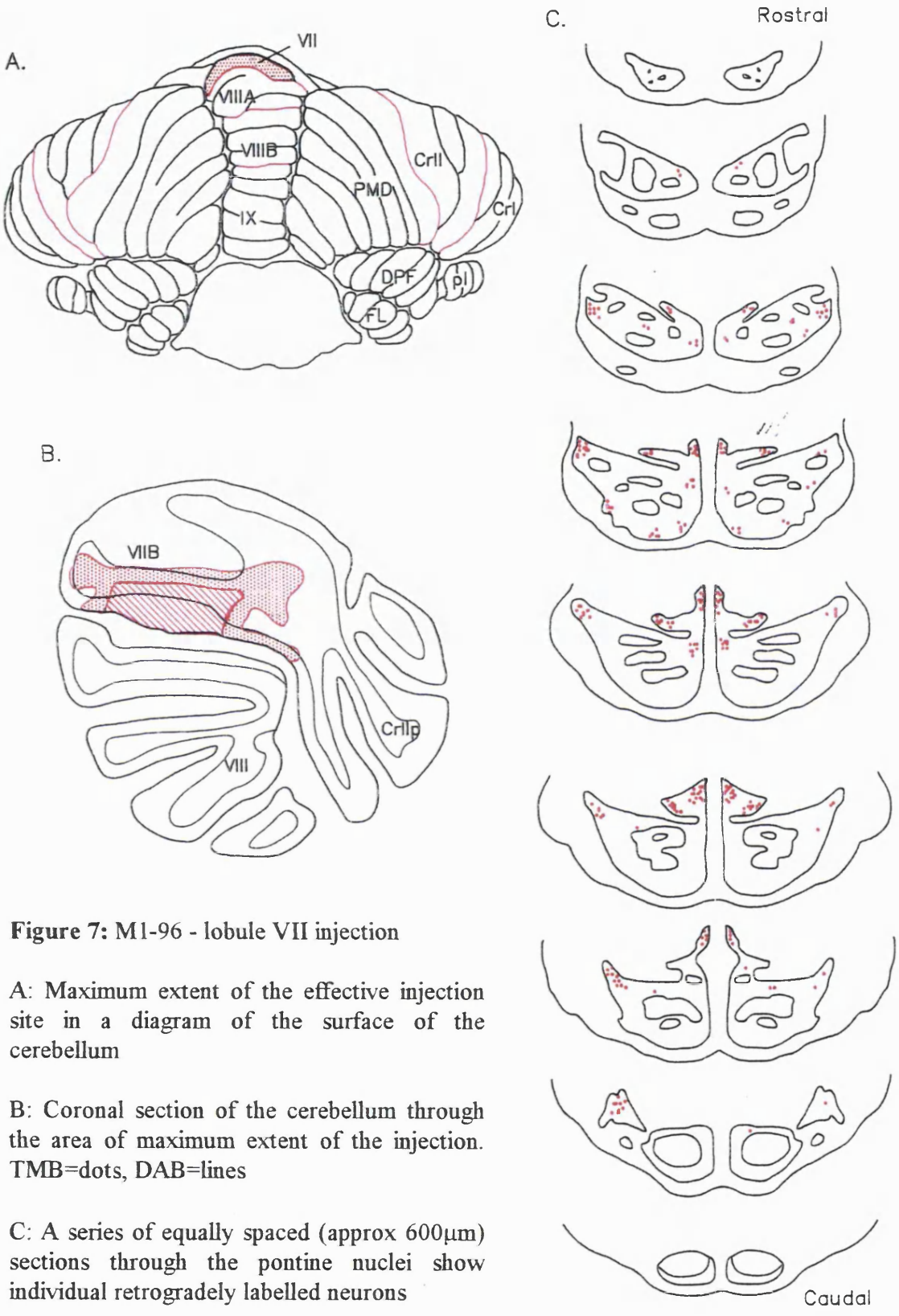

Figure 7: M1-96 - lobule VII injection

A: Maximum extent of the effective injection site in a diagram of the surface of the cerebellum

B: Coronal section of the cerebellum through the area of maximum extent of the injection. TMB=dots, DAB=lines

C: A series of equally spaced (approx 600μm) sections through the pontine nuclei show individual retrogradely labelled neurons

3.1.1.2 Lobule VIII

Case Pyr1

This case had been cut parasagittally, making comparison with other cases somewhat more difficult. It was a good case, however, which warrants inclusion here.

Injection site

See figures 8 and 9

This case was confined medially in the vermis, with the lateral edges having no labelled Purkinje cells. The injection was positioned on the two dorsal sublobules of the vermal lobule VIII, with the centre of the injection site over the fissure separating them. Although the injection was well centred, such that it stretched approximately equal distances away from the midline, the right hand side of the injection site had a slightly greater rostro-caudal extent.

The olivo-cortico-nuclear projection

The olivary label was located bilaterally in the lateral edge of the cMAO. More cells were found in the left medial accessory and the label on this side extended more caudally than it did on the right.

There was additional, albeit sparser, label bilaterally in the subnucleus β and the caudal dorsomedial cell column. This data indicates that the injection covered the entire breadth of the A zone, but since there was no label in the rMAO, DAO or PO, the injection had clearly not spread laterally to include any other zones.

Fibres could be traced coursing down from the cortical injection site to produce a strong terminal band across almost the entire the mediolateral extent of the ventro-caudal half of the fastigial nuclei bilaterally, although the most lateral edge of the fastigial had no label. The fastigial nucleus is contained within cerebellar zone A.

The ventral posterior interposed nucleus also contained a dense terminal field throughout almost its entire rostrocaudal extent bilaterally. The terminal field spanned much of the mediolateral extent of this nucleus, but again the lateral edge was spared. The posterior interposed nucleus belongs to zone C2.

The NRTP/Pontocerebellar projection

The pontine nuclei contained two main cell groups located bilaterally in the dorsolateral and dorsomedial nuclei. The dorsolateral group was the smaller of the two, but covered the entire rostrocaudal length of the pons. The dorsomedial group disappeared just rostral to the caudal end of the pons.

Additional small cell groups were seen ventromedially throughout most of the length of the pons and a few were also seen around the fascicles of the CST.

A large number of labelled cells found bilaterally in the NRTP, covering its entire rostrocaudal extent. Labelled cells were found distributed along its ventral border rostrally, but more caudally, the labelled area contracted into only ventro-medial label, with the lateral half of the nucleus free from label.

Although the groups of labelled cells remained separated in the pons and NRTP individually, the label in the dorsomedial pons and ventromedial NRTP merged to form a continuous band of afferent cells throughout the majority of the length of the NRTP.

The nucleo-cortical projection

The only retrogradely labelled cells in the deep cerebellar nuclei were found bilaterally in the dentate nucleus. Cells were found in the ventrolateral portion of the dentate, at mid-rostrocaudal levels. There was no indication of reciprocity in the nucleo-cortical and cortico-nuclear projections.

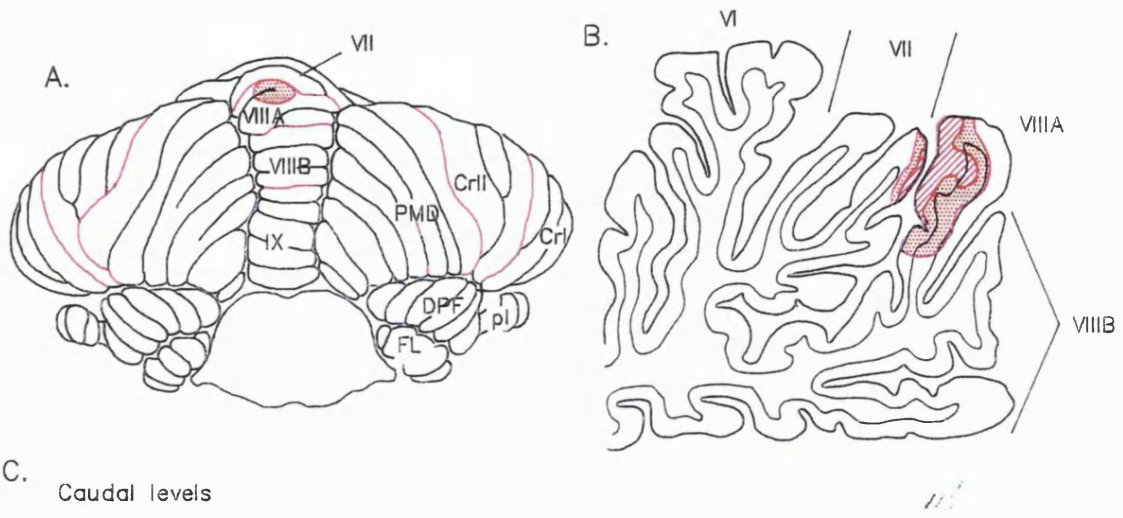

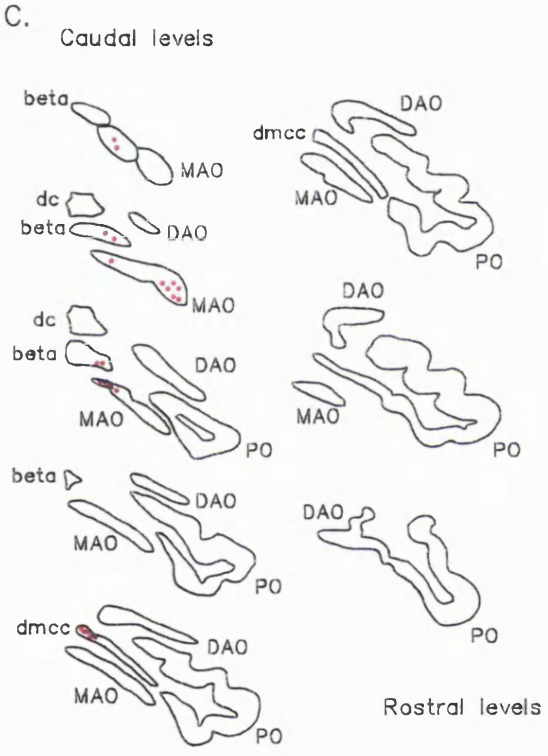

Figure 8: Pyr1 - lobule VIII injection

A: Maximum extent of the effective injection site in a diagram of the surface of the cerebellum.

B: Coronal section of the cerebellum through the area of maximum extent of the injection.
TMB=dots, DAB=lines

C: A series of equally spaced sections (approx 750μm) through the inferior olive showing the location of individual retrogradely labelled nuclei.

D: A series of equally spaced (500μm) coronal sections through the deep cerebellar nuclei showing position and density of anterogradely labelled terminals.

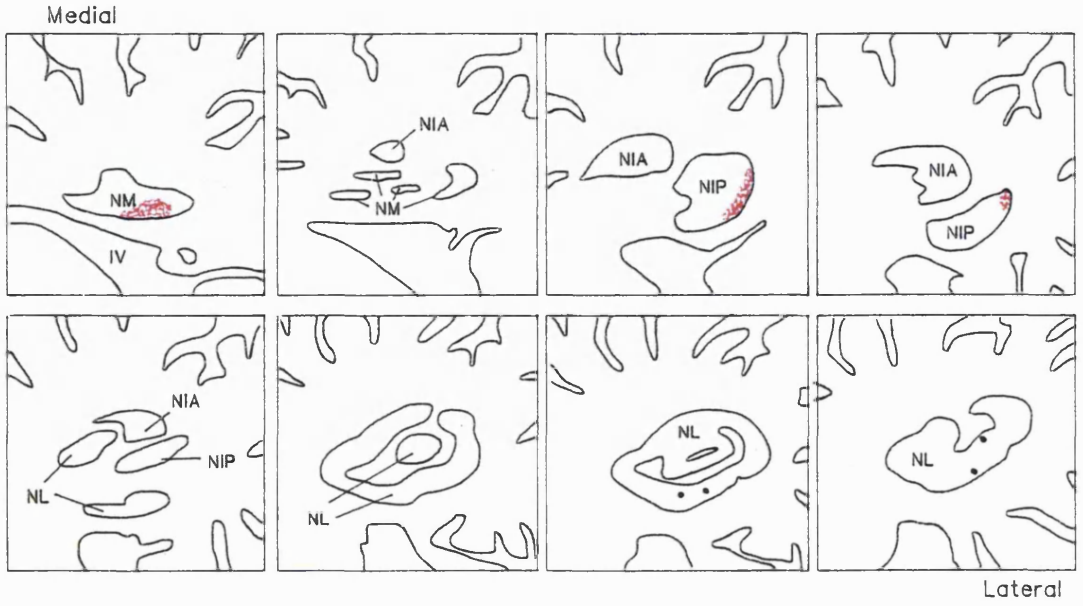

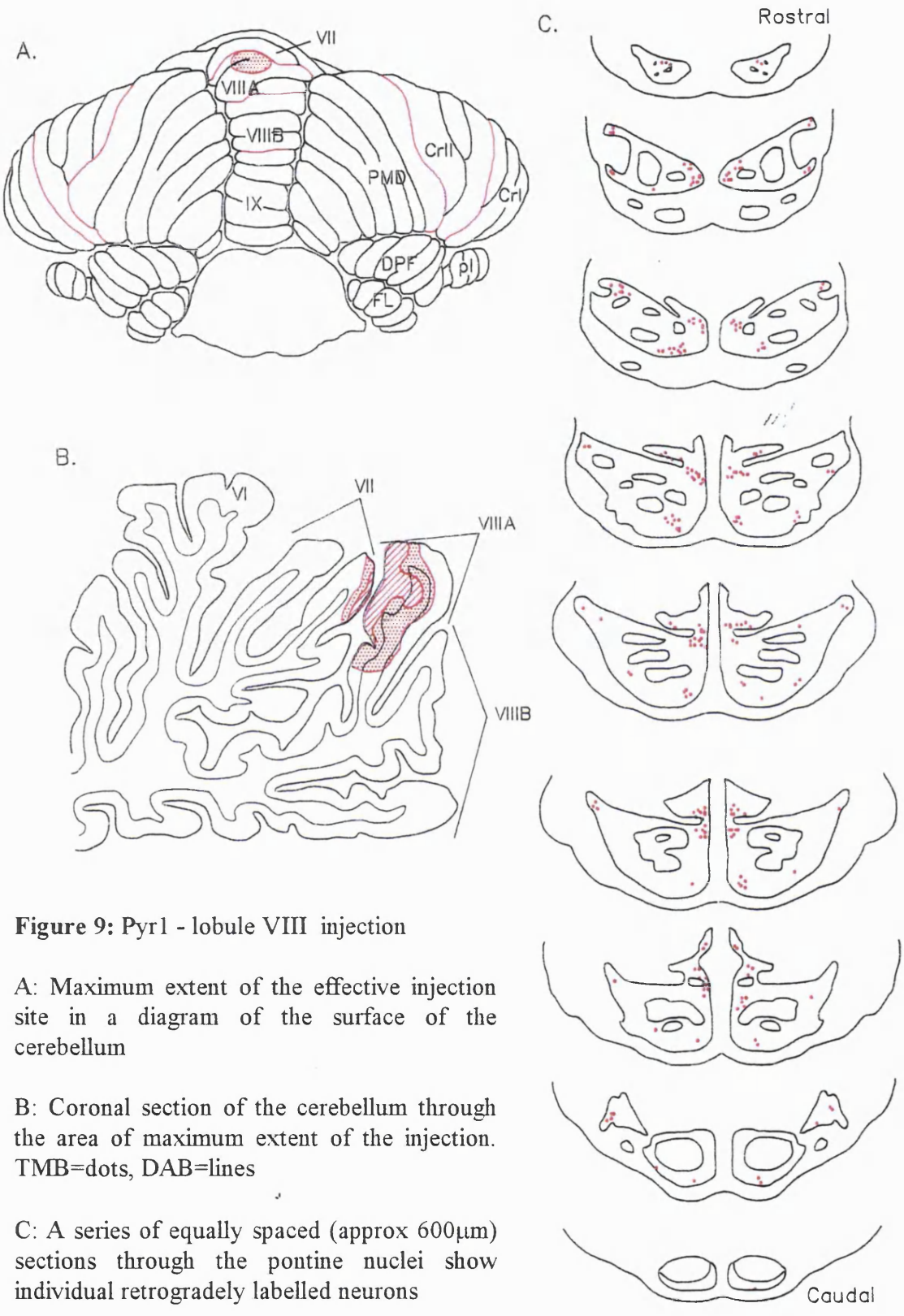

Figure 9: Pyr1 - lobule VIII injection

A: Maximum extent of the effective injection site in a diagram of the surface of the cerebellum

B: Coronal section of the cerebellum through the area of maximum extent of the injection. TMB=dots, DAB=lines

C: A series of equally spaced (approx 600µm) sections through the pontine nuclei show individual retrogradely labelled neurons

3.1.1.3 Lobule IX

a) Case UV2

Injection site

See figures 10 and 11.

The injection site in this case was centred in sublobule IXa, spanning three folia. There was only minimal overlap between the two cases, between the rostral edge of UV1 and the caudal edge of UV2. The injection site in this case spread laterally only on the right hand side, and the left hand border of the vermis was free of labelled Purkinje cells.

The olivo-cortico-nuclear projection

Retrogradely labelled cells clustered centrally in caudal subnucleus β and at the rostral pole of this label, the cMAO also contained a small number of cells. All label was bilateral, although noticeably sparser on the right hand side.

The injection site was therefore totally restricted to zone A1-2.

Labelled terminals in the deep nuclei were focused ventrocaudally in the fastigial (zone A), but the terminal field did extend into the rostral half of the nucleus. The fastigial label was located medially, and at no point in the terminal field did it cover the entire mediolateral extent of the nucleus. Fastigial label was present bilaterally.

The caudalmost posterior interposed (zone C2) contained terminals at its ventromedial border, and the dentate contained terminals at its caudomedial edge (zone D1).

The terminals fields in the posterior interposed and the dentate nucleus were only evident on the right hand side.

The NRTP/pontocerebellar projection

Labelled pontine cells were restricted to the rostral half of the pons. On the left hand side (thus contralateral to the main body of the injection site), they clustered adjacent to the dorsolateral nucleus, as two groups lying medial and ventral to it. On the right hand side, a couple of cells were found in the dorsolateral nucleus at caudal levels of the label's extent.

No labelled cells were seen anywhere in the NRTP

The nucleo-cortical projection

No labelled cells were found seen anywhere in the deep cerebellar nuclei.

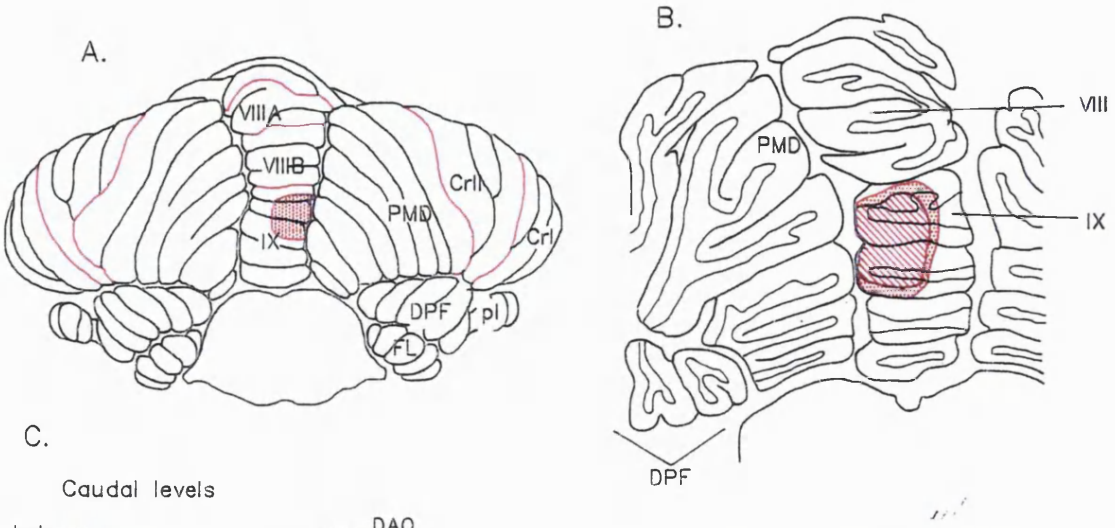

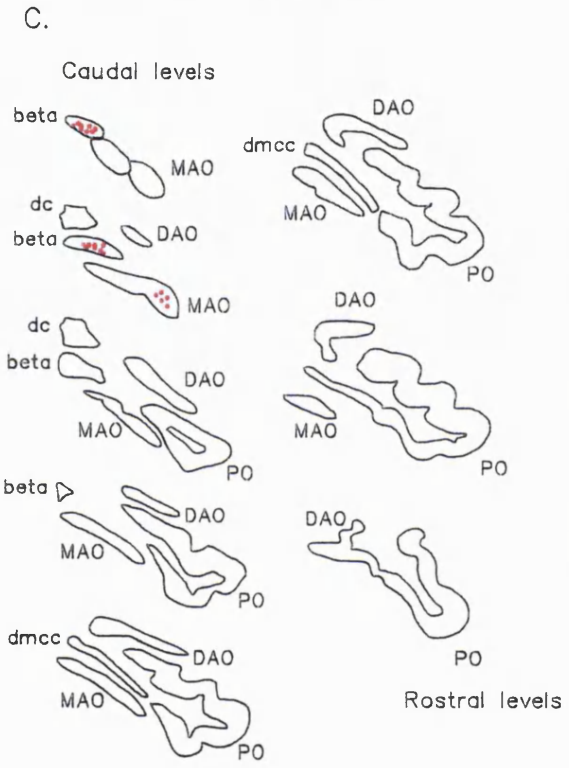

Figure 10: UV2 - lobule IXa injection

A: Maximum extent of the effective injection site in a diagram of the surface of the cerebellum.

B: Coronal section of the cerebellum through the area of maximum extent of the injection.
TMB=dots, DAB=lines

C: A series of equally spaced sections (approx 750μm) through the inferior olive showing the location of individual retrogradely labelled nuclei.

D: A series of equally spaced (500μm) coronal sections through the deep cerebellar nuclei showing position and density of anterogradely labelled terminals.

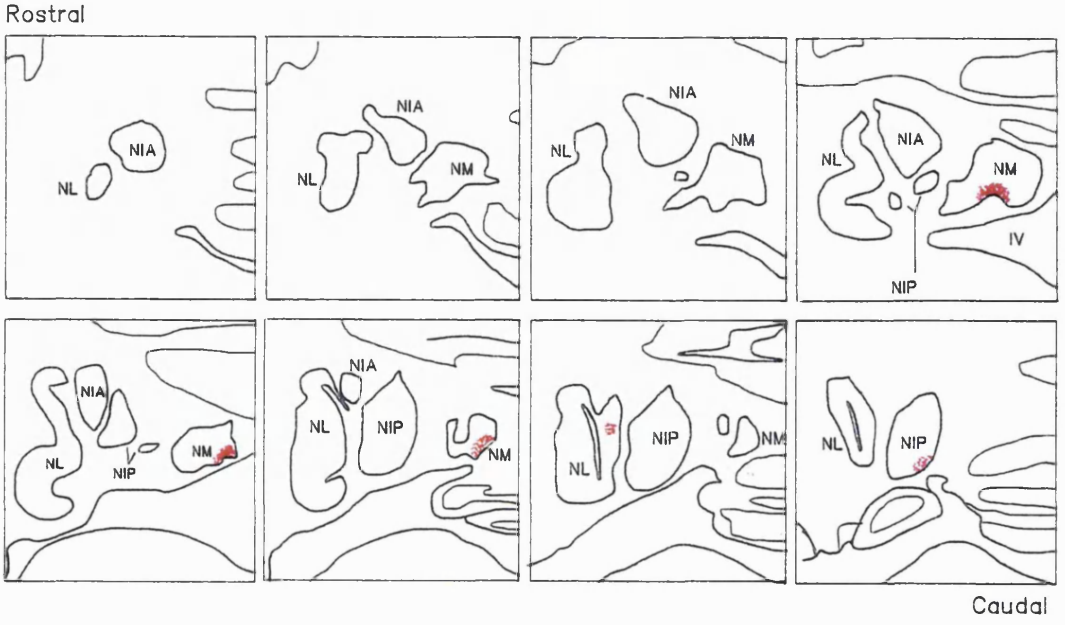

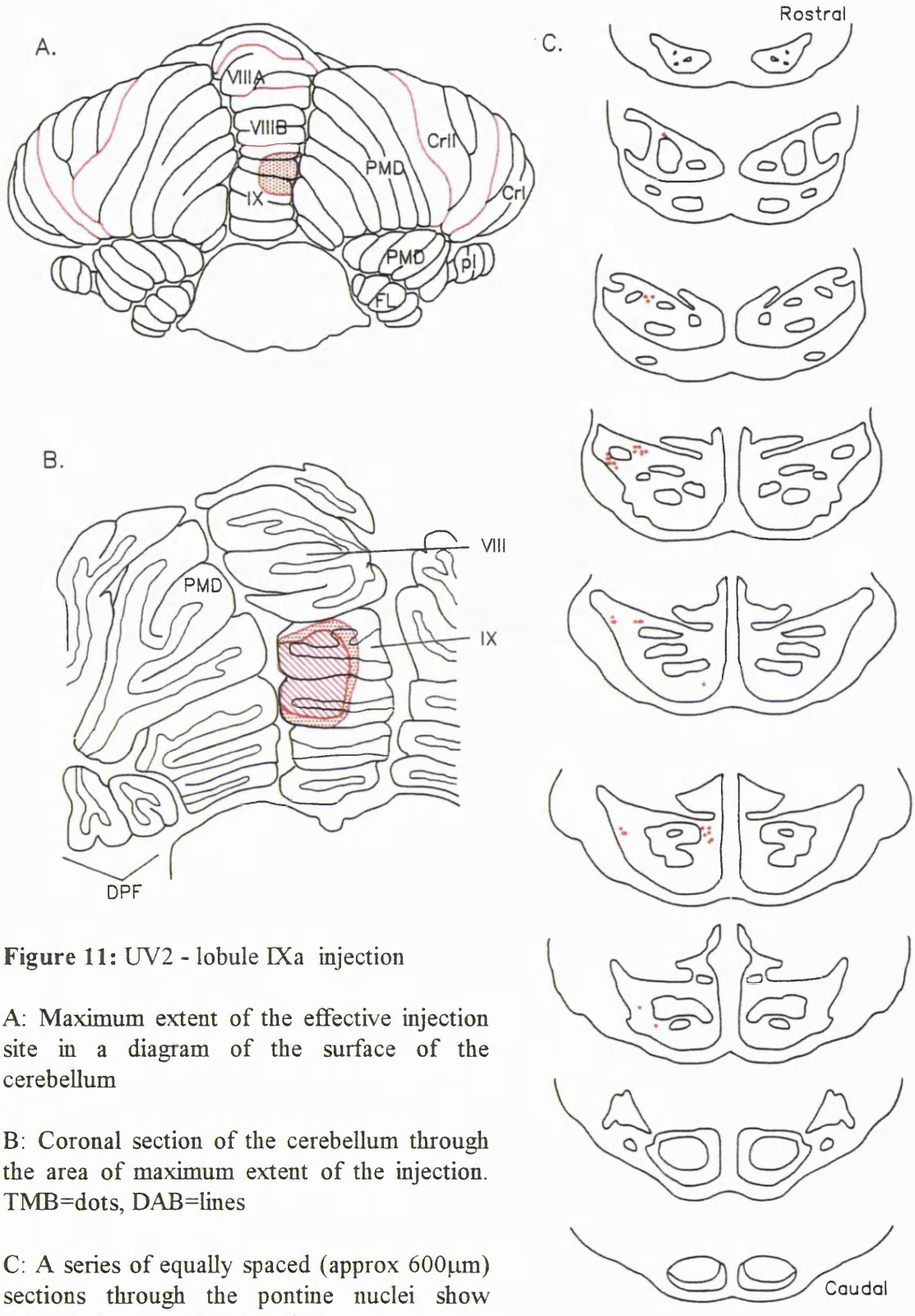

Figure 11: UV2 - lobule IXa injection

A: Maximum extent of the effective injection site in a diagram of the surface of the cerebellum

B: Coronal section of the cerebellum through the area of maximum extent of the injection. TMB=dots, DAB=lines

C: A series of equally spaced (approx 600µm) sections through the pontine nuclei show individual retrogradely labelled neurons

b) Case UV1

Injection site

See figures 12 and 13

The injection site was situated over two sublobules of IXb. On the right hand side, the injection spread laterally to the vermal border with the paramedian lobule. Both the cortex and the white matter of the hemisphere were unstained. The spread of the injection site on the left hand side was more restricted, such that the lateral border of the vermis contained no labelled Purkinje cells.

The olivo-cortico-nuclear projection

Retrogradely labelled cells clustered in the medial edge of subnucleus β and dmcc. Subnucleus β label was restricted to rostral levels of the nucleus; dmcc label was more extensive, covering almost 80% of its length. Although the nucleus β label was found bilaterally, the dmcc label was only seen on the left hand side, indicating that the injection site had covered zones A1-3 on the right hand side, but only zones A1 and 2 on the left.
In addition, there were two or three labelled cells in the ventral leaf of the rostral principal olive, corresponding to zone D2.

Fibres were traced from the injection site to a terminal field in the ventro-caudal edge of the fastigial nucleus bilaterally (zone A). The bulk of the terminal label covered the entire mediolateral span of the fastigial, but at the terminal field's rostral and caudal poles, the label was restricted to the medial edge of the nucleus.
Additional, sparse terminal label was found at the ventral edge of the anterior interposed nucleus (C1 and C3), at the same level as the rostral end of the fastigial terminal field.
Interpositus label was only seen on the right hand side.

The NRTP/pontocerebellar pathway

There was very restricted pontine labelling in this case. On the side contralateral to the injection site, there was a large clump of cells found in the dorsolateral nucleus in the rostral half of pons and an additional smaller clump located slightly more medially. On the side ipsilateral to the injection, there were a few labelled cells in the dorsolateral nucleus at caudal levels.

No labelled cells were found anywhere in the NRTP.

The nucleo-cortical projection

No retrogradely labelled cells were seen anywhere in the deep nuclei.

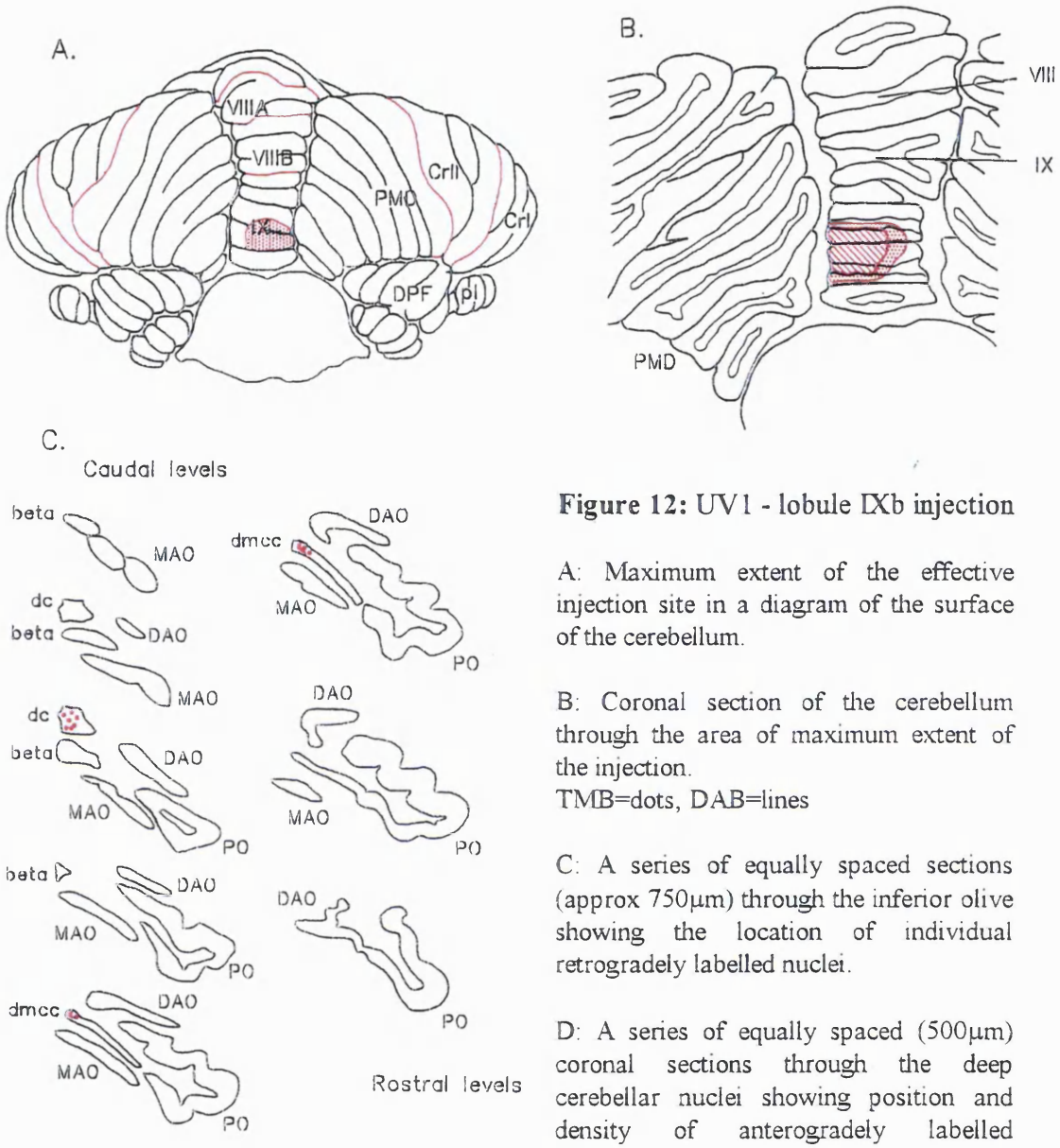

Figure 12: UV1 - lobule IXb injection

A: Maximum extent of the effective injection site in a diagram of the surface of the cerebellum.

B: Coronal section of the cerebellum through the area of maximum extent of the injection.
TMB=dots, DAB=lines

C: A series of equally spaced sections (approx 750μm) through the inferior olive showing the location of individual retrogradely labelled nuclei.

D: A series of equally spaced (500μm) coronal sections through the deep cerebellar nuclei showing position and density of anterogradely labelled terminals.

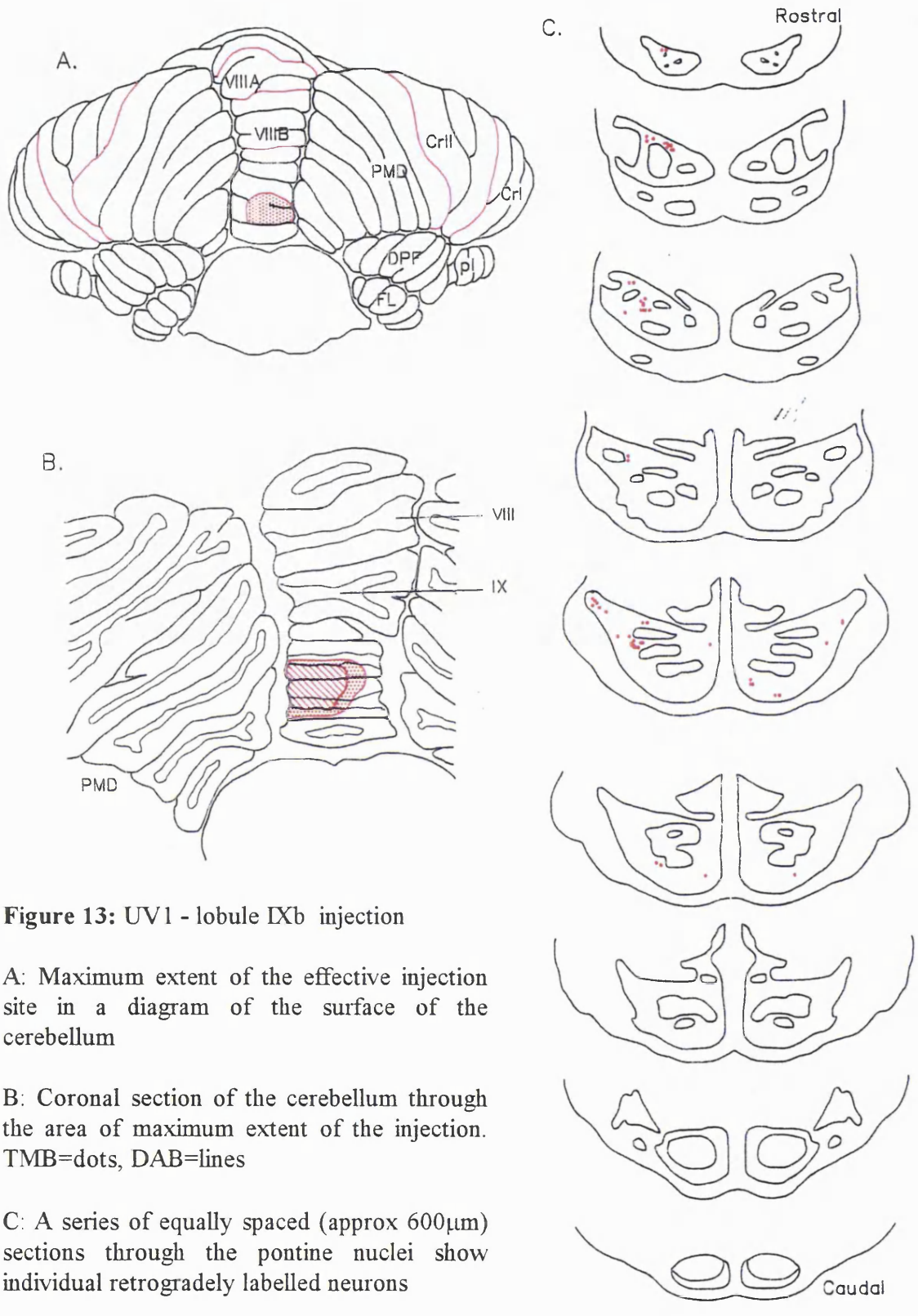

Figure 13: UV1 - lobule IXb injection

A: Maximum extent of the effective injection site in a diagram of the surface of the cerebellum

B: Coronal section of the cerebellum through the area of maximum extent of the injection. TMB=dots, DAB=lines

C: A series of equally spaced (approx 600μm) sections through the pontine nuclei show individual retrogradely labelled neurons

3.1.1.4 SUMMARY

The olivocerebellar projection

The bulk of the olivocerebellar pathway in the monkey posterior vermis arises in the caudal medial accessory olive, which projects onto the cortical zones A1-2 in the midline vermis. The more lateral A3 zone receives input from the dmcc in all vermal lobules except IXa. The B zone lies adjacent to the A zone (see vermal lobule VII case M1-96: section 3.1.1.1) and receives olivary input from the caudal dorsal accessory olive.

The uvula receives the majority of its input from the subnucleus β, with smaller contributions from the cMAO. In addition, its most caudal folia (see case UV1: section 3.1.1.3b) receive an input from the ventral leaf of the principal olive, corresponding to zone D2

The olivocortical projection to vermal lobules VII and VIII did not show a striking rostrocaudal or mediolateral topography: the olivary efferents for both cases arose from very similar parts of the medial accessory. The was, however, a striking difference in the olivary input to the subdivisions of the uvula from the subnucleus β. The olivary input to the more rostral folia of the uvula (IXa - UV2) arose from more caudal areas of the subnucleus β than that to caudal uvula IXb.

.

The cortico-nuclear projection to the fastigial

The midline vermis projects strongly onto the fastigial nucleus (nuclear zone A). Purkinje cells in the posterior vermis project preferentially to the ventral border of the caudal fastigial, part of which contained overlapping projections from all vermal lobules. The cortico-fastigial projection did demonstrate a marked rostrocaudal topography, however. The projection from the vermal lobule VII terminated in more rostral levels of the ventral fastigial than other cases. The projection from vermal lobule IXb terminated most caudally of all within this nucleus. This rostrocaudal difference was only apparent at the rostral edge of the fastigial terminal label, as in all the cases, the terminal fields ended at the same level caudally.

Although in all cases the projection focused towards the medial edge of the fastigial, none of the cases terminated in the most medial edge, even when the mediolateral extent of the

terminal fields was at their greatest. As each of the injections covered the complete hemivermis, it was not possible to discern a mediolateral topography in this projection.

The olivocorticonuclear projection

The parasagittal zonation of this pathway deviates markedly from the midline in the monkey vermis. Although the bulk of the olivocorticonuclear pathway does follow strict parasagittal zonation, there were striking deviations in the cortico-nuclear projections away from the midline into areas normally attributed to projections from non-vermal cortical areas. These "extra-zonal" cortico-nuclear projections were evident in the absence of olivary input appropriate to the nuclear zone.

Extra-zonal projections were apparent in every case in the vermis, but separate lobules deviated differently from their neighbours. The most common deviation was to the interposed complex, and projections to the anterior or posterior division appeared to alternate between lobules. Vermal lobules VII and IXa projected to the anterior interposed while the VIII and IXb projected to the posterior division. Due to rostrocaudal differences between the cortical areas, the extra-zonal terminal fields did not overlap (i.e. the lobule VII projection to anterior interposed terminated more rostrally then the lobule IXa-AIP projection). It should be noted, however, that cases VIII and IXa were cut in different planes, and thus it was difficult to compare terminal fields precisely. In addition, the vermal lobule VII case contained cDAO olivary label indicating zone B involvement in the injection site. Zone B projects preferentially to the lateral vestibular nucleus, but may have additional projections to the interposed nuclei. These details will be covered in more depth in section 4.2.2.1 of the discussion.

The NRTP/pontocerebellar projection

The vermal lobule VII received the strongest projection from the visual/oculomotor dorsolateral pons. Not only was the projection stronger at each individual level, but also had a greater rostrocaudal spread. The clearest example is derived from comparison between lobule VII and the uvula; the latter only receives dlpn input from its rostral levels. Following vermal lobule VII, the strongest projection was to IXa, then IXb and vermal lobule VIII. However, all vermal cases did show some degree of label in the dorsolateral pons.

Pontine cerebellar afferents arise from multiple nuclei, although one particular nucleus tends to dominate. For example, in addition to its dlpn input, lobule VII receives projections from dorsomedial, ventromedial and lateral pontine nuclei; lobule VIII receives its greatest input from the dorsomedial nucleus, but additional projections from satellite cell groups in the ventromedial and ventrolateral nuclei. The uvula was unusual in having more sparsely labelled and scattered satellite cell groups, such as those seen ventrally in IXb.

Overall, the pontocerebellar projection shows simultaneous convergence and divergence. Numerous pontine cell groups converge their input onto one area in the cerebellar cortex and individual nuclei projected to different areas in the vermis.

NRTP efferents are much more lobule specific than those from the pontine nuclei. The distribution of efferents to lobule VII and VII are markedly different, and the NRTP sends no projections at all to the uvula.

Vermal lobule VII received strong input from the dorsolateral and a smaller input from the medial NRTP nuclei, paralleling the arrangement in the pontine nuclei. VIII was dominated by a large ventromedial group, which spread laterally at more rostral levels, giving the opportunity for overlap of the two efferent cell groups. VIII also showed a clear continuity of a cerebellar projection across the medial lemniscus from the ventromedial NRTP and dorsomedial pons.

The NRTP efferent system does not show the same clustering into clearly separable small cell groups, as in the pontine nuclei, but nonetheless NRTP efferents do tend to group together as one or two large cell masses.

The nucleo-cortical projection

Lobule VII and VIII both receive a purely ipsilateral input from the deep cerebellar nuclei. This input does not reciprocate the cortico-nuclear pathway completely, however. In the lobule VII case, there were labelled cells found both inside and beyond terminal fields, but in the lobule VIII case, nucleo-cortical cells were only located in the dentate, which contained no terminal fields whatsoever. There was no consistent size differences between reciprocal and non-reciprocal afferents.

In all cases, the nuclear areas which received extra-zonal input from the cortex did not project back to the vermis.

There is no projection from the deep nuclei to the uvula.

3.1.2 PARS INTERMEDIA AND HEMISPHERE

The cerebellar hemispheres of the posterior lobe are formed by the medially directed loop of a folial chain (Bolk, 1906): the rostral part is crus II and more the caudal parts, as the chain approaches the vermis, produce the paramedian lobule. The parasagittal zones within the cerebellar cortex run parallel to this folial chain and orthogonal to the long axes of individual folia.

Due to surgical limitations, the paramedian lobule and crus II injections presented in this thesis are all focused along the posterior edge of the cortex, just dorsal to the paraflocculi. On a posterior view of the cerebellum, the cases appear to be mediolaterally separated. However, the role of the folial chain in parasagittal zonation must be recalled, and therefore within this context, the cases are rostrocaudally rather than mediolaterally segregated.

3.1.2.1 Paramedian lobule

a) Case PMD2

Injection site

See figures 14 and 15.

The injection site in this case was located on the ventral surface of the cerebellum, and thus caudally in the paramedian folial chain, at the medial edge of the paramedian lobule. Its medial border abutted the vermal lobules IXb and X. It straddled the medial halves of two folia, but did not spread into the vermis.

The Olivo-cortico-nuclear projection

Retrogradely labelled olivary cells were primarily located laterally in the middle levels of the contralateral MAO. Additional labelled cells were located in the most rostromedial aspect of the dorsal leaf of the principal olive. This pattern of olivary label suggests that this injection site involved C2 and D1 zones. The lack of label in the dmcc (zone A3) supports the contention that the injection site had not involved the lateral edge of the vermis.

Labelled terminals within the deep nuclei were located ipsilaterally in the interposed and dentate nuclei. The anterior interposed contained label rostrodorsally (C1 and C3 zones), while the terminal field in the posterior interposed (C2) was located centrally at mid-rostrocaudal levels. Two patches of label were seen in the dorsal aspect of rostral NL (D2): they were situated at the medial and lateral edges of the nucleus.

The NRTP/pontocerebellar projection

Retrogradely labelled cells were found throughout the contralateral pontine nuclei. Clumps of cells were seen in the ventromedial, lateral, dorsal, peduncular and paramedian nuclei (in descending order of strength). There was no indication of a particular pattern to the pontine efferents, although those in the ventromedial nucleus were only found caudally. No cells were seen ipsilateral to the injection site.

No labelled cells were encountered in the NRTP.

The nucleo-cortical projection

Labelled nuclear cells in this case were found ipsilaterally, only in the caudal two-thirds of the terminal label areas within the dentate. The cells were located within the terminal field, and were arranged along the same axis as the terminal field, as a strip running dorsoventrally.

No cells were seen contralaterally.

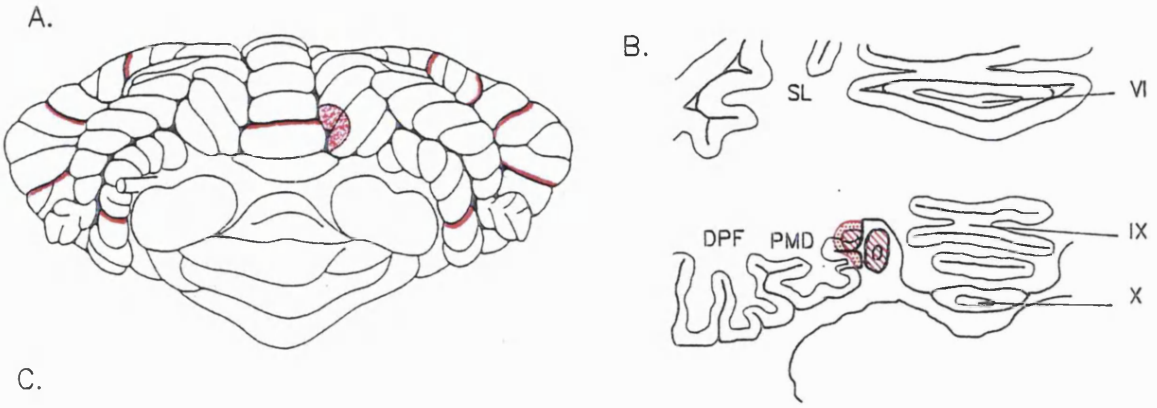

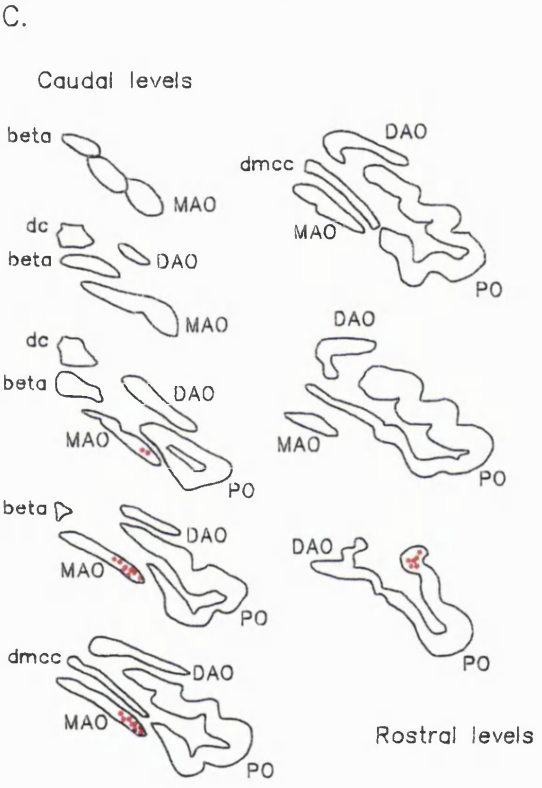

Figure 14: PMD2 - paramedian lobule injection

A: Maximum extent of the effective injection site in a diagram of the surface of the cerebellum.

B: Coronal section of the cerebellum through the area of maximum extent of the injection.
TMB=dots, DAB=lines

C: A series of equally spaced sections (approx 750μm) through the inferior olive showing the location of individual retrogradely labelled nuclei.

D: A series of equally spaced (500μm) coronal sections through the deep cerebellar nuclei showing position and density of anterogradely labelled terminals.

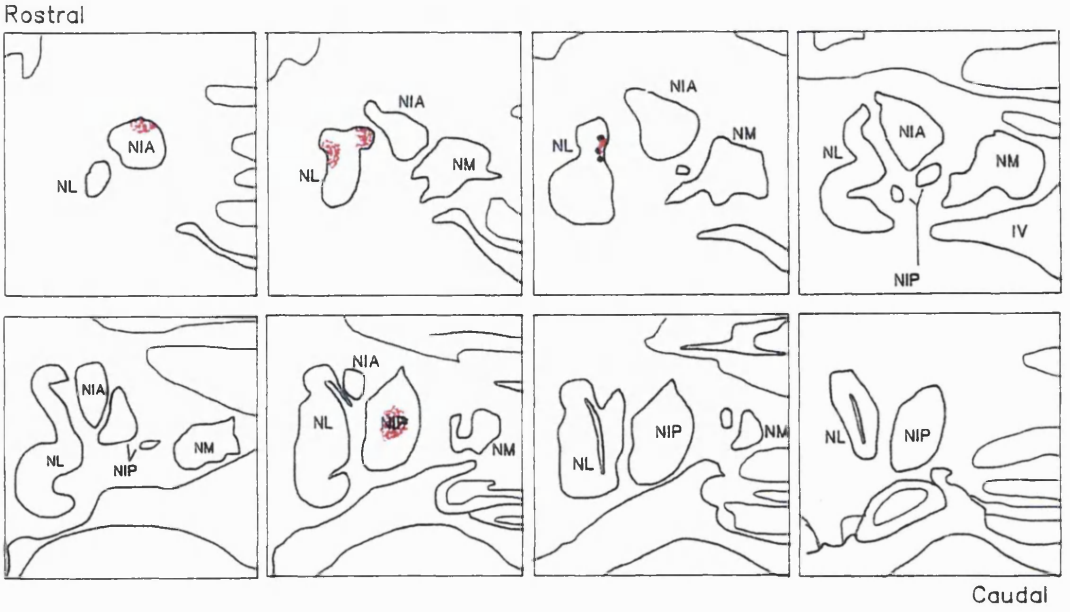

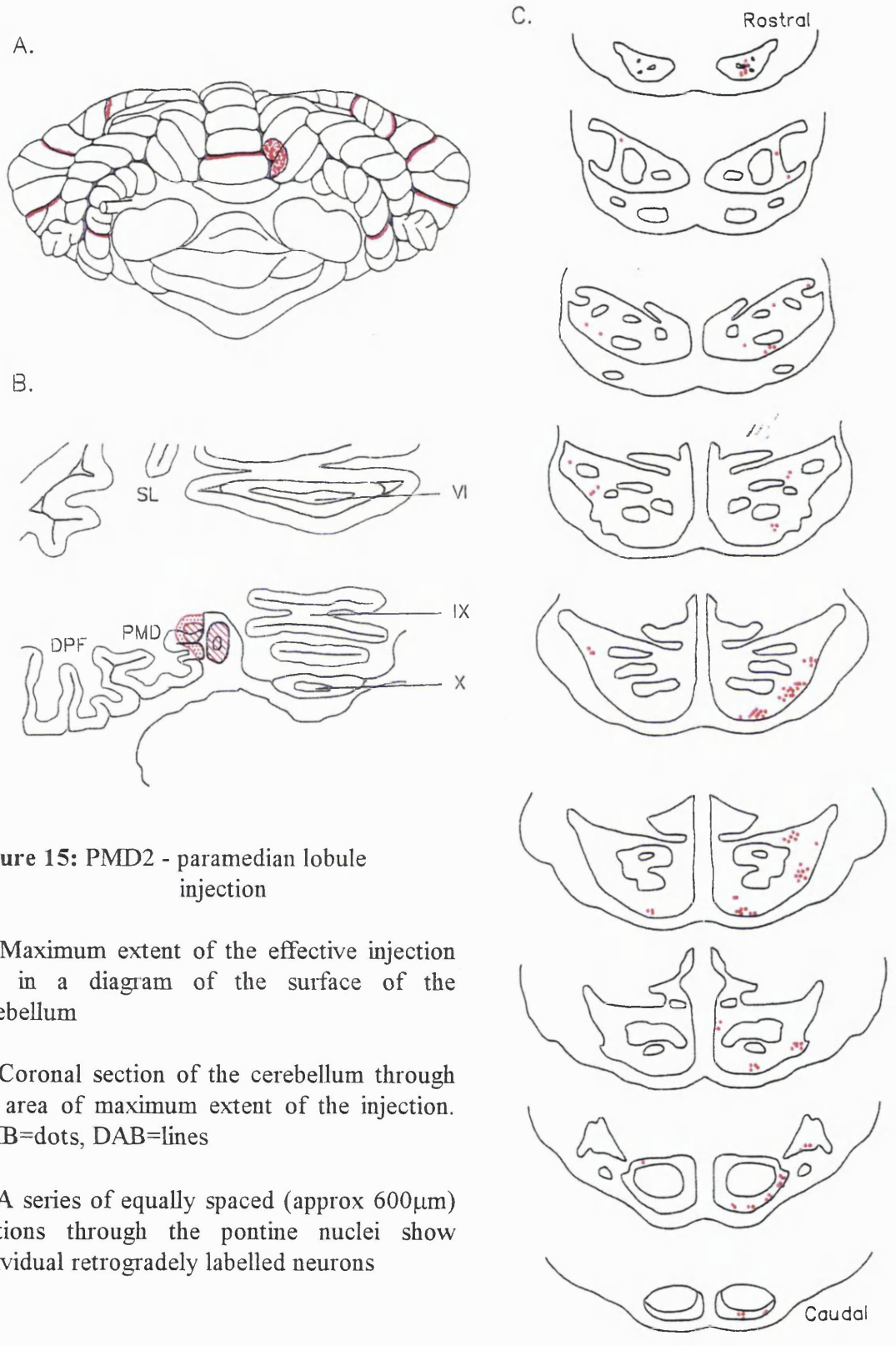

Figure 15: PMD2 - paramedian lobule injection

A: Maximum extent of the effective injection site in a diagram of the surface of the cerebellum

B: Coronal section of the cerebellum through the area of maximum extent of the injection. TMB=dots, DAB=lines

C: A series of equally spaced (approx 600µm) sections through the pontine nuclei show individual retrogradely labelled neurons

b) Case GR-95

Injection site

See figures 16 and 17.

The bulk of this injection site was located at the posterior edge of the paramedian lobule. Viewed posteriorly, the injection site was situated laterally, at the border with crus II, and therefore rostrally within the paramedian folial chain. The injection site spanned the caudal third of two folia.

There was additional spread of WGA-HRP into the tip of folium 6 of the dorsal paraflocculus immediately beneath the paramedian lobule.

The olivo-cortico-nuclear projection

Olivary label was largely confined to the contralateral principal olive. It covered the caudal third of this nucleus, and the labelled cells were located in the middle of the dorsal leaf. In one section, there was also a number of cells collected in the lateral bend. One or two cells were found in the rMAO rostral to the principal olive label. Overall, these results indicate that the injection site mostly comprised zone D1 and an almost negligible contribution from C2.

The majority of terminal label was located in ipsilateral mid-rostral NL (D2). The terminal band ran from the ventral indentation medially to the lateral edge of the nucleus. Immediately caudal to this, another, smaller terminal field was located in the ventrolateral corner of mid-PIP (C2).

The NRTP/pontocerebellar projection

Pontine label in this case was very sparse. However, labelled cells were found contralaterally in the ventral peduncular nucleus rostrally and ventrally at more caudal levels. There was no label in the dorsolateral or lateral nuclei. Very few cells were seen ipsilaterally.

No labelled cells were found in the NRTP

The nucleo-cortical projection

No retrogradely labelled cells were found in this case. However, the injection in this animal was very superficial, and there was little labelling of the granular layer (as evidenced by the comparatively sparse label in the pontine nuclei), where the nucleo-cortical fibres terminate.

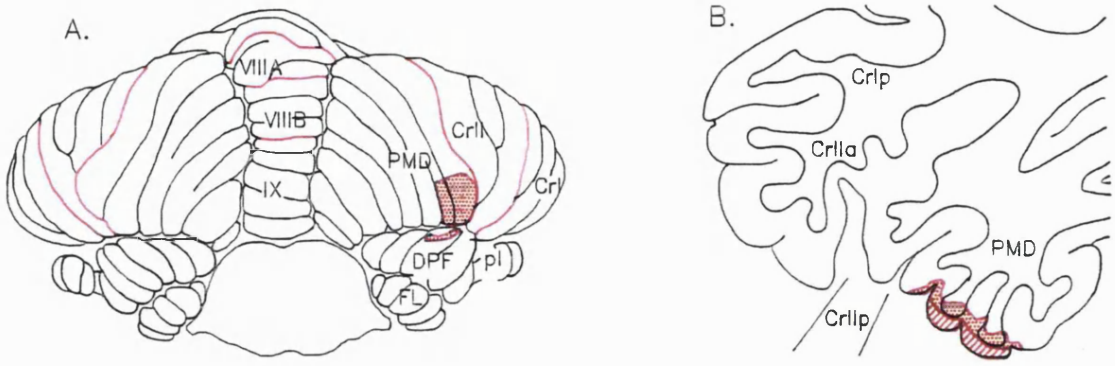

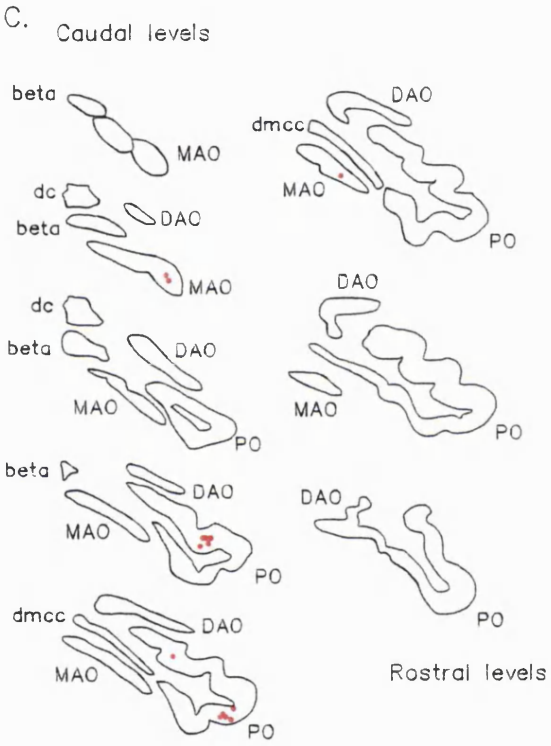

Figure 16: GR-95 - paramedian lobule injection

A: Maximum extent of the effective injection site in a diagram of the surface of the cerebellum.

B: Coronal section of the cerebellum through the area of maximum extent of the injection.
TMB=dots, DAB=lines

C: A series of equally spaced sections (approx 750µm) through the inferior olive showing the location of individual retrogradely labelled nuclei.

D: A series of equally spaced (500µm) coronal sections through the deep cerebellar nuclei showing position and density of anterogradely labelled terminals.

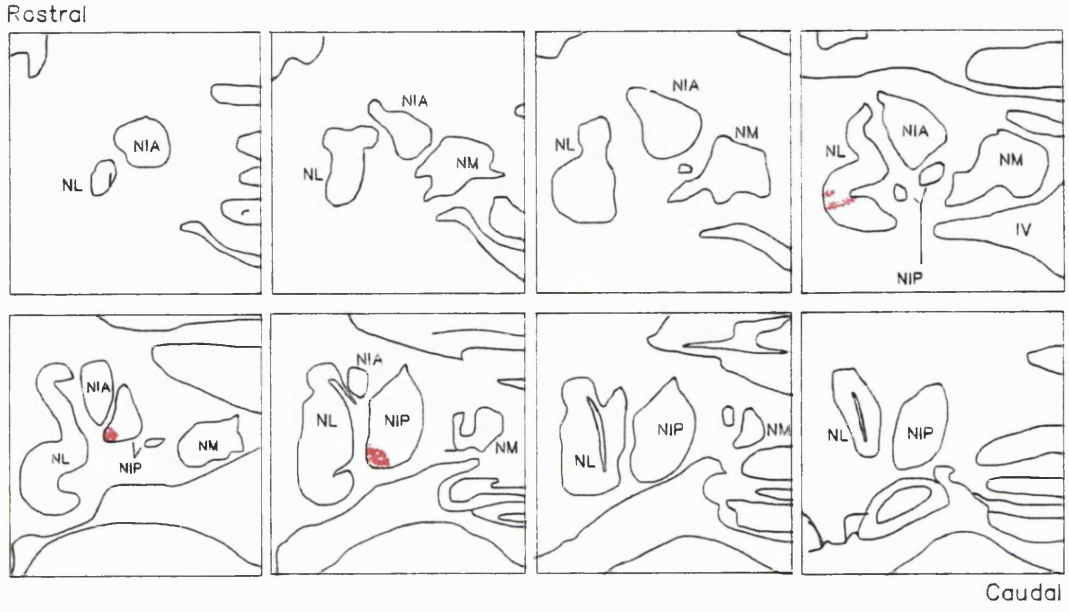

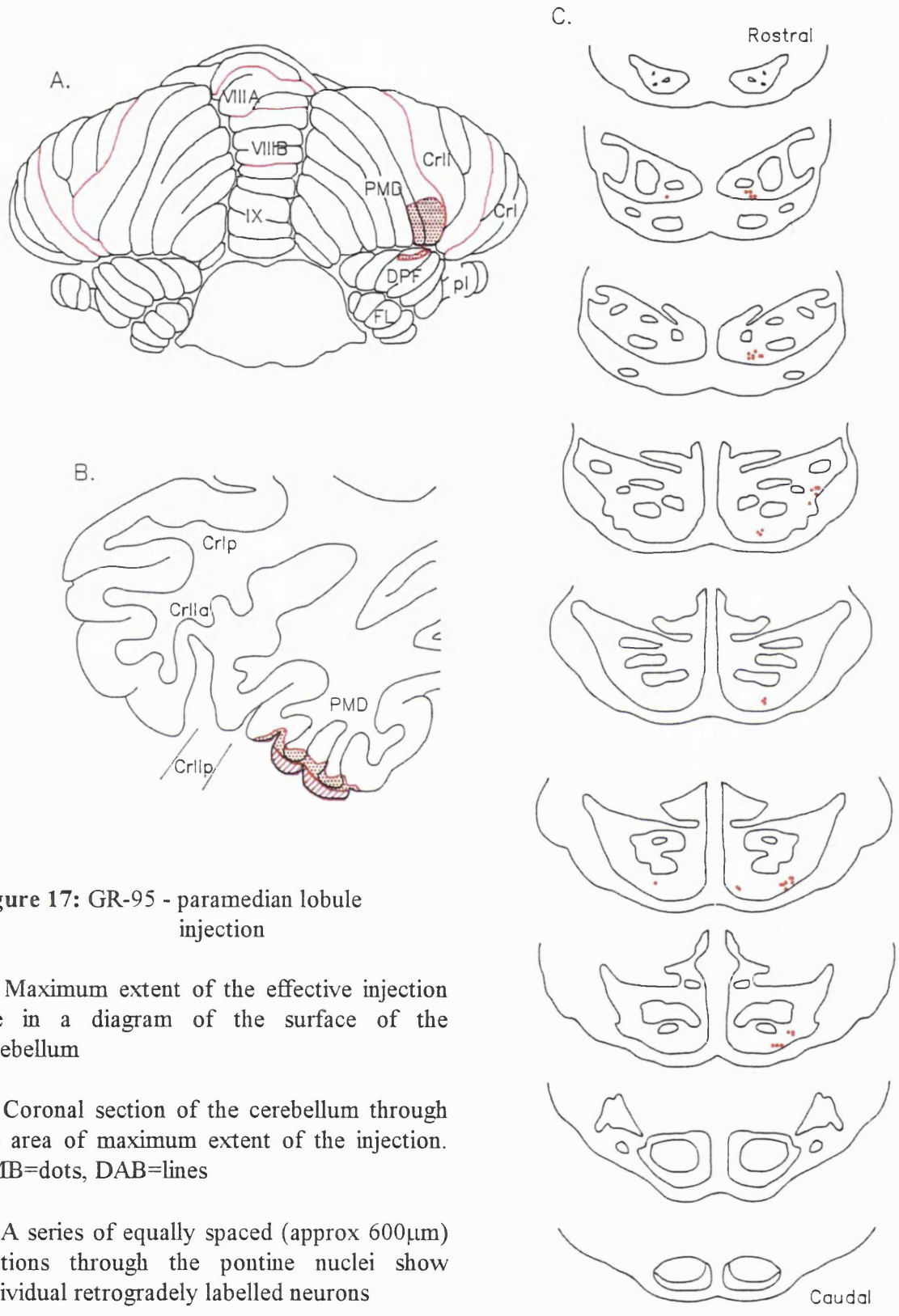

Figure 17: GR-95 - paramedian lobule injection

A: Maximum extent of the effective injection site in a diagram of the surface of the cerebellum

B: Coronal section of the cerebellum through the area of maximum extent of the injection. TMB=dots, DAB=lines

C: A series of equally spaced (approx 600µm) sections through the pontine nuclei show individual retrogradely labelled neurons

c) Case Co5

Injection site

See figures 18 and 19.

The injection site in this case was positioned in the fissure separating the two most lateral folia in the paramedian lobule, and thus rostrally in the paramedian folial chain. There was no leak of the WGA-HRP into either the dorsal paraflocculus or crus IIp.

The olivo-cortico-nuclear projection

Retrogradely labelled olivary cells in this area were entirely restricted to the contralateral principal olive, forming a small clump of cells in the dorsal part of the lateral bend. The cells were found to be positioned caudally in the principal olive, just at the level at which it starts to become invaginated medially.

This olivary label corresponds to zone D1.

Labelled terminal fields within the nuclei were found only in the caudal quarter of the dentate nucleus (D1). The terminal field formed two thin stripes (three at the labels most rostral level, but the most dorsal one disappears caudally) running across the nucleus in a medial to lateral direction. The stripes were slanted such that the stripes run somewhat ventrally as the lateral edge of the nucleus was reached, and dorsally at its more medial locations. There was evidence of a few fibres running between the stripes. The most medial part of the dentate was free of label until the most caudal sections. The terminal stripes were located in the ventral half of the dentate, but did not fill its most ventral area.

The NRTP/Pontocerebellar projection

The entire rostrocaudal length of the contralateral pons contained labelled cells. The majority of the cells clumped ventrally and formed a ring following the ventral surface of the pons round from dorsomedial to ventral to a few cells in the dorsolateral nucleus. There were very few cells found dorsally.

Only a very few cells were found ipsilaterally, and all of these were found in ventromedial divisions, scattered throughout the rostro-caudal span of the pons.

No labelled cells were found within the NRTP.

The nucleo-cortical projection

No retrogradely labelled cells were seen anywhere in the deep nuclei. This result is unlikely to be a false negative, since the pontine nuclei, which are retrogradely filled from the same layer of the cerebellar cortex contained numerous labelled cells.

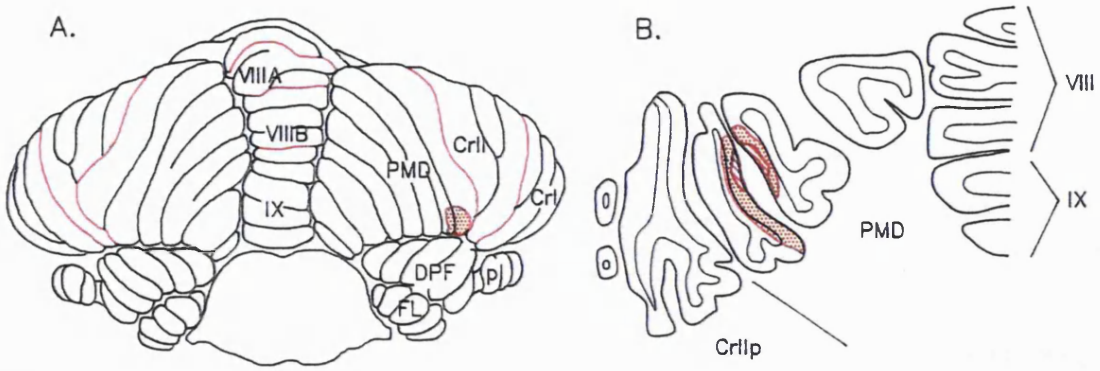

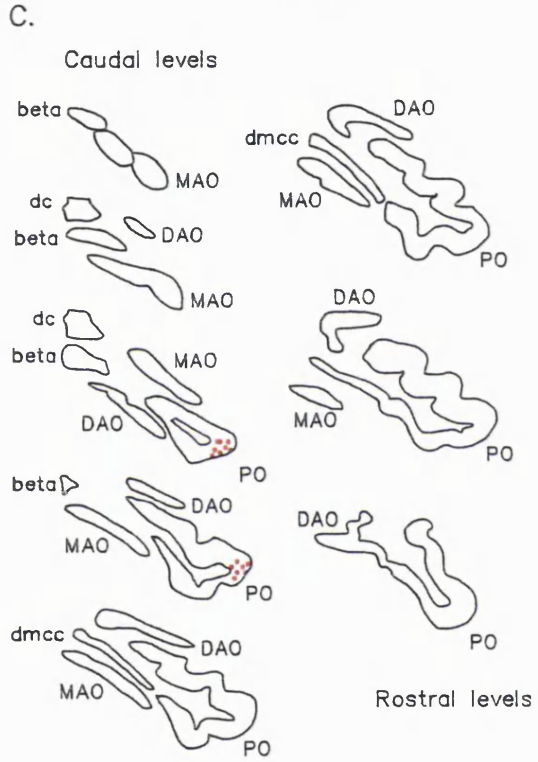

Figure 18: Co5 - paramedian lobule injection

A: Maximum extent of the effective injection site in a diagram of the surface of the cerebellum.

B: Coronal section of the cerebellum through the area of maximum extent of the injection.
TMB=dots, DAB=lines

C: A series of equally spaced sections (approx 750μm) through the inferior olive showing the location of individual retrogradely labelled nuclei.

D: A series of equally spaced (500μm) coronal sections through the deep cerebellar nuclei showing position and density of anterogradely labelled terminals.

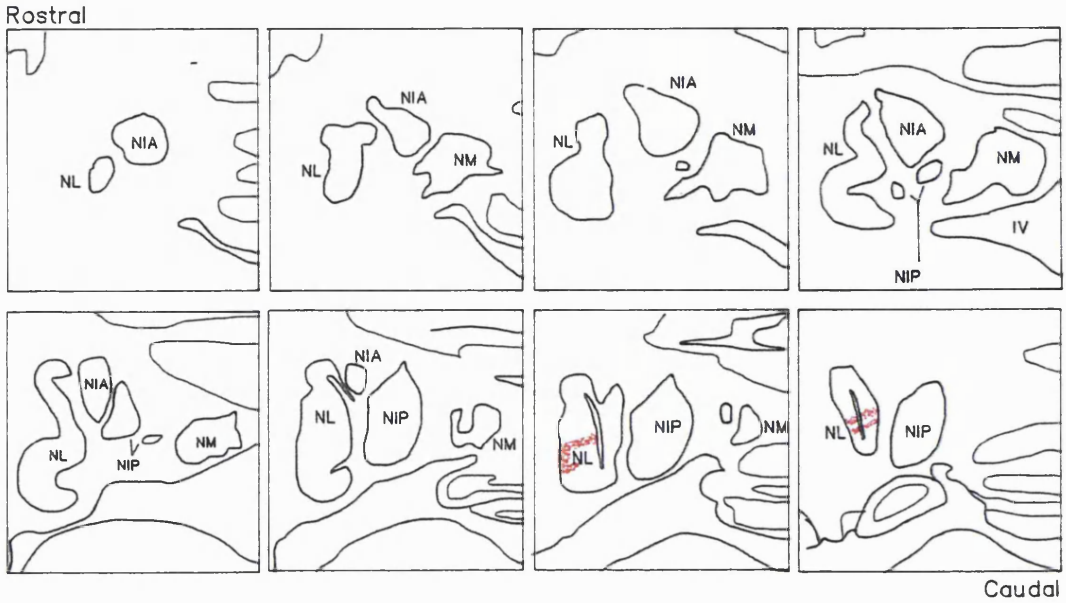

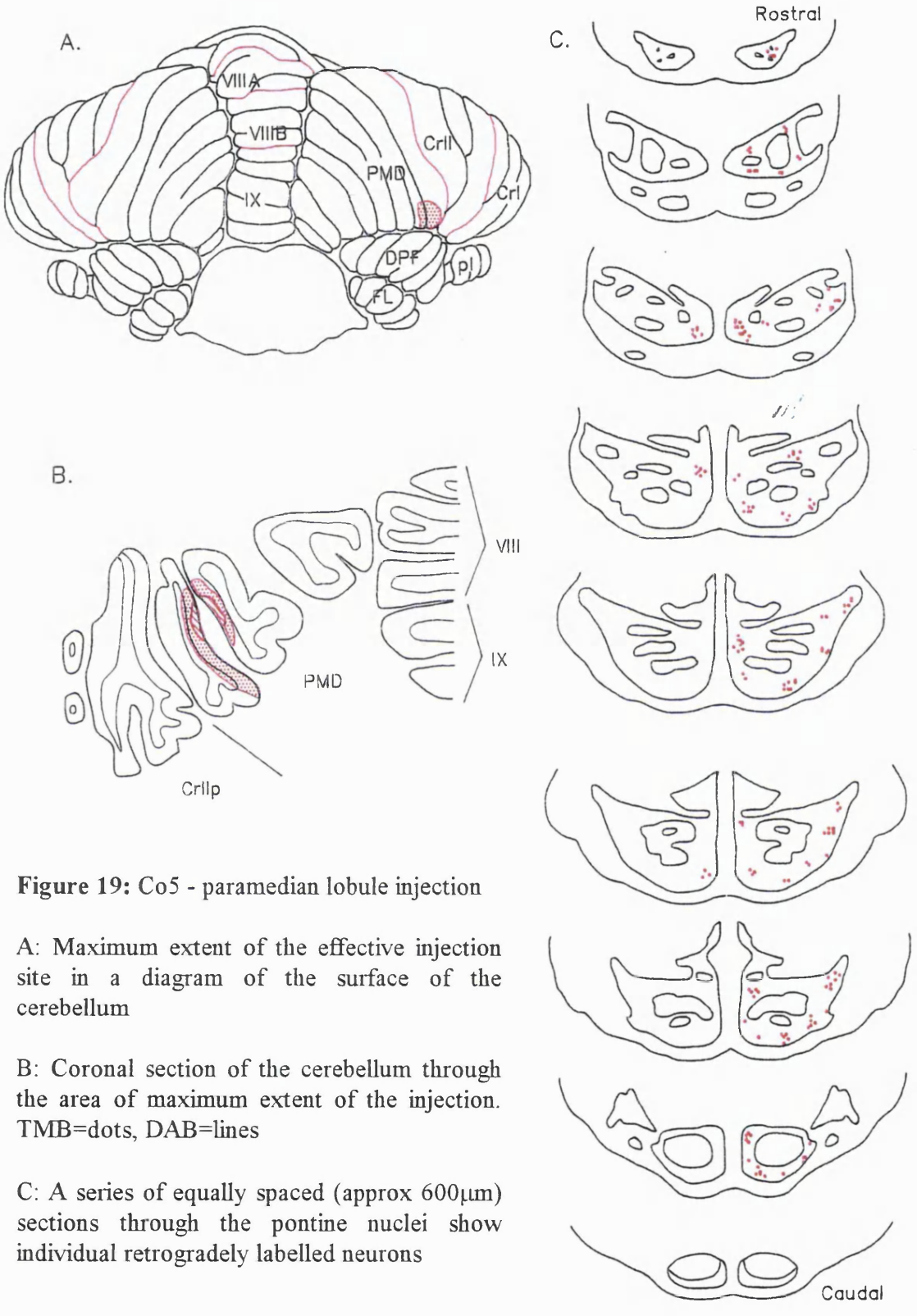

Figure 19: Co5 - paramedian lobule injection

A: Maximum extent of the effective injection site in a diagram of the surface of the cerebellum

B: Coronal section of the cerebellum through the area of maximum extent of the injection. TMB=dots, DAB=lines

C: A series of equally spaced (approx 600μm) sections through the pontine nuclei show individual retrogradely labelled neurons

d) Case M 2-96 (Left hemisphere)

Injection site

See figure 20 and 21.

This animal received two cerebellar cortex injections, one either side of the midline. The injection into the left hemisphere was centred in fissure that divides the paramedian lobule. There was a small amount of leak into the tips of the dorsal paraflocculus (folia 4 - 6).

The olivocorticonuclear projection

Labelled cells were found in four nuclei in the contralateral inferior olive. They were (in descending order of label strength): the dorsal leaf of the principal olive, immediately adjacent to the dorsal lamella's lateral indentation; the mid-MAO, just medial to the middle of the nucleus; the rDAO, in the middle of its mediolateral span; and the caudal ventral leaf of the principal olive, two small cell groups near its lateral and medial edge. This indicates that the majority of the injection site was in Voogd's zone D1, a smaller contribution from zone D2 and some involvement from C2 and C1 and 3 zones.

The vast majority of labelled terminals in this case were confined to the ipsilateral dentate nucleus. Additional label was also found in the NIP.

The ventral dentate contained a very large amount of terminal label in its caudal half (zone D1). The areas of densest dentate label formed stripes running in a somewhat slanted medio-lateral direction across much of the nucleus. At its greatest extent, the terminal field consisted of stripes filling the entire ventral half of the nucleus, although frequently the medial portions of the nucleus were free from label. At the caudal end of the dentate, the stripes disappeared and there was a solitary terminal patch at the medial edge of the nucleus, opposite a similar one in the caudal NIP (zone C2). The solitary dentate terminal patch resembled a medial extension of one of the terminal stripes that had been broken off by the white matter islands that run in through the caudal dentate.

Patches of labelled terminals were seen in the caudal half of the posterior interposed nucleus (zone C2). The rostral levels of the NIP terminal fields consisted of two patches. One was situated in the very dorsal tip of the nucleus, and the other at the lateral edge in mid-dorsoventral levels, immediately adjacent to the medial patch in the dentate. At more

caudal levels, a single large terminal patch was found in the very ventro-caudal tip of the nucleus.

The NRTP/pontocerebellar projection

It would be impossible to form any rigorous conclusions about this particular set of data as the animal received two injections, and there is a bilateral component (albeit small) to the pontocerebellar projection. For both injections in this animal, I shall briefly describe the contralateral pontine label, with the caveat that it cannot be a completely accurate picture.
Label in the pontine nuclei was extremely widespread, with labelled cells evident in every nucleus at some rostrocaudal level. The cell groups form a ring around the perimeter of the pons with midline predominance. There was dorsolateral label present only in the rostral half of the pons.

Labelled cells were only present in the rostral half of the NRTP. They were seen in central, dorsomedial and ventromedial areas of the nucleus.

The nucleo-cortical projection

Previous reports have shown that the nucleo-cortical projection may, too, have a contralateral component, which would preclude rigorous conclusions drawn from an experimental animal with bilateral injections. However, none of the nucleo-cortical data presented in this thesis shows any evidence of a contralateral projection, so I shall describe the nucleo-cortical projections for both injection sites in this animal.

A large number of retrogradely labelled cells were found in this case, the majority of which were again located outside the main terminal fields in NIP and NL.
Labelled cells were found in the posterior interposed rostral to the terminal label. The collection of cells grouped together in such a way as to form a dorsally-directed arrowhead, spanning the medio-lateral extent of the nucleus.
Overall less retrograde cellular label was found in the dentate than in NIP. Label was seen in the caudal three-quarters of the NL terminal field's extent. At caudal levels of the retrograde label, the cells were located ventral to the terminal field. The majority of the

labelled cells, however, were seen at slightly more rostral levels where they were situated in a medio-lateral strip dorsal to the terminal field.

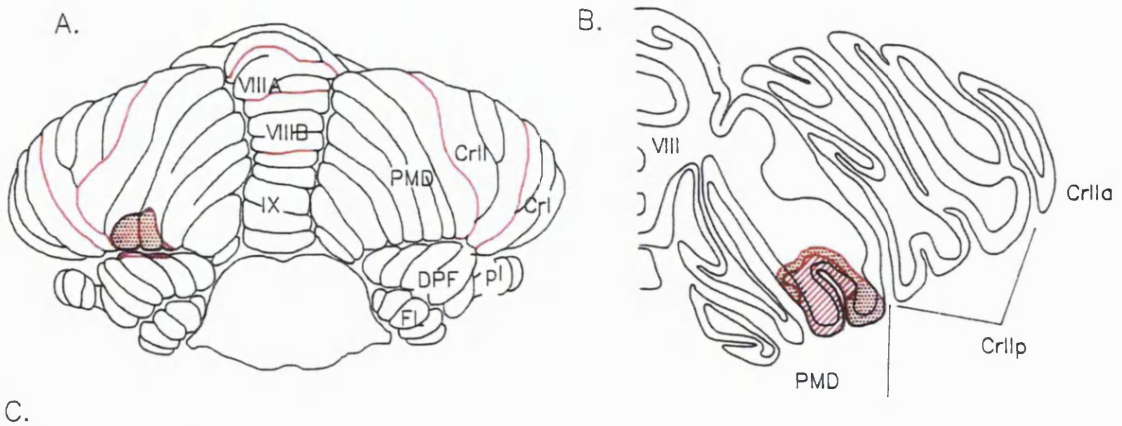

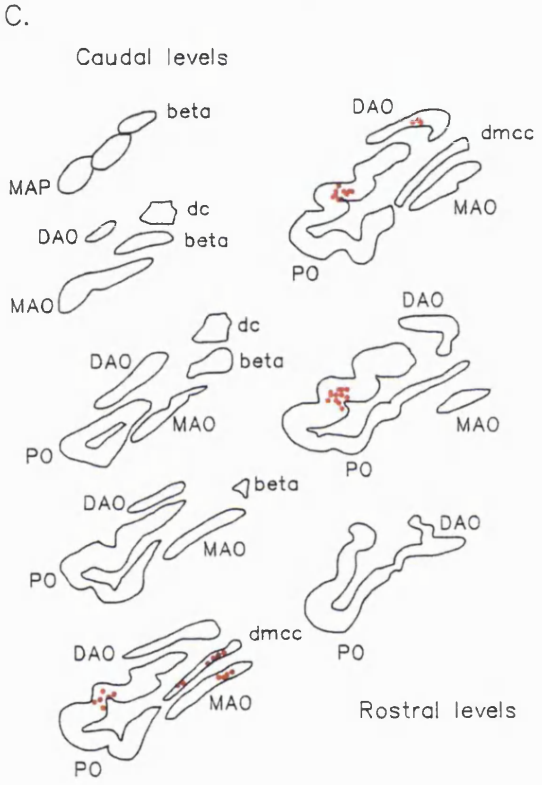

Figure 20: M2-96left - paramedian lobule injection

A: Maximum extent of the effective injection site in a diagram of the surface of the cerebellum.

B: Coronal section of the cerebellum through the area of maximum extent of the injection.
TMB=dots, DAB=lines

C: A series of equally spaced sections (approx 750μm) through the inferior olive showing the location of individual retrogradely labelled nuclei.

D: A series of equally spaced (500μm) coronal sections through the deep cerebellar nuclei showing position and density of anterogradely labelled terminals.

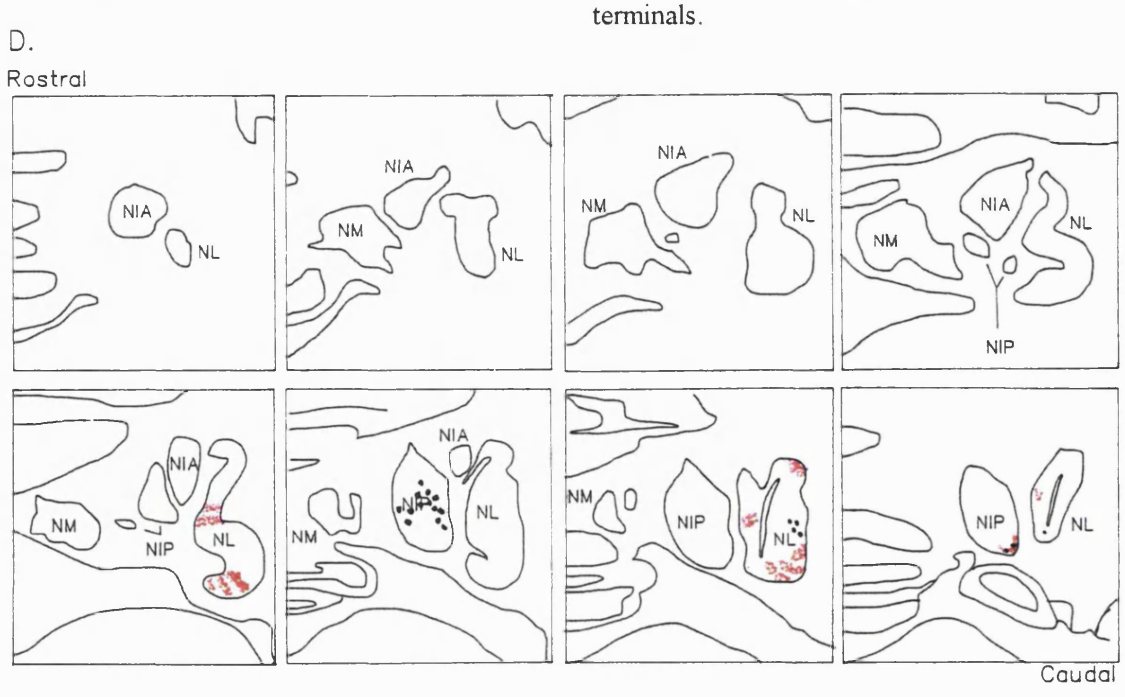

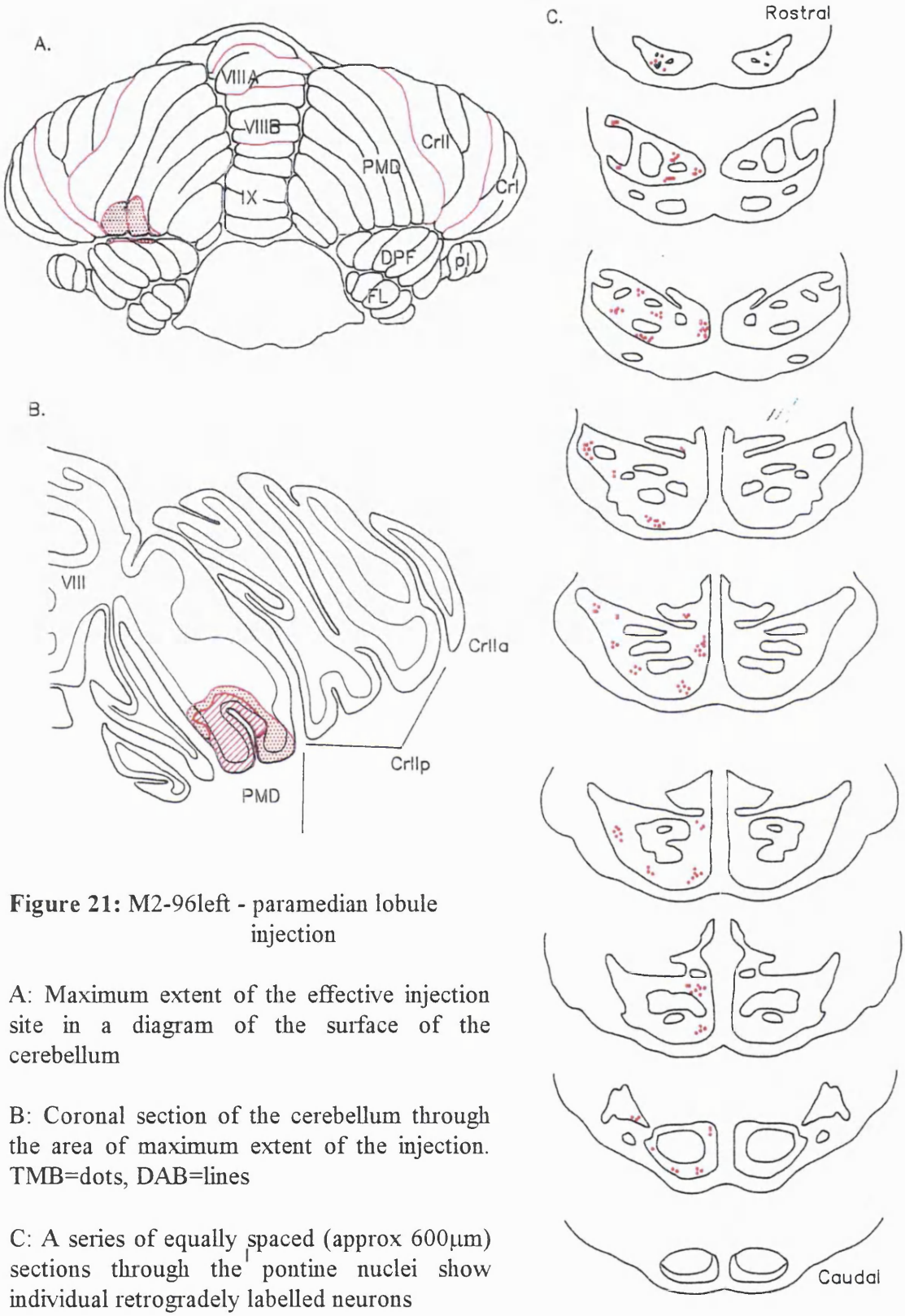

Figure 21: M2-96left - paramedian lobule injection

A: Maximum extent of the effective injection site in a diagram of the surface of the cerebellum

B: Coronal section of the cerebellum through the area of maximum extent of the injection. TMB=dots, DAB=lines

C: A series of equally spaced (approx 600µm) sections through the pontine nuclei show individual retrogradely labelled neurons

3.1.2.2 Crus II lobule

a) Case M2-96 (Right hemisphere)

Injection site

See figures 22 and 23.

The injection in this case was placed in the centre of the most medial folium in crus IIp, at the border with the paramedian lobule, and therefore caudally in the crus II folial chain. It did not extend right to the base of the folium, nor did it spread into the paramedian lobule.

The olivocorticonuclear projection

Retrogradely labelled cells in the olive were focused in the ventral edge of the lateral bend in the principal olive. The cells were clumped tightly together and lay very close to the outside border of the olive at its mid and mid-rostral levels. The injection was therefore very discrete and lay in Voogd's zone D1.

Nuclear terminal label was found in the dentate and both interposed nuclei. The terminal patch in the posterior interposed consisted of a single strip that lay in the ventrolateral corner of the mid-caudal NIP (C2). The anterior interposed (C1 and C3) contained only one small patch of terminal label in its extreme dorsolateral corner, adjacent to a number of terminal stripes in dorsal levels of the dentate.

Terminal label in the dentate covered the caudal half of the nucleus (zone D1). The majority of the terminal label was arranged as stripes directed mediolaterally in the ventral half of the nucleus. The extreme rostral end of the terminal field, contained three stripes of anterograde terminal label in the dorsal tip of the dentate.

The NRTP/pontocerebellar projection

This animal received a second injection in the left hemisphere, so it is hard to make rigorous conclusions on this pathway in this case, in view of the limited bilateral component to the pontocerebellar pathway. The following results are based on the strongest label found in the pontine nuclei and NRTP contralateral to the injection site.

The entire rostrocaudal length of the pontine nuclei contained labelled cells. The majority of cells were arranged in clumps in an arc around the medial aspect of the CST fascicles, with cells being seen in the dorsal, dorsomedial, paramedian, ventromedial and ventral nuclei. In addition, at more rostral levels, many labelled cells were seen in between the fascicles of the CST in the peripeduncular nucleus, and in the extreme dorsolateral nucleus.

Labelled cells were only found in the rostral half of the NRTP. They were seen in a ventromedial clump, which seemed to be continuous with a dorsomedial patch in the pons directly ventral to the NRTP. At a slightly more caudal level, there was a patch of labelled cells in the central NRTP.

The nucleo-cortical projection

Cellular label was encountered in the posterior interposed and the dentate. Within these nuclei, the bulk of the labelled cells were located outside the terminal fields.

Labelled cells in the posterior interposed nucleus were only found dorsal to the most rostral level of the terminal field in this nucleus. The cells grouped laterally in the space between the terminal field and the indentation of the posterior interposed.

The dentate contained labelled cells across its entire mediolateral extent at the same rostrocaudal level as the label in the posterior interposed. The cells were situated dorsal to the terminal field, although a few cells were located in the lateral edge of the most dorsally located terminal strip. A few more cells were again seen in this same strip more caudally, although at this level, they lie more centrally within it. Cells lying within and outside terminal fields were of similar size ranges.

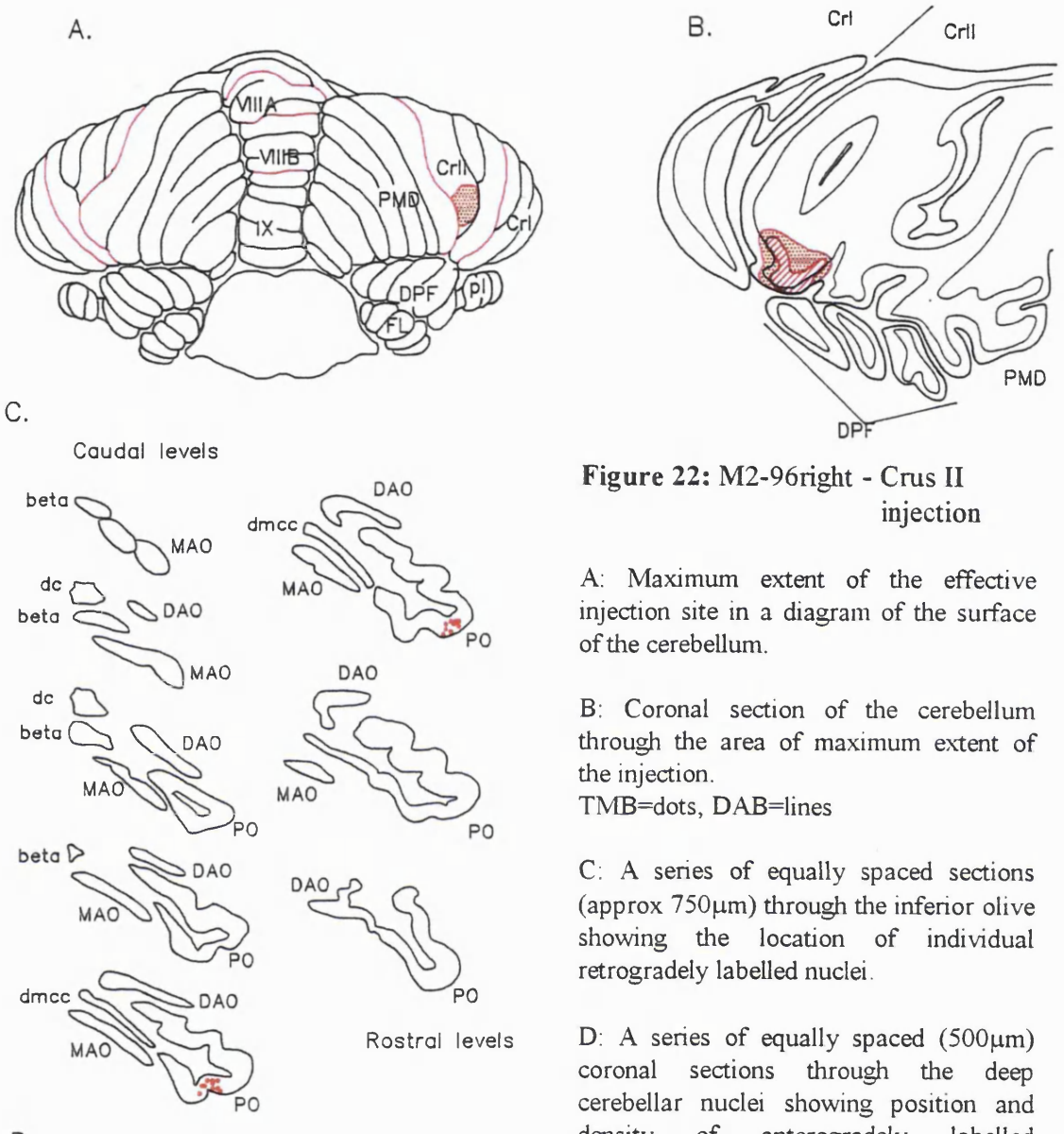

Figure 22: M2-96right - Crus II injection

A: Maximum extent of the effective injection site in a diagram of the surface of the cerebellum.

B: Coronal section of the cerebellum through the area of maximum extent of the injection.
TMB=dots, DAB=lines

C: A series of equally spaced sections (approx 750µm) through the inferior olive showing the location of individual retrogradely labelled nuclei.

D: A series of equally spaced (500µm) coronal sections through the deep cerebellar nuclei showing position and density of anterogradely labelled terminals.

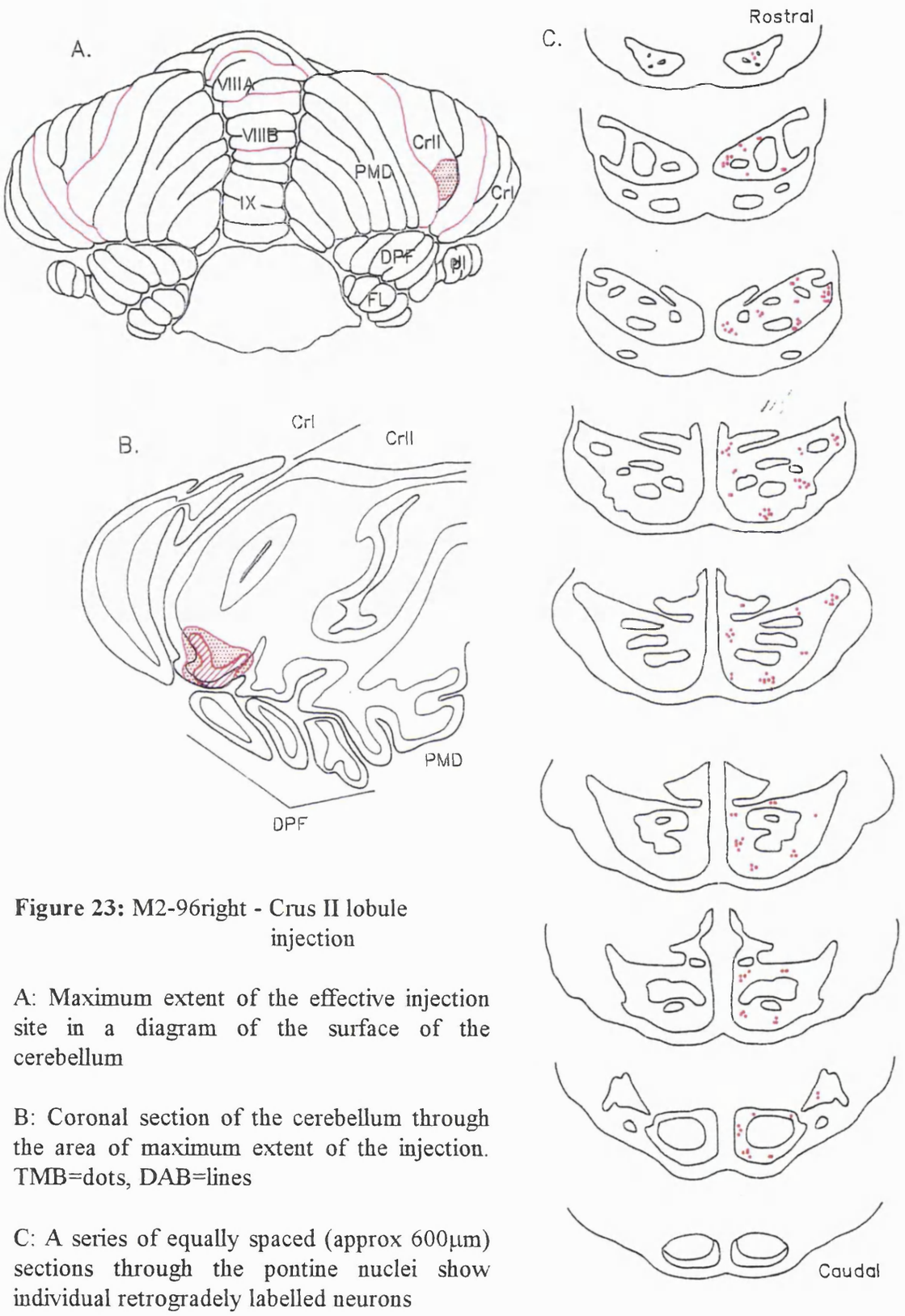

Figure 23: M2-96right - Crus II lobule injection

A: Maximum extent of the effective injection site in a diagram of the surface of the cerebellum

B: Coronal section of the cerebellum through the area of maximum extent of the injection. TMB=dots, DAB=lines

C: A series of equally spaced (approx 600μm) sections through the pontine nuclei show individual retrogradely labelled neurons

b) Case SB6

Injection site

See figures 24 and 25.

This animal received a WGA-HRP injection into crus II of the right hemisphere. The injection was centred on the intracrural fissure that separates crus IIp and crus IIa, and thus lay at mid-levels of the crus II chain. The spread of the tracer was almost equal on either side of the fissure, and there was no leak of the injection site into either the paramedian lobule or the dorsal paraflocculus.

The olivocorticonuclear projection

Retrogradely labelled cells in the inferior olive were confined contralaterally to the ventral portion of the principal olive's lateral bend. The cells clumped tightly together to form a discrete group in this region, and the label started at mid-levels and extended almost to the rostral end of the olive. The olivary label indicates that the injection site was completely restricted to zone D1.

Nuclear terminal label was located primarily in the ipsilateral dentate nucleus, with a small contribution to the posterior interposed. The single patch of labelled terminals in the posterior interposed was confined to the ventrolateral edge at mid-caudal levels (zone C2). The dentate terminal field covered the caudal two-fifths of the nucleus (zone D1). The terminal field was arranged into stripes running round medial to lateral across the entire width of the nucleus. At the most rostral levels of the terminal label, the stripes covered the dorso-ventral length of the dentate too, with very dense bands of label being interleaved with strips of sparsely labelled fibres. At more caudal levels, however, the number of stripes decreased, and at the most caudal level, they broke up into smaller islands of labelled terminals.

The NRTP/pontocerebellar projection

Clusters of labelled cells were seen contralaterally throughout all but the most caudal pontine nuclei. The labelled cells formed a ring right the way round the CST fibres, such that all of the nuclei within the pons contained labelled cells, with the exception of the

area in between the fascicles of the descending CST. There was a slight predominance of the medial nuclei, with two large cell groups in the ventromedial and dorsomedial nuclei. A considerable level of ipsilateral label was present too. These cells mirrored the largest cell groups on the contralateral side, i.e. the dorsomedial, ventromedial and dorsolateral nuclei at mid-levels of the pons.

Labelled cells in the contralateral NRTP were found ventrally and centrally throughout its extent, with a few labelled cells found dorsolaterally at mid-rostrocaudal levels. The ipsilateral NRTP also contained labelled cells in approximately corresponding numbers and positions to those on the contralateral side.

The nucleo-cortical projection

Retrogradely labelled cells in this case were found only in the ipsilateral dentate. None were seen in the posterior interposed, even within the terminal label fields. The population of labelled cells in the dentate extended for all but the most caudal part of the terminal field. Approximately half of the labelled cells were located outside the terminal fields, and even those that were within label were consistently encountered ventrally in the lighter rather than denser terminal fields. All nucleo-cortical cells were of similar size ranges, regardless of their position relative to the nuclear terminal field.
The cells showed no indication of grouping in a recognisable pattern.

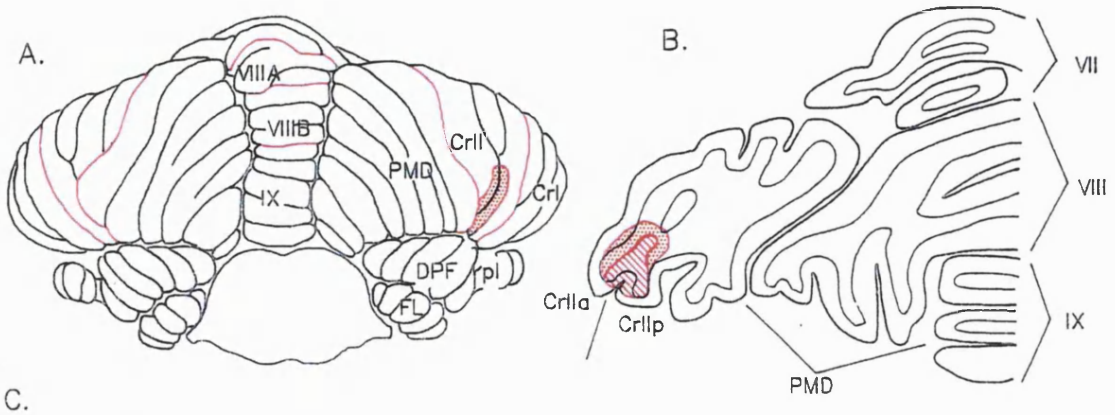

C.

Caudal level

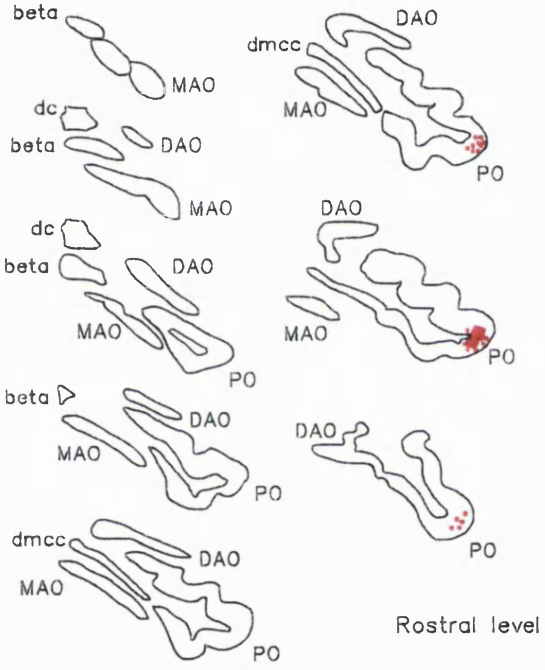

Figure 24: Sb6 - Crus II injection

A: Maximum extent of the effective injection site in a diagram of the surface of the cerebellum.

B: Coronal section of the cerebellum through the area of maximum extent of the injection.
TMB=dots, DAB=lines

C: A series of equally spaced sections (approx 750µm) through the inferior olive showing the location of individual retrogradely labelled nuclei.

D: A series of equally spaced (500µm) coronal sections through the deep cerebellar nuclei showing position and density of anterogradely labelled terminals.

D.

Rostral

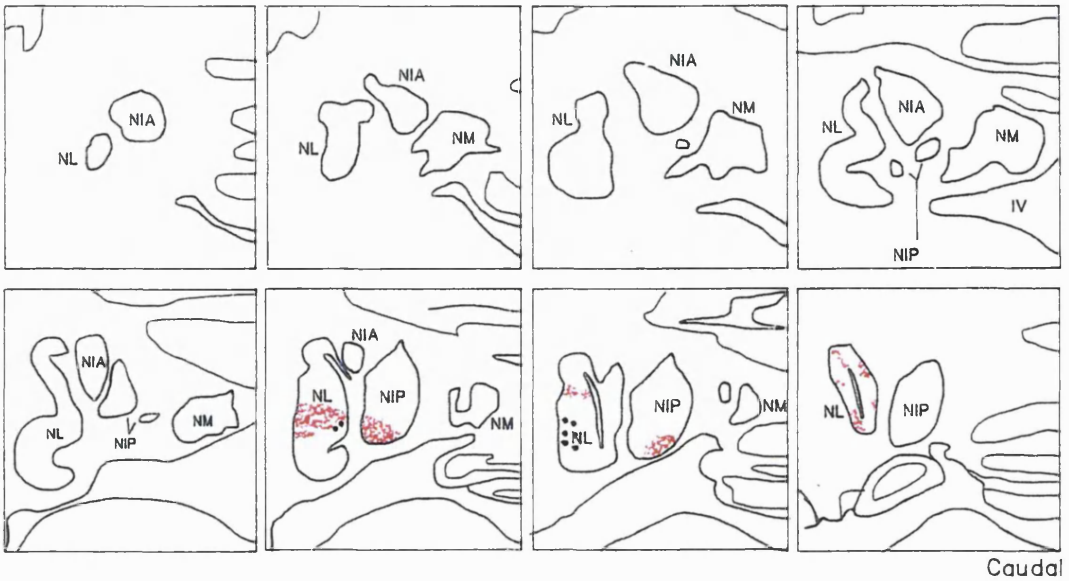

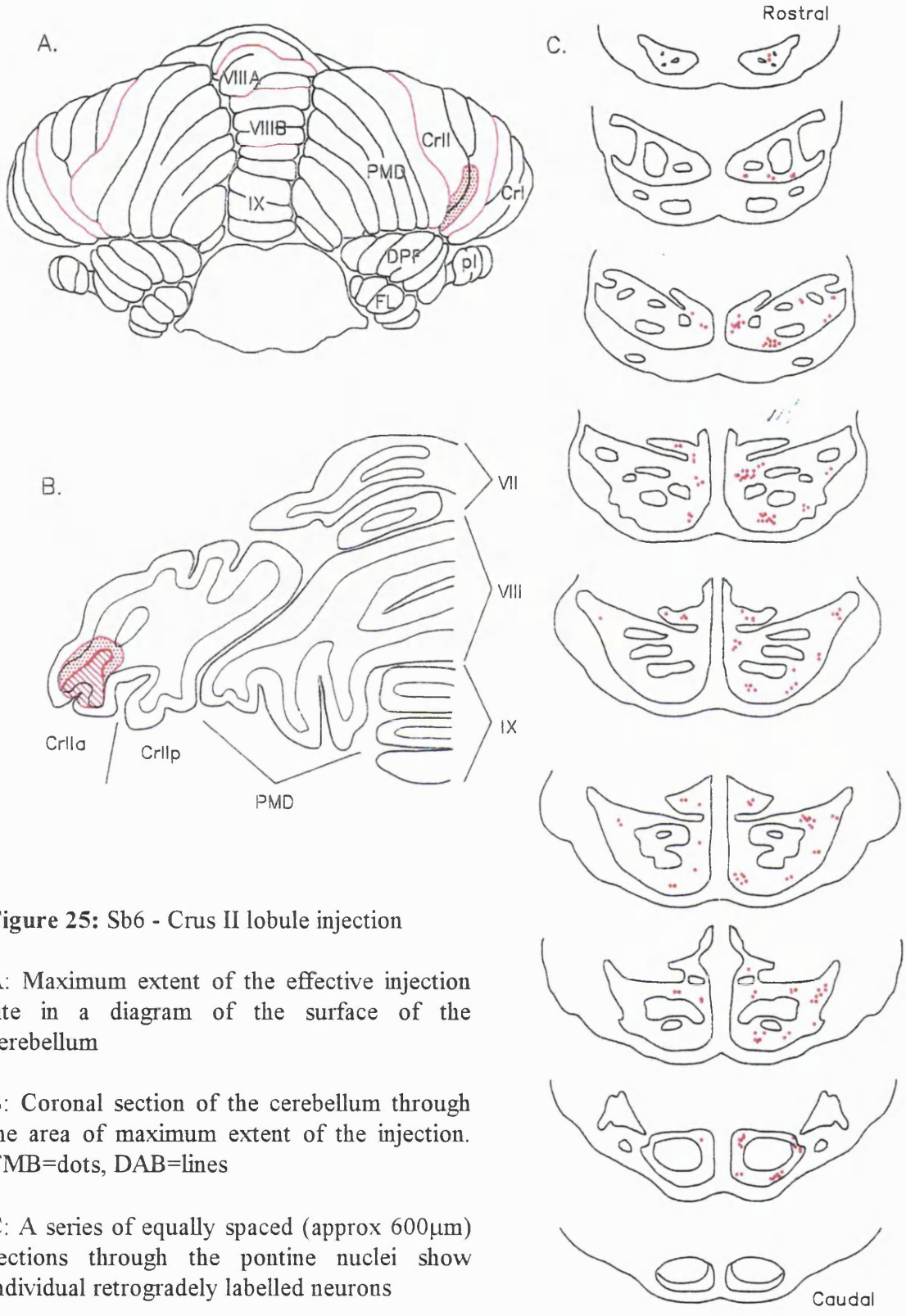

Figure 25: Sb6 - Crus II lobule injection

A: Maximum extent of the effective injection site in a diagram of the surface of the cerebellum

B: Coronal section of the cerebellum through the area of maximum extent of the injection. TMB=dots, DAB=lines

C: A series of equally spaced (approx 600μm) sections through the pontine nuclei show individual retrogradely labelled neurons

3.1.2.3 SUMMARY

The conclusions portion of this results chapter will begin with a separate consideration of connections of the paramedian lobule and crus II. The final analysis will comprise a comparison of the two cerebellar areas.

As the summary will discuss the injection sites in terms of the zonal subdivisions of the cortex, descriptions of the injection sites will focus on their rostro-caudal position within the folial chain.

A. Paramedian lobule

<u>The olivocerebellar projection</u>

Three of the four paramedian lobule cases (GR-95, Co5 and m2-96left) were all situated in the lateral folia of the lobule, at the border with the medial edge of crus II. These cases therefore were positioned *rostrally* with respect to the folial chain.

PMD2, on the other hand lay ventromedially, in a folium adjacent to the vermis, and thus *caudally* in the paramedian folial chain.

All of the paramedian lobule cases involved injections into cortical zone D1, as evidenced by retrogradely labelled olivary cells in the dorsal leaf and lateral bend. There was evidence of a more detailed topography in the olivocerebellar projection: for the cases in the rostral levels of the chain (in lateral paramedian folia), the olivary label was situated at mid-to-rostral levels, and mid-mediolateral distance, focusing around the two invaginations within dorsal lamella. The caudal case, adjacent to the vermis, however, contained dorsal lamella and thus still D1 label, but at extreme medial and rostral levels.

There was also some indication of a very detailed olivocerebellar topography within the rostral cases, as in spite of very similar injection sites and olivary label, there were slight variations in the mediolateral or rostrocaudal positions of the olivary label. However, it was impossible to discern a consistent topography, and more cases would be required to satisfactorily suggest a pattern.

The cortico-nuclear projection

A difference between the rostral and caudal paramedian folial chain (lateral and medial folia) was also apparent in the cortico-nuclear projection. All the rostral cases projected preferentially to the caudal dentate (zone D1), with additional smaller projections to the posterior interposed. Instead, the caudal area projected to the most rostral levels of the dentate (zone D2), with additional projections to the anterior and posterior interposed. Nuclear projections from the caudal and rostral levels of the paramedian folial chain did not overlap in either the dentate or the interposed.

The terminal fields in the caudal dentate were consistently striped. The strips of terminal label ran mediolaterally from the hilus of the nucleus, with the interdigitating areas being free from label.

The olivocorticonuclear system in the paramedian lobule did not follow the parasagittal zonation precisely. A number of cases (e.g. cases PMD2 and M2-96left) contained olivary label appropriate to particular zones which were then not represented in the nuclear terminal field, while others (e.g. GR-95) contained nuclear projections into a zone which was not represented at the olivary level. Therefore both convergence and divergence from the parasagittal system occurs in the paramedian lobule. A particularly powerful example of the convergence in the olivocorticonuclear system was evident in the dentate nucleus. All of the cases in the rostral paramedian chain (lateral folia) contained olivary label in zone D1 and projected to the caudolateral D1 zone in the dentate. However, case M2-96left which contained olivary label in both the dorsal and ventral lamella simultaneously (and therefore included zones D1 and the D2), contained only one focus of striped terminal field - it was located in the caudal half of the dentate, a nuclear area associated with D1. Thus, this case demonstrated "intra-zonal" convergence as cortical D1 and D2 zones converged onto a single nuclear zone.

The NRTP/pontocerebellar projection

Due to the (limited) bilaterality of the pontocerebellar projection, the data from case M2-96left will not be discussed.

All paramedian lobule cases received input from the pontine nuclei, with no marked variation between the cases. GR-95 was unusual in having very sparse label, due to the superficiality of the injection site, with restricted label of the granular layer. The dorsolateral pontine nucleus contained fewer cells than the vermal cases, and although no nucleus was consistently over-represented, medial and ventral cell groups tended to dominate.

The clusters of labelled pontine cells covered the entire rostrocaudal length of the pons. Although the majority of cells were seen contralaterally, when ipsilateral label was found, it was usually a mirror-representation of the medial cell groups seen on the contralateral side.

The NRTP does not project to the paramedian lobule.

The nucleo-cortical pathway

The nucleo-cortical projection to the paramedian lobule is relatively sparse. The sparseness in some cases could be attributed to superficial injection sites, although correlation with the amount of pontine label, which arises as retrograde transport from the same cortical layer, would suggest that the projection is indeed small. There was no evidence of topography in the projection, and labelled cells were found both within and beyond terminal fields. The nucleo-cortical projection to the paramedian lobule therefore has reciprocal and non-reciprocal components, with no consistent morphological differences between them.

The nucleo-cortical projection has no contralateral component in the paramedian lobule.

B. CRUS II

The olivocerebellar projection

Both cases of crus II injections contained labelled cells restricted to the lateral bend of the principal olive, corresponding to zone D1. Olivary afferents to the more caudal areas of the crus II chain (case M2-96right) began at more caudal levels of the olive than those to the more rostral case (sb6). There was a small amount of overlap between the two at the rostral levels of m2-96right and caudal levels of sb6 olivary label.

The cortico-nuclear projection

Both cases contained terminal fields in the posterior interposed and the dentate nuclei. The terminal fields overlapped completely in the posterior interposed, but there was no overlap of dentate terminal fields: terminal fields in case m2-96right (caudal chain) began more rostrally than those in sb6 (rostral chain). When there was overlap in the rostrocaudal dimension, the terminal fields in the two cases were separated dorsoventrally until the most caudal levels of the nucleus. As in the paramedian lobule cases, the terminal fields in the dentate were striped.

The crus II cases provided another example of divergence from the parasagittal zonation of the olivocorticonuclear projection. Both cases lacked olivary label for the C2 zone (rostral medial accessory), but contained strong, overlapping terminal fields in the C2 nuclear zone (posterior interposed nucleus). There was no indication of convergence of two cortical D zones onto a single nuclear zone.

The NRTP/pontocerebellar projection

Case m2-96right will not be discussed here, due to the bilaterality of the pontocerebellar projection.

The majority of retrogradely labelled pontine cells were seen contralaterally, forming a ring around the fascicles of the cortico-spinal tract. A few cells were seen near or inside the dorsolateral pontine nucleus, but on the whole, they were focused in ventral and dorsomedial nuclear groups. The ipsilateral component was modest and in general mirrored the medial groups on the contralateral side.

The NRTP projects to the crus II, albeit moderately. Labelled cells were found in the central areas of the contralateral nucleus, with a relatively strong ipsilateral component.

The nucleo-cortical projection

Both cases in crus II showed evidence of a purely ipsilateral nucleo-cortical pathway. The projection from the deep nuclei is both reciprocal and non-reciprocal to the cortico-nuclear projection, with no evidence of topography. There was no evidence of morphological differences between reciprocal and non-reciprocal cortical afferents.

C. COMPARISON OF PARAMEDIAN LOBULE AND CRUS II

The olivocerebellar projection

Although all paramedian and crus II cases contained olivary label in the dorsal leaf and lateral bend, often situated close together, there were no instances of complete overlap in olivary afferents to these separate cortical areas. The crus II and paramedian cases with the most similar olivary label were Co5 (lateral paramedian lobule) and sb6 (medial crus II) which lay either side of the prepyramidal fissure and contained label in the lateral bend of the principal olive. In terms of the folial chain, case Co5 lay caudal to sb6, and its olivary label began at more caudal levels than that from sb6, indicating a rostrocaudal topography in the olivocerebellar pathway across the hemisphere.

The similarity, but segregation of olivary afferents to these cortical areas is a testament to the precision of the olivocerebellar pathway.

The cortico-nuclear projection

Projections from both crus II and neighbouring paramedian lobule focus onto the caudal dentate. Caudal levels of the paramedian folial chain project more rostrally in the dentate. The stripes inherent to the terminal fields were arranged similarly in both areas, but it is impossible to say from these single tracer studies whether they overlapped or interdigitated with one another. Projections from the crus II and paramedian lobule to the caudal posterior interposed showed clear overlap at mid-rostrocaudal levels of the nucleus. Both the crus II and paramedian lobule had connections which converged and diverged from the classical parasagittal zonation of the olivocorticonuclear projection.

The NRTP/pontocerebellar projection

Pontine labelling was similar following injections into the crus II and paramedian lobule, but it is impossible to determine from single-tracer studies whether the pontocerebellar projections to the crus II and paramedian lobule overlap or interdigitate.

There is, however, a clear dichotomy in projections from the NRTP to the paramedian lobule and crus II. There are no NRTP projections to the paramedian lobule, but moderately strong ones to crus II.

The nucleo-cortical projection

Both crus II and paramedian lobule received projections from the deep nuclei, both reciprocally and non-reciprocally. There was no evidence of overlap in the retrogradely labelled cell populations between the crus II and paramedian lobule cases. No symmetrical projections were encountered.

3.1.3 PARAFLOCCULAR AND FLOCCULAR COMPLEX

The folial chain bends laterally from the paramedian lobule into the rostrally directed portion of the loop, the petrosal lobule, which includes the dorsal and ventral paraflocculi. The caudalmost section of the chain as it bends medially again is the flocculus. Injection sites in the floccular complex can be described in terms of medial or lateral folia (and therefore rostral and caudal parts of the chain respectively). Due to difficulty in reaching the dorsal paraflocculus during surgery, all of the cases in this chapter are focused on approximately identical folia, which precluded any attempts at detailed descriptions of mediolateral/caudorostral topography. Thus these cases will be described purely in terms of their positions in the floccular complex as a whole, without reference to their position in the folial chain

3.1.3.1 Dorsal paraflocculus

a) Case M 696

In this case, the cerebellum was cut parasagittally, making comparisons more difficult. Nonetheless, it was a good case which merited study.

Injection site

See figures 26 and 27.

The injection site in this case straddled folia 5 and 6 of the dorsal paraflocculus, but did not cover the entire extent of either. The lateral edge of folium 6 and the medial edge of folium 5 did not contain labelled Purkinje cells, nor did the very anterior and posterior portions of this area. As a result, the injection site was very discrete and restricted to the dorsal paraflocculus, and there was no spread of the label into the flocculus beneath or the ventral paraflocculus rostrally.

The olivocorticonuclear projection

The majority of labelled olivary cells were found in the principal olive: most were grouped in the ventral leaf, although a number were also found in the dorsal leaf and

lateral bend. The label in the principal olive covered the caudal half of the nucleus, and in the most rostral of the labelled sections, cells were also seen in the rostral MAO.
The olivary data indicated that Voogd's zones C2, D1 and D2 had been involved in the injection site.

Nuclear terminal label was confined to the posterior interpositus and dentate nuclei. The terminal field in the posterior interpositus formed a band covering the edges of the caudolateral half of the nucleus (C2). The lateral edge of the terminal field appeared to cover a greater dorsoventral extent of the nucleus than the medial edge, particularly at rostral levels of the label.
The dentate label was less restricted than that of the posterior interpositus - it covered a greater mediolateral proportion of its nucleus, and was not confined simply to caudal levels (and therefore included D1 and D2 zones). The very medial edge of the dentate contained no labelled terminals. As the middle of the nucleus is reached, the terminal field formed two patches ventrally, one rostral and one caudal, the latter being the larger of the two. More laterally, the caudal patch expanded to fill the entire rostrocaudal extent of the caudal end of the nucleus. In the most lateral portions of the dentate, the labelled terminals formed a strip over the ventral edge of the nucleus in its caudal third quarter.

The NRTP/pontocerebellar projection

Pontine label was very strong contralaterally in this case, and evident at all levels except only the most rostral ones. The labelled cells formed a ring round the extreme perimeter of the pontine nuclei, such that label was encountered in every division of the pons, and in addition, a number of labelled cells were also found in between the fascicles of the CST. The label in the dorsolateral pontine nucleus was particularly dense. The ipsilateral component of this projection was restricted to those levels and nuclei which are heaviest labelled contralaterally, i.e. the dorsolateral, lateral and midline nuclei at mid to caudal levels.

The NRTP contained four cells centrally, just caudal to its middle level. In addition, a few cells were encountered ventromedially immediately caudal to the central label. These cells were only found contralateral to the injection site.

The nucleo-cortical projection

Labelled cells in this case were found in both nuclei displaying a terminal field, namely the NIP and NL.

Cells in the posterior interposed were found lying centrally within the terminal fields throughout their rostro-caudal and mediolateral extents (except for the most medial areas). At middle levels of the posterior interposed, the cells were less clearly grouped within the labelled terminals and indeed a number of cells were found outside the labelled areas.

The dentate contained retrogradely labelled cells in a number of its terminal fields, and only a very few cells were found outside terminal label.

There were no consistent differences in cell sizes of reciprocal and non-reciprocal cortical afferents.

No cells were found contralaterally.

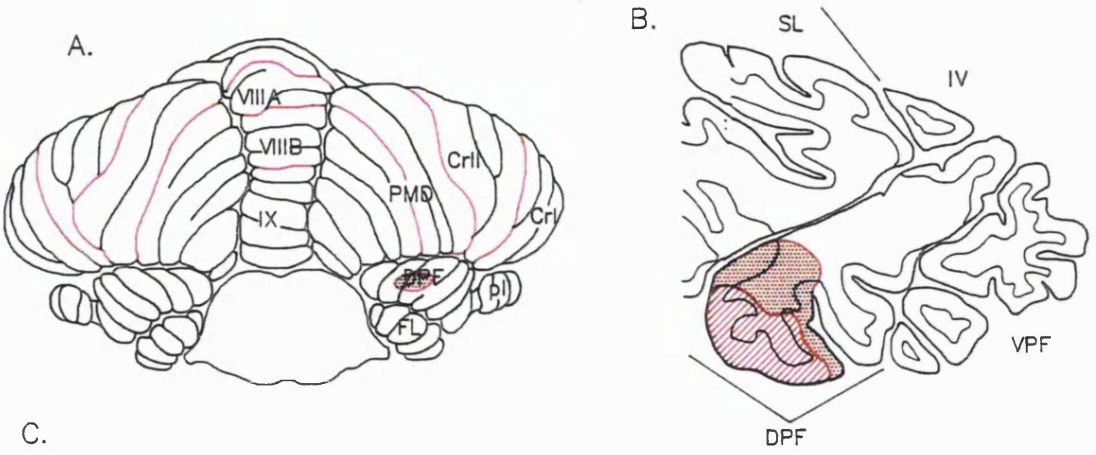

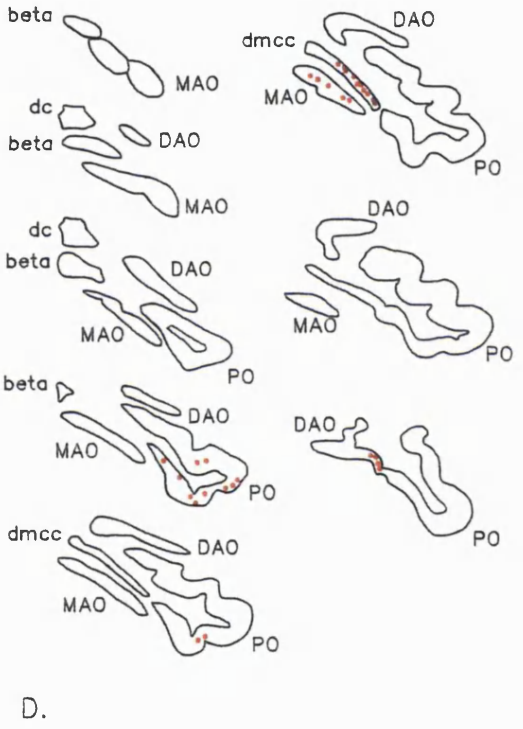

Figure 26: M696 - Dorsal paraflocculus injection

A: Maximum extent of the effective injection site in a diagram of the surface of the cerebellum.

B: Coronal section of the cerebellum through the area of maximum extent of the injection.
TMB=dots, DAB=lines

C: A series of equally spaced sections (approx 750μm) through the inferior olive showing the location of individual retrogradely labelled nuclei.

D: A series of equally spaced (500μm) coronal sections through the deep cerebellar nuclei showing position and density of anterogradely labelled terminals.

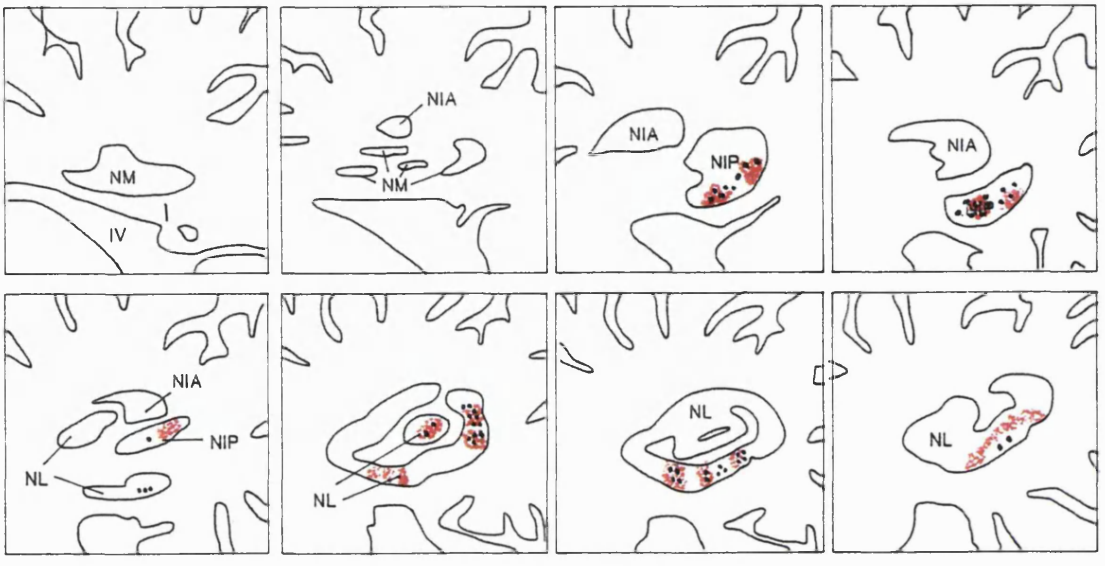

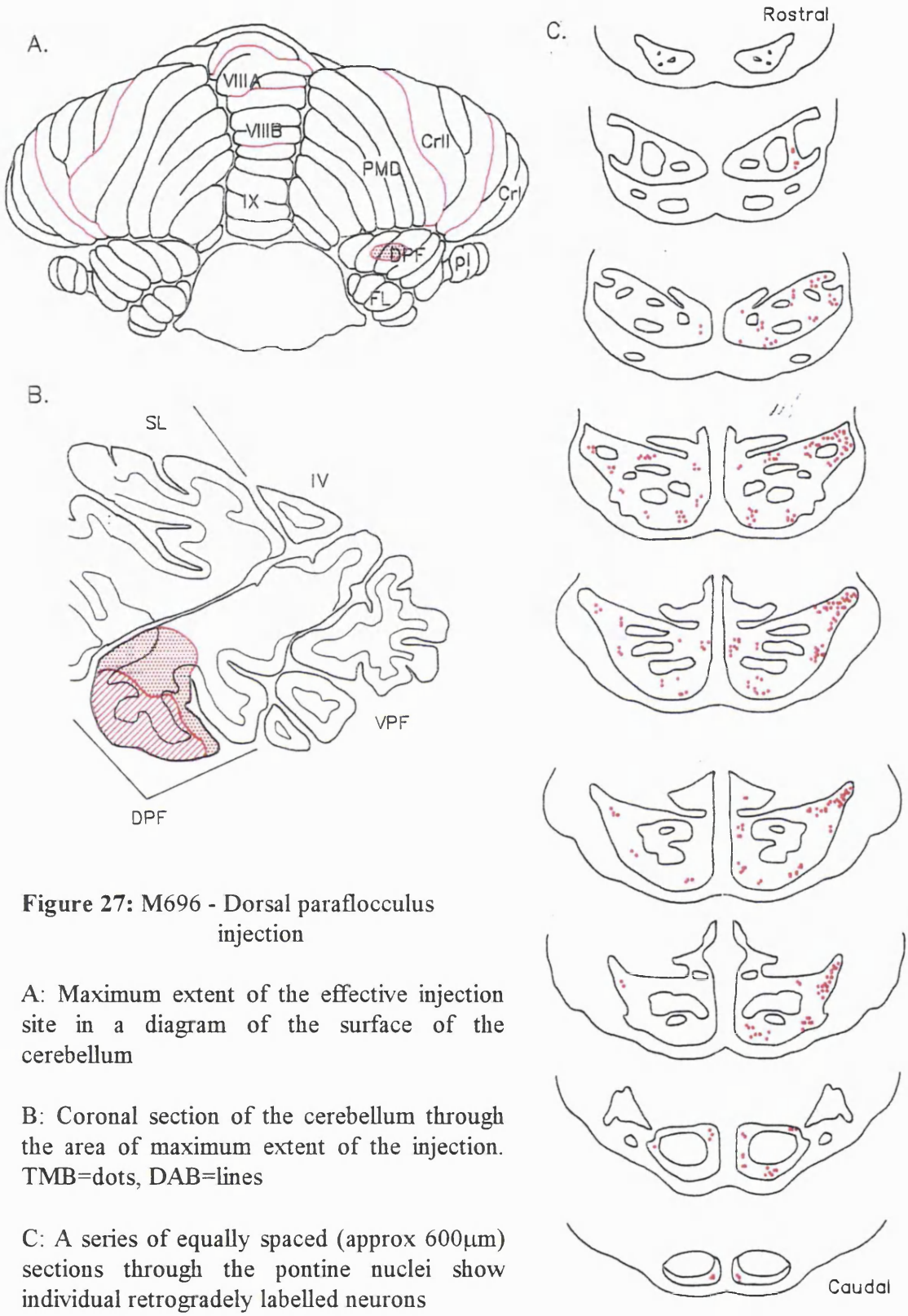

Figure 27: M696 - Dorsal paraflocculus injection

A: Maximum extent of the effective injection site in a diagram of the surface of the cerebellum

B: Coronal section of the cerebellum through the area of maximum extent of the injection. TMB=dots, DAB=lines

C: A series of equally spaced (approx 600μm) sections through the pontine nuclei show individual retrogradely labelled neurons

b) Case DPF1

Injection site

See figures 28 and 29.

The injection site in this case was totally confined to folium 6 of the dorsal paraflocculus. There was no spread of the label medio-laterally or rostro-caudally. Indeed, the areas abutting the overlying paramedian lobule were devoid of labelled Purkinje cells.

The olivocorticonuclear projection

Labelled cells in this case were restricted to only two divisions of the inferior olive. The majority of cells were found in the rMAO, and a few were seen in the caudal ventral leaf of the principal olive.

The label in the inferior olive indicates that the injection site mostly comprised Voogd's zone C2, with a small contribution from D2.

The majority of labelled terminals were found in the caudal quarter of the posterior interpositus nucleus (C2). At its rostral end, the terminal field formed a strip running dorsolaterally from the medial portion of the nucleus. This strip appeared to continue into the lateral edge of the caudal dentate (D1). Moving more caudally, the terminal field in the dentate disappeared, and that of the posterior interposed became restricted to the ventrolateral edge of the nucleus.

The NRTP/pontocerebellar projection

Labelled cells were found contralaterally throughout the rostro-caudal extent of the pons in this case. The heaviest label was focused within the dorsolateral and lateral nuclei. Additional small cell groups were found ventrally, dorsomedial and in between the fascicles of the CST.

Ipsilateral to the injection site, labelled cells were seen in the lateral, ventral and dorsomedial nuclei.

No labelled cells were found anywhere within the NRTP.

The nucleo-cortical projection

A few labelled cells were found only in the ipsilateral posterior interposed, at the level of the densest terminal field. The cells inside and outside the terminal field were morphologically similar.

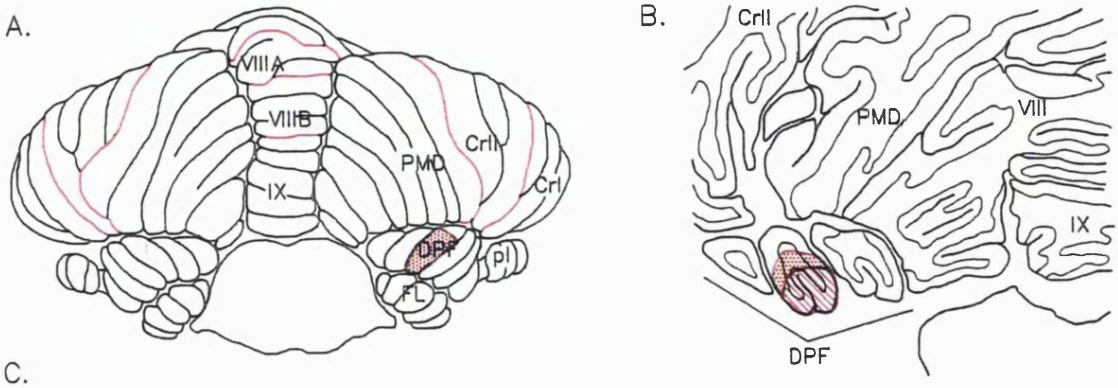

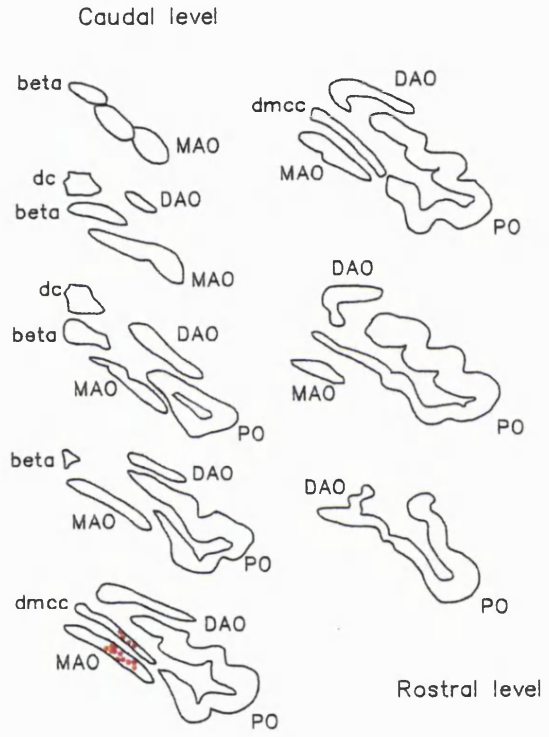

Figure 28: dpf1 - Dorsal paraflocculus injection

A: Maximum extent of the effective injection site in a diagram of the surface of the cerebellum.

B: Coronal section of the cerebellum through the area of maximum extent of the injection.
TMB=dots, DAB=lines

C: A series of equally spaced sections (approx 750µm) through the inferior olive showing the location of individual retrogradely labelled nuclei.

D: A series of equally spaced (500µm) coronal sections through the deep cerebellar nuclei showing position and density of anterogradely labelled terminals.

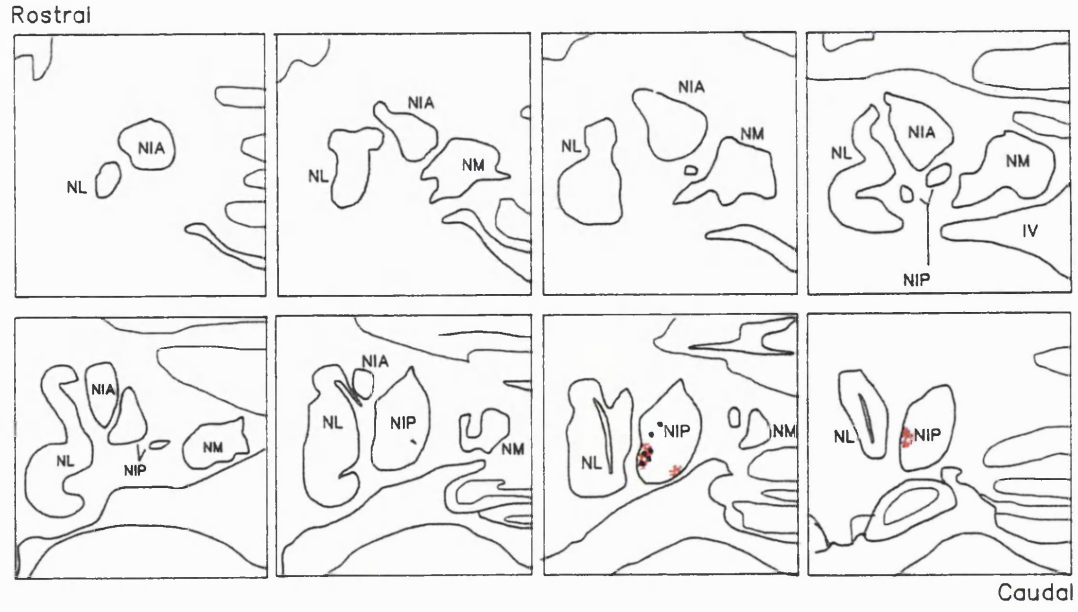

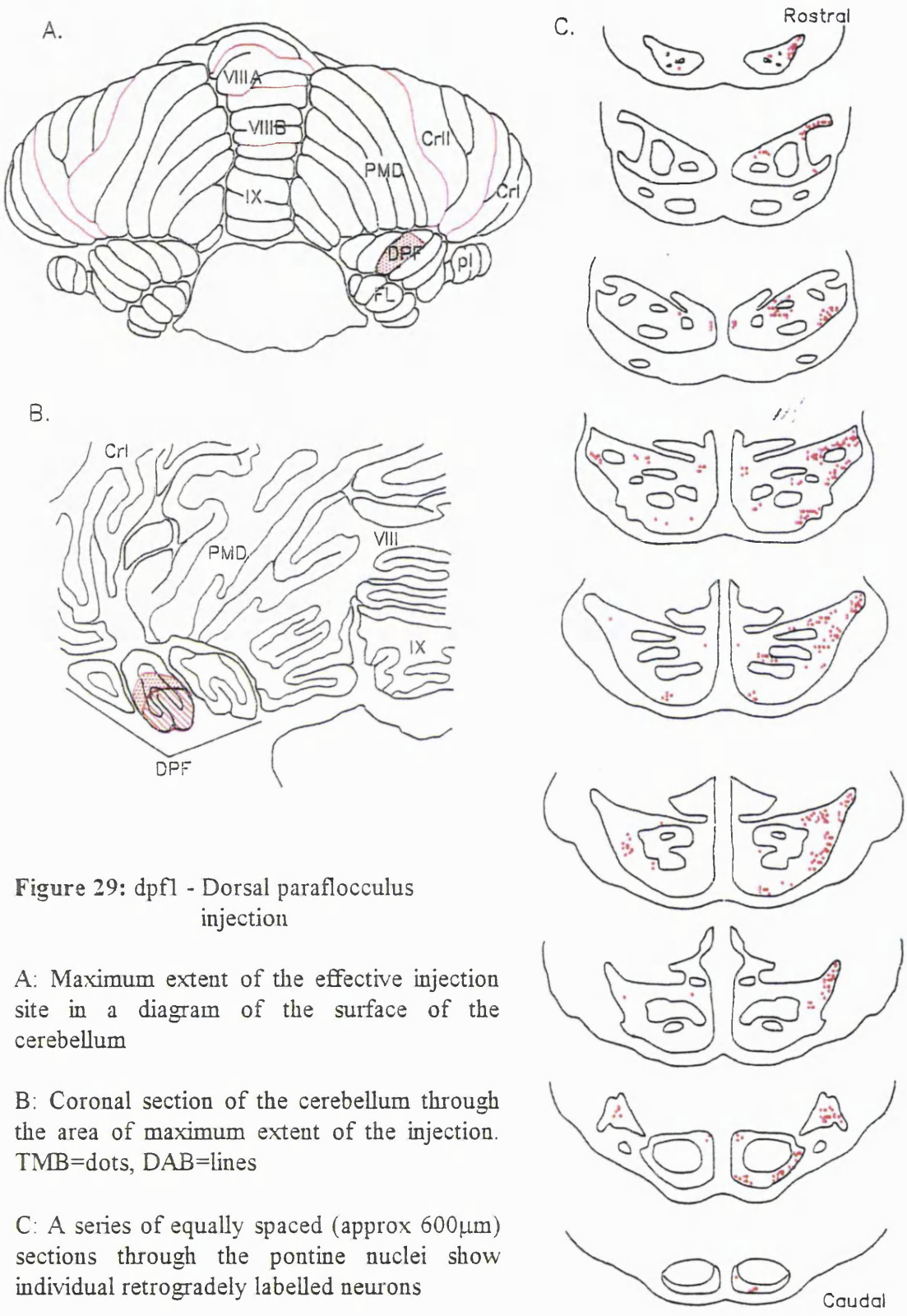

Figure 29: dpfl - Dorsal paraflocculus injection

A: Maximum extent of the effective injection site in a diagram of the surface of the cerebellum

B: Coronal section of the cerebellum through the area of maximum extent of the injection. TMB=dots, DAB=lines

C: A series of equally spaced (approx 600µm) sections through the pontine nuclei show individual retrogradely labelled neurons

c) Case HN-95

Injection site

See figures 30 and 31.

The injection site in this animal covered the whole of folium 6 of the dorsal paraflocculus. The injection site spread along the fissure separating the paramedian lobule and crus II, such that the base of crus IIp was included.

The olivocorticonuclear pathway

The majority of labelled cells in the inferior olive were found in the dorsal leaf and lateral bend of the caudal principal olive. They formed three clumps of cells, separated by areas in which the somata contained no WGA-HRP granular deposit. In addition, a number of cells were seen laterally in the middle levels of the ventral leaf. The position of the retrogradely labelled cells is typical of an injection into Voogd's D1 and D2 zones.

Labelled terminals were found in the caudal half of the deep nuclear complex. Moving caudally, the terminal field began in the dentate (D1) as a narrow strip running mediolaterally towards the ventromedial indentation. At more caudal levels, this strip became orientated at an angle, with the lateral end being ventral to the medial one. In the caudal third of the posterior interposed (C2), terminals formed a band arising adjacent to the terminal field in the dentate, and following a U-shaped course around the ventrolateral edge of the nucleus. At its most caudal pole, the terminal field consisted of a small clump in the medial dentate, with a collection of terminals directly adjacent to it in the ventrolateral corner of the posterior interposed.

The NRTP/pontocerebellar projection

Pontine label was somewhat restricted for this case. Contralaterally, labelled cells were found in mid-rostrocaudal levels and were focused into clusters of cells, forming an arc around the ventral and lateral edge of pons. The densest collection of labelled cells was found in the dorsolateral nucleus. In addition, there were a few clumps of cells found in the dorsomedial nucleus.

Ipsilaterally, a few cells were seen in the ventral, lateral and dorsolateral nuclei.

The NRTP contained a few labelled cells in the midline and laterally. Both cell groups were found bilaterally at more caudal levels of the label's extent, but the vast majority of labelled cells were found contralaterally.

The nucleo-cortical projection

No retrogradely labelled cells were found anywhere in the deep nuclei. The injection site was somewhat superficial, and may not have labelled a sufficient area of granular layer to produce retrograde labelling of the nuclear cells. This is supported by the observation that pontine and NRTP label was also relatively sparse.

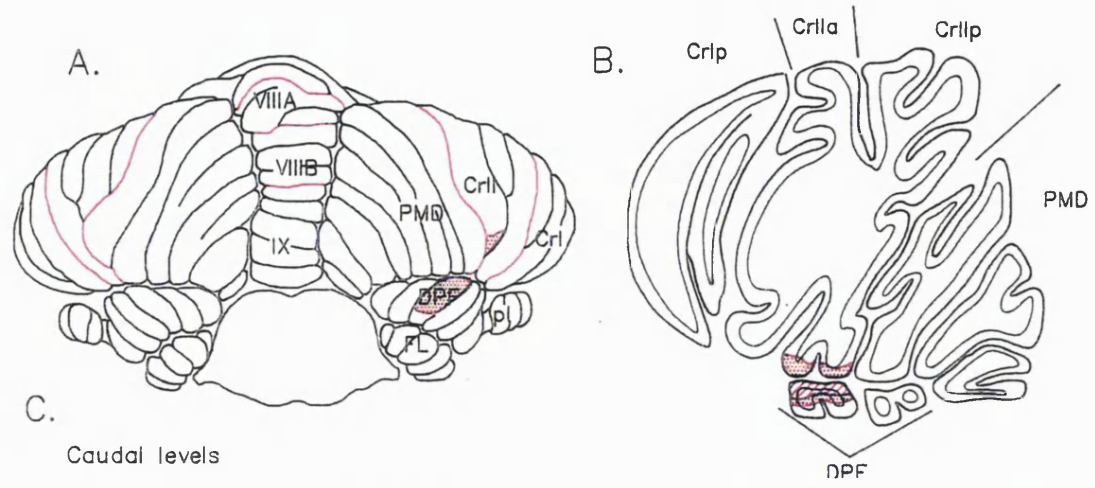

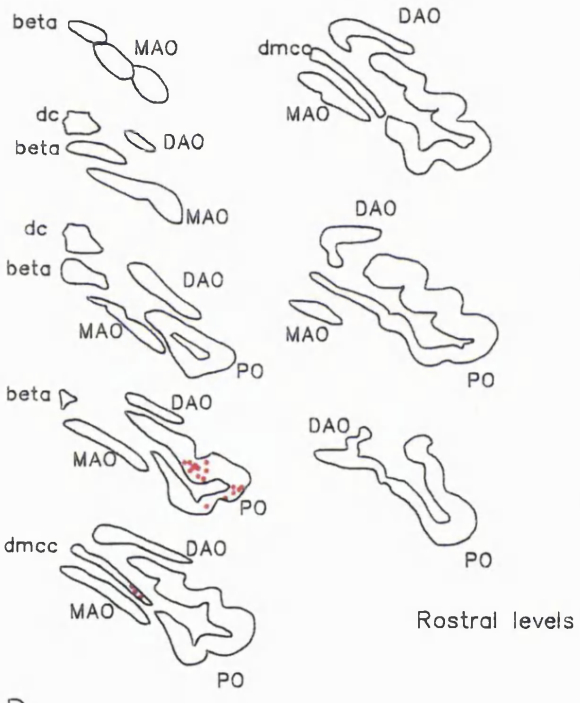

Figure 30: HN-95 - Dorsal paraflocculus injection

A: Maximum extent of the effective injection site in a diagram of the surface of the cerebellum.

B: Coronal section of the cerebellum through the area of maximum extent of the injection.
TMB=dots, DAB=lines

C: A series of equally spaced sections (approx 750μm) through the inferior olive showing the location of individual retrogradely labelled nuclei.

D: A series of equally spaced (500μm) coronal sections through the deep cerebellar nuclei showing position and density of anterogradely labelled terminals.

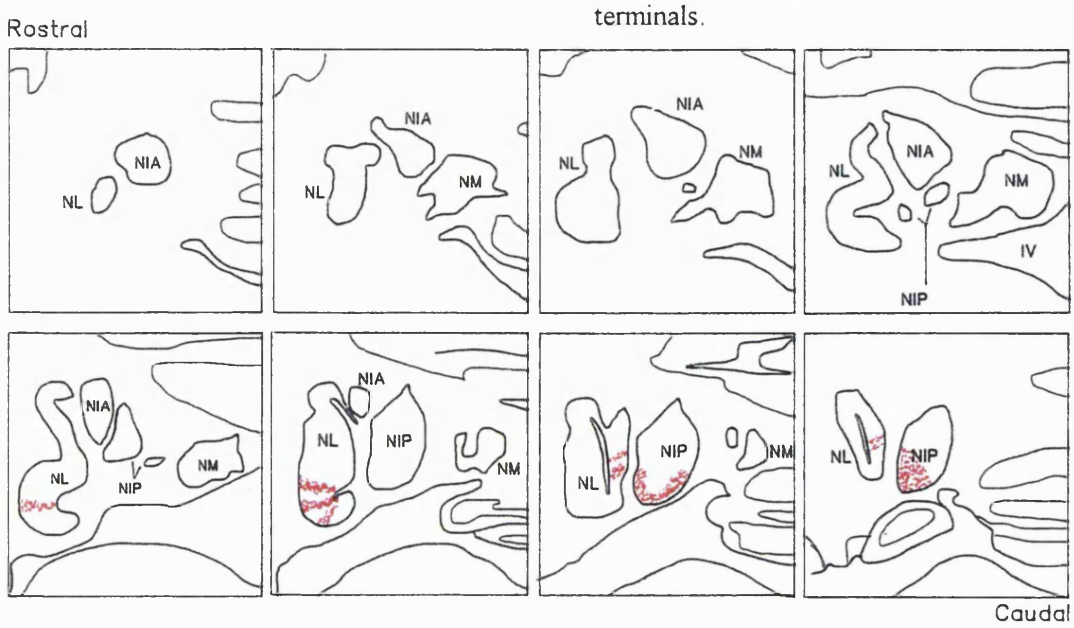

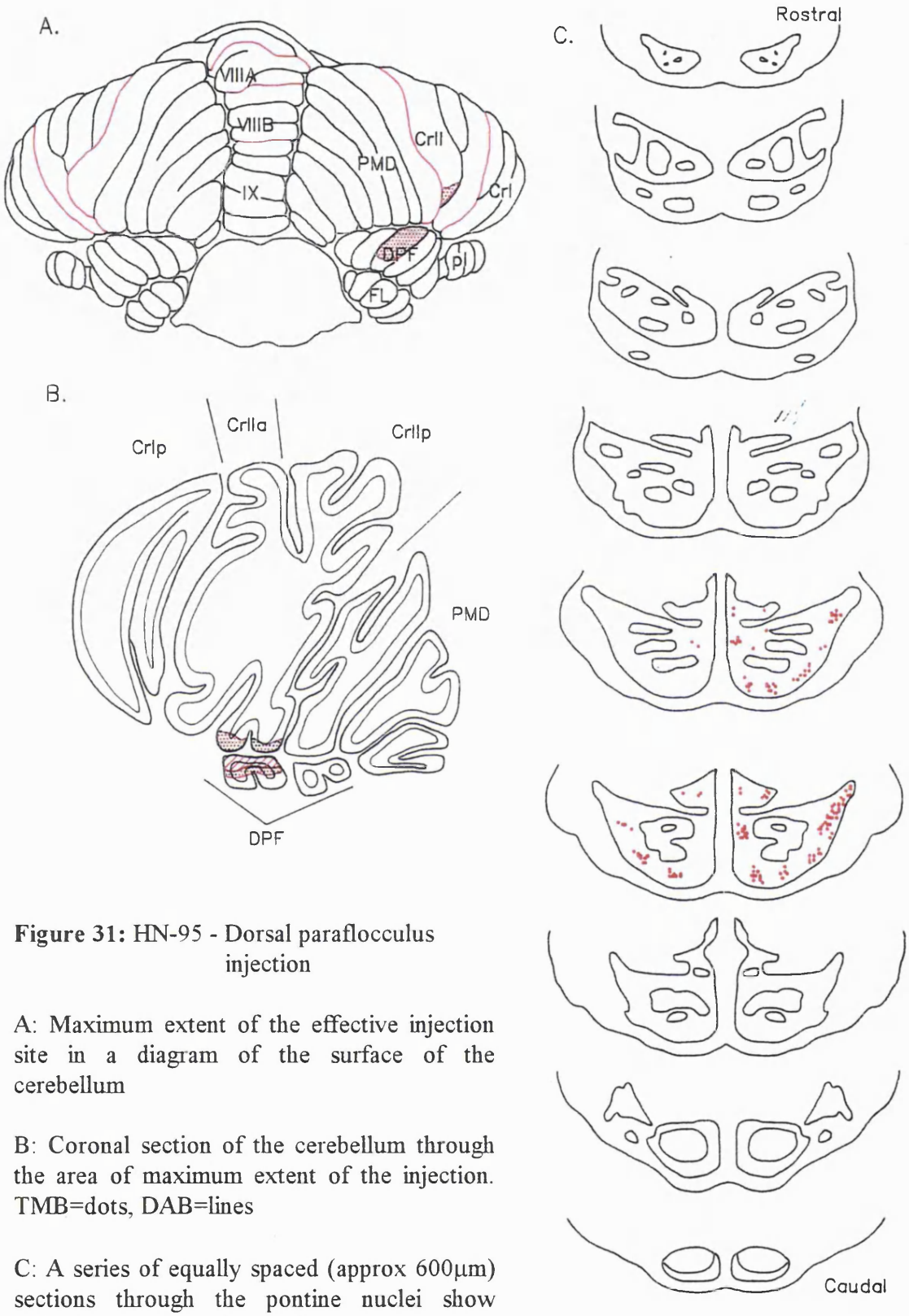

Figure 31: HN-95 - Dorsal paraflocculus injection

A: Maximum extent of the effective injection site in a diagram of the surface of the cerebellum

B: Coronal section of the cerebellum through the area of maximum extent of the injection. TMB=dots, DAB=lines

C: A series of equally spaced (approx 600µm) sections through the pontine nuclei show individual retrogradely labelled neurons

d) Case BG-95

Injection site

See figures 32 and 33.

BG-95 had a very large injection site, covering folia both of the dorsal paraflocculus and the flocculus. In the dorsal paraflocculus, the injection site was centred on folium 5, with some spread mediolaterally into the medial half of folium 4 and the lateral third of folium 6. The leakage into folium 6 was greater than that into folium 4, with the caudal third being almost totally filled. The spread into the flocculus covered the rostral half of folia 3 and 4, and the rostromedial quarter of folium 5. There was no spread of the injection site into the paramedian lobule or crus II.

The olivocorticonuclear pathway

The caudal half of the inferior olive showed extensive retrograde cell labelling. The most caudal cells were found throughout the medial dorsal cap and the ventrolateral outgrowth. Moving rostrally, cells were subsequently found in the lateral bend of the principal olive, mid-to-rostral levels of the MAO and middle levels of the ventral leaf of the principal olive. The labelled cells in the ventral leaf collected immediately dorsal to those in the MAO, but continued somewhat more rostrally.

This data indicates that the injection site included C2, D1-2 and the floccular zones FZI-IV.

Labelled terminals again focused caudally in the deep cerebellar nuclei. The terminal field in the posterior interposed (C2) began as a clump in the ventrolateral corner of the nucleus, but at more rostral levels this was replaced by a strip running ventromedially. At the most caudal levels, this strip was joined by another collection of terminals in the mid-dorsoventral area of lateral posterior interposed. The ventromedial strip then swept ventrolaterally to combine with it, and the resulting terminal field almost covered the entire ventrolateral half of the nucleus.

Dentate label was found only in the caudal quarter of the deep nuclei (D1). It was consistently found laterally, adjacent to the lateral edge of the ventromedially directed strip in the posterior interposed.

The NRTP/pontocerebellar projection

Contralateral to the injection site, retrogradely labelled cells were found throughout the entire rostro-caudal length of the pons. At rostral levels, the label was found in three clumps of ventrally-located cells, but at caudal levels, more labelled cells appeared at lateral, dorsolateral and paramedian locations.

Ipsilaterally, there were small components in the paramedian, ventrolateral and dorsolateral nuclei.

The NRTP contained labelled cells at its midline at rostral levels, and laterally at most caudal levels. The midline label was present bilaterally. The lateral label was purely contralateral.

The nucleo-cortical projection

Labelled cells were encountered in both the posterior interposed and dentate, although the majority were found in the NIP. Regardless of location, all nucleo-cortical cells were of similar sizes.

Labelled cells were found at all the rostrocaudal levels of the posterior interposed in which terminal label was seen. However, only a quarter of the cells were found lying within a terminal field: the majority of the others were located nearby, but some lay considerably dorsal to the terminal field.

The nucleo-cortical cells the cells did not clump together, but lay in lines either running parallel to the strip of the terminal field or dorsally away from the labelled terminals in a zigzag pattern.

The dentate contained only five labelled cells, lying in a line within the terminal field in the caudomedial dentate.

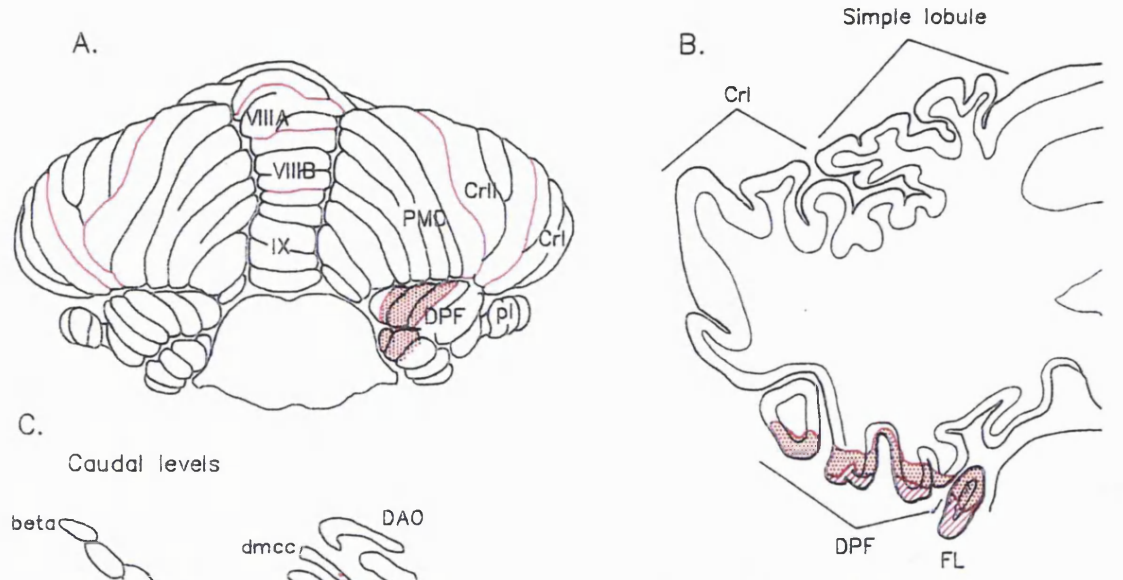

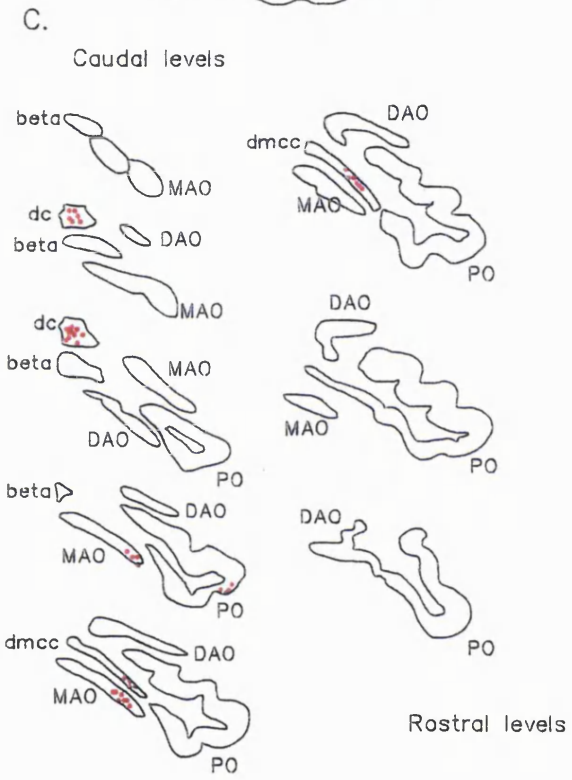

Figure 32: BG-95 - Dorsal paraflocculus injection

A: Maximum extent of the effective injection site in a diagram of the surface of the cerebellum.

B: Coronal section of the cerebellum through the area of maximum extent of the injection.
TMB=dots, DAB=lines

C: A series of equally spaced sections (approx 750µm) through the inferior olive showing the location of individual retrogradely labelled nuclei.

D: A series of equally spaced (500µm) coronal sections through the deep cerebellar nuclei showing position and density of anterogradely labelled terminals.

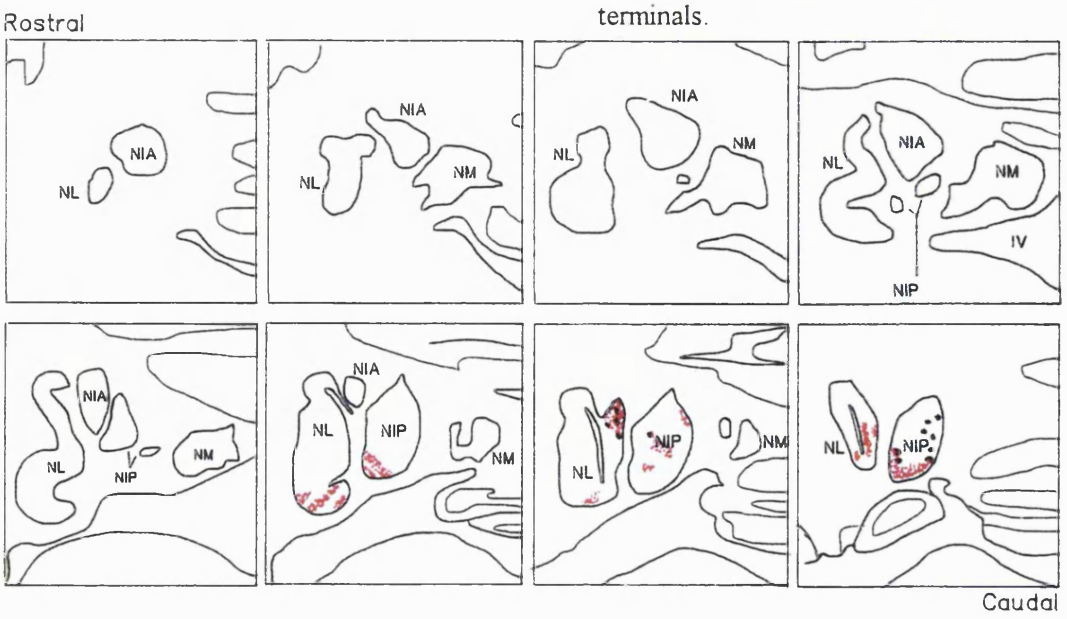

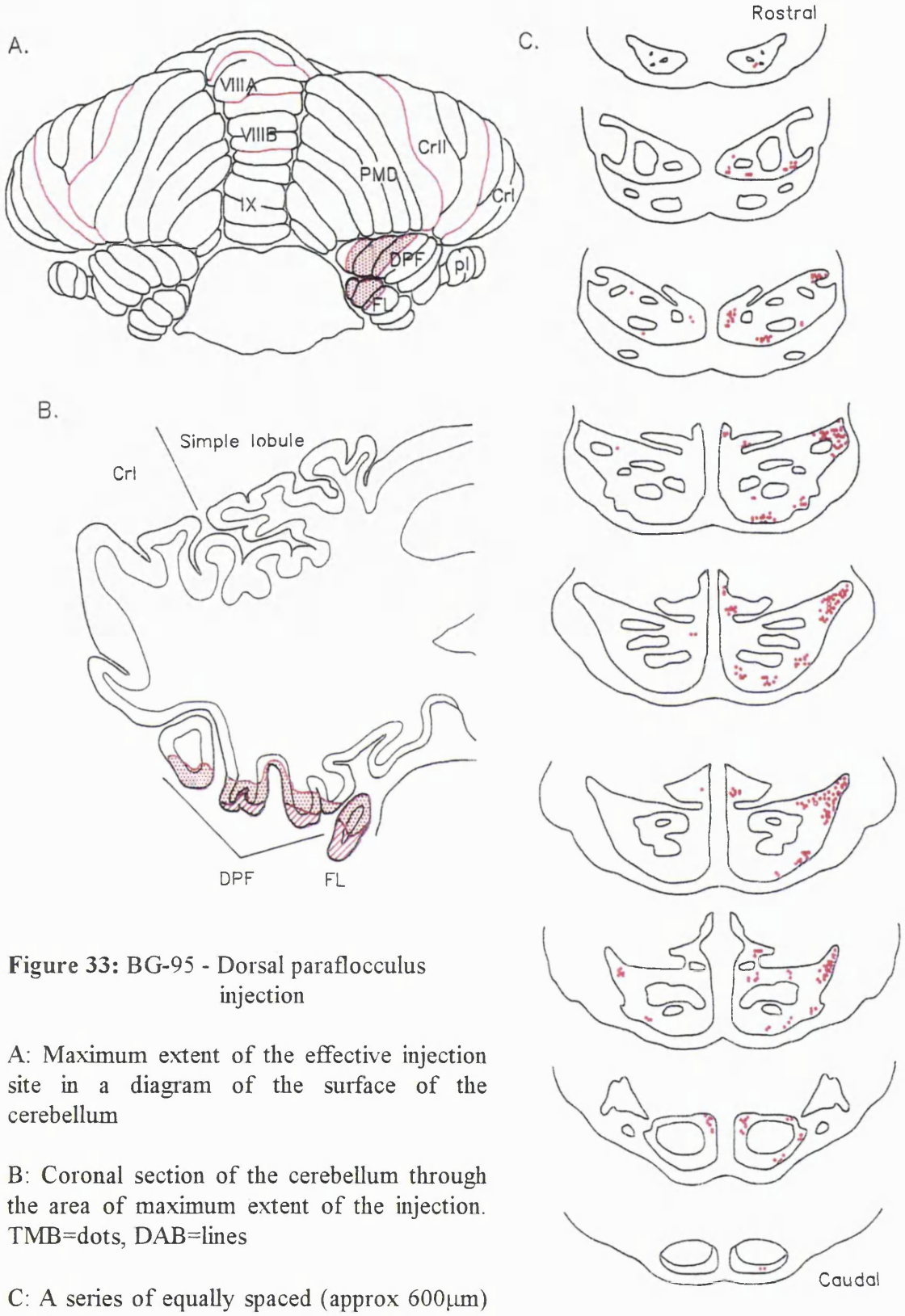

Figure 33: BG-95 - Dorsal paraflocculus injection

A: Maximum extent of the effective injection site in a diagram of the surface of the cerebellum

B: Coronal section of the cerebellum through the area of maximum extent of the injection. TMB=dots, DAB=lines

C: A series of equally spaced (approx 600μm) sections through the pontine nuclei show individual retrogradely labelled neurons

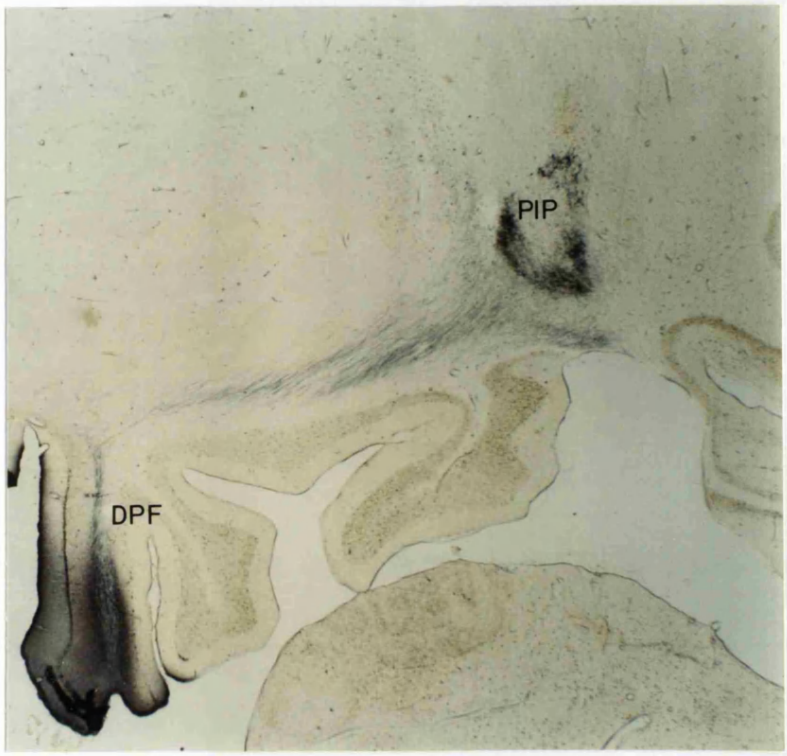

1mm

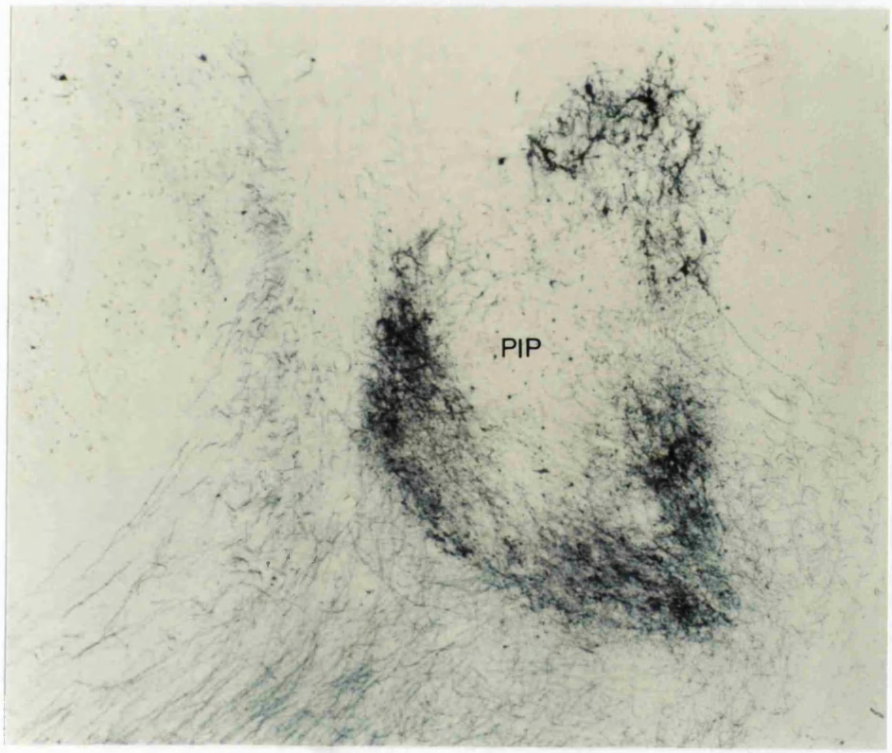

0·25mm

Photomicrograph 2: BG-95

A: Transverse cerebellar section following injection of WGA-HRP into the flocculus and dorsal paraflocculus and reaction with chromogen TMB. Fibres can be seen coursing up from the medial edge of the dorsal parafloccular region in the injection site, and terminating in a characteristic U-shaped terminal field in the ventrocaudal posterior interposed nucleus.

B: High power photomicrograph of the terminal field in A. Note the dense U-shaped terminal field, and the retrogradely-labelled cells in a dorsally-located group.

3.1.3.2 Flocculus plus ventral paraflocculus -

Case M228

Injection site

See figures 34 and 35.

The injection site in this case was centred on the flocculus, and covered most of folia 3 to 5. However, the lateral part of the injection site crossed the posterolateral fissure and labelled the first folium of the ventral paraflocculus, also known as the medial extension (M.E.). There was no spread of label into the overlying dorsal paraflocculus.

The olivocorticonuclear pathway

Labelled olivary cells were restricted to those parts of the inferior olive known to project to the flocculus: the dorsal cap and the ventrolateral outgrowth. The dorsal cap contained labelled cells throughout its rostrocaudal extent. At caudal levels, it seemed as though every cell in the dorsal cap was labelled, but at more rostral levels, the cells seemed to collect in the lateral corner, stretching dorsomedially. The label in the ventrolateral outgrowth was minor, lateral, and only found at most caudal levels. The olivary label indicates that the injection site had included floccular zones FZI-IV.

Terminal label in the deep cerebellar nuclei was very sparse and restricted to the caudal posterior interposed (C2). The terminal field formed two stripes which lay in the ventrolateral corner of this nucleus.

The NRTP/pontocerebellar projection

Retrogradely labelled cells were found contralaterally in the dorsomedial and dorsolateral pontine nuclei at rostral levels. More caudally, the dorsomedial label disappears and labelled cells were additionally encountered in the dorsal and lateral nuclei. At the most caudal levels, a few cells were found in the dorsolateral nucleus.

Ipsilaterally, labelled cells were found mostly in the dorsolateral pons at caudal levels, although a few were additionally found in the paramedian nucleus.

All of the pontine cells were weakly labelled.

The NRTP was strongly labelled at its caudal levels. The majority of labelled cells formed a strip running along the dorsal aspect of this nucleus, from the lateral corner. In addition, there was a large clump of labelled cells located in the medial nucleus of the caudal NRTP. The midline label was seen bilaterally but the dorsolateral strip was only found contralateral to the injection site.

The nucleo-cortical projection

No labelled cells were found anywhere in the deep nuclei.

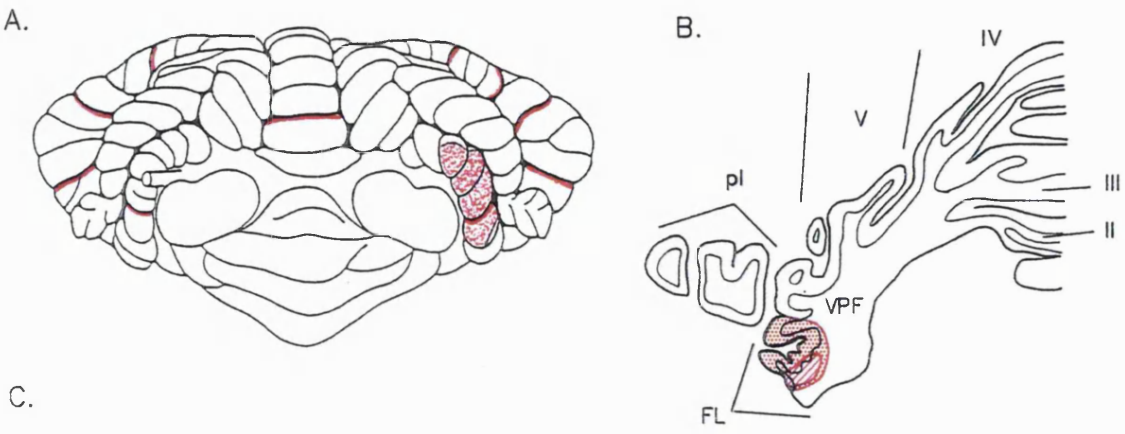

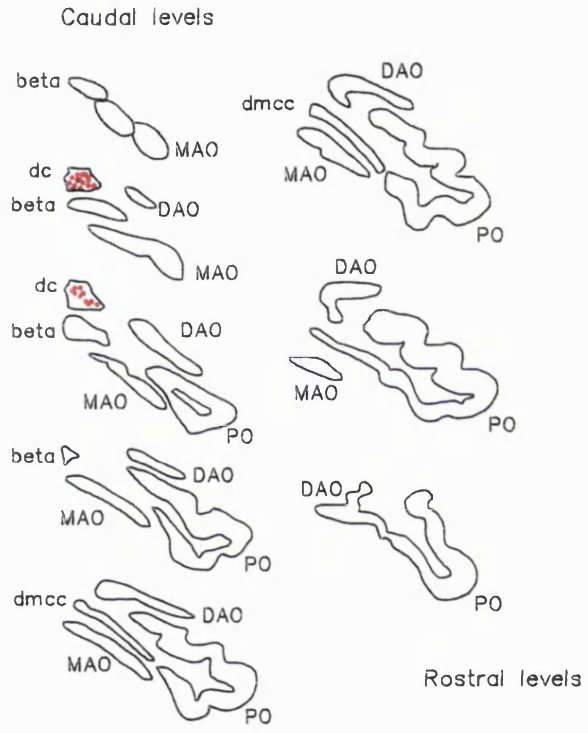

Figure 34: M228 - Flocculus/ventral paraflocculus injection

A: Maximum extent of the effective injection site in a diagram of the surface of the cerebellum.

B: Coronal section of the cerebellum through the area of maximum extent of the injection.
TMB=dots, DAB=lines

C: A series of equally spaced sections (approx 750μm) through the inferior olive showing the location of individual retrogradely labelled nuclei.

D: A series of equally spaced (500μm) coronal sections through the deep cerebellar nuclei showing position and density of anterogradely labelled terminals.

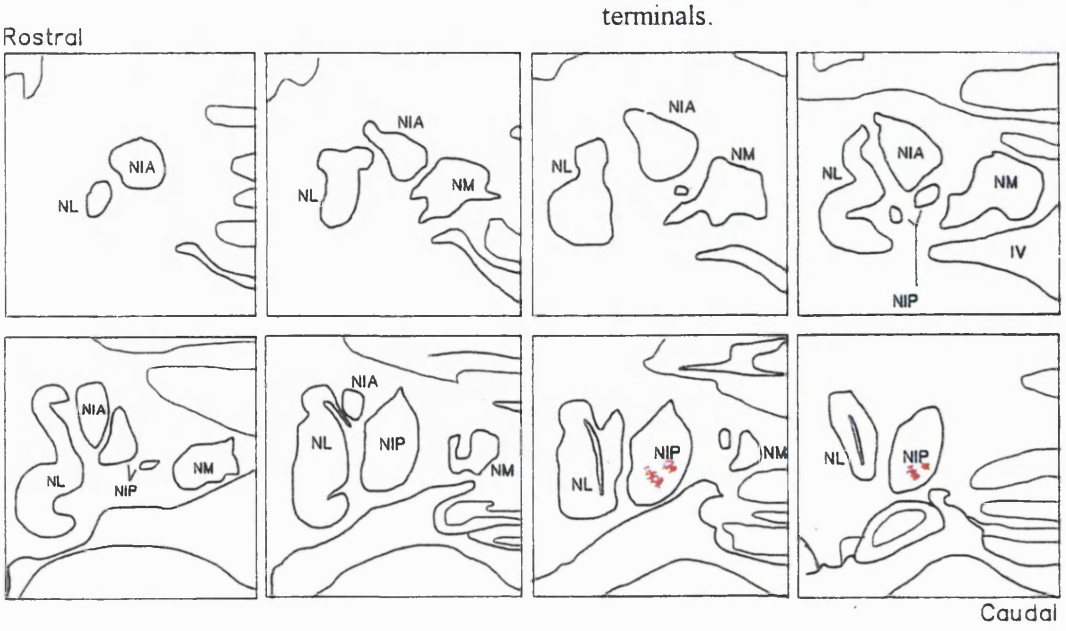

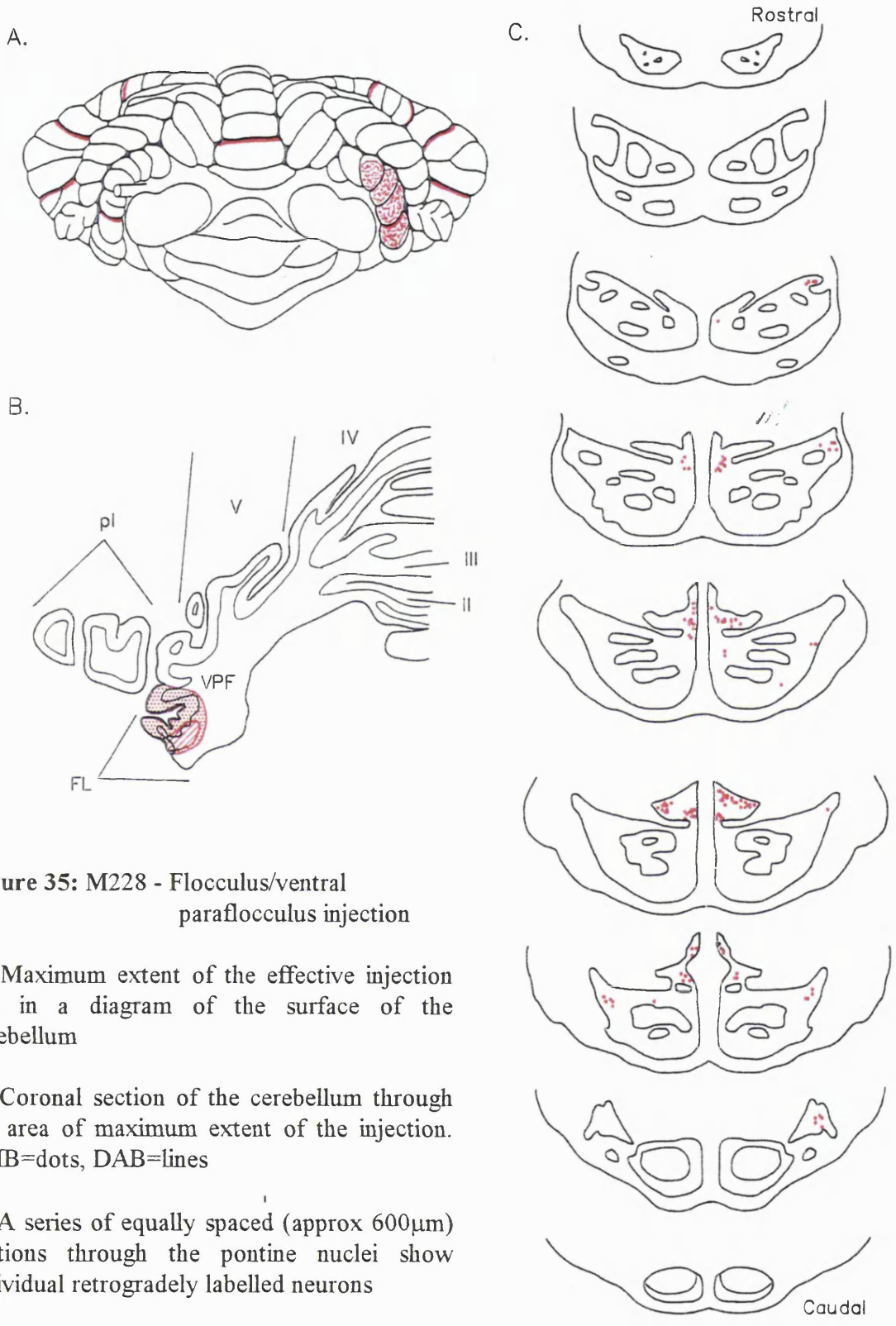

Figure 35: M228 - Flocculus/ventral paraflocculus injection

A: Maximum extent of the effective injection site in a diagram of the surface of the cerebellum

B: Coronal section of the cerebellum through the area of maximum extent of the injection. TMB=dots, DAB=lines

C: A series of equally spaced (approx 600µm) sections through the pontine nuclei show individual retrogradely labelled neurons

3.1.3.3 Pure flocculus -

Case D669

Injection site

See figures 36 and 37.

The injection site was restricted to the flocculus in this case. There was no leak into the ventral paraflocculus along the posterolateral fissure, nor dorsally into the dorsal paraflocculus.

The olivocorticonuclear pathway

The majority of cells in this case were found in the dorsal cap and the ventrolateral outgrowth. The dorsal cap contained label medially throughout its rostrocaudal extent. In the ventrolateral outgrowth, the cells also collected medially within the main body of the nucleus. In addition, labelled cells were seen in the extreme lateral edge of the middle levels of the MAO. This olivary label indicates that the injection site had included C2 and the floccular zones FZI-IV.

Terminal label in this case was confined to the posterior interposed and the dentate nuclei. The terminal field in the posterior interposed (C2) was situated caudally in this nucleus, and consisted of two stripes in the ventrolateral corner of the NIP.

Two stripes of dense terminal label were present in the caudolateral dentate nucleus (D1), directly adjacent to the label in the NIP. Two extremely faint strips of terminal were also identified, running ventrally down from the white matter island in the centre of the dentate.

The NRTP/pontocerebellar projection

The contralateral dorsomedial and dorsal pontine nuclei contained a very few, sparsely labelled cells at rostral levels. Otherwise, the pontine nuclei were free of labelled cells.

The NRTP contained a huge number of cells ventromedially. This label was bilateral and found at all levels of the nucleus. The lateral NRTP contained labelled cells only at rostral levels, and this was predominantly contralateral.

The nucleo-cortical projection

No labelled cells were found in the deep cerebellar nuclei.

Photomicrograph 3: The extent of the floccular injection site, as demonstrated using DAB histochemistry.

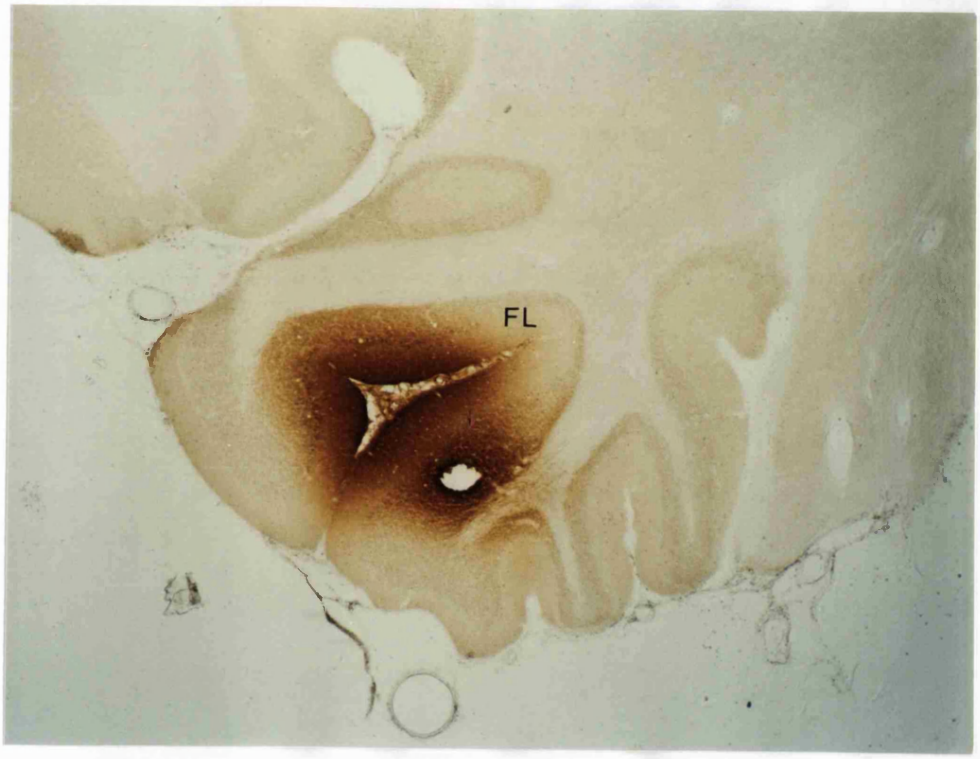

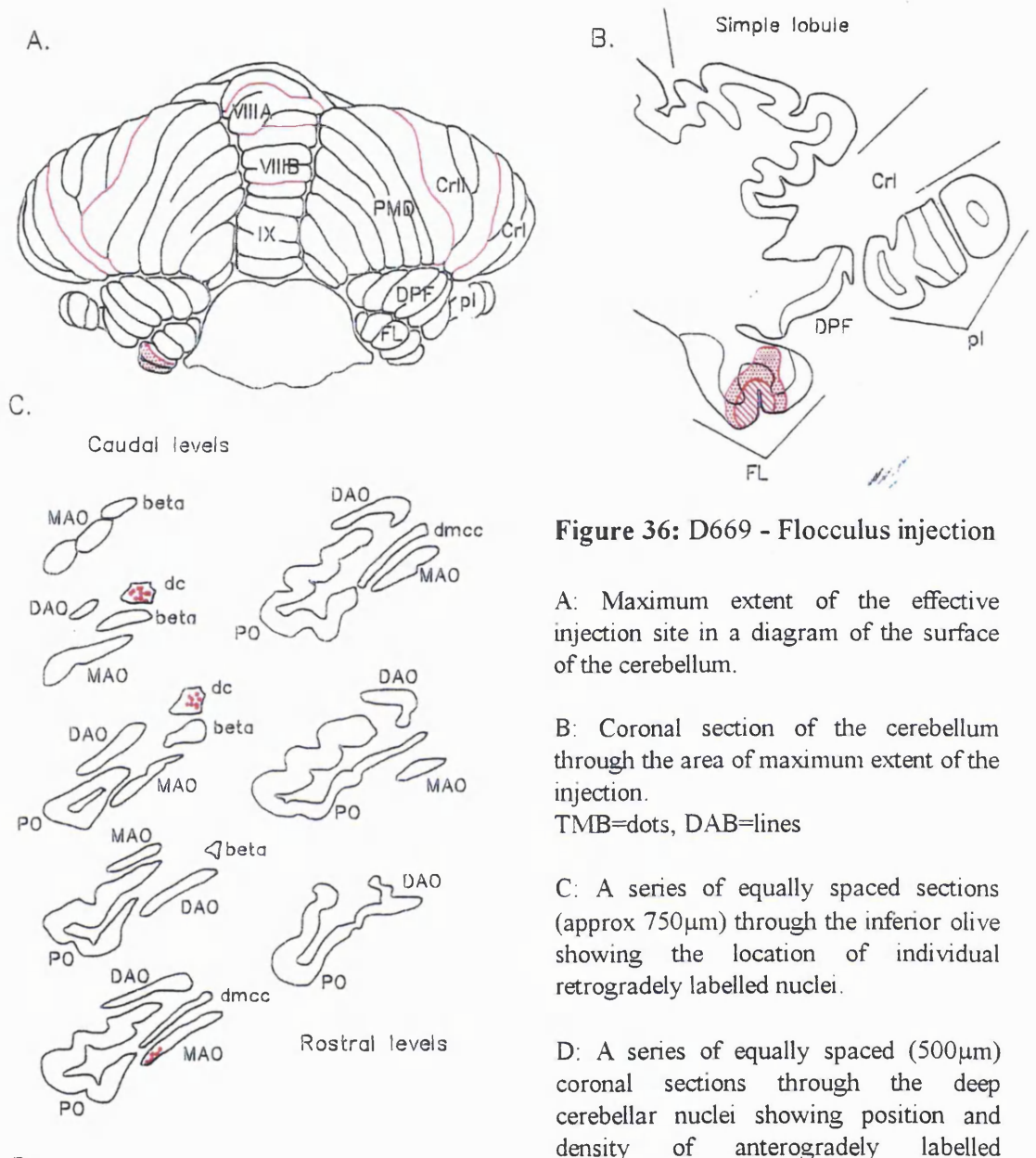

Figure 36: D669 - Flocculus injection

A: Maximum extent of the effective injection site in a diagram of the surface of the cerebellum.

B: Coronal section of the cerebellum through the area of maximum extent of the injection.
TMB=dots, DAB=lines

C: A series of equally spaced sections (approx 750μm) through the inferior olive showing the location of individual retrogradely labelled nuclei.

D: A series of equally spaced (500μm) coronal sections through the deep cerebellar nuclei showing position and density of anterogradely labelled terminals.

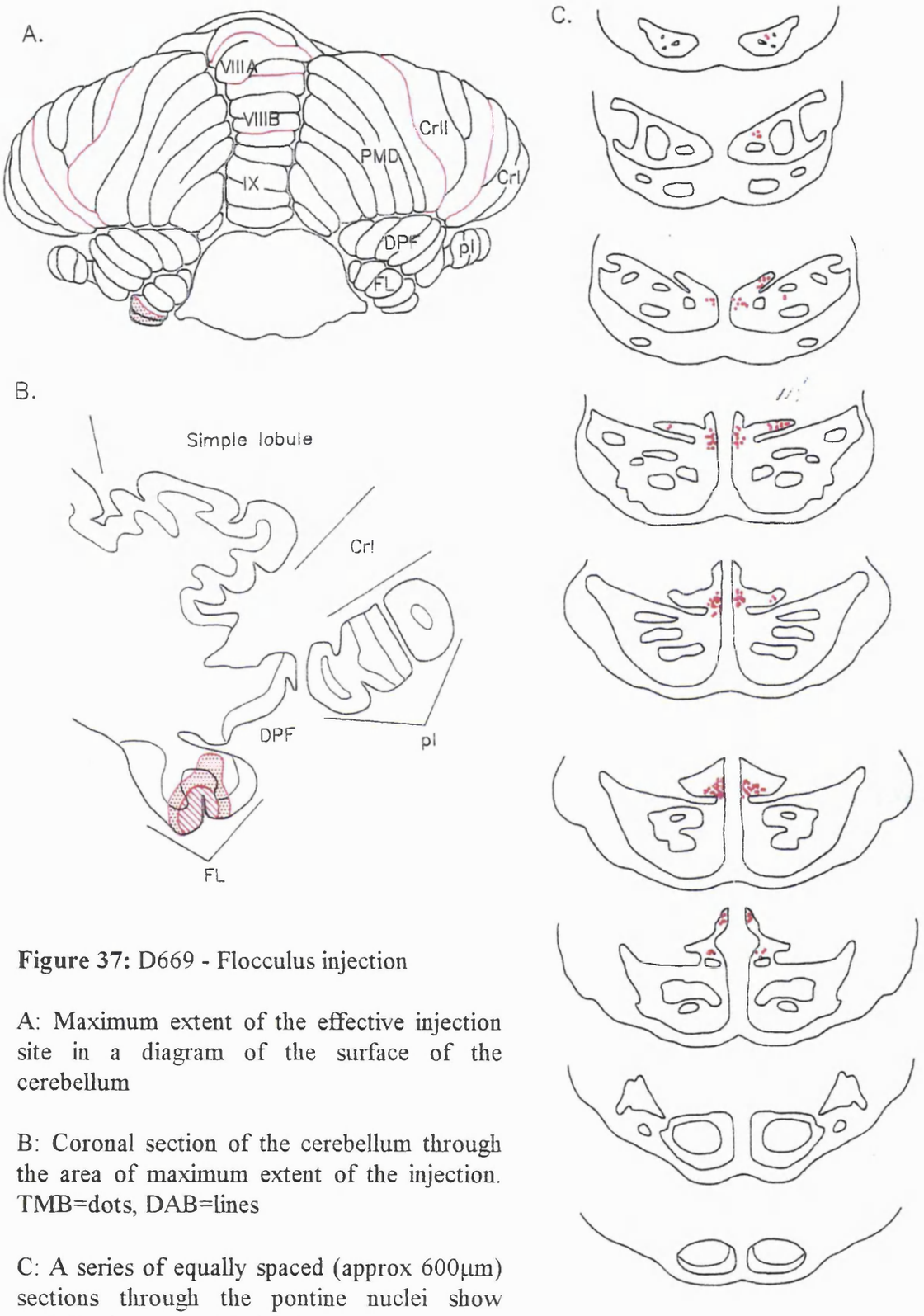

Figure 37: D669 - Flocculus injection

A: Maximum extent of the effective injection site in a diagram of the surface of the cerebellum

B: Coronal section of the cerebellum through the area of maximum extent of the injection. TMB=dots, DAB=lines

C: A series of equally spaced (approx 600μm) sections through the pontine nuclei show individual retrogradely labelled neurons

3.1.3.4 SUMMARY

The conclusions portion of this results chapter will begin with a separate consideration of connections of the dorsal paraflocculus and the floccular complex. The final analysis will comprise a comparison of the two cerebellar areas.

A. Dorsal paraflocculus

The dorsal paraffloccular cases presented in this thesis comprised injections into almost identical folia of the dorsal paraflocculus. Due to the difficulty of reaching the dorsal paraflocculus during surgery, we were unable to inject folia medial or lateral to folia 5 and 6, and, as a result, it is impossible to comment on the presence or absence of mediolateral and rostrocaudal topographies in the anatomical connections of this area. However, the majority of the cases were pure dorsal paraflocculus injections, with no spread of the neural tracer into neighbouring structures such as the ventral paraflocculus or the flocculus itself, which would confound the results.

<u>The olivocerebellar projection</u>

The dorsal paraflocculus contains three zones D2, D1 and C2 moving dorsoventrally, and as a result, each dorsal paraflocculus injection resulted consistently in retrograde labelling in the principal olive and the medial accessory olive. BG-95 contained additional labelled cells in the dorsal cap and ventrolateral outgrowth due to the spread of the injection site into the flocculus.

Labelling in the ventral leaf of the principal olive (D2) was unusual in that it was consistently restricted to the thin, cell-poor division of the ventral lamella, as opposed to the larger, more lateral areas of the ventral leaf. The only other case displaying this type of olivary label was is m2-96left, which, although the injection was focused on lateral paramedian lobule, had some leak into the most dorsal areas of folia 5 and 6 of the dorsal paraflocculus. The implications of this topography will be discussed in section 4.2.1.3 of the discussion.

The D1 zone, as evidenced by label in the dorsal leaf and lateral bend of the principal olive, is intercalated between D2 and C2. Note that when dorsal leaf/lateral bend label is present (cases 696, HN-95 and BG-95), the labelled cells are found in virtually identical locations due to the similarity of the injection sites in these cases.
The rostral medial accessory olive contained label in mid-lateral areas in almost every case, corresponding to label in cortical zone C2 within the dorsal paraflocculus. The only case without label in this area was HN-95, which contained an injection site restricted to more dorsal parts of the folium.

A remarkable feature of the olivary label was that in each case of rMAO and ventral lamella label, the labelled cells in the medial accessory division lay immediately beneath labelled cells in the ventral lamella, and covered the same mediolateral span as those in the ventral lamella. The functional consequences of this topography will also be discussed in section 4.2.1.3 of the discussion.

Cortico-nuclear projection from the dorsal paraflocculus

All dorsal parafloccular cases projected to the caudal posterior interposed. The projection to the posterior interposed nucleus produces a characteristic U-shaped terminal field, covering the caudolateral corner of the nucleus. This nuclear label corresponds to a cortical C2 injection and is normally accompanied by rostral medial accessory olivary label. In the case of HN-95, terminal label was present in the posterior interposed label even though olivary label was restricted to the dorsal and ventral lamella of the principal olive; the rMAO contained no labelled cells. This implies that divergence of cortical zones to "extra-zonal" nuclear targets may be not be a purely vermal or intermediate hemispheric phenomenon, and that one or both of the cortical D zones also send(s) a small projection to the posterior interposed.

The ventrocaudal dentate nucleus (zone D1) contained label in all cases except dpf1, which clearly had spare D zone involvement due to its minimal label in the principal olive. The terminal field in the dentate was consistently arranged into numerous stripes of punctate label patches separated by areas devoid of label. The terminal field spanned almost the entire mediolateral width of the nucleus, and was consistently found

immediately adjacent to the terminal field in the posterior interposed. The terminal fields in these cases appeared to be a continuum across the dentate/posterior interposed border, interrupted only by the passage of white matter between the nuclei.

The most unusual finding on the cortico-nuclear system from the dorsal paraflocculus was the singularity of the terminal fields in the dentate. The olivary label indicated that in many cases, both cortical zones D1 and D2 were injected, and yet there was only one focus of terminal label in the caudal dentate (zone D1). The rostral dentate was consistently free from label. This indicates that intra- as well as extra-zonal convergence occurs in the dorsal paraflocculus.

The NRTP/pontocerebellar projection

Following dorsal parafloccular injections, the pontine nuclei contained label in the dorsolateral, lateral, ventral, ventromedial and medial nuclei. The labelled cells were arranged as a cluster, forming a ring around the border of the pontine nuclei and corticospinal tract fascicles. In each case, however, by far the largest number of cells were found in the dorsolateral pontine nucleus. In addition, the dorsolateral pontine label extended throughout the rostrocaudal length of the basilar pons, whereas the labelled cell groups in other nuclei had a more limited rostrocaudal distribution.

The pontocerebellar projection to the dorsal paraflocculus is predominantly contralateral, although labelled cells are regularly encountered ipsilaterally. In general, it is the cell groups most strongly represented contralaterally that appear ipsilaterally.

The NRTP does not project to the dorsal paraflocculus. Cases with pure dorsal parafloccular injection sites contained no NRTP label. Cases BG-95 and HN-95 contained labelled cells in the medial NRTP and medial and lateral NRTP respectively due to their injection sites spreading beyond the dorsal paraflocculus into the flocculus and crus II. Indeed, the NRTP areas containing label in cases BG-95 and HN-95 were identically labelled following pure crus II and flocculus injection.

The nucleo-cortical projection

The dorsal paraflocculus has the strongest nucleo-cortical pathway relative to size of terminal field of all the cortical areas investigated. The deep nuclei in case HN-95

contained no labelled cells, but it is likely that this results from the superficial location of the injection site rather than the lack of a nucleo-cortical projection. The observation that HN-95 also contained very sparse pontine/NRTP label, which also arises following retrograde transport of WGA-HRP from the granular layer, supports this explanation.

In all cases, the projection is purely ipsilateral. The cells are located in nuclear zones containing terminal fields, although the cells may be present either inside or outside a terminal field, with no clear evidence of greater topography. The nucleo-cortical pathway therefore has reciprocal and non-reciprocal components. There was no consistent difference in cell size between the reciprocal and non-reciprocal cortical afferents.

B. Flocculus and ventral paraflocculus

The olivocerebellar projection

Both cases 228 and D669 had injections including the flocculus. D669 was a pure flocculus injection, with no leak into either division of the paraflocculus. In case 228, however, the injection site spread rostrally to include the most medial folium of the ventral paraflocculus (folium p or the medial extension, M.E.). Both cases received more or less identical olivary input from the dorsal cap and the ventrolateral outgrowth. As both cases were in similar locations, it was impossible to discern any rostrocaudal topography - in both cases, the entire length of the dorsal cap and ventrolateral outgrowth contained labelled cells, indicating that every floccular zone had been injected.

A limited amount of mediolateral topography was evident. The dorsal cap label in case D669 was confined largely to its medial edge. However, in the combined flocculus and ventral paraflocculus case, the dorsal cap label spread laterally from the medial border of the nucleus. The difference in mediolateral spread olivary label may suggest that the flocculus receives from medial areas in the dorsal cap, the ventral paraflocculus from lateral areas within the same nucleus.

Additional rostral medial accessory olive label in the pure flocculus D669 case is explicable because its injection site covered the entire dorsoventral height of the floccular folia, whereas case 228, which, although it was the larger injection site, didn't cover the

most dorsal areas of the flocculus, in which the floccular zone C2 (receiving input from the rMAO) is known to reside.

The cortico-nuclear projection

Both floccular complex cases projected to the posterior interposed nucleus (C2). 228 (flocculus plus ventral paraflocculus) had a restricted nuclear projection, terminating only in the posterior interposed, whilst the D669 (pure flocculus) projection not only starts more rostrally and has a larger projection to the posterior interposed, but also projects to the dentate. The ostensibly more restricted injection site may have produced a larger nuclear projection because it spread situated more deeply into the white matter than the flocculus and ventral paraflocculus case (228). This is supported by the fact that case 228 contained less olivary label than the flocculus case.

Both 228 and D669 projected into overlapping striped terminal fields. In case 228, the terminal fields were actually separated completely by areas without terminal label or labelled fibres, whereas in case D669, the corner was filled with terminal stripes of varying intensity.

The stripes in case 228 appeared to correspond with the densest stripes in case D669.

The floccular projection to the dentate also terminated as stripes in the caudomedial edge of the nucleus (D1). The stripes in the dentate appeared to be continuous with those in the posterior interposed, indicating some form of anatomical continuity in the cortico-nuclear projection to these nuclei, interrupted only by the passage of white matter between the nuclei.

The NRTP/pontocerebellar projection

Both cases were dominated by label in the ventromedial NRTP..

228 (flocculus and ventral paraflocculus) case contained a greater degree of NRTP label, presumably because of ventral paraflocculus involvement. The additional NRTP label due to ventral paraflocculus involvement suggests that the ventral paraflocculus receives input from a dorsal strip of cells at mid-levels. Again, within the NRTP label, midline cell groups are represented bilaterally, whereas the more lateral cell groups are predominantly

found contralaterally. In rare cases when they are seen ipsilaterally, they appear at very reduced levels.

The few pontine cells that are present are more faintly labelled than others in the NRTP or the pontine nuclei of other cases, suggesting that they may send collaterals to the flocculus, but send their main axon to alternative cerebellar sites, such as the dorsal paraflocculus or vermal lobule VII, in the case of the dlpn.

The nucleo-cortical projection

The deep cerebellar nuclei do not project to the flocculus.

C. Comparison of dorsal paraflocculus and flocculus

The olivocerebellar projection

The flocculus and dorsal paraflocculus receive different climbing fibre input. There was no overlap in the retrogradely labelled olivary cells between the floccular and dorsal parafloccular cases, except in the case of BG-95. This dorsal parafloccular case contained labelled cells in the dorsal cap and ventrolateral outgrowth due to the spread of the tracer into the floccular folia beneath the main dorsal parafloccular injection site.

The cortico-nuclear projection

In spite of the difference in climbing fibre input to the dorsal paraflocculus and flocculus, the nuclear projections from these cortical areas overlap in the ventrocaudal posterior interposed and ventromedial dentate nuclei.

The cortico-nuclear projections to the ventrolateral corner of the caudal posterior interposed are arranged somewhat differently between the dorsal parafloccular and the floccular cases, but this may result simply from the fact that in no injection site had covered the entire breadth of the cortical C2 zone. The dentate projection in case D669 (pure flocculus) overlapped completely with that seen in dorsal parafloccular cases. In all cases, the dentate terminal field looked like a continuation of that in the posterior interposed, interrupted only by the passage of fibres between the nuclei.

The floccular input to the deep nuclei is more sparse than that from the dorsal paraflocculus since the majority of its efferents terminate in the vestibular nuclei in the brainstem.

NRTP/ pontocerebellar projection

There was no overlap in pontine and NRTP afferents to the dorsal paraflocculus and the flocculus. Indeed, a sharp dichotomy existed between efferent projections to the dorsal paraflocculus and flocculus. The flocculus receives massive input from the NRTP and virtually none from the pontine nuclei. The dorsal paraflocculus, on the other hand, receives its major input from the dorsolateral pons, and no projections from the NRTP. Those dorsolateral pontine cells that were labelled in the flocculus/ventral paraflocculus case 228 were more lightly labelled than cells in both the neighbouring NRTP and the pontine nuclei of all other cases. These cells may form a collateral population, which sends their main axon to another cortical location, such as the dorsal paraflocculus, and a small collateral to the flocculus or ventral paraflocculus.

Thus, although the flocculus and dorsal paraflocculus receive totally separate inputs via both the climbing fibre system and the pontine/NRTP mossy fibre system, they project to overlapping areas in the deep cerebellar nuclei. The implications of this will be detailed in section 4.1.3 and 4.3 of the discussion.

Nucleo-cortical

This data again pointed to a stark dichotomy between the flocculus and dorsal paraflocculus. The flocculus receives no nucleo-cortical projection, whereas the dorsal paraflocculus receives the strongest input from the nuclei of all the areas investigated.

3.2 ZEBRIN STUDIES

3.2.1 Purkinje cells

Purkinje cells in the cerebellar cortex showed immunoreactivity throughout their somata, plus the dendrites, dendritic spines, axons, axon collaterals and their terminals in the deep cerebellar nuclei and the lateral vestibular nucleus (see photomicrographs 2 and 5).
All of the Purkinje cells in the cortex showed some degree of immunoreactivity to zebrin II. In no case were there unlabelled cells. The degree of immunoreactivity in the macaque, therefore seems to be much more of a continuum of degrees of staining, rather than an all-or-nothing property. The clearest differences in levels of immunoreactivity were encountered within the vermis, such that parasagittal strips could be clearly seen, even with the naked eye. Within the pars intermedia, hemispheres and floccular complex, however, almost all cells were equally strongly labelled, and it was hard to discern the presence of differences in staining intensity between subsets of Purkinje cells.

The dendritic trees of the Purkinje cells were also clearly stained, and could be traced in their entire length into the molecular layer, which is only weakly immunoreactive. As the dendritic trees are arranged orthogonal to the direction of the folial chain, they appeared flattened in the vermis. In the more lateral parts of the hemisphere, and more clearly at the base of the folia, however, the dendritic trees could be seen branching repeatedly as they travelled through the molecular layer.

The entire axon of Purkinje cells were also clearly labelled, and could be seen coursing through the white matter towards the deep nuclei or the brainstem. Recurrent axon collaterals were seen coursing back towards the Purkinje cells, forming a heterogenous network of collateral fibres immediately beneath the Purkinje cell layer.

3.2.2 Cerebellar cortex

As mentioned previously, clear parasagittal strips of zebrin positive and negative subsets were only clearly discernible in the vermis. There were patches within the more lateral

cortical areas that showed small variations in the degrees of staining, but, due to the complex folding and twisting of the folial chain in these areas, it was not possible to recognise a consistent pattern, and a complete reconstruction of immunoreactivity in these areas was therefore not attempted. As a general rule, however, the vast majority of Purkinje cells in the hemispheres, particularly posteriorly and in the floccular complex, were highly immunoreactive.

Differences in immunoreactivity were actually more clearly displayed in the dendrites and axons of the Purkinje cells than the somata themselves. Therefore, a subset of Purkinje cells were deemed to be zebrin-positive if there was a difference in staining intensity that could be followed through the molecular layer.

Within the vermis, four stripes of highly immunoreactive Purkinje cell subsets were seen. The midline strip, P1+, was the thinnest of the strips, but could be followed throughout the rostrocaudal length of the vermis. The neighbouring P2+ also reached throughout the vermis, but was much wider than P1+, and became broader as it was followed into the more posterior vermal lobules. P3+ and P4+ were more difficult to follow through the vermis. The P3+ strip was much more clearly seen posteriorly in the vermis - the more anterior lobules did not display as clear a difference in immunoreactive intensity. P4+ was seen at the border of the vermis and hemispheres, but, as for P3+, was only clearly evident in the posterior lobe (see photomicrograph 4).

On the whole, staining intensity of both the P+ and P- stripes increased in the more posterior parts of the vermis. This, combined with the increasing breadth of P2+, and the fact that P3+ and P4+ are more clearly discernible in the posterior lobe, resulted in the posterior lobe of the cerebellum having larger zebrin-positive population that the anterior lobe.

Photomicrograph 4: Zebrin-reacted cerebellar cortex.

A: Purkinje cells, their dendritic trees and axons can be clearly visualised using the Purkinje cell-specific marker zebrin II.

0·25mm

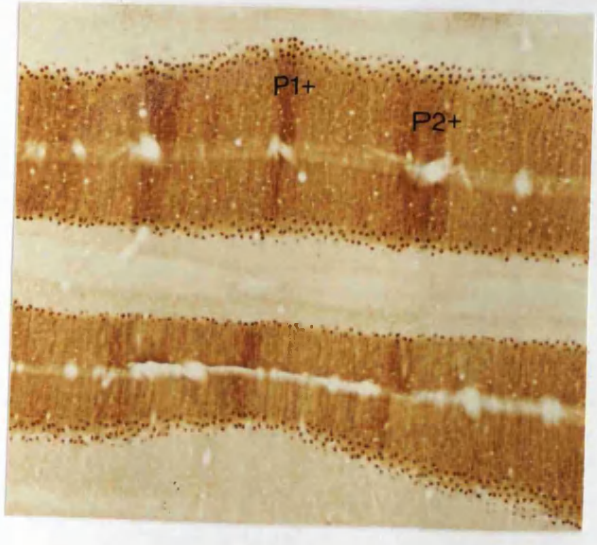

B: Zebrin-reacted section through the anterior vermis, displaying alternating zebrin-positive and negative stripes. P1+ and P2+ are evident at this level.

0·5mm

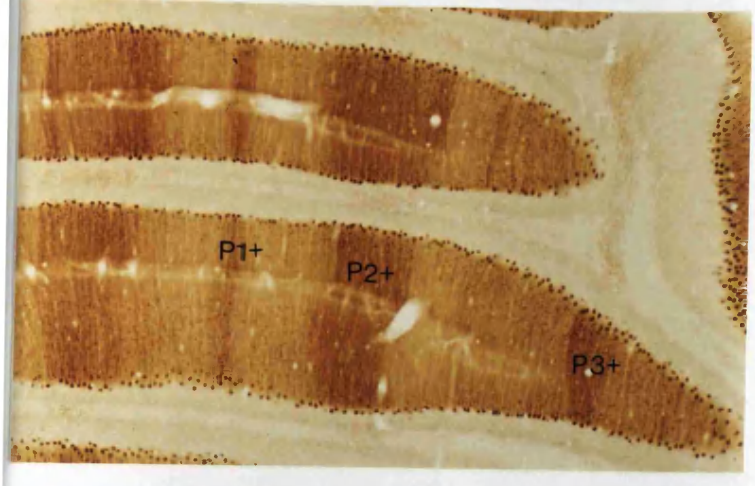

0·8 mm

C: Zebrin-reacted section through the middle vermis, at which level the zebrin-positive stripes P1+, P2+ and P3+ can be discerned.

0·5mm

D: Zebrin-reacted section through posterior vermis. Almost all Purkinje cells are zebrin-positive at this level.

3.2.3 White matter

Purkinje cell axons could be followed down from the cortex to the deep nuclei and the brainstem through the white matter. Within the posterior lobe, and particularly evident within the floccular complex, it was evident that the projections from individual folia, although travelling together, remained distinct en route to the nuclei (see photomicrograph 6). Bundles of labelled axons could be seen emanating from the base of a folium, travelling alongside that from another folium, with a thin strip of white matter interleaved between them which did not contain labelled Purkinje cell axons. Once the deep nuclei were reached, this separation was impossible to pursue as the white matter became increasingly densely stained and homogenous. Fibres to the dentate travelled along to its lateral edge, those to the anterior and posterior interposed reached them via dorsal and ventral routes respectively and the fastigial was reached via its medial edge.

3.2.4 Deep cerebellar nuclei

Each of the deep cerebellar nuclei contained labelled Purkinje cell axon terminals. The dentate contained the same amount of terminal label throughout its rostrocaudal length, whereas the interposed nuclei were more densely filled in caudal sections. The fastigial nucleus was the least densely labelled of all of the nuclei throughout its extent, and, as for the interposed, was more densely filled in its caudal levels.

In certain parts of the nuclei, fibres could be discerned, but the majority was a homogenous mass of punctate terminal labelling, which was so dense that in the dentate the weakly immunoreactive cells were barely visible beneath the plexus of terminal label. Fibres destined for the vestibular nuclei and decussating efferent fibres from the opposite fastigial could be seen coursing through in the lateral edge of the fastigial, giving it a striated appearance.

There was no evidence of alternating zebrin-positive and negative terminal stripes in any of the deep nuclei (see photomicrograph 5).

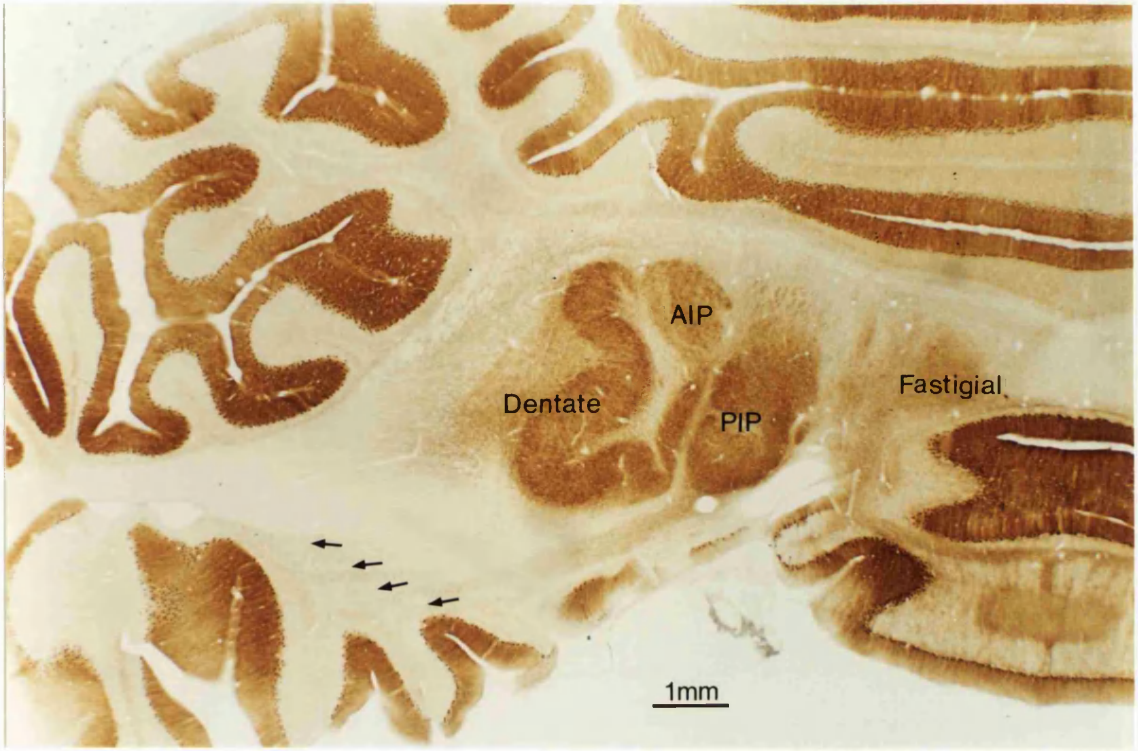

Photomicrograph 5: The deep cerebellar nuclei

Photomicrograph of the deep cerebellar nuclei and cerebellar white matter in coronal section following reaction with the Purkinje cell-specific antibody zebrin II. All areas of the deep cerebellar nuclei receive input from the cerebellar cortex. Separate laminae of cortico-nuclear projections can be discerned in the white matter (arrows).

3.2.5 SUMMARY

Following WGA-HRP injections in the lateral cerebellum, terminal fields in the deep nuclei are striped: mediolaterally directed strips of label are intercalated with areas free from fibre or terminal label. It was therefore necessary to confirm that those unlabelled nuclear areas did indeed receive Purkinje cell input, and to rule out the possibility that the nuclear afferent systems in the monkey are segregated into strips. This was achieved using the monoclonal antibody mabQ113.

MabQ113 labels the entire Purkinje cell, including the soma, the dendritic tree, axon and, crucially, its terminations within the deep nuclei. In spite of differences in label strengths between different nuclei, and rostrocaudal variation within a particular nucleus, there were no nuclear areas that were free from punctate label. Purkinje cells terminate throughout the deep cerebellar nuclei, and moreover, there was no indication of stripes within Purkinje cell terminal fields in the deep nuclei.

The differences in nuclear label strength can be explained by the difference in labelling of Purkinje cell subsets in the cortex. Although all Purkinje cells showed some degree of immunoreactivity, and there was a continuum of labelling intensity rather than an all-or-none relationship, there were differences in Purkinje cell labelling that are subsequently reflected in the deep nuclei.

Considered as a whole, the vermis contains fewer highly-immunoreactive cells than the lateral hemispheres, and hence the fastigial is on the whole more lightly stained than either the interposed or the deep nuclei. In addition, immunoreactivity of the Purkinje cells increase in a antero-posterior direction, such that projections from the anterior lobe to the rostral areas of the deep nuclei will be less immunoreactive than those from posterior regions to the caudal nuclei. Small variations in immunoreactivity can also be explained with consideration for the passage of cortico-nuclear fibres. The lateral edge of the dentate, for example, frequently appeared more immunoreactive than the rest of the nucleus. However, this is probably due to the labelling of fibres that emanate from the cortex and are known to stream down the lateral edge of the nucleus (Chan-Palay, '77). These fibres are also viewed in cross-section in coronally-cut sections, thereby increasing

the apparent degree of label. The complex curvature of the deep cerebellar nuclei may also account for some of the differences in label strength.

The demonstration that Purkinje cells project onto all parts of the deep nuclei excludes the possibility of segregation of cortical and subcortical nuclear afferents. Thus, one can conclude that Purkinje cells from areas other than those injected project into the unlabelled stripes within the deep nuclei. The functional implication of this are discussed in section 4.3 of the discussion.

4. DISCUSSION

The cerebellum plays a critical role in the visual guidance of movement. In this study of the anatomical connections of those cerebellar cortical areas that receive visual information, I focused on those areas receiving the majority of their visual input from the dorsolateral pons. The cells in the dlpn receive input from dorsal stream extrastriate cortical areas and subcortical visual structures, such as the superior colliculus. All of the cells within the dlpn are visually activated, eye-movement related, or both (Suzuki and Keller, '84; '90; Smooth pursuit: May et al., '85, '88; Mustari et al., '88; Thier et al., '89; Saccades: Thier et al., '96; Ocular following: Kawano et al., '92, '96), and project with varying strengths onto the posterior cerebellar cortex (Glickstein et al., '94). The cerebellar areas which I investigated cannot, however, be described as purely visually-activated or eye-movement related like the dlpn cells serving them, although many populations of Purkinje cells in these areas do demonstrate these type of relations (Ron and Robinson, '73; Noda and Suzuki, '79; Miles et al., '80; Noda and Mikami, '86; Stone and Lisberger, '87; Suzuki and Keller, '88a and b).

Difficulties in characterising areas of the cerebellum as "visual" based on their input from the dorsolateral pons are multiple. The borders of the dorsolateral pons containing visual/oculomotor cells are not precisely demarcated, and thus it is impossible to claim categorically that all the cerebellar afferents from the dorsolateral corner of the pons (as seen in retrograde tracing studies) have these physiological characteristics. Secondly, there are no cases in which the pontine projection emanates solely from the dlpn; additional, non-visual information is transmitted via other pontine nuclear cells. In addition, climbing fibre-mediated information is largely somatosensory in origin. Indeed, only the dorsal cap of the inferior olive contains purely visual/oculomotor-related cells such as those found in the dlpn.

However, studies on the anatomical basis of visuomotor control must focus on those cerebellar areas known to receive visual information. Thus this study was confined to the posterior cerebellar cortex.

This discussion is divided into six parts, covering mossy fibre input from the pontine nuclei and NRTP, the parasagittal organisation of the olivo-cortico-nuclear projection,

the cortico-nuclear and nucleo-cortical projections, deep nuclear eye movement areas and technical considerations.

4.1 MOSSY FIBRE INPUT

4.1.1 Pontine efferents

The ponto-cerebellar pathway has been clearly elucidated in many mammals (Rats: Burne et al., '78; Eisenman and Noback, '80; Burne and Woodward, '83, '84; Azizi et al., '85; Azizi and Woodward, '90. Cats: Hoddevik, '77; Brodal and Hoddevik, '78; Mower et al., '80; Robinson et al., '84; Broch-Smith and Brodal, '90. Monkey: Brodal, '79, '82a,b, Langer et al., '85; Glickstein et al., '94), and my results were in broad agreement with all of them. Injections of WGA-HRP into the cerebellar cortex resulted in retrogradely labelled cells which cluster together in and around the descending fascicles of the corticospinal tract. In agreement with Brodal's ('82a) observations in the monkey, my results demonstrate that the pontocerebellar pathway is simultaneously convergent (with multiple pontine subnuclei projecting onto a single cerebellar area) and divergent (each pontine subnucleus also projecting to separated areas of the cerebellar cortex).

The pontocerebellar pathway - anatomy

The visual and oculomotor responsive cells in the monkey dlpn nuclei project most heavily to the dorsal paraflocculus, vermal lobule VII and the uvula, and more moderately to crus II and paramedian lobule, in agreement with previous studies (Glickstein et al., '94). For cases in which the pontocerebellar projection was dominated by the dorsolateral pons, there were other pontine nuclei which contributed more moderate input, and label at any level of the pontine nuclei included the major dlpn cell group and smaller satellite groups of labelled cells. In cases such as crus II, paramedian lobule and VIII, which were not dominated by dorsolateral pontine input, there was a much more even distribution of pontine efferents from the various nuclei.

The flocculus and ventral paraflocculus receive virtually no projections from the pontine nuclei. The few cells that were present were much more sparsely labelled than pontine cells encountered in any other case, suggesting that they provided a smaller calibre projection to the flocculus. A likely explanation is that these projections may be collateral fibres from a main axon heading elsewhere in the cerebellar cortex. Two (or more) cortical areas would thus receive identical input via the pontine mossy fibre system, but different information via the other mossy fibre sources (such as NRTP) or the climbing fibre system. However, it should be noted that this collateral system would be very restricted, with only one or two cells providing collaterals from a pontine nucleus at any particular rostrocaudal level.

Those cerebellar areas that receive the greatest input from the dorsolateral pons (dorsal paraflocculus and vermal lobule VII) receive input throughout its rostrocaudal length. Those areas which receive a less powerful projection (uvula) or only a moderate one (crus II, paramedian lobule), receive projections from a more restricted rostrocaudal span of the basilar pons. The dorsal stream extrastriate cortical visual areas focus their projections onto the rostral levels of the dlpn, while the superior colliculus focuses its projection caudally (Glickstein et al., '90), although there is some overlap between their terminal fields in mid-pons.

Differences in rostrocaudal heights of retrogradely labelled pontine cells following separate cerebellar cortical injections could be taken to indicate that particular cerebellar areas receive cortical in preference to subcortical visual information. This is only true for the *direct* pontine projections from individual visual areas. It should be recalled that the cortical and subcortical visual areas are interconnected.

Both the MT and MST which are themselves interconnected (Ungerleider and Desimone, '86), project individually to the dlpn (Glickstein et al., '80, '90a), and also project onto the superior colliculus. MT projects onto the purely visual superficial and intermediate layers, whilst the MST input terminates in the polysensory deeper layers (Maioli et al., '92). All layers of the superior colliculus project to the dlpn (Glickstein et al., '90).

The frontal eye fields and superior colliculus are also topographically interconnected and project independently to the pontine nuclei. The ventrolateral FEFs code for small

saccades and project onto the rostral areas of the superior colliculus which represent perifoveal vision and which, upon stimulation, elicit small saccades. The dorsomedial FEFs code for large saccades and project onto the entire rostrocaudal length of the superior colliculus, reaching areas representing the peripheral visual field, and which produce large saccades on stimulation (Robinson, '72; Bruce et al., '85; Stanton et al., '88). Both the frontal eye fields and the superior colliculus project to the dlpn: the frontal the fields project with no particular topography onto the entire rostrocaudal length of the pons, in the dorsal, medial and dorsolateral nuclei (Stanton et al., '88). The collicular input focuses caudally (Harting et al., '77; Glickstein et al., '90) in the dlpn. Therefore, the bulk of visual input to the rostral dlpn is indeed cortical in origin. The caudal dlpn, however, receives a mixture of cortically and sub-cortically derived visual information: a few cortical areas do project directly to caudal dlpn; those that do not, send inputs indirectly via a relay in the superior colliculus. This, combined with the overlap of cortical and subcortical projections to mid-pons *and* the divergence of cortico-pontine projections to nuclei other than the dlpn suggest that cerebellar cortical areas receive visual input from a wide range of cortical and subcortical areas.

The pontocerebellar pathway indicates sharp dichotomies between cerebellar cortical areas. The most obvious example of this is in the floccular complex, in which the dorsal paraflocculus receives the most powerful dlpn input, while flocculus and ventral paraflocculus receive only a tiny collateral input. A more subtle example of this is seen in the uvula, in which rostral folia receive a more powerful projection than the caudal ones. An interesting point to note is that a dichotomy between rostral and caudal folia of the uvula is maintained throughout the olivo-cortico-nuclear system too. The dichotomy between the flocculus and dorsal paraflocculus is mirrored in the climbing fibre input, but is lost in the cortico-nuclear projection (see section 4.2.2).

Physiology

The dlpn is the only discretely visual and/or oculomotor nucleus within the pons. Electrophysiological and lesion studies in a number of animals have demonstrated that it contains directionally selective neurons (Cats: Baker et al., '76; Mower et al., '80; Monkeys: Suzuki and Keller, '84; Mustari et al., '88; Thier et al., '88, '89; Suzuki et al.,

'90) and have assigned it roles in smooth pursuit eye movements (Suzuki and Keller, '84; May et al., '85; May et al., '88; Mustari et al., '88; Thier et al., '88, '89), saccades (Thier, '96) and ocular following (Kawano, '96).

Each of the roles it plays in oculomotor control are attributable to the cortical and/or subcortical visual inputs that it receives. Directional selectivity and smooth pursuit relations are derived from its input from dorsal stream extrastriate visual areas such as MT and MST. Cells in these areas not only provide the dlpn with detail on visual motion resulting both from movement of the visual scene relative to a stationary observer and the movement of an observer through a visual scene, but also signals relating to smooth pursuit (Maunsell and van Essen, '83; Thier, '92; Tanaka et al., '93). The FEFs, which are normally associated with saccadic eye movements, have been recently shown to contain smooth pursuit signals (MacAvoy et al., '91) which are also transmitted to the dorsolateral pons (Stanton et al., '88).

The saccadic signals recently found in the dlpn (Thier, '96) presumably result from its input from the superior colliculus, FEFs, LIP and VIP, whilst the dlpn cells related to the ocular following response (Kawano et al., '96), may do so due to input from the nucleus of the optic tract (Buttner-Ennever, '96), the cells of which also contain cells related to ocular following (Kawano et al., '96).

The dlpn, therefore, contain a range of signals relevant to the visual guidance of voluntary movement, and of eye movements particularly. These signals are distributed across the posterior cerebellar cortex, but the most powerful projections are to those areas frequently associated with eye movements, such as the dorsal paraflocculus (Noda and Mikami, '86) and the vermal lobule VII (Fujikado and Noda, '87; Suzuki and Keller, '88; Sato and Noda, '92; Ohtsuka and Noda, '95).

The distribution of the dlpn afferents to these regions of greatest input seems to be equal within each particular area: for example, anterograde tracing studies following dlpn injections demonstrate that all folia in the dorsal paraflocculus receive equal amounts of input from the dlpn (see figure 3, Glickstein et al., '94). However, the physiology of the dlpn cerebellar targets vary both between different cerebellar regions, and within individual cortical areas. Vermal lobule VII is dominated by saccade-related Purkinje cells, with a smaller population controlling smooth pursuit eye movements, and a tiny

minority responding to optokinetic stimulation (Suzuki and Keller, '88; Sato and Noda, '92). Purkinje cells in the dorsal paraflocculus seem to be related to saccades (Noda and Mikami, '86), but not smooth pursuit. In addition, regional differences in the Purkinje cell responses *within* a particular cerebellar cortical areas indicates that the dlpn afferents do not transmit all of the signals inherent to their cell population to every cerebellar cortical region. In their study of the dorsal paraflocculus, for example, Noda and Mikami ('86) only found eye movement relations in folia 4-6 of the dorsal paraflocculus. The more medial and lateral folia were not responsive to their saccadic paradigms. Therefore, although the dlpn has the potential to distribute all types of visual/oculomotor information to each individual area of the cerebellar cortex, clearly physiological subsets of dlpn afferents project to different cerebellar locations. Support for this arises from anatomical double-label studies investigating collateral projections from the dlpn. Thielert and Thier ('93) injected fast blue and fluorogold retrograde tracers into vermal sublobules VIIAa/b and VIIAd, and cholera toxin and fast blue into VIIA/B and VIIIA, and found that no dlpn cells were double-labelled. They concluded that adjacent lobules in the posterior vermis, receive input from overlapping cell groups, but "different populations" of pontine neurons. Similar studies in the rat indicate that dlpn cells do not provide collateral systems to more widely separated cerebellar cortical areas (Hans: personal communication).

4.1.2 NRTP efferents

Fewer studies have been dedicated to the NRTP-cerebellar projection than the pontocerebellar projection (Hoddevik et al., '78; Gerrits and Voogd, '83; Gerrits et al., '84; Brodal, '80; Azizi and Woodward, '90; Broch-Smith and Brodal, '90; Armengol and Salinas, '91; Thier and Thielert, '93).

Data presented in this thesis is in broad agreement with previous studies in the monkey, although there are points of difference. In addition, it provides new details on the pathway that have not been discussed hitherto.

Anatomy

The cerebellar efferents from the NRTP are more lobule specific than those from the basal pons, and there are large areas of the cerebellar cortex which do not appear to receive an input from the NRTP, such as the uvula, paramedian lobule and the dorsal paraflocculus. Of those areas that do receive input from the NRTP, the flocculus and vermal lobule VII receive by far the largest amount, in agreement with previous reports (Brodal, '80; Yamada and Noda, '87; Thier and Thielert, '93).

In his paper on basal pontine efferents, Brodal ('80) describes efferent cell groups as "clustering" and cites this as a major difference with NRTP cerebellar efferents which he suggested are more diffusely scattered. However, in their double-label retrograde study, Thielert and Thier ('93) describe NRTP efferents to the vermis as being clustered in a comparable way to the pontocerebellar system. Each of the cases presented in this thesis show NRTP clustering reminiscent of that in the pontocerebellar system, Thielert and Thier's data, and the pattern of input to the NRTP from the cerebral cortex or superior colliculus (Harting, '77; Brodal, '80; Stanton et al., '88; Glickstein et al., '90). Indeed, scrutiny of Brodal's figures indicate that the more scattered NRTP projections terminated in the anterior lobe of the cerebellum, whereas those to the posterior lobe were clustered in a similar way to the cases presented here.

The NRTP-cerebellar pathway in the monkey is predominantly contralateral, although it has a much greater ipsilateral component than the pontocerebellar pathway. Armengol and Salinas ('91) observed a similar phenomenon to a greater degree in the rat, and suggested that the NRTP-cerebellar pathway in this mammal is bilateral. Data presented here suggests that, in the monkey, only cerebellar projections from the medial NRTP are bilateral.

Previous studies (Brodal, '80; Thielert and Thier, '93) on NRTP projections in the monkey compare well with the data presented here, in spite of a few differences. The powerful projection from the entire rostrocaudal length of dorsomedial NRTP to vermal lobule VII is in agreement with all previous studies on this system (Brodal, '80; Yamada and Noda, '87; Thielert and Thier, '93). However, Brodal's cases failed to

show label in the more lateral regions of the NRTP, found in the cases presented here and in other studies (Yamada and Noda, '87; Thielert and Thier, '93).

Following a lobule VII injection, central and ventral portions of the NRTP were unlabelled: this area contains floccular afferents (Brodal, '80; Langer et al., '85; present study). Additional projections to the flocculus arise from lateral regions of rostral NRTP, from areas partially overlapping with lobule VII afferents. This rostrolateral NRTP group also projects to lobule VIII, although at more caudal levels NRTP afferents to VIII arise more medially.

Brodal's paper suggested that the lateral NRTP also projects to the paramedian lobule. With the exception of M2-96left which contained labelled cells within centrolateral areas of the NRTP, none of the paramedian cases presented here demonstrated any input from NRTP. Animal M2-96, however, received bilateral injections of WGA-HRP, and, as the NRTP-cerebellar pathway has a moderately strong ipsilateral component, the lateral NRTP label may have arisen as retrograde transport from the injection site centred on the right, in crus II. There is good correspondence between the NRTP label in M2-96left and a pure crus II case (sb6).

Thus, it is likely that the NRTP does not project to the paramedian lobule.

The NRTP does not project to the dorsal paraflocculus. Those dorsal paraflocular cases which did contain label in the NRTP all had injection sites spreading beyond the paraflocculus into either crus II or the flocculus. The NRTP label in these dorsal paraflocular cases correlates with that found in pure crus II or flocculus cases.

The NRTP sends its strongest projections to the flocculus.

Thus, the dichotomy between the dorsal paraflocculus and the flocculus is present in both the pontine and NRTP efferent systems. The dorsal paraflocculus receives the largest input from the dlpn, but none from the NRTP, while the flocculus receives virtually no projections from the dlpn, but a massive input from the NRTP.

Physiology

The flocculus and vermal lobule VII receive the greatest input from NRTP-cerebellar cortical efferents. The arrangement of floccular and lobule VII afferents from the NRTP

are of particular interest due to the involvement of the NRTP in oculomotor control (Gamlin and Clarke, '85; Zhang and Gamlin, '87; Yamada and Noda, '87; Yamada et al., '96).

Electrophysiological and lesion studies have implicated the medial areas of NRTP in the regulation of smooth pursuit eye movements (Yamada et al., '96), saccades (Gamlin and Clarke, '85) and vergence and ocular accommodation (Gamlin and Clarke, '95). Smooth pursuit-related cells are located in the rostral two-thirds of the NRTP. Saccadic and vergence-responsive cells are found in the caudal half of the NRTP, such that there is some overlap between saccadic and smooth pursuit-related areas in the NRTP, although vergence-related neurons are always segregated caudally. The saccadic and vergence-responsive neurons are found in close proximity, but none of the recorded cells showed firing modulation to both stimuli. Within the population of vergence-responsive neurons, both far and near-response relations were encountered.
Although lateral areas of the NRTP project both to the flocculus and vermal lobule VII, and receive an input from the posterior parietal cortex (Leichnetz et al., '84; Schmahmann and Pandya, '89) there are no single-unit recording studies on this area.

Electrophysiological and anatomical studies on the medial NRTP, combined with the recent description of smooth pursuit neurons in the FEFs (May and Andersen, '86; Lynch et al., '87; MacAvoy et al., '91) have indicated the presence of three cerebro-NRTP-cerebellar pathways controlling smooth pursuit, saccadic and vergence eye movements. The data presented in this thesis clarifies the role that the NRTP plays in transmitting these oculomotor-related signals to the cerebellar cortex.

Smooth pursuit signals from the FEFs are transmitted to rostral levels of the medial NRTP (Stanton et al., '80); saccadic and vergence signals from the FEFs/superior colliculus and prearcuate cortex respectively are transmitted to caudal levels of the medial NRTP(Leichnetz et al., '84; Stanton et al., '88).
The medial NRTP is known to project most heavily to the flocculus and lobule VII in the cerebellar cortex (Brodal, '80; Yamada and Noda, '87; Thielert and Thier, '93). However, my data indicates that inputs to dorsomedial regions of the NRTP are

transmitted to vermal lobule VII, whilst those to ventromedial regions are transmitted to the flocculus. The only region of overlap between medial NRTP cell groups projecting to VII and flocculus is in the dorsomedial nucleus at the most caudal levels of NRTP.

Thus, the present study shows that signals used in smooth pursuit, saccadic and vergence eye movements are transmitted to vermal lobule VII *and* the flocculus via rostrocaudally and dorsoventrally segregated relays in the NRTP. The functional implications that this segregation produces therefore depend on differences between dorsal and ventral regions of the oculomotor medial NRTP. Single unit recordings and anatomical tracing studies restricted to the different dorsoventral levels of lobule VII and floccular projecting NRTP cell groups are warranted, as are single-unit recording and double-label retrograde anatomical tracing studies to clarify the role that the hitherto uninvestigated lateral NRTP plays in oculomotor control.

4.1.3 The dlpn and NRTP - dual pathways in oculomotor control

Cerebellar control of smooth pursuit and saccadic eye movements is achieved via two parallel pathways.

Cerebellar input from the smooth pursuit and saccadic systems arise via relays in the dlpn or the medial NRTP. Considered together, the most likely cerebellar targets for these precerebellar nuclei are the vermal lobule VII, the dorsal paraflocculus and the flocculus. Due to the strict dichotomy between dlpn projections to the dorsal paraflocculus and the flocculus, and the division of the medial NRTP into lobule VII-projecting dorsal areas and floccular-projecting ventral areas, there is an interesting distribution of smooth pursuit or saccadic signals over the cerebellar cortex.

Vermal lobule VII receives smooth pursuit and saccadic information via converging inputs from both the dorsolateral pons and dorsomedial NRTP. The dorsal paraflocculus, on the other hand, receives input purely from the dlpn, with no contribution from the NRTP. Finally, the flocculus, receives input from the ventromedial NRTP but none from the dlpn.

The overall picture is complicated further if one considers the input to the NRTP and dlpn from the nucleus of the optic tract (Mustari et al., '90; Buttner-Ennever, '96; Kawano, '96) and other extrastriate visual areas in the dorsal stream (Glickstein et al., '94).

At the simplest level, however, these parallel pathways which employ different precerebellar nuclei and/or subregions of the same precerebellar nucleus must play different but complementary roles in the cerebellar control of voluntary eye movements (see figure 38).

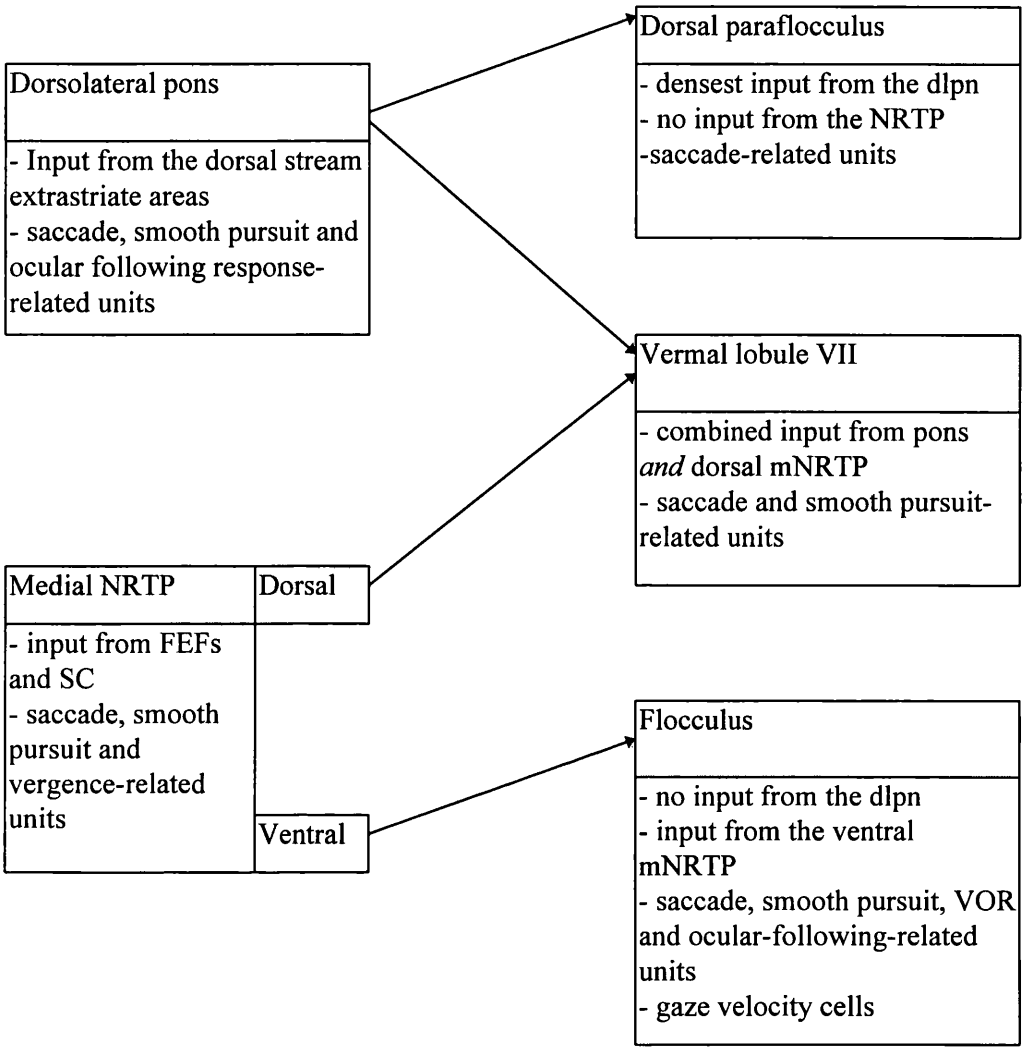

Figure 38 Multiple cortico-ponto/NRTP-cerebellar pathways in oculomotor control.

4.2 THE OLIVO-CORTICO-NUCLEAR PROJECTION

The first section of this discussion will be concerned with the olivocerebellar projection in isolation. The olivo-cortico-nuclear projection will be discussed in section 4.2.2. Details on the specific topography of the cortico-nuclear projection will be presented in section 4.3.

4.2.1 The olivocerebellar pathway.

The inferior olive is the sole source of climbing fibres to the cerebellum. The topography of this pathway has been thoroughly investigated in a number of mammals and its topography and relationship to cortical efferents is reasonably well understood (Rat: Bernard, '87; Buisseret-Delmas, '88; Ruigrok and Voogd, '90; Cat: Groenewegen and Voogd, '77; Groenewegen et al., '79; Walberg et al., '79, '87; Rosina and Provini, '82, '83, '87; Kanda et al., '89; Dietrichs and Walberg, '90; Rabbit: Sato and Barmack, '85; Monkey: Brodal and Kawamura, '80; Brodal and Brodal, '80, 81).
Axons from different olivary subnuclei project through distinct white matter compartments, visible in anticholinesterase or myelin-stained material, and terminate as on Purkinje cells as parasagittal strips running orthogonal to the length of a folium (Groenewegen and Voogd, '77, '79 etc). The cortical efferents share these white matter compartments, and the parasagittally-arranged olivocorticonuclear projections form zones across the mediolateral dimension of the cerebellar cortex. These zones have been ascribed letters from A to D2, and are considered to be the functional module of the cerebellum. However, as will be discussed in the next section, the cortico-nuclear projection in the monkey does not maintain precision of the parasagittal projection in the olivocerebellar pathway, and the decision as to which zone a cortical region should therefore be determined by its olivary afferent, not its nuclear projection.

Brodal and Brodal's HRP studies on the olivocerebellar system in the monkey ('81, '82) have demonstrated a parasagittal organisation within the pathway, but have not been able to describe a more detailed topography within particular olivary zones. Reports of very precise topographies in individual olivocortical parasagittal zones are, however,

available on non-primate systems (Rat: Bernard, '87; Rabbit: Sato and Barmack, '85; Cat: Kanda et al., '89).

The olivary data in this thesis was collected principally to investigate the overall topography of the olivocorticonuclear projection and therefore concerns relatively large areas of the cerebellar cortex. Nevertheless, it confirms and extends previous studies on this system and presents some interesting patterns which have not been reported previously.

4.2.1.1 The vermis

The olivocerebellar projection to the vermis in the monkey is very similar to that reported for non-primates (Rat: Bernard, '87; Buisseret-Delmas, '88a and b; Buisseret-Delmas et al., '93; Buisseret-Delmas and Angaut, '93; Cat: Kanda et al., '89; Rabbit: Sato and Barmack, '85). The vermis contains a medially located zone A, receiving input primarily from the cMAO and subnucleus β, and zone B, which receives projections from the caudal DAO.

Brodal and Brodal ('81) confirmed that vermal lobules VII and VIII in the monkey receive olivary efferents from medial (cerebral) and lateral (spinal) divisions of the cMAO respectively, with additional contributions from the subnucleus β, which are not evident in the cat. Data from this study supports these findings, and additionally supports the suggestion that vermal lobule VII receives a greater overall olivary input than lobule VIII.

Interestingly, data from this study suggests that the vermal zone B has a greater rostrocaudal length in the monkey than it does in the cat, reaching and including vermal lobule VII. The medial zone A areas in vermal lobule VII that project to the fastigial oculomotor region control both saccadic and smooth pursuit eye movements (Fujikado and Noda, '87; Noda and Fujikado, '87; Suzuki and Keller, '88; Noda, '91; Sato and Noda, '92; Ohtsuka and Noda, '95). The more lateral vermal zone B projects to cells in the lateral vestibular nucleus that give rise to the vestibulospinal tract known to control the muscles of the neck. Thus, the combined output of vermal lobule VII in the monkey

may be used to control combinations of eye and head movements to track targets of interest.

Previous reports of zone C1 encroachment into the vermal lobule VIII of the cat and monkey (Oscarsson and Sjolund, '77; Groenewegen et al., '79; Kawamura and Hashikawa, '79; Brodal and Brodal, '81) could not be confirmed in this study, due to the restricted mediolateral spread of the injection site in this lobule.

The uvula receives a powerful topographic input from subnucleus β (cat: Brodal, '76; Kanda et al., '89; Rabbit: Sato and Barmack, '85; monkey: Brodal and Brodal, '81; present study). Data presented here suggests that the rostral subnucleus β and ventral leaf project to the caudal uvula; the caudal subnucleus β and cMAO project to the rostral uvula. Differences between the rostral and caudal uvula are well documented and not confined to the olivary input: rostral and caudal uvula also receive different mossy fibre inputs (Sato et al., '89; Eisenman and Noback, '80), different degrees of primary vestibular input (Brodal and Hoivik, '63; Carpenter et al., '72) and have different nuclear projections (Tabuchi et al., '89). As a result, it has been suggested that the rostral and caudal uvula serve different functions (Eisenman and Noback, '80).

Recent HRP studies in the cat and rabbit (Sato and Barmack, '85; Kanda et al., '89) have demonstrated a more finely-detailed parasagittal organisation in the uvula than that previously described by Voogd and colleagues. The parasagittal zones in the uvula of these animals receive input from caudal and then rostral subnucleus β to the most medial uvula; subsequently lateral divisions of the uvula receive olivary efferents from the cMAO, the dorsomedial cell column, ventral lamella and finally the rostral MAO. Data presented here is not able to confirm or dispute the presence of a similar parasagittal system in the monkey, but one small interspecies difference is evident. The ventral lamella of non-primates project preferentially to rostral folia of the uvula. Data presented here indicates that the ventral lamella of the monkey projects to the caudal uvula instead (see case UV1). However, in view of the overall interspecies similarities in the olivocerebellar vermal projections, it is likely that some degree of detailed olivo-uvula topography is present in all mammals.

The nodulus was not investigated in this study, since it receives little or no visual input via the dorsolateral pontine nuclei. Recent double-label retrograde tracing studies in the rabbit (Takeda and Maekawa, '89), however, have demonstrated that up to 8% of uvula-projecting cells in the nucleus β send collaterals to the nodulus. An equivalent collateral system is likely to exist in the monkey.

4.2.1.2 The pars intermedia and hemispheres

Olivary input to the cerebellar hemispheres is dominated by projections from the principal olive, confirming that zone D covers much of the paramedian lobule and crus II. There has been some debate as to whether projections to cortical zones D1 and D2 arise from different lamellae in the principal olive (see Brodal and Kawamura, '80; Bigare and Voogd, '80). According to autoradiographic and fluorescent retrograde tracing studies in the cat, it appears that the ventral lamella supplies D1 and the dorsal lamella/lateral bend D2 (Groenewegen and Voogd, '77; Groenewegen et al., '79; Bigare and Voogd, '80; Rosina and Provini, '83). In HRP studies in the cat, however, it has been reported that the lateralmost zone in the paramedian lobule, D2, receives input from the ventral lamella, whilst the more medial D1 zone receives its afferents from the dorsal lamella (Brodal and Walberg, '77b; Walberg and Brodal, '79).
Brodal and Brodal ('81) explored the olivocerebellar projection of the monkey using retrograde transport of HRP. In the paramedian lobule and crus II cases, they found that the dorsal lamella projected to more medial areas of these lobules than the ventral lamella. Hence they concluded that the dorsal lamella/lateral bend of the principal olive projects to cortical zone D1, whilst the ventral lamella projects to cortical zone D2, in agreement with their studies in the cat. Their data also suggests that the cortical zone D2 is narrow in both species.

Data presented in this thesis supports Brodal and Brodal's conclusions on the dorsal and ventral lamella projections to the cerebellar hemispheres. The figures in the results chapters do not present the cerebellar cortex as unfolded, and it should be borne in mind that when the cerebellum is viewed posteriorly, the very lateral edges of the

hemispheres are curled underneath the hemispheres and are out of sight. Hence, only two cases (GR-95 and M2-96left) had injection sites located at the very lateral edge of the paramedian lobule. These were the only cases containing label in the ventral lamella. In both cases, the injection site spread into the dorsal tip of the dorsal paraflocculus folia, but due to the twisting of the folial chain as it leaves the paramedian lobule, these most dorsal levels of the paraflocculus also contain zone D2 (see next section). The crus II cases were also restricted to more medial areas of the cortex and contained retrograde olivary label only in the dorsal lamella.

The paramedian lobule cases investigated by Brodal have injection sites and olivary label in very similar locations to the data presented in this thesis. Thus, data in this thesis supports the contention that in the monkey the dorsal leaf of the principal olive projects to the more medially situated D1 zone, and the ventral lamella to D2 of the paramedian lobule and crus II.

Within paramedian lobe cases, there was evidence of a more detailed olivocerebellar topography: caudal areas of the folial chain receive inputs from extreme rostromedial areas of the dorsal lamella; olivary projections to more rostral levels of the paramedian folial chain arise from more caudal and lateral areas of the dorsal lamella. The rostrocaudal topography of the olivary projection to the folial chain is paralleled by differences in their nuclear projections, which will be discussed in the next section. There were hints of an extremely detailed olivo-cortical topography when cases at rostral levels of the paramedian chain were studied: there were very slight variations in both the injection sites and the olivary label, but unfortunately it was not possible to discern a clear and consistent pattern. No doubt investigations with smaller injection sites, and employing a tracer such as biocytin which has fewer interpretative difficulties in the extent of the injection site would demonstrate a clear topography in the dorsal lamella projections to the paramedian lobe.

The crus II cases were also dominated by dorsal lamella input, and were thus located in cortical zone D1. In spite of this, there was no overlap between olivary afferents to the crus II and paramedian lobule: a testament to the precision of the olivocerebellar pathway.

A rostrocaudal topography was also evident in olivary projections to crus II. Caudal levels of the olive projected to caudal levels of the crus II chain, nearest the paramedian lobule. Rostral dorsal leaf projected to rostral levels of the folial chain.

Thus, when the paramedian lobule and crus II cases are looked at as a whole, a general pattern of D1/dorsal lamella projections to the pars intermedia and hemispheres becomes evident. Moving from caudal to rostral through the folial chain which comprises the paramedian lobule and crus II, there is a progression of dorsal lamella output from rostral to caudal olivary levels along the paramedian lobule, up to the prepyramidal fissure, and then from caudal to rostral olivary levels along crus II.

Data presented here confirms and extends previous reports on olivocerebellar projections to the pars intermedia and hemispheres of cats (Groenewegen and Voogd, '77; Groenewegen et al., '79; Walberg et al., '79, '87; Rosina and Provini, '82, '83, '87; Kanda et al., '89; Dietrichs and Walberg, '90) and monkeys (Brodal and Brodal, '81). The hemispheres are dominated by the D1 zone, which appears to be expanded in the posterior lobe (Brodal and Brodal, '81; Haines et al., '82), but zones C2 and C1-3 are also in evidence, as demonstrated by the appearance of label in the rostral MAO and DAO respectively. However, this data also supports the contention held by Voogd and his colleagues (Groenewegen and Voogd, '77; Groenewegen et al., '79; Bigare and Voogd, '80) that parasagittal cortical zones are not necessarily present throughout the rostrocaudal length of a cerebellar subdivision. In PMD2, for example, there is no olivary label indicating the involvement of cortical zone C3 in the injection site, but there is label attributable to its neighbouring C2 and D1 zones. This may suggest that the cortical zone C3 vanishes from the most caudal areas of the paramedian lobule.

4.2.1.3 Floccular complex

Data presented in this thesis lend further support to Brodal's ('81) contention that the ventral lamella projects to the D2 zone in the cortex.

Due to the twisting of the folial chain as it moves into the paraflocculus from the paramedian lobule, the lateral edge of the folial chain is positioned dorsally in the

paraflocculus, such that the D2 zones in the paramedian lobule and dorsal paraflocculus face each other across the parafloccular sulcus. The majority of dorsal parafloccular cases covered the entire dorsoventral height of the parafloccular folia, and therefore included the D2 zone. These cases all contained olivary label in the ventral lamella, and indeed, the only case which did not (dpf1) had an injection site restricted to ventral areas, and did not cover the levels in which the D2 zone resides. In addition, case M2-96left contained a leak through lateralmost paramedian lobule into the dorsalmost tip of the dorsal paraflocculus and concomitant label in the ventral lamella.

The olivocerebellar projection to the dorsal paraflocculus raised some interesting issues. In the majority of cases, label was found in the ventral lamella of the principal olive (zone D2) and the rostral medial accessory (C2). The absence of olivary label in the dorsal leaf in these cases suggests that zone D1 in the dorsal paraflocculus, unlike its representation in the hemisphere, is either very thin or absent. The dorsal paraflocculus is difficult to inject due to its ventral position beneath the paramedian lobule, and, as a result, all the injection sites in this study are situated in similar folia within the dpf. The breadth of individual zones clearly varies across cerebellar subdivisions (Voogd, '69; Groenewegen et al., '79; Bigare and Voogd, '80; Buisseret-Delmas, '88, '93), and it is possible, therefore, that the D2 zone in the dorsal paraflocculus is larger in folia medial or lateral to those which are described here.

The retrogradely labelled cells in the ventral lamella were strikingly confined to the cell-poor thin division of this subnucleus. No cells were seen more laterally in the larger division which is continuous with the lateral bend and dorsal lamella. Two possible conclusions can be made. Firstly, that projections to cortical D2 zones from the cell-poor thin division of the ventral lamella are confined to the dorsal paraflocculus. This suggestion is complicated, however, by the observation that in hemispheric cases (GR-95 and M2-96left) with leak into the dorsal paraflocculus, this type of ventral lamella label is evident, and it is impossible to determine whether it arose from injection into the D2 zone of the dorsal paraflocculus or the overlying paramedian lobule.
The other possible conclusion is that in the monkey, the D2 zone is greatly reduced, and it is only this cell-poor thin ventral lamella that projects to *any* cortical D2 zone,

regardless of location within the hemisphere. The remaining principal olivary nucleus would consist only of dorsal lamella and lateral bend, comprising the projection to the cortical D1 zones. Indeed, the lateral bend and dorsal lamella are conceived as a combined efferent unit to D1 cortical areas due to their morphological similarities. Brodal ('81) comments that:

> "...Compared with the pattern in the cat and other subprimate species, the lateral bend appears to be mainly a further development of the dorsal lamella, indicating that this shows a more marked growth and expansion than does the ventral lamella, which, furthermore, both in the cat and the monkey, is relatively cell poor in comparison to the dorsal lamella....."

Bowman and Sladeck ('73) and Brodal and Brodal ('81, '82) used arbitrary limits to differentiate between the lamellae of the principal olive of the monkey. Data on the olivocerebellar projection presented in this thesis, however, may indicate that only the cell-poor thin area in the principal olive comprises the ventral lamella, and thereby may provide a more rigorous and reproducible differentiation between the lamellae of the principal olive based on these morphological differences. Retrograde tracing studies with injection sites confined to D2 areas in various cortical subdivisions are needed to confirm or exclude this possibility.

Cases containing rMAO and cell-poor ventral lamella label simultaneously were remarkable in that the label in both subdivisions consistently appeared at the same rostro-caudal and mediolateral positions: the label in the ventral lamella completely overlaid that in the rMAO. The figures in Brodal and Brodal's paper ('81) indicate that this phenomenon is not restricted to the D2 and C2 zones, but is a more consistent feature of the cerebellar projection from all subnuclei in the inferior olive. The rostral dorsal accessory olive is known to contain a refined cutaneous map of the entire contralateral body surface in the cat (Gellman et al., '83), due to topographic projections from the dorsal column nuclei (Boesten and Voogd, '75; Groenewegen et al., '75; Berkely and Hand, '78; Kalil, '79). Similar detailed cutaneous maps are not evident in the other olivary subnuclei. However, broad somatotopic maps relaying different parameters of information about particular body parts may be evidence. For example, the cells of the cat MAO have more complex receptive fields than those found in the

DAO, and transmit predominantly deep rather than cutaneous information. The complexity of the receptive fields precludes the description of a detailed somatotopy such as that in the DAO, but nonetheless a broad mediolateral somatotopy has been discerned. It is likely that each subnucleus of the olive contains some degree of somatotopy, since each receives topographical projections from the deep cerebellar nuclei (Graybiel et al., '73; Tolbert et al., '76; Berkely and Worden, '78; Chan-Palay, '78; Dietrichs and Walberg, '81, '85, '86; Angaut and Cicirata, '82; Ruigrok and Voogd, '90), each of which has been shown both anatomically and physiologically to contain an individual somatotopic map (Thach, '68, '70, '72; Strick, '76; Asanuma et al, '83a-c; Thach et al., '92, '93; Van Kan et al., '93; Gibson et al., '96).

The possibility arises therefore, that some kind of body map is distributed across the rMAO and cell-poor ventral lamella. In comparing the medial principal olive and the DAO of the cat, Gellman et al. observed that:

> "....The medial region of the principal olive has a preponderance of responsiveness to taps, many bilaterally symmetric fields, and conforms with the general medial forelimb and lateral hindlimb trend seen in the *overlying* MAO...." [my italics]

Thus, the broad somatotopic maps evident in the olivary subnuclei may be in register with those directly above or below. The cells in the rMAO and overlying vlPO presented in this study, and equivalent neighbouring populations in other studies, may transmit different parameters of information about a particular body part onto the same area of the cerebellar cortex. In addition, both sets of olivary neurons would send collateral branches to somatotopically corresponding areas in different parts of the hemispheres (Armstrong et al., '74; Brodal et al., '80; Rosina and Provini, '83, '87).

The flocculus and ventral paraflocculus receive the majority of their olivary input from the dorsal cap and ventrolateral outgrowth. The dorsal cap was almost completely filled throughout its rostrocaudal length, indicating that almost all floccular zones had been included in the injection site. Due to the size and similarity of the injection sites, it was impossible to discern a clear mediolateral topography for projections from the dorsal cap to the flocculus. Comparison between the pure flocculus and flocculus/ventral paraflocculus case suggests that the lateral edge of the dorsal cap may project to the

ventral paraflocculus and the medial edge to the flocculus proper, as the lateral areas of the dorsal cap only contained labelled cells when there was involvement of the medial extension of the ventral paraflocculus. In the cat, the nodulus is reported to receive its olivary afferents from the same region as the flocculus (Brodal and Kawamura, '80). Indeed, recent double-label retrograde studies in the rabbit (Takeda and Maekawa, '89) demonstrated that olivary axons from the dorsal cap and the ventrolateral outgrowth bifurcate to supply both the flocculus and the nodule. There are however, few (if any) bifurcating axons from either the dorsal cap or the nucleus β that project to both the flocculus and the uvula.

The fact that the dorsal paraflocculus and flocculus receive different olivary input has important functional consequences, particularly when considered within the context of the parasagittal zonation of the olivo-cortico-nuclear pathway. It is to this system that we will now turn.

4.2.2 The olivo-cortico-nuclear projection - divergence from parasagittal zonation

The basic functional module of the cerebellum consists of a parasagittal strip of cerebellar cortex, its afferent projections from a particular inferior olivary subnucleus and efferent projections to a deep cerebellar nucleus, or part thereof (Voogd, '64, '69, '89; Haines, '76, '84, '89; Chan-Palay et al., '77; Brodal and Walberg , '77a, b; Groenewegen and Voogd, '77; Haines and Rubertone, '77, '79; Dietrichs and Walberg, '79, '80; Groenewegen et al., '79; Bigare and Voogd, '80; Brodal, '80; Oscarsson, '80; Brodal and Kawamura, '80; Walberg, '80; Eisenman, '89; Dietrichs, '81a, b, '83; Brodal and Brodal, '82; Haines et al., '82; Beyerl et al., '82; Trott and Armstrong, '87a, b, c; Bernard, '87; Buisseret-Delmas, '88a, b; Tabuchi et al., '89; Trott, '89; Paallysaho et al., '90; Haines and Dietrichs, '91; Umetani, '93; Yatim et al., '95; Rosina et al., '96). With the exception of an extensive study on the cortico-nuclear system of the anterior lobe of the primate (Haines et al., '82), the primate olivocorticonuclear system has not been thoroughly investigated since Jansen and Brodal's original lesion study ('40 and '42) produced the concept of longitudinal cerebellar organisation. Indeed, Haines' study was confined to the anterior lobe, and did not correlate the cortico-nuclear projections with the olivocerebellar system. In view of the extensive information on the parasagittal

zonation of non-primate olivocorticonuclear systems, and the increasing appreciation of somatotopy in the deep cerebellar nuclei of the primate, this thesis focused on the olivocorticonuclear system of the posterior lobe of the macaque cerebellum. The posterior lobe was chosen for study due to its input from the visual and oculomotor dorsolateral pons, and therefore its role particularly in the visual guidance of voluntary movement.

The parasagittal zones across the cerebellar cortex are characterised and defined by their afferent and efferent connections. The vermis is composed of zones A (divisible into A1-3), x and B, the intermediate cortex of zones C1-3, and the lateral cortex of zones D1 and D2. Although some zones have a limited rostrocaudal extent (Armstrong and Campbell, '78a, Dietrichs, '81a; Haines and Dietrichs, '91), others may narrow and widen through the cerebellum (Haines et al., '82) or deviate from the midline (Buisseret-Delmas, '88). These zonal characteristics vary between species, but parasagittal zones are evident in all mammals investigated to date, and their connections are largely comparable across mammalian lines (see above citations).

Data presented in this thesis, however, indicates a more complex organisation of the olivocorticonuclear system in the monkey than in non-primates. Although the strict parasagittal zonation is still evident in the monkey, the majority of cortical areas investigated also show a marked divergence from the zonal system of olivocorticonuclear projections. Purkinje cells from a particular zone frequently projected into nuclear areas in the absence of olivary input appropriate to that nuclear zone. The "extra-zonal" element to the monkey parasagittal organisation increases the complexity of deep nuclear circuitry relative to that in non-primates, since:

i) input to a deep nucleus from Purkinje cells beyond its zone allows cross-talk between functional modules, and

ii) the nuclear cells receiving these extra-zonal inputs will not receive the topographically organised collaterals from climbing fibres projecting into the cortical zone from which the extra-zonal projection arose.

These extra-zonal projections are most marked in the posterior vermis, but also occur in the hemispheres and floccular complex. This section of the discussion will deal with each of these cerebellar subdivisions in turn, commenting on the topography of the strictly parasagittal cortico-nuclear projections before focusing on those to extra-zonal nuclei.

4.2.2.1 The vermis

Cortico-nuclear projections from the monkey posterior vermis terminate in caudomedial fastigial, in agreement with previous studies (Rat: Armstrong and Schild, '78a; Bernard, '87; Buisseret-Delmas, '88; Tabuchi et al., '89; Paallysaho et al., '90; Cat: Dietrichs, '83; Monkey: Yamada and Noda, '87). The projection demonstrated a clear rostrocaudal topography: Purkinje cell axons from vermal lobule VII terminated more rostrally within the fastigial than those from lobule VIII, which is turn had a more rostrally located terminal field than the uvula. There was no difference in the projections from the dorsal and ventral uvula to the fastigial. The injection sites were too large to comment on a likely mediolateral topography.
This vermo-fastigial projection corresponds to Voogd's zone A.

Zone B in the vermis is reported in other species to extend only as far as the end of vermal lobule VI (Groenewegen and Voogd, '77; Groenewegen et al., '79; Kawamura and Hashikawa, '79; Bigare and Voogd, '80; Walberg, '80; Dietrichs, '83; Buisseret-Delmas, '88). However, this zone is longer in the monkey than in non-primates, and extends up to and including lobule VII. The functional implications of this have already been discussed.
The question of whether the B zone projects to the deep nuclei as well as the lateral vestibular nucleus of Deiter's (posterior interposed in the Galago: Haines and Rubertone, '79E; anterior interposed in the cat: Dietrichs and Walberg, '79), however, cannot be satisfactorily answered by this study. Case M1-96 did contain labelled cells in the caudal DAO, attributable to zone B, and terminal label was found in the interpositus. The label, however, was located in the anterior division, whereas previous studies on the Galago indicated an input to the posterior division. The terminal field in M1-96 also

covered the entire mediolateral width of the nucleus, while reports describing cortico-nuclear projections from the B zone have limited the cortical input to the extreme medial edge of the interposed, whether in the anterior or posterior division. Finally, the dorsal uvula injection (case UV1) did not include zone B, but also contained a strong terminal field in the ventral anterior interposed, indicating that this terminal field may actually arise from an extra-zonal input rather than an independent projection from zone B. It is likely therefore, that most (if not all) of the terminal field in the anterior interposed is attributable to extra-zonal inputs from vermal lobule VII, but it is equally possible, of course, that the anterior interposed of the macaque contains an overlapping terminal field from the extra-zonal A projection and the strict parasagittal projection from zone B.

No cases contained labelled cells in the mid-rostral levels of the MAO, indicating that the vermal x zone is indeed confined to the anterior lobe in the monkey (Haines and Dietrichs, '91).

The vermal extra-zonal projections are discrete and specific for the vermal lobule from which they arise. Although every vermal lobule projected into the interpositus, neighbouring lobules projected into different divisions, and projections to the anterior or posterior interposed division alternated between lobules Thus vermal lobule VII and IXa both projected to the anterior interposed, while vermal lobule VIII and IXb projected to the posterior division. Due to the rostrocaudal topography of the vermal efferents, there was no overlap of inputs within these extra-zonal nuclear fields (see figure 39).

Attempts to assign these extra-zonal projections to one of the vermal A zones was difficult to do conclusively. However, case UV2 (IXb) was striking in that it contained dorsomedial cell column only on the left hand side, and its extra-zonal projection to the anterior interposed was only apparent on the right hand side, implying that these extra-zonal projections arise from the lateral A3 zone. However, scrutiny of the other vermal cases was unable to confirm this issue. For lobules VII and VIII, both dorsomedial cell column and extra-zonal label were present bilaterally, and, in case IXa, the extra-zonal projection was present, even though the dorsomedial cell column contained no label.

The only other report of divergence of vermal Purkinje cells into the interposed nuclei in the monkey is Yamada and Noda's ('87) WGA-HRP study of the afferent and efferent connections of the oculomotor vermis (lobule VIc-VII). They noted that when the injection site in animal Rh encroached upon the paravermal region:

> "... Labelled fibres increased in the white matter lateral to the fastigial nucleus and terminated in the marginal zones of the anterior and posterior interposed nuclei..."

In this case, however, the olivary label was restricted to the caudal MAO (zone A), and thus this was an example of a divergent vermal projection, as described in this thesis.

There are reports of inconsistent projections from the vermis to the interposed nuclei in other mammals (Rat: Dietrichs, '83; Bernard, '87; Tabuchi et al., '89; Cat: Angaut and Brodal, '67; Galago: Haines, '77). Each of these studies, however, lacked correlation between the olivocortical and cortico-nuclear projections. The border between the vermis and hemispheres is indistinct in many mammals, and thus conclusions regarding parasagittal zonation based simply on the location of the injection site and resultant terminal field are unrigorous. Indeed, it is highly improbable that cortico-nuclear projections from the vermis of the rat diverge into the interposed, since recent WGA-HRP studies (Buisseret-Delmas, '88) which correlated the afferent and efferent connections of the vermis, indicated that the vermal A zone deviates laterally from the midline and encroaches upon the paramedian lobule and crus II

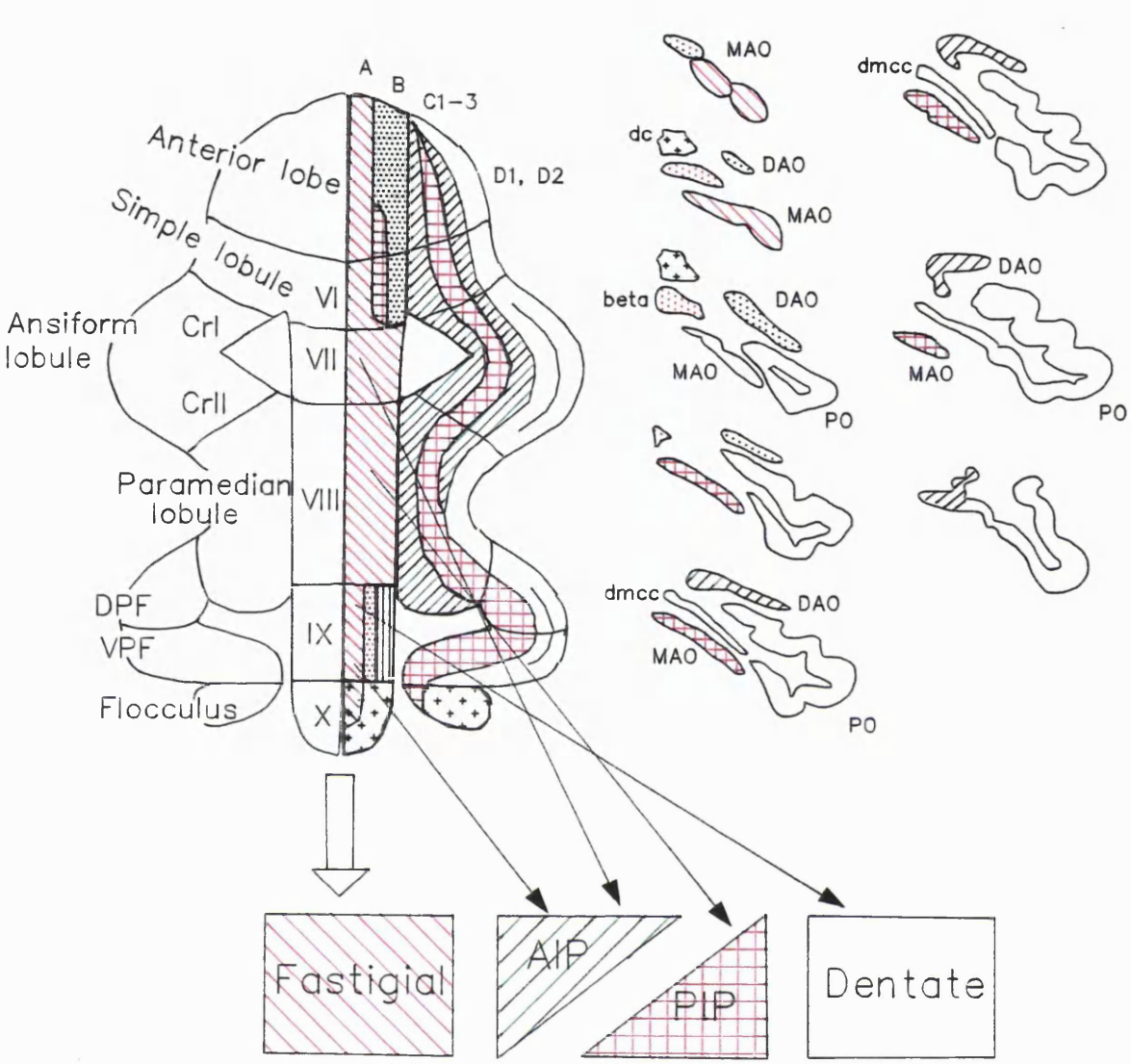

Figure 39: Divergence of olivo-cortico-nuclear projections

Vermal olivo-cortico-nuclear projections in the macaque diverge beyond the classical parasagittal zonation seen in other mammals. Purkinje cells project into nuclear areas attributable to zones that are not represented at the olivary level. "Extra-zonal" projections were encountered in all cerebellar subdivisions.

4.2.2.2 The hemispheres

Due to the massive expansion of the D zones in primates, all the paramedian lobule and crus II cases were dominated by D1 input from the dorsal leaf/lateral bend of the inferior olive. Consistent with this olivary input, the majority of the terminal fields were found in the nuclear D1 zone in the caudal parvicellular dentate nucleus (Hess and Voogd, '86). All of the terminal fields were striped and focused ventrally within the dentate.

The cortico-nuclear projection from the paramedian lobule showed indications of a rostrocaudal topography, as the more caudal case (PMD2) in the folial chain produced a terminal field in dorsorostral rather than the ventrocaudal levels of the dentate which received input from the more rostral levels of the chain. Although the more rostral paramedian chain cases varied in their injection sites and olivary input within the D1/dorsal lamella areas, it was impossible to determine a consistent pattern to the variation in dentate labelling, and therefore no clearer pattern to the paramedian olivocorticonuclear projection could be ascertained. Interestingly, the cases which showed a moderate overlap of the dentate terminal fields (Co5 and M2-96left - rostral and middle paramedian chain respectively) did not show overlap in the olivary afferents - an indication that the olivocerebellar pathway is more discrete than the cortico-nuclear projection, and an example of *intra-zonal* convergence. Thus, cortical areas in the same zone, but receiving different olivary input from the appropriate olivary subnucleus project into the same area of the deep nucleus appropriate for that zone.

The paramedian lobule also contains cortical areas associated with Voogd's C zones. Two of the four paramedian cases (PMD2 and m2-96left) received input from the rMAO and projected into the posterior interposed nucleus, thus comprising the C2 zone, but curiously only m2-96left contained olivary and nuclear label associated with the zones C1 and 3, indicating that the C3 zone vanishes from the paramedian lobule at its most caudal end.

Projections from the paramedian lobule to the posterior interposed displayed rostrocaudal topography. Nuclear input derived from caudal levels of the chain (PMD2) focused in central regions of the caudal posterior interposed; projections from more rostral areas (m2-96left) terminated ventrolaterally in the most caudal limit of the PIP.

The olivocorticonuclear projections within the crus II are also localised to Voogd's zone D1 and the dentate terminal fields are obviously striped. Within the rostrocaudal dimension, there was overlap of the terminal fields within the caudal dentate. However, projections from sb6 (middle chain) terminated dorsal to those emanating from M2-96right (caudal chain), and, as a result, there was only a negligible overlap at the extreme caudal end of the dentate.

Differences in the segregation of olivocorticonuclear inputs between the paramedian lobule and crus II suggest that the cortico-nuclear projection from crus II is more discrete than that from the paramedian lobule. The only example of intra-zonal convergence for crus II cases was at the very caudal end of the dentate.

There was no complete olivo-cortico-nuclear representation of the C zones in either crus II case.

The olivocorticonuclear system in the paramedian lobule and crus II of the monkey both deviate from the strict parasagittal zonation; both cortical areas contained Purkinje cell axons which projected a nuclear zone that had not been represented at the olivary level.

Only two paramedian lobule cases demonstrated extra-zonal projections - PMD2 and GR-95. Differences in the extra-zonal projections were apparent between the caudal paramedian case and those positioned more rostrally in the chain. Projections from the extreme caudal injection site (PMD2) terminated dorsally in the rostralmost anterior interposed nucleus, while the more rostral case (GR-95) projected to ventrolateral PIP. There was no overlap between the extra-zonal projection from this latter case and "strict" PIP terminal fields in the other paramedian lobule cases.

Unlike the nuclear projections within the strictly zonal olivocorticonuclear system, the crus II cases overlapped in their extra-zonal projections into the ventrocaudal posterior interposed.

Overlap in the extra-zonal projections from the paramedian lobule and the crus II were therefore restricted to mid-caudal levels of the posterior interposed nucleus, which received input from the crus II cases (sb6 and m2-96right) and GR-95 in the rostral paramedian chain.

The terminal field in the dentate nucleus showed an interesting degree of convergence from different cortical zones. Previous studies have assigned zone D1 to caudomedial and D2 to rostromedial dentate (Hess and Voogd, '86). Case M2-96left contained olivary label associated with both D zones - labelled cells were located in both the dorsal and ventral lamella of the principal olive, but the terminal field in the dentate was confined to its caudal half. Thus, it appears that in the posterior lobe, zone D1 and D2 projections converge onto a nuclear region normally associated with only the D1 zone. In each case, the terminal fields are striped, but unfortunately it was impossible to say whether the inputs from the separate zones converged or interdigitated within the nuclear terminal field.

Previous evidence of this type of *inter-zonal* convergence is available from Haines and Patricks' lesion study on the cortico-nuclear projections of the squirrel monkey ('82). They lesioned lateral (D2) and medial (D1) areas of the D zone in lobule V intermediate cortex and found that:

> "...the terminal fields in the NL for fibres arising in these two respective areas of cortex are found in slightly different positions in the NL....one can clearly see the axonal debris was located in two different portions of the *rostral* NL..." [my italics]

Haines and Patrick determined the cortical zones according to their positions, and did not correlate these cortical nuclear projections with the olivocerebellar pathway. However, if their assertion that they lesioned cortical areas D1 and D2 is correct, this would be further evidence of inter-zonal convergence, with the two cortical zones projecting onto one (rostral) nuclear zone in the dentate. If this were the case, one might assume that the rostral areas of the dentate would be reserved for converging inputs from the cortical D1 and D2 zones in the anterior lobe.

Thus, the parasagittal division of the monkey dentate nucleus into rostral D2 and caudal D1 zones would be inaccurate. Indeed, Demole's ('27) and Larsell's ('34, '37) original cerebellar studies divided the dentate rostrocaudally, terming the caudal parvicellular division the "neodentate" due to its association with phylogenetically more recent parts of the cerebellar hemispheres, such as the hemispheres of the posterior lobe.
In addition, the relation of the rostral dentate with the anterior lobe and the caudal with the posterior lobe, made possible by intra-zonal convergence, is reminiscent of Clarke and Horsley's observations on the cortico-nuclear system, made over 90 years ago:

> "....Our series of sections also show that all efferent cerebellar cortical fibres in the first instance pass.....to the [deep cerebellar nucleus] which is nearest to their origin..."

4.2.2.3 The floccular complex

The dorsal paraflocculus consists of zones C2, D1 and D2 (Voogd, '64, '69; Haines and Whitworth, '78; Voogd and Bigare, '80; Dietrichs, '81; Umetani, '93). Consistent with these previous observations, cases presented here contain olivary label in the rostral MAO (C2) and the both lamellae of the principal olive (D1 and D2) and terminal label in the posterior interposed and the dentate nuclei. The terminal fields were located caudally and showed evidence of stripes in both nuclei. Due to the difficulty in injecting the monkey dorsal paraflocculus, all the injection sites were focused on similar folia. However, in spite of almost identical rostrocaudal and mediolateral positioning of olivary afferents, there were slight variations in the location of the nuclear terminal fields from the cases, but a consistent mediolateral or rostrocaudal topography was difficult to ascertain.

Extra-zonal projections from the dorsal paraflocculus followed a similar pattern to those from crus II or the paramedian lobule. As the dorsal paraflocculus is known to contain a zone C2, and the injection sites covered more of an individual folium than injections into the paramedian lobule or crus II, there were fewer clear cases of extra-zonal projections into caudal posterior interposed. However, HN-95 had no olivary label relating to zone C2 (rMAO) and yet displayed a strong terminal field in the caudal

posterior interposed, indicating that this extra-zonal projection is also in evidence from the dorsal paraflocculus. There was moderate overlap in the caudal posterior interposed between extra-zonal projections from the dorsal paraflocculus and both crus II cases, but not that from the paramedian lobule; the extra-zonal projection from this cortical area terminated more rostrally.

HN-95 also displayed evidence of the inter-zonal convergence of two cortical D zones onto the single nuclear D zone in caudal dentate. One floccular complex case, BG-95, displayed convergence in the olivocerebellar projection, since it contained the olivary, but not nuclear representation of zone D2. This phenomenon was not witnessed in any other case.

Zonal projections from the flocculus concern the dorsal cap and vestibular nuclei rather than the principal olive and the cerebellar nuclei, although the C2 zone shows continuity with that in the dorsal paraflocculus. The flocculus projects into the ventrolateral posterior interposed and ventromedial dentate at caudal levels, in a similar fashion to the overlying paraflocculus. Case 228 (flocculus and ventral paraflocculus) showed only extra-zonal projections into the ventrocaudal posterior interposed in the absence of label in the rMAO.
The strictly zonal projection from case d669 (pure flocculus) and the extra-zonal projection from case 228 (flocculus and ventral paraflocculus) overlapped in the ventrolateral posterior interposed nucleus at caudal levels.

The ventrocaudal PIP receives overlapping extra-zonal inputs from dorsal paraflocculus and flocculus, and the stricter zonal projections from the flocculus. Thus, two different cortical areas with entirely segregated climbing fibre and mossy fibre (pontine/NRTP) input project in an overlapping fashion onto the caudal posterior interposed nucleus. In addition, the extra-zonal projections from crus II terminate in this nuclear region. Recent single-unit recording studies (van Kan et al., '93; Zhang and Gamlin, '94; Robinson et al., '96) have indicated that the ventrocaudal PIP area which displays this overlap between dorsal paraflocular, floccular and crus II inputs has some interesting

physiological responses during eye movements. The functional implications of this overlap will be discussed in section 4.5 of the discussion.

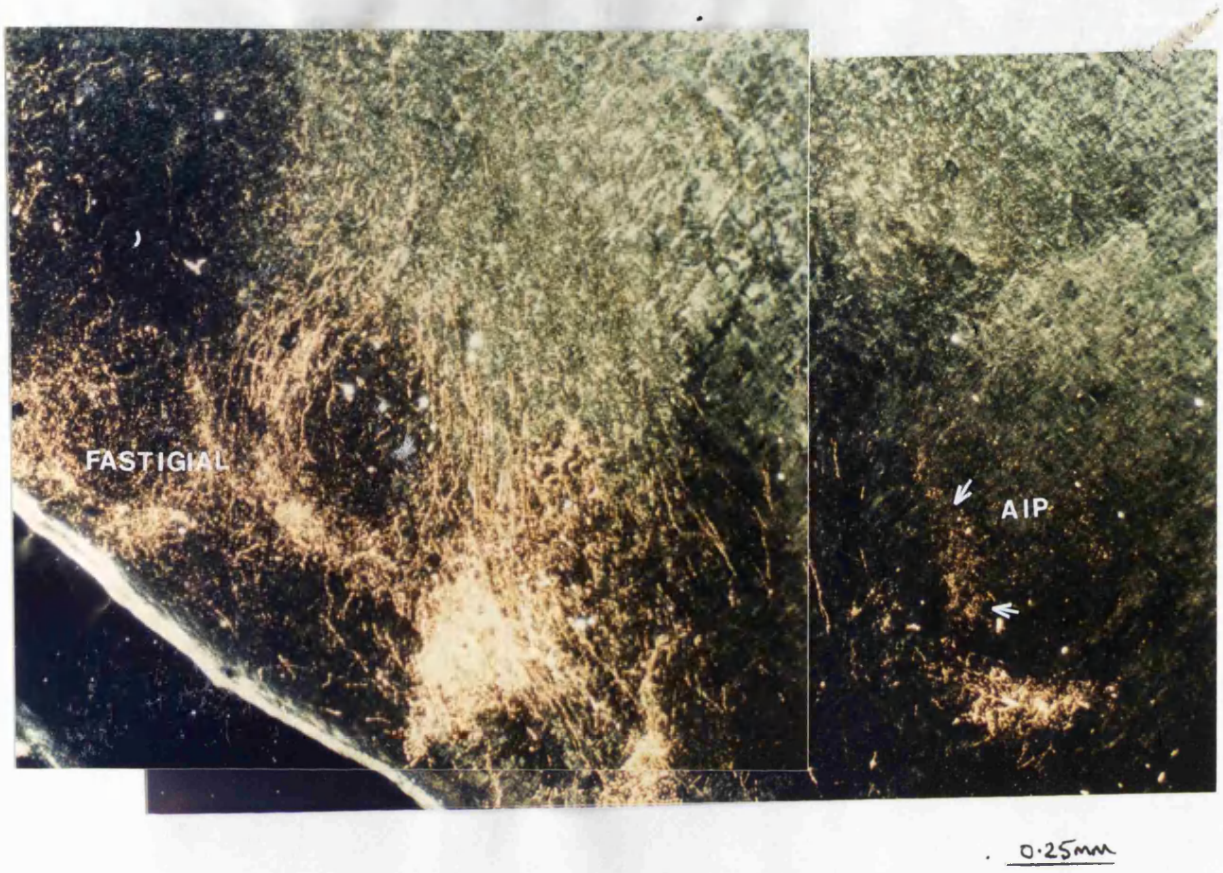

Photomicrograph 6: Divergence from the olivo-cortico-nuclear parasagittal zonation. Section from vermal lobule VII/case M1-96, showing dense terminal label in the fastigial nucleus, and a discrete field at the ventral tip of the anterior interposed nucleus (arrow). The olivary zone appropriate for the AIP terminal field did not contain labelled cells.

4.3 CORTICO-NUCLEAR STRIPES

Injections in the hemispheres and floccular complex resulted in striped terminal fields in the interposed and dentate nuclei. In each case, the terminal fields followed the same approximate mediolateral direction fanning out from the hilus of the dentate, while those in the posterior interposed were orientated obliquely or vertically.

Inspection of the terminal fields in the dentate at high power showed streams of fibres running down the lateral edge of the nucleus, and groups of fibres coursing laterally to enter the nucleus and terminate in bands across the entire mediolateral breadth of the nucleus. Immediately above and below the terminal stripes lay stripes of approximately equal thickness that were unlabelled. There were no terminals and only very occasionally a few fibres in these inter-stripe areas.

The cortico-nuclear projection to the posterior interposed nucleus also show this striped topography. Often the stripes were not as clear as those in the dentate, appearing more as stripes of terminal fields of differing intensities, although in some cases, such as BG-95 (dorsal paraflocculus and flocculus) or 228 (flocculus and ventral paraflocculus), the stripes were much more evident. It was not possible to account consistently for the difference in number or intensity of the stripes in the terminal fields relative to each injection site. Although the stripes were clearer in cases involving the lateral paramedian lobe or medial crus II (see m2-96left and right), the number of stripes did not correspond closely to the size or depth of the injection site.

Haines et al. ('82) investigated the cortico-nuclear projections of the anterior lobe of the primate cerebellum, and also observed the appearance of striped terminal fields. Following a lesion in intermediate cortex of lobule V, he comments on the terminal degeneration in the PIP:

> "....[terminal degeneration] was arranged as two dorsoventrally orientated lamina separated by a narrow region which contained no degenerated axons..."

and following a lesion in lateral lobule V, he describes the terminal field in the dentate thus:

> "....At more dorsal planes, the terminal field appeared to be relatively homogenous. However, at more ventral levels, it consisted of two mediolaterally orientated laminae separated by a region completely devoid of preterminal debris...a remarkable feature of the pattern of degeneration....was the sharp interface between the terminal field and directly adjacent areas of the NL which were essentially devoid of debris...".

Chan-Palay ('77 and '82) studied Golgi preparations of Purkinje cells and described the course of the axon as it:

> "....runs along the outside of the nucleus, gives off a branch that enters the nucleus, and may continue further to serve another portion of the nucleus..."

Clearly, the cortico-nuclear projection to the dentate and posterior interposed is striped in the primate. However, this important detail has been somewhat overlooked since these early reports.

Data from zebrin immunocytochemical studies (Hawkes and Leclerc, '86; Leclerc et al, '90; Hawkes et al., '92; present study) demonstrate that all areas of the deep cerebellar nuclei receive input from the Purkinje cells. Although streams of labelled Purkinje cell axons could be seen coursing towards the nuclei in segregated bands, the bands coalesced at the border of the nuclei and there was no evidence of striping of the total cortico-nuclear termination (see 2.2.4). Therefore, Purkinje cells from cortical regions other than those injected must project to the interleaving areas (see photomicrograph 7).

Why would the cortico-nuclear projection in the monkey consist of interdigitating inputs from separate areas of the cerebellar cortex? The most likely answer focuses on the somatotopic representation in the cortex relative to that in the deep nuclei.

The cerebellar cortex, by virtue of widely distributed and overlapping mossy fibre inputs and parasagittal organisation in the climbing fibre input, contains multiple representations of the body surface. Each sagittal zone within the cortex serves a different control function and thus multiple somatotopic representations are required to provide each sagittal zone with a spectrum of information concerning the body part that is to be controlled.

The deep cerebellar nuclei contain simpler somatotopic maps than the multiple representations in the cortex. Anatomical (Thach and Jones, '79; Stanton, '80; Kalil, '82; Asanuma et al., '83b) and electrophysiological (Thach, '68, '78; Thach et al., '82,

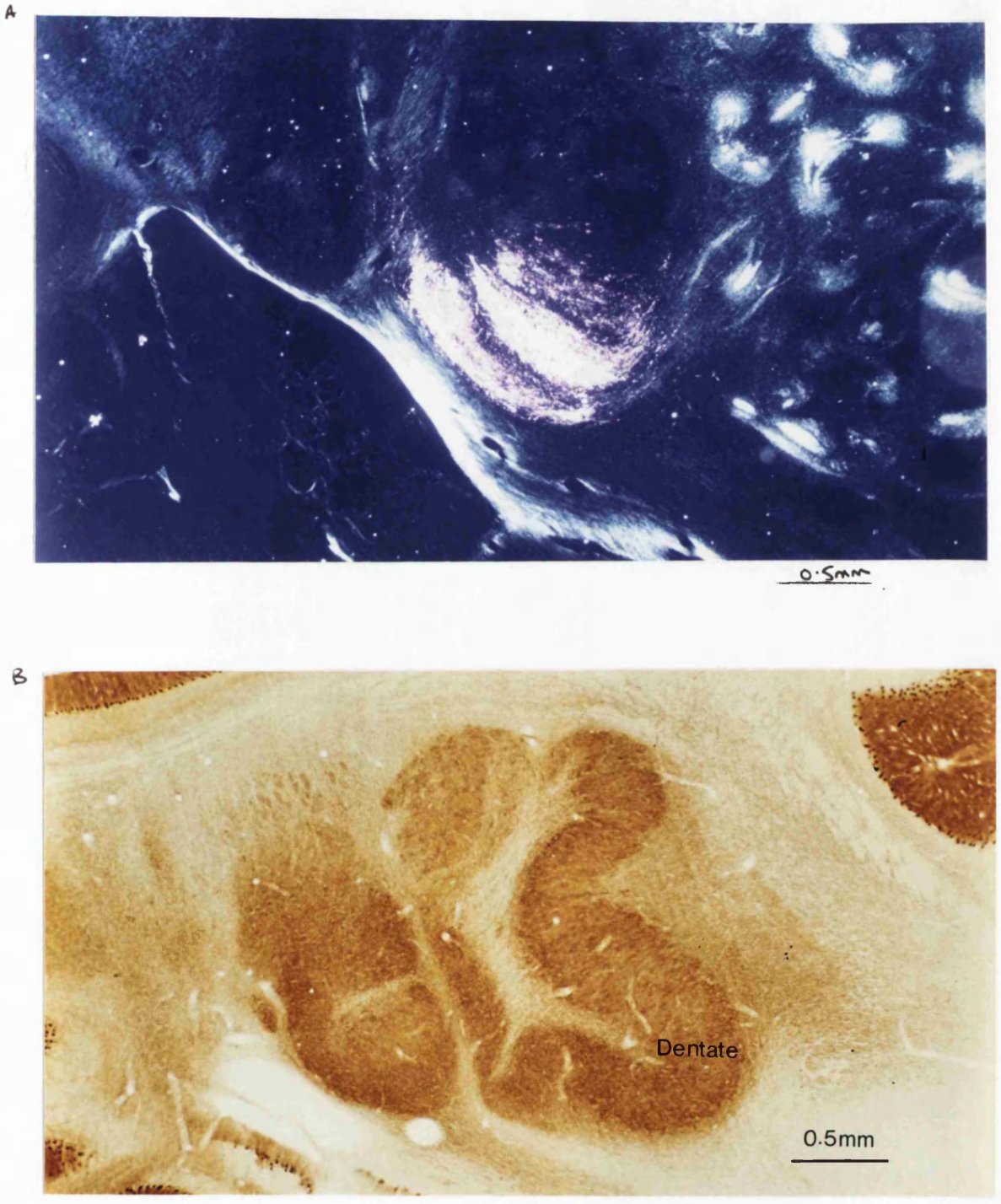

Photomicrograph 7: Cortico-nuclear stripes.

A: Following an injection of WGA-HRP into the hemisphere, the labelled terminal fields (as displayed by TMB histochemistry in a coronal section) had a characteristically striped appearance. Stripes of dense label were separated by areas devoid of terminal label. Taken from case M2-96left.

B: Height-matched coronal section through the deep cerebellar nuclei following reaction with the Purkinje cell-specific antibody zebrin II. The whole dentate is innervated by Purkinje cell fibres.

'93; Van Kan et al., '93; Gibson et al., '96) studies have indicated the presence of an approximate body representation in each of the deep cerebellar nuclei. The hindlimb is represented anteriorly, the forelimb in the middle, and the head posteriorly. The limbs are medial and the trunks are lateral.

The interleaving topography of the cortico-nuclear projection may be used to compress the multiple body representations in the cortex onto one in each of the deep cerebellar nuclei. Thus, several different cerebellar cortical areas concerned with a particular body part will project in an interleaving fashion into the area of the deep nuclei appropriate for control of that limb.

Electrophysiological and anatomical evidence supports this concept. Climbing fibres bifurcate to supply functionally homologous, but anatomically segregated areas of the cerebellar cortex (Rosina and Provini, '83, '87; Trott and Armstrong, '87). Garwicz and Ekerot's ('94) stimulation study on the forelimb area of the cat anterior lobe demonstrated that microzones in the C1, C3 and Y zones with similar climbing fibre input project to a common set of neurons in the anterior interposed. They go on to comment that:

> "...it is proposed that the cortico-nuclear projection is organised according to climbing fibre receptive fields and microzones and not strictly according to sagittal zones..."

Rosina et al., ('96) recently extended this concept. C1 and C3 face-forelimb responsive regions in more widely separated areas of the cat cerebellar cortex (anterior lobe, paramedian and ansula lobules (crus I and II)) were identified electrophysiologically and then injected with retro-anterograde markers. The resultant terminal label formed interdigitating and only occasionally overlapping patches of the anterior interposed. They concluded that:

> "...Purkinje cells in individual forelimb areas of the cortical body maps in the intermediate cerebellar compartments have a finely differentiated pattern of projections to specifically localised neurons in the forelimb nuclear groups....."

Thus, by virtue of its collateralised climbing fibre input, the cerebellar cortex contains functionally homologous areas both within one particular cortical region (e.g. anterior

lobe), and in more widely separated areas of the cortex (e.g. anterior, paramedian and ansula lobules). Projections from functionally homologous areas which reside within the *same* cortical area converge upon similar groups of nuclear neurons (Garwicz and Ekerot, '94). However, these nuclear neurons will not receive additional convergent inputs from cortical areas which respond to the same body part but reside in a *different* division of the cerebellum (Rosina et al., '96). Inputs from more distant but functionally homologous area are directed to adjacent populations of nuclear neurons.

These observations may suggest that the cortico-nuclear stripes seen following injections in one cortical subdivision would interdigitate with those from another (e.g. paramedian lobule and crus II).

Consider the combination of inputs to the ventrocaudal posterior interposed nucleus. The cPIP receives convergent inputs from the dorsal paraflocculus, crus II and the flocculus, such that their terminal fields interdigitate ventrally in the nucleus. The dpf, crus II, flocculus *and* the cPIP have all been shown to contain eye movement-related neurons. The interdigitation of cortical eye movement inputs onto a nuclear eye movement area would thus allow combination of different mossy fibre-mediated eye movement information from the dlpn and NRTP, as described in section 4.1.3 of this discussion. The co-operation between this ventrocaudal PIP and other eye movement related areas in the deep cerebellar nuclei will be discussed in section 4.5.

The striped topography of the cortico-nuclear projection also lends support to a recent contention by Thach and his colleagues ('92) on the role of the parallel fibre in cerebellar co-ordination of muscle synergies. The action of parallel fibres and cortical interneurons on Purkinje cells forms a coronal "beam" of Purkinje cell inhibition onto the deep nuclei. The orientation of the somatotopic map in the deep nuclei indicates that myotomes (which run orthogonal to the long axis of the body) run mediolaterally across each nucleus and thus parallel both to the beam of Purkinje cells and the parallel fibres activating them. Thach suggests that:

> "...the parallel fibre in this way would be a single neural element spanning and co-ordinating the activities of multiple synergies and joints..."

Data from this thesis presents anatomical evidence that Purkinje cells from functionally homologous areas project into the deep nuclei as interdigitating mediolateral beams which run across the representation of myotomes in the body.
In addition, since the parallel fibre is known to stretch up to 6mm (Mugnaini et al., '83), this coronal beam activation of cortico-nuclear projections is capable of spanning separate nuclei, and therefore:

> "....have a co-ordinating effect on the outputs of the different nuclei (e.g. of stance, of stretch reflex gains and of voluntary movements)..."

Anatomical evidence for this idea is supplied by the results in this thesis. Many injection sites in the hemispheres and floccular complex produced terminal fields that spanned two nuclei, such that the terminal fields appeared as a continuous nuclear input, interrupted only by the passage of white matter tracts between the nuclei.

Overall, the parallel fibres and the interleaving coronal stripes of cortico-nuclear projections are optimally designed for cerebellar coordination of muscle synergies and joints and the complex multi-jointed actions they allow (see figure 40). Indeed, coordination of movement is one of the oldest postulated functions of the cerebellum (Fluorens, 1823).

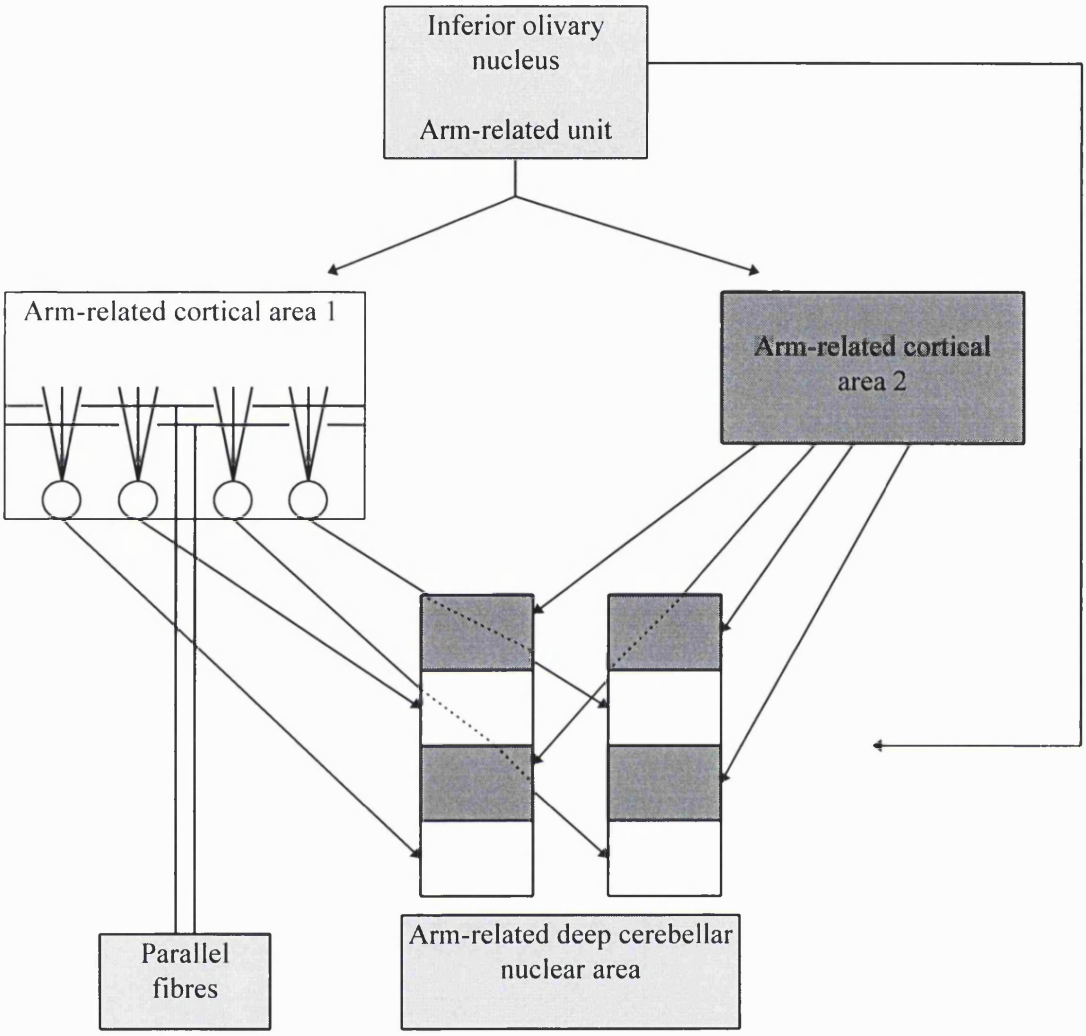

Figure 40 Interdigitation of projections from functionally homologous cortical areas into the deep cerebellar nuclei

4.4 THE NUCLEO-CORTICAL PROJECTION

The presence of a nucleo-cortical pathway was first suggested by Cajal in 1911. A variety of techniques (anterograde and retrograde tracers, degeneration and antidromic stimulation) used on a number of species have confirmed its presence in all mammals studied thus far (Rat: Buisseret-Delmas, '88, '89; Paallysaho et al., '90; Umetani, '90; Yatim et al., '95; Cat: Dietrichs and Walberg, '79, '80; Dietrichs, '81, '83; Monkey: Tolbert et al., '76, '77, '78; Chan-Palay, '77, '79; Gould, '79; Haines, '88). Most nucleo-cortical projections are collaterals of nuclear efferent axons destined for extracerebellar targets such as the ventral lateral thalamus and the inferior olive or both (Tolbert et al., '78; Payne, '83). Each nucleo-cortical axon splits into numerous branches before entering the cortex, resulting in a somewhat diffuse mossy fibre-like termination in the granular layer. The nucleo-cortical axon forms synaptic contacts within cortical glomeruli, most frequently with granule cells and more rarely with Golgi cells (Tolbert et al., '80). There is no consensus on the transmitter used, or the action of the nucleo-cortical projection. Some immunocytochemical studies have suggested that the nucleo-cortical pathway is GABAergic and inhibitory (Chan-Palay, '79; Batini et al., '89; Hamori and Takacs, '89), while others dispute it (Kolston et al., '95; Angaut, '96) Electron microscopic investigations have described the synapses as asymmetrical, and the vesicles within them as clear and round (Tolbert et al., '80), features characteristic of an excitatory pathway.

The topography of the nucleo-cortical pathway is clearest in the rat and the cat. In spite of small interspecies differences, the pathway is comprised of reciprocal, non-reciprocal and symmetrical divisions; (Tolbert et al., '78; Gould, '79; Dietrichs and Walberg, '79, '80; Dietrichs, '81, '83; Buisseret-Delmas and Angaut, '88, '89; Paallysaho et al., '90; Trott et al., '90; Umetani, '90; Kolston et al., '95; Yatim et al., '95). Reciprocal projections are strictly arranged in the sagittal direction, following the zonal distribution. Symmetrical projections arise contralaterally from nuclear regions symmetrical to that giving rise to the reciprocal projection. The non-reciprocal projections arise from nuclear areas outside the cortico-nuclear projection.

Nucleo-cortical projections to different cerebellar areas employ different combinations of the reciprocal, non-reciprocal and symmetrical pathways. For example, in the cat paramedian lobule, the nucleo-cortical pathway consists of all three divisions (Dietrichs and Walberg, '79). In the paraflocculus of the same animal, however, the same pathway is arranged totally reciprocally to the cortico-nuclear projection (Dietrichs, '81). Dietrichs and Walberg ('79) have suggested that the non-reciprocal portion of the pathway is a false positive, since retrograde transport of HRP has been reported to occur from a larger area than does the anterograde. More recent studies, including the data in this thesis, relied on the bi-directional transport of WGA-HRP, which is considered to have a more equal uptake by somata and axonal or dendritic terminals. The non-reciprocal pathway is therefore considered to be a legitimate division of the nucleo-cortical projection.

The nucleo-cortical projection has not been as thoroughly investigated in the primate as it has in the rat and cat. The available studies indicate a profound species difference in this pathway. Although it also is comprised of reciprocal, non-reciprocal and symmetrical components, the majority of the primate nucleo-cortical projections arise from the caudal dentate nucleus with no obvious topography (Chan-Palay, '77; Tolbert et al., '78, '82; Haines, '78, '88). The caudal dentate comprises the "neodentatum" of Demole ('27). Data from this thesis suggests that this nuclear area projecting all over the cerebellar cortex actually receives converging D1 and D2 zone inputs from the those areas also attributed to the "neocerebellum" (the lateral hemispheres of the posterior lobe).

A recent double-label retrograde tracing study (Haines, '88) suggested that a fraction of the reciprocal and non-reciprocal projections arise as collaterals from one nuclear cell. Thus, the nucleo-cortical projection may in part be used to contact functionally homologous areas in different cortical zones. Data presented in this thesis suggest that a comparable system exists in the cortico-nuclear projection (see section 4.3).

Nucleo-cortical data presented in this thesis is in partial agreement with previous studies. The projection suggested by this data is sparser than has been previously reported. However, the majority of reciprocally-projecting cells were found in the

densest part of the terminal fields, and in some cases, the labelling in the terminal field was so dense that it was impossible to discern whether individual cells were located within the plexus of axons and terminal label. Therefore, it is likely that the data on the reciprocal projection is an underestimate of the actual situation.

All of the deep nuclei project to the cerebellar cortex. Nucleo-cortical cells were of various sizes, although medium sized neurons were most frequently represented. This latter observation may purely be a reflection of the distribution of neuronal sizes within the nuclei. Nucleo-cortical projections are almost equally divided between reciprocal and non-reciprocal, and there were no obvious differences in cell sizes according to their location with respect to the terminal field.

Reciprocal nucleo-cortical cells were generally found in areas of densest terminal label. The populations of non-reciprocal cells could be subdivided according to their degree of separation from the cortico-nuclear terminal field. One sub-group of non-reciprocal cells were located in nuclei (most frequently the dentate) which received no input from the cortex (see case Pyr1). The other non-reciprocal nucleo-cortical cells were located in the appropriate nucleus for their cortical zone: they were divided into groups which were separated from the terminal field rostrocaudally (see case m2-96left) and those at the same height as the terminal field, but lying just outside it (see case m2-96right). Many cases showed combinations of the various nucleo-cortical projection types.
There was no evidence of a more detailed topography in the monkey nucleo-cortical projection, although Chan-Palay has reported a mediolateral and rostrocaudal organisation within the dentato-cortical projection. In addition, cells were never encountered contralaterally, and thus no symmetrical projections could be described. The deep nuclei do not project to the flocculus or the uvula.

Drawing conclusions on the functional implications of the rather diffuse nucleo-cortical pathway would be premature in view of the lack of knowledge on the precise action of the nucleo-cortical projection on its target cells. The role that the nucleo-cortical projection plays in cerebellar function is defined by facts that are still not known. Firstly, it is still unclear whether the pathway is inhibitory or excitatory, or contains a

mixed population of projections, which has profound ramifications for it effect on cortical circuitry. Secondly, the relevance of nucleo-cortical topography to cerebellar function also hinges on greater knowledge about the target neurons themselves. If, as is suggested by Tolbert et al. ('80), the nucleo-cortical projection terminates preferentially on granule cells within the glomeruli, the final input from the nucleo-cortical system to Purkinje cells would only be via the parallel fibre system. Parallel fibres are extremely long, and any precise topography of the projection would be masked by its distribution over 6mm of the cerebellar cortex. In this context, the reciprocity (or otherwise) of the projection would be of diminished relevance. The contact with Golgi cells is of more interest in terms of topography since their dendritic fields are circular, arranged in a plane orthogonal to the dendritic fields of the Purkinje cell, and somewhat more localised in their cortical contacts than the granule cell.

Clearly, further studies on both the electrophysiology and intra-cortical relationships of the nucleo-cortical projection are needed in order to draw any firm conclusions on the role of the pathway in cerebellar function.

4.5 EYE MOVEMENT AREAS IN THE DEEP CEREBELLAR NUCLEI

The cortico-nuclear topography in the monkey is of particular interest in view of recent studies on eye movement areas within the deep cerebellar nuclei (Gardner and Fuchs, '74, '75; Ritchie, '76; Vilis and Hore, '81; Chubb and Fuchs, '82; Hepp et al., '82; MacKay, '88b; Noda et al., '88; Fuchs et al., '93, '94; Robinson et al., '93). Eye movement neurons in the fastigial (Noda et al., '88; Ikeda et al., '89; Fuchs et al., '93a, '94; Robinson et al., '93b; Zhang and Gamlin, '96) and dentate (Gardner and Fuchs, '75; Chubb and Fuchs, '82; Hepp et al., '82) nuclei have been well characterised for some time, but there have been recent descriptions of oculomotor units in the less well-studied posterior interposed nucleus (Hepp et al., '82; MacKay, '88b, van Kan et al., '93; Zhang and Gamlin, '94; Robinson, et al., '96).

The oculomotor-responsive units in the caudal posterior interposed are located in the ventrolateral corner of the nucleus, adjacent to a similar patch in the dentate, and describe a discrete U-shape. The PIP eye-movement area is of particular relevance to this thesis, since data presented here has demonstrated the convergence of projections from oculomotor-responsive cortical regions (Crus II: Ron and Robinson, '73; Flocculus: Miles et al., '80; Stone and Lisberger, '86; Dorsal paraflocculus: Noda and Mikami, '86) onto U-shaped terminal fields in this eye movement-related nuclear zone.

Neurons in the caudolateral posterior interposed and caudal fastigial modulate their firing in relation to saccadic and vergence eye movements (van Kan et al., '93; Robinson et al., '96; Zhang and Gamlin, '96). Single-unit recording and lesion studies have shown that PIP neurons burst for nearly every vertical saccadic eye movement, decelerating upward and accelerating downward saccades. The vergence and accommodative neurons in the PIP are related predominantly to the dynamics of the far response, and the neuronal population is divisible into cells that are related predominantly to vergence, or to accommodation, or to both.

Caudal fastigial neurons, however, accelerate contralateral and decelerate ipsilateral horizontal saccades (Fuchs et al., '93a; Robinson et al., '93b, '96), while the vergence responses are predominantly related to the near response (Zhang and Gamlin, '96).

The anatomical connections of these oculomotor nuclear regions support their different physiological responses.

Injections of WGA-HRP into the midbrain near-response supraoculomotor area (May et al., '92) or the superior colliculus (May et al., '90) result in labelled cells in both the caudal fastigial and the caudal posterior interposed/dentate. The position and shape of the labelled cell group in the PIP corresponds almost exactly with the U-shaped oculomotor and convergent input areas (see p.103, fig 3g-k).

The fastigial and PIP have identical connections to midbrain near-response regions in the supraoculomotor area (May et al., '92), which is connected to the medial rectus division of the oculomotor nucleus. It would seem likely that the near and far-response centres would be interconnected, assuming that they function as a push-pull pair, and that projections from the far-response related PIP region would be inhibitory in nature. There is, in fact, evidence for GABAergic projection neurons in the posterior interposed (Border et al., '86).

The cerebello-tectal pathways, however, differ between the fastigial and posterior interposed. Neurons in the caudal fastigial project bilaterally onto the intermediate grey layer in the rostral superior colliculus, while the caudal posterior interposed neurons project ipsilaterally onto the intermediate and deep grey layers of the superior colliculus throughout its rostrocaudal extent. The collicular levels to which the fastigial neurons project contain a representation of the perifoveal visual field, and stimulation at these sites elicits small saccades. Terminations from interposito-tectal neurons reach areas of the colliculus representing the whole visual field, and stimulation at the more caudal levels elicits large saccades.

Animals with laterally-placed eyes have a very reduced fastigio-tectal pathway, but the interposito-tectal pathway is evident in all mammals studied so far. This fact, combined with the visual field properties and firing characteristics of collicular areas receiving deep nuclear input, produced the commonly held belief that the cerebello-tectal pathways exert a modulatory feedback influence on saccades. The fastigio-tectal pathway controls the small corrective saccades used to maintain accurate foveation,

while the posterior interposed oculomotor area controls those scanning saccades performed to discern a new target of interest.

In their paper on the cerebello-tectal system in the macaque, May et al. ('90) disputed the idea of a feedback system:

> "...The specific areas of the precerebellar nuclei that receive collicular input, mNRTP, the MAO and the dlpn all have lobule VII as their main target, which only projects to the fastigial and its restricted fastigio-tectal pathway....The dentate and interposed do not receive major inputs from the precerebellar targets of the descending collicular pathways..."

and they suggest that:

> "...only the premotor cells at the very rostral end of the colliculus would be in a position to receive feedback via this [fastigio-tectal] pathway...".

Recent anatomical studies (Glickstein et al., '94; present study) show that in actual fact those areas of the precerebellar nuclei that receive collicular input, i.e. the dlpn and the medial NRTP not only project to vermal lobule VII as May states, but also project in a non-overlapping fashion to the flocculus and dorsal paraflocculus (see section 4.1.3 of discussion); indeed, the dorsal paraflocculus and flocculus receive the strongest projections from the dlpn and medial NRTP respectively. Projections from the flocculus and dorsal paraflocculus have been shown to converge onto areas of the posterior interposed which show saccade-related responses (van Kan et al., '93) and project to the entire rostrocaudal length of the superior colliculus (Gonzalo-Ruiz et al., '88; May et al., '90). Thus, premotor cells throughout the rostrocaudal extent of the colliculus would receive feedback via *both* cerebellotectal pathways. In the rostral colliculus, premotor cells in the intermediate grey receive feedback both from the fastigial bilaterally and the posterior interposed contralaterally; premotor cells in the deep grey layers receive feedback from the contralateral posterior interposed both at all levels of the colliculus.
In spite of this anatomical support for a more straightforward cerebellar feedback circuit, the physiological data relating to firing characteristics of Purkinje cells and deep nuclear neurons argue against it (see May et al., '90). Clearly, studies focusing on the precise signals transmitted via the fastigio- and interposito-tectal pathways (and their

effects on their target collicular neurons) are needed to clarify the roles of these projections in the cerebellar control of saccadic eye movements.

Results from physiological and anatomical studies suggest therefore that the caudal fastigial controls of horizontal saccades and the near-response, while the caudal posterior interposed controls vertical saccades and the far-response. Reasons for the massive convergence onto the posterior interposed from almost all oculomotor areas in the cerebellar cortex area, as demonstrated in this thesis, are not clear.
This convergence, however, should be considered in the context of the interdigitating nuclear projections from homologous areas of the cerebellar cortex, as described in section 4.3. Although the striped topography of the cortico-nuclear projection was not as clear in the posterior interposed as it was in the dentate nucleus, there were clear suggestions that a similar organisation was present in the two nuclei. Therefore, the nuclear projections that appear to converge on the posterior interposed from cortical eye movement areas may produce a terminal field consisting of stripes of input from the different oculomotor-related cortices.

The areas that converge onto the caudal posterior interposed are the flocculus, dorsal paraflocculus and crus II. Each of these cortical areas are eye-movement related. Crus II, the dorsal paraflocculus have been reported to show saccadic activity (Ron and Robinson, '73; Noda and Mikami, '86) and the flocculus is involved in the VOR (Miles et al., '80; Miles and Lisberger, '81; Watanabe, '84, '85; Stone and Lisberger, '86, '90), vergence (Judge, '87), smooth pursuit (Buttner and Waespe, '84) and saccades (Noda and Suzuki, '79).
As described in part 4.1, crus II, dorsal paraflocculus and flocculus receive mossy fibre input from separate areas of the NRTP or pontine nuclei (crus II from the dmpn and vmNRTP, dpf from the dlpn and flocculus from vmNRTP). It is likely that the information transmitted via the different precerebellar nuclei will vary, either as different parameters of information on the same eye movement, or information regarding different eye movements altogether. Thus, the caudal PIP would receive a broad spectrum of oculomotor-related information from different cortical areas, each carrying different information from their segregated mossy and climbing fibre inputs.

Trans-synaptic tracing studies (West and Strick, '96) on the nuclear efferents bound for the cerebral cortex have given no indication that the efferent nuclear projections are striped. Therefore, inputs from the interdigitating cortico-nuclear projections must be integrated, perhaps via interneurons, before the information is relayed out to the thalamus and cortex as a single projection. The integrative load on the deep cerebellar nuclear neurons is increased still further by direct nuclear projections from the NRTP (Brodal et al., '86; Gerrits and Voogd, '87; Mihailoff, '93) and dlpn (although this latter pathway is disputed). As data from zebrin studies in this thesis demonstrate (see section 3.2.4), all areas of the deep nuclei receive Purkinje cell input. Thus, collateral projections from the mossy fibre system will also converge onto nuclear neurons receiving Purkinje cell input

Vermal lobule VII projects to the fastigial. Does the oculomotor region of the fastigial nucleus not receive convergent inputs? Interestingly, the convergence in this pathway occurs one step "upstream" from that in the hemisphere-PIP pathway. The vermal lobule VII receives convergent information from the precerebellar nuclei. As described in section 4.1.3, both the dlpn and the dorsomedial NRTP project to the vermal lobule VII. Cells in the dlpn are directionally selective and carry signals related to smooth pursuit (Suzuki and Keller, '84 and '90; May et al., '85, '88; Mustari et al., '88; Thier et al., '89), ocular following (Kawano et al., '96) or saccades (Thier et al., '96). The rostral dmNRTP transmits information on smooth pursuit (Yamada et al., '96), whilst the caudal half is concerned with saccades (Crandall and Keller, '85) and vergence eye movements (Gamlin and Clarke, '95). Rostral levels of the dmpn contains cells that are directionally selective and respond to during optokinesis, smooth pursuit, or both (Keller and Crandall, '83). All these different oculomotor signals in the precerebellar nuclei converge onto the vermal lobule VII, which subsequently projects onto the caudally-located fastigial oculomotor region of Noda et al. ('88). Hence the caudal fastigial contains neurons related to saccadic (Noda et al., '88; Ohtsuka and Noda, '91; Fuchs et al., '93a; Robinson et al., '93b), smooth pursuit (Fuchs et al., '94a) and vergence (Zhang and Gamlin, '96) eye movements.

4.6 INTERPRETATION OF EXPERIMENTAL METHODS

4.6.1 Evaluation of the primary injection site

The size of the injection site varies according to post-operative survival times. The maximum effective injection site is reached within about two hours of administration (Vanegas et al., '78), although the size of the injection site under microscopic evaluation (the so-called virtual injection site (Mesulam, '82)) continues to expand for another five hours. After a following 18 hours it contracts and disappears within 5 days (La Vail and La Vail, '74; Nauta et al., '74; Hedreen and McGrath, '77; Vanegas et al., '78). These data are all based on material utilising unconjugated HRP and reacted with the chromogen DAB, but it is thought that parameters are similar with WGA-HRP and TMB. Survival times of 17-72 hours post-injection are considered to give the most accurate interpretation of the injection site.
In the present series of experiments, a constant 48 hour survival time was used.

TMB is a more sensitive chromogen than DAB, and, as a result, the two compounds provide differing estimates of the injection site. Although TMB-evaluated injection sites are consistently larger than those using DAB, injection sites using either chromogen consist of a very dense reaction product centrally surrounded by a halo of lighter reaction product. There is conflicting evidence regarding the true zone of HRP uptake. Some authors believe that transport of HRP only occurs from the dense central zone (Jones, '75; Horton et al., '79), whereas others believe that uptake occurs from an area expanding beyond the densely stained cortical area, corresponding to the total halo of diffuse HRP (Bunt et al., '75; Dursteler et al., '77). Due to the cortical location of injection sites in this thesis, there was little difference in the extent of the injection site under TMB and DAB histochemistry, since the outer halo of TMB label was much reduced compared to injection sites in less densely cellular CNS areas. In addition, spread of the injection site into neighbouring areas was minimal. In each case, Purkinje cells were assumed to contribute to the injection if their somata were completely labelled and labelled axons could be discerned emanating from their somata. In practice, the area defined by these criteria generally corresponded with the inner densest reaction

product under TMB and the entire extent of the injection site under DAB histochemistry.

The level of neuronal activity within the injection site has been shown to affect the amount of free HRP transported (Singer et al., '77). Free HRP molecules are actively endocytosed and transported by the neuron. However, since the HRP molecules are not bound to the neural membrane, there must be a high concentration of molecules available at the neuron terminals for endocytosis to occur. Conjugated WGA-HRP is thought to be less influenced by neuronal activity because of the way it is bound to the neuronal membrane (Stockel et al., '78). The wheat-germ agglutinin lectin portion of the tracer is specifically bound to the cell membrane by high affinity bonds. Once bound to the membrane, the tracer is taken up into specific organelles within the neuron.

The amount of HRP taken up at terminals and transported retrogradely to the soma is dependent on the extent of the terminal axonal field contained within the injection site (Jones and Leavitt, '74; Jones, '75). Variation in both climbing and mossy fibre terminal fields in the molecular and granular layer respectively may account for differing staining densities within populations of olivary, pontine or NRTP neurons.

WGA-HRP was chosen specifically for these experiments due to its capacity for bi-directional transport from the site of injection. However, the climbing and mossy fibre input and Purkinje cell output reported in this study all focus in different layers of the cerebellar cortex. If an injection site covered a far greater area of molecular layer than underlying Purkinje cell layer for example, one might expect that the *afferent* and *efferent* effective injection sites would differ, and that the labelled olivary population would be projecting to a cortical area far greater than that projecting to the deep cerebellar nuclei from the Purkinje cell layer. However, attempts at creating separate afferent and efferent effective injection sites demonstrated that the differences were negligible in each case. Hence a single delimitation of each injection site was used for studying both afferent and efferent connections.

4.6.2 Uptake of WGA-HRP by fibres of passage.

Free HRP is not taken up by intact fibres of passage in the CNS (La Vail et al., '73; Lynch et al., '74; Nauta et al., '74; Wakefield and Shonnard, '79) but reports on uptake in the PNS are conflicting (Krishnan and Singer, '73; Oldfield and McLachlan, '77; Sparrow and Kiernan, '79). There is strong evidence to suggest that the conjugate WGA-HRP is not taken up by passing fibres (Brodal et al., '83).
Crushed or cut axons in both the PNS (Krishnan and Singer, '73) and CNS (Kristensson and Olsson, '74; Bunt et al., '75; Grob et al., '82) readily take up free HRP. Indeed, some authors believe that HRP uptake is greater in damaged axons than at undamaged axon terminals (Halperin and La Vail, '75; Sherlock and Raisman, '75).

Evidence for WGA-HRP is conflicting. Injections of 125I-WGA into the corpus callosum results in almost no uptake of WGA-HRP by passing fibres and little uptake by fibres damaged by the injection pipette (Grob et al., '82). However, WGA experiments utilising an unlabelled antibody technique to demonstrate transport shows clearly labelled cells whose axons were damaged by the injection cannula (Philipson and Griffiths, '83)
Due to the cortical location of the injection sites, fibres of passage themselves do not present a major problem in these experiments, and thus the problem of false positives is minimal. However, in a number of cases, the introduction of the Hamilton syringe damaged a small amount of cortex at the centre of the injection site, introducing the risk of false negatives. The "lesioned" area, however, only covered a tiny fraction of the total amount of tissue showing uptake of WGA-HRP, so the effect was assumed to be negligible.

The use of WGA-HRP as an anterograde tracer inevitably introduces the risk of confusion between terminal label and fibres of passage cut in cross-section. In actual fact, this difficulty was rarely encountered if the course of cortico-nuclear fibres were considered in their entirety. Difficulty with recording labelled terminal fields only occurred in the lateral border of the fastigial, when cut cortico-vestibular fibres complicated the picture. The majority of cortico-vestibular fibres, however, ran in the raphe between the fastigial and the interpositus nuclei and on the whole, cortico-nuclear fibres separated themselves from

the cortico-vestibular fibres and clearly travelled towards granular deposits in the nuclei. The possibility that terminal boutons arising from the Purkinje cell axon would be disguised by the strength of WGA-HRP deposit in the fibre itself is unavoidable, but considered to be small and consistent across all cases.

4.7 SUMMARY

This thesis sought to address the following questions:

i) does the visual and oculomotor-related dorsolateral pontine nucleus project to the flocculus?

ii) How is the olivo-cortico-nuclear parasagittal zonation represented in the monkey?

iii) Do cerebellar cortical projectipns overlap in the deep cerebellar nuclei?

iv) Is the nucleo-cortical pathway reciprocal to the cortico-nuclear projection?

i) Following an injection into the pure flocculus, as described by Gerrits and Voogd ('87), no retrogradely labelled cells were found in the dorsolateral pons. The five labelled cells found in the pontine nuclei were located in the dorsomedial nucleus. These cells, however, were more faintly labelled than those in the dlpn following injections into other cortical sites, or in the NRTP. Such limited labelling may indicate that projections from these cells to the flocculus comprise a collateral pathway from a major axon projecting to an alternative cortical area. The flocculus receives visual input from the climbing fibre system via the dorsal cap and ventrolateral outgrowth. Part of the mossy fibre-mediated visual information is supplied by input from discrete subnuclei of the NRTP. Comparison of NRTP efferents to the flocculus, vermal lobule VII and the dorsal paraflocculus, all of which play a part in oculomotor control permitted conclusions on the multiplicity of cortico-ponto/NRTP-cerebellar pathway involved in the control of eye movements.

ii) The classic parasagittal zonation of the olivo-cortico-nuclear projections (see Bigare and Voogd, '80 for review) is also evident in the macaque. However, important deviations from the strict parasagittal system were also evident in this animal.

Cortical areas receiving input from an olivary subdivision attributable to a particular parasagittal zone frequently sent additional projections into a deep nucleus not normally associated with that parasagittal zone. This "extra-zonal" divergence was found in the majority of cases, regardless of whether the injection site was located in the vermis, hemispheres or floccular complex.

In addition to divergence from the parasagittal zone, convergence within the olivo-cortical projection was seen. This convergence resulted from two olivary zones projecting to a particular cortical location which subsequently sent output to a single deep nuclear zone. Such "intra-zonal" convergence only occurred in the D zones. Cortical injection sites producing olivary label attributable to the D1 and D2 zones produced terminal fields purely in the caudal D1 zone of the dentate. The D1 and D2 zones in the posterior lobe therefore appear to converge onto the parvicellular, neocerebellar dentate nucleus.

iii) The cortico-nuclear projection s very precise, and projections that obeyed the strict parasagittal zonation did not show complete overlap of their nuclear terminal fields. However, extra-zonal projections from different cortical areas such as crus II, the flocculus and the dorsal paraflocculus did terminate in overlapping areas of the deep nuclei. Overlapping projections to the deep nuclei (in the above example, the ventrocaudal PIP) are unlikely to converge onto the same nuclear neurons. Data presented in this thesis demonstrates the striped topography of the cortico-nuclear projection, and combined with electrophysiological studies (Rosina et al., '96) that functionally homologous areas of the cerebellar cortex project onto interdigitating patches of the same deep cerebellar nucleus suggests that overlapping projections interdigitate rather than converge onto identical nuclear neurons.

iv) The nucleo-cortical pathway in the macaque is purely ipsilateral. It has three components:

a) Purely reciprocal

b) Localised non-reciprocity, in which the labelled cells lie just outside the terminal field, but

in the deep nucleus appropriate for that zone.

c) Nuclear non-reciprocity, in which the retrogradely labelled cells are located in a nucleus with no terminal field.

There were no consistent size differences between neuronal populations supplying any of the above projections.

Further conclusions of the role of the nucleo-cortical pathway cannot be drawn until the precise intra-cortical circuitry that includes the nucleo-cortical projections is established more precisely.

5. APPENDIX

5.1 PROTOCOLS

5.1.1 WGA-HRP

5.1.1.1 Fixation

The animal is sedated with 0.5-1 ml "Ketalar" i/m. The anaesthesia is prolonged with barbiturates until the lethal dose is reached. The animal's fore and hind limbs are stretched and tied to the base. After opening the thorax, the infusion needle is introduced to the left ventricle and up to the aorta and tied down.

The animal is then perfused with:

2 litres 0.9% sodium chloride (NaCl) + 2 ml heparin at room temperature

2 litres of 4% paraformaldehyde at room temperature

1 litre 10% buffered sucrose at 4°C

1 litre 20% buffered sucrose at 4°C.

All fluids are introduced at a flow rate of about 120ml/min.

Solutions required:

0.2M phosphate buffer = Solution a: 11g sodium dihydrogen orthophosphate in 400ml distilled water

Solution b: 45.427g di-sodium hydrogen orthophosphate in 1600ml distilled water.

Mix together solutions a and b.

0.9% NaCl (normal saline) = 9g NaCl dissolved in 1000ml distilled water.

4% paraformaldehyde = 40g paraformaldehyde dissolved in 100ml distilled water at 70°C. Add drops of 1N NaOH till clear. Cool to below 40°C. Add distilled water to 500 ml. Filter. Add 500ml 0.2M phosphate buffer. Check pH = 7.2-7.6.

10% buffered sucrose = 50g sucrose dissolved in 250ml distilled water + 250ml 0.2M phosphate buffer

20% buffered sucrose = 100g sucrose dissolved in 250ml distilled water + 250ml 0.2M phosphate buffer

5.1.1.2 Chromogen TMB

Reaction goes as follows:

Sections are placed in a dish with 0.1M phosphate buffer (in the fridge) prior to reacting

1. Sections rinsed 6 times in chilled distilled water.
2. Sections undergo pre-reaction soak for 40 minutes in TMB solution (in the fridge)
3. Reaction initiated by adding 1ml of 0.3% hydrogen peroxide per 100ml reaction fluid - 10 minutes in the fridge.
4. Reaction fluid is replaced and 1ml hydrogen peroxide per 100ml reaction fluid added - 10 minutes in the fridge.
5. Step 4 repeated two more times.
6. Sections rinsed 6 times in rinsing solution using agitating apparatus (5 minutes each rinse)
7. Sections mounted from rinsing solution onto subbed slides, using albumen to cover the slides prior to mounting.
8. Dry overnight.

N.B. for TMB reaction.

- All the dishes to be used must be clean and free of any bleach.
- Mix 585ml solution A and 15ml solution B. These solutions must be prepared fresh and mixed immediately prior to reacting the sections.
- To cut down on background, when first changing the reaction fluid, add 0.5ml 0.3% hydrogen peroxide per 100ml of reaction fluid.

Solutions required:

Acetate buffer = 200ml 1M sodium acetate added to 200ml distilled water and 190ml 1M HCl added. Make to 1 litre with distilled water and keep in the fridge. Check pH = 3.1-3.3

TMB solution = Solution A: 1850ml distilled water + 100ml HaC + 1800mg sodium ferracyanide

Solution B: 100mg TMB dissolved in 50ml absolute alcohol

Mix together above solutions just before reacting solutions

Solution for rinsing = 100ml acetate buffer (HaC) diluted in 1900ml distilled water.

5.1.1.3 Chromogen DAB

Reaction goes as follows:

1. Incubate sections in DAB solution for 30 minutes at room temperature
2. Rinse in three changes of 0.1M phosphate buffer
3. Mount onto subbed slides from fresh phosphate buffer.

Solution required:

50mg DAB + 100ml 0.1M phosphate buffer + 6ml 0.3% hydrogen peroxide. Dissolve in ultrasonicator

N.B. DAB is a possible carcinogenic compound and must be handled with caution.

5.1.1.4 Volumes of WGA-HRP injected in each case

M1-96	75nl	Co5	190nl
Pyr1	70nl	Sb6	200nl
UV1	100nl	GR-95	170nl
UV2	WGA-HRP soaked gelfoam sponge	696	100nl
PMD2	250nl	DPF1	100nl
M2-96right	200nl	HN-95	110nl
M2-96left	180nl	BG-95	140nl
228	120nl	D669	100nl

5.1.2 Zebrin

1. Rinse sections 3 times in TBS+
2. mabQ113, 1:150 in TBS+ for 12-24 hours at room temperature or 48 hours at 4°C
3. Rinse three times in TBS+
4. Biotine anti-mouse, 1:200 in TBS+ for 1-2 hours

5. Rinse 3 times in TBS+

6. ABC kit - incubate sections in this for 30 minutes

7. Rinse sections 6 times in 0.05M phosphate buffer at pH 7.2

8. React with DAB solution

9. Rinse with 0.05M phosphate buffer

10. Mount on subbed slides, dry overnight

Solutions required:

TBS+ = Tris-buffer saline with Triton

6.06g trizma base, 29.22g NaCl, 5ml tritonx100. Dissolve above ingredients in 750ml distilled water and titrate hydrochloric acid to pH 8.6. Add distilled water to 1 litre.

5.1.3 Stains

5.1.3.1 Cresyl violet

1. xylene - 3 minutes

2. 100% alcohol - 3 minutes

3. 95% alcohol - 3 minutes

4. 70% alcohol - 3 minutes

5. Distilled water - 3 minutes

6. Cresyl stain - 5-10 minutes depending on age of stain

7. Distilled water - rinse

8. 70% alcohol - 3 minutes

9. 95% alcohol - 3 minutes

10. 100% alcohol - 3 minutes

11. Xylene - 2 changes, 5 minutes each

12. Apply DPX and cover.

Solutions required:

Dissolve 1g of cresyl violet in 1000ml distilled water heated to 60°C. Add 10ml 10% acetic acid. Filter.

Alternatively, use 950ml distilled water and 50ml acetate buffer.

5.1.4 General

5.1.4.1 Gelatine embedding for HRP brain:

1. Place brain in 5% gelatine solution for 1 hour into vacuum oven at 42°C.
2. Place brain in 10% gelatine solution for 1 hour into vacuum oven at 42°C.
3. Allow brain to cool in 10% gelatine solution in a suitable vessel to form a block. Remove block from vessel and place in 20% buffered sucrose solution and leave in fridge overnight.
4. Carefully trim gelatin block to leave an even 2mm thickness of gelatin around the entire brain.
5. Harden the gelatin in approximately 200ml of 4% paraformaldehyde solution for 2 hours with gentle agitation.
6. Rinse thoroughly in a large volume of 20% buffered sucrose solution for 20 minutes with agitation. Change again and leave in fresh 20% buffered sucrose until ready to cut.

Solutions required:

5% gelatin = 5g gelatin, 20g sucrose, 100ml distilled H20

10% gelatin = 10g gelatin, 20g sucrose, 100ml distilled H20.

Heat distilled water to 42°C and carefully add gelatin while stirring. Add sucrose when gelatin is completely dissolved.

5.1.4.2 Subbing solution for microscope slides

Wash slides in hot water and detergent. Rinse thoroughly in hot running water and then leave slides in distilled water for a short time (10 minutes). Using slide racks, dip bodily into the following solution (at room temperature)* and dry in a hot oven for several hours or overnight (60°C).

Solution required:

5g gelatin, 0.5g chromium potassium sulphate, 1000ml distilled water.

Dissolve gelatin in a small quantity of the distilled water in a warm oven (or just warm water on a hot plate to a temperature of 37-42°C). The add chromium potassium sulphate and the rest of the water to make 1000ml. Filter before use.

* Leave slides in subbing solution for about 1 hour for better results.

6. REFERENCES

Aas, J.E., O.P. Ottersen, and P. Brodal (1989) Profiles enriched in GABA-like immunoreactivity participate in serial synapses in the pontine nuclei of baboon (Papio anubis). .Exp.Brain Res. *78*:641-645.

Aas, J.E. and P. Brodal (1990) GABA and glycine as putative transmitters in subcortical pathways to the pontine nuclei. A combined immunocytochemical and retrograde tracing study in the cat with some observations in the rat. .Neuroscience. *34*:149-162.

Ahn, A.H., S. Dziennis, R. Hawkes, and K. Herrup (1994) The cloning of zebrin II reveals its identity with aldolase C. .Development. *120*:2081-2090.

Akaike, T. (1986) Differential localization of inferior olivary neurons projecting to the tecto-olivo-recipient zones of lobule VII or crus II in the rat cerebellum. Brain Res. *386*:400-404.

Akaogi, K., Y. Sato, K. Ikarashi, and T. Kawasaki (1994) Mossy fiber projections from the brain stem to the nodulus in the cat. An experimental study comparing the nodulus, the uvula and the flocculus. Brain Res. *638*:12-20.

Albus, K., F. Donate Oliver, D. Sanides, and W. Fries (1981) The distribution of pontine projection cells in visual and association cortex of the cat: an experimental study with horseradish peroxidase. .J.Comp.Neurol. *201*:175-189.

Allen, G.I. and N. Tsukahara (1974) Cerebrocerebellar communication systems. .Physiol.Rev. *54*:957-1006.

Andersen, R. A. and J. W. Gnadt (1989) Posterior parietal cortex. Rev. Oculo. Res. 3: 315-35.

Andersen, R. A., P. R. Brotchie, and P. Mazzoni (1992) Evidence for the LIP area as the parietal eye field. Curr. Opin. Neurobiol. 2(6):840-6.

Andersson, G. and O. Oscarsson (1978) Climbing fiber microzones in cerebellar vermis and their projection to different groups of cells in the lateral vestibular nucleus. .Exp.Brain Res. *32*:565-579.

Andersson, G. and O. Oscarsson (1978) Projections to lateral vestibular nucleus from cerebellar climbing fiber zones. .Exp.Brain Res. *32*:549-564.

Andersson, G. and L. Eriksson (1981) Spinal, trigeminal, and cortical climbing fibre paths to the lateral vermis of the cerebellar anterior lobe in the cat. Exp.Brain Res. *44*:71-81.

Andersson, G. (1984) Mutual inhibition between olivary cell groups projecting to different cerebellar microzones in the cat. Exp.Brain Res. *54*:293-303.

Andersson, G. and G. Hesslow (1987) Activity of Purkinje cells and interpositus neurones during and after periods of high frequency climbing fibre activation in the cat. .Exp.Brain Res. *67*:533-542.

Andersson, G. and G. Hesslow (1987) Inferior olive excitability after high frequency climbing fibre activation in the cat. .Exp.Brain Res. *67*:523-532.

Angaut, P. and A. Brodal (1967) The projection of the "vestibulocerebellum" onto the vestibular nuclei in the cat. .Arch.Ital.Biol. *105*:441-479.

Angaut, P. (1970) The ascending projections of the nucleus interpositus posterior of the cat cerebellum: an experimental anatomical study using silver impregnation methods. Brain Res. *24*:377-394.

Anguat, P. and F. Cicirata (1982) Cerebello-olivary projections in the rat. An autoradiographic study. Brain Behav.Evol. *21*:24-33.

Angaut, P., F. Cicirata, and M. R. Panto (1985) An autoradiographic study of the cerebello-pontine projections from the interposed and lateral cerebellar nuclei in the rat. J. Hirnforsch. *26(4):* 463-470.

Angaut, P., F. Cicirata, and F. Serapide (1985) Topographic organization of the cerebellothalamic projections in the rat. An autoradiographic study. Neuroscience. *15*:389-401.

Angaut, P., C. Compoint, C. Buisseret Delmas, and C. Batini (1996) Synaptic connections of Purkinje cell axons with nucleocortical neurones in the cerebellar medial nucleus of the rat. .Neurosci.Res. *26*:345-348.

Apps, R., J.R. Trott, and E. Dietrichs (1991) A study of branching in the projection from the inferior olive to the x and lateral c1 zones of the cat cerebellum using a combined electrophysiological and retrograde fluorescent double-labelling technique. .Exp.Brain Res. *87*:141-152.

Armengol, J.A. and P. Salinas (1991) Analysis of the ipsi- and contralateral location of the neurons of the nucleus reticularis tegmenti pontis projecting to the cerebellum and of the trajectory of their axons within the pons to the brachium pontis. An "in vivo" and "in vitro" study. .J.Hirnforsch. *32*:715-724.

Armstrong, D.M. and R.F. Schild (1978) An investigation of the cerebellar corticonuclear projections in the rat using an autoradiographic tracing method. II. Projections from the hemisphere. .Brain Res. *141*:235-249.

Armstrong, D.M. and S.A. Edgley (1984) Discharges of nucleus interpositus neurones during locomotion in the cat. J.Physiol.Lond. *351*:411-432.

Armstrong, D.M. and S.A. Edgley (1988) Discharges of interpositus and Purkinje cells of the cat cerebellum during locomotion under different conditions. J.Physiol.Lond. *400*:425-445.

Armstrong, D.M. (1990) Topographical localisation in the projections from the inferior olive to the paravermal cortex of the anterior lobe and paramedian lobule in the cerebellum of the cat. A brief review. Arch.Ital.Biol. *128*:183-207.

Asanuma, C., W.R. Thach, and E.G. Jones (1983) Anatomical evidence for segregated focal groupings of efferent cells and their terminal ramifications in the cerebellothalamic pathway of the monkey. Brain Res. *286*:267-297.

Asanuma, C., W.T. Thach, and E.G. Jones (1983) Brainstem and spinal projections of the deep cerebellar nuclei in the monkey, with observations on the brainstem projections of the dorsal column nuclei. Brain Res. *286*:299-322.

Asanuma, C., W.T. Thach, and E.G. Jones (1983) Distribution of cerebellar terminations and their relation to other afferent terminations in the ventral lateral thalamic region of the monkey. Brain Res. *286*:237-265.

Azizi, S.A., R.A. Burne, and D.J. Woodward (1985) The auditory corticopontocerebellar projection in the rat: inputs to the paraflocculus and midvermis. An anatomical and physiological study. .Exp.Brain Res. *59*:36-49.

Azizi, S.A., G.A. Mihailoff, R.A. Burne, and D.J. Woodward (1981) The pontocerebellar system in the rat: an HRP study. I. Posterior vermis. J.Comp.Neurol. *197*:543-548.

Azizi, S.A. and D.J. Woodward (1987) Inferior olivary nuclear complex of the rat: morphology and comments on the principles of organization within the olivocerebellar system. J.Comp.Neurol. *263*:467-484.

Azizi, S.A. and D.J. Woodward (1990) Interactions of visual and auditory mossy fiber inputs in the paraflocculus of the rat: a gating action of multimodal inputs. .Brain Res. *533*:255-262.

Baker, J., A. Gibson, M. Glickstein, and J. Stein (1976) Visual cells in the pontine nuclei of the cat. .J.Physiol.Lond. *255*:415-433.

Baker, J., A. Gibson, G. Mower, F. Robinson, and M. Glickstein (1983) Cat visual corticopontine cells project to the superior colliculus. .Brain Res. *265*:227-232.

Balaban, C.D., Y. Kawaguchi, and E. Watanabe (1981) Evidence of a collateralized climbing fiber projection from the inferior olive to the flocculus and vestibular nuclei in rabbits. .Neurosci.Lett. *22*:23-29.

Barbas, H. and M. M. Mesulam (1981) Organisation of afferent input to subdivisions of area 8 in the Rhesus monkey. J. Comp. Neurol. *200(3):* 407-31.

Barmack, N.H., R.W. Baughman, P. Errico, and H. Shojaku (1993) Vestibular primary afferent projection to the cerebellum of the rabbit. J.Comp.Neurol. *327*:521-534.

Batini, C., C. Buisseret Delmas, J. Corvisier, O. Hardy, and D. Jassik Gerschenfeld (1978) Brain stem nuclei giving fibers to lobules VI and VII of the cerebellar vermis. Brain Res. *153*:241-261.

Batini, C., C. Buisseret Delmas, C. Compoint, and H. Daniel (1989) The GABAergic neurones of the cerebellar nuclei in the rat: projections to the cerebellar cortex. .Neurosci.Lett. *99*:251-256.

Batton, R.R., A. Jayaraman, D. Ruggiero, and M.B. Carpenter (1977) Fastigial efferent projections in the monkey: an autoradiographic study. .J.Comp.Neurol. *174*:281-305.

Bauswein, E., F.P. Kolb, B. Leimbeck, and F.J. Rubia (1983) Simple and complex spike activity of cerebellar Purkinje cells during active and passive movements in the awake monkey. .J.Physiol.Lond. *339*:379-394.

Becker, W. and A.F. Fuchs (1969) Further properties of the human saccadic system: eye movements and correction saccades with and without visual fixation points. .Vision.Res. *9*:1247-1258.

Beitz, A.J. (1976) The topographical organization of the olivo-dentate and dentato-olivary pathways in the cat. .Brain Res. *115*:311-317.

Bentivoglio, M. and M. Molinari (1981) Axonal branches of the same cerebellar neurons terminate bilaterally in the thalamus. Neurosci.Lett. *23*:291-296.

Berkley, K.J. and P.J. Hand (1978) Projections to the inferior olive of the cat. II. Comparisons of input from the gracile, cuneate and the spinal trigeminal nuclei. J.Comp.Neurol. *180*:253-264.

Bernard, J-F. (1987) Topographical organisation of olivocerebellar and corticonuclear connections in the rat - an WGA-HRP study: I. Lobules IX, X and the flocculus. J. Comp. Neurol. *263*: 241-258.

Beyerl, B.D., L.F. Borges, B. Swearingen, and R.L. Sidman (1982) Parasagittal organization of the olivocerebellar projection in the mouse. .J.Comp.Neurol. *209*:339-346.

Bishop, G.A., R.A. McCrea, and S.T. Kitai (1976) A horseradish peroxidase study of the cortico-olivary projection in the cat. .Brain Res. *116*:306-311.

Bishop, G.A., R.A. McCrea, J.W. Lighthall, and S.T. Kitai (1979) An HRP and autoradiographic study of the projection from the cerebellar cortex to the nucleus interpositus anterior and nucleus interpositus posterior of the cat. J.Comp.Neurol. *185*:735-756.

Bjaalie, J.G. and P. Brodal (1983) Distribution in area 17 of neurons projecting to the pontine nuclei: a quantitative study in the cat with retrograde transport of HRP-WGA. .J.Comp.Neurol. *221*:289-303.

Bjaalie, J.G. and P. Brodal (1989) Visual pathways to the cerebellum: segregation in the pontine nuclei of terminal fields from different visual cortical areas in the cat. .Neuroscience. *29*:95-107.

Blanks, R.H., W. Precht, and Y. Torigoe (1983) Afferent projections to the cerebellar flocculus in the pigmented rat demonstrated by retrograde transport of horseradish peroxidase. Exp.Brain Res. *52*:293-306.

Blatt, G.J., R.A. Andersen, and G.R. Stoner (1990) Visual receptive field organization and cortico-cortical connections of the lateral intraparietal area (area LIP) in the macaque. .J.Comp.Neurol. *299*:421-445.

Boesten, A.J. and J. Voogd (1975) Projections of the dorsal column nuclei and the spinal cord on the inferior olive in the cat. .J.Comp.Neurol. *161*:215-237.

Bolk, L. (1906) Das Cerebellum der Saugetiere, Jena G. Fisher.
Border, B.G. and G.A. Mihailoff (1985) GAD-immunoreactive neural elements in the basilar pontine nuclei and nucleus reticularis tegmenti pontis of the rat. I. Light microscopic studies. .Exp.Brain Res. *59*:600-614.

Border, B.G., R.J. Kosinski, S.A. Azizi, and G.A. Mihailoff (1986) Certain basilar pontine afferent systems are GABA-ergic: combined HRP and immunocytochemical studies in the rat. .Brain Res.Bull. *17*:169-179.

Boussaoud, D., L.G. Ungerleider, and R. Desimone (1990) Pathways for motion analysis: cortical connections of the medial superior temporal and fundus of the superior temporal visual areas in the macaque. .J.Comp.Neurol. *296*:462-495.

Boussaoud, D., R. Desimone, and L.G. Ungerleider (1992) Subcortical connections of visual areas MST and FST in macaques. .Vis.Neurosci. *9*:291-302.

Bowman, J.P. and J.R. Sladek (1973) Morphology of the inferior olivary complex of the rhesus monkey (Macaca mulatta). .J.Comp.Neurol. *152*:299-316.

Broch Smith, T. and P. Brodal (1990) Organization of the cortico-ponto-cerebellar pathway to the dorsal paraflocculus. An experimental study with anterograde and retrograde transport of WGA-HRP in the cat. .Arch.Ital.Biol. *128*:249-271.

Brochu, G., L. Maler, and R. Hawkes (1990) Zebrin II: a polypeptide antigen expressed selectively by Purkinje cells reveals compartments in rat and fish cerebellum. .J.Comp.Neurol. *291*:538-552.

Brodal, P. (1968) The corticopontine projection in the cat. I. Demonstration of a somatotopically organized projection from the primary sensorimotor cortex. .Exp.Brain Res. *5*:210-234.

Brodal, A. and P. Brodal (1971) The organization of the nucleus reticularis tegmenti pontis in the cat in the light of experimental anatomical studies of its cerebral cortical afferents. .Exp.Brain Res. *13*:90-110.

Brodal, A., J. Destombes, A.M. Lacerda, and P. Angaut (1972) A cerebellar projection onto the pontine nuclei. An experimental antaomical study in the cat. .Exp.Brain Res. *16*:115-139.

Brodal, A., A.M. Lacerda, J. Destombes, and P. Angaut (1972) The pattern in the projection of the intracerebellar nuclei onto the nucleus reticularis tegmenti pontis in the cat. An experimental anatomical study. .Exp.Brain Res. *16*:140-160.

Brodal, A. and G. Szikla (1972) The termination of the brachium conjunctivum descendens in the nucleus reticularis tegmenti pontis. An experimental anatomical study in the cat. .Brain Res. *39*:337-351.

Brodal, P. (1972) The corticopontine projection from the visual cortex in the cat. II. The projection from areas 18 and 19. .Brain Res. *39*:319-335.

Brodal, P. (1972) The corticopontine projection from the visual cortex in the cat. I. The total projection and the projection from area 17. .Brain Res. *39*:297-317.

Brodal, A. and J. Courville (1973) Cerebellar corticonuclear projection in the cat. Crus II. An experimental study with silver methods. .Brain Res. *50*:1-23.

Brodal, A., F. Walberg, and G.H. Hoddevik (1975) The olivocerebellar projection in the cat studied with the method of retrograde axonal transport of horseradish peroxidase. J.Comp.Neurol. *164*:449-469.

Brodal, P. and F. Walberg (1977) The pontine projection to the crebellar anterior lobe. An experimental study in the cat with retrograde transport of horseradish peroxidase. .Exp.Brain Res. *29*:233-248.

Brodal, A. and F. Walberg (1977) The olivocerebellar projection in the cat studied with the method of retrograde axonal transport of horseradish peroxidase. VI. The projection onto longitudinal zones of the paramedian lobule. .J.Comp.Neurol. *176*:281-294.

Brodal, A. and F. Walberg (1977) The olivocerebellar projection in the cat studied with the method of retrograde axonal transport of horseradish peroxidase. IV. The projection to the anterior lobe. .J.Comp.Neurol. *172*:85-108.

Brodal, A. and G.H. Hoddevik (1978) The pontocerebellar projection of the uvula in the cat. .Exp.Brain Res. *32*:105-116.

Brodal, P. (1978) The corticopontine projection in the rhesus monkey. Origin and principles of organization. .Brain *101*:251-283.

Brodal, P. (1978) Principles of organization of the monkey corticopontine projection. .Brain Res. *148*:214-218.

Brodal, P. (1979) The pontocerebellar projection in the rhesus monkey: an experimental study with retrograde axonal transport of horseradish peroxidase. .Neuroscience. *4*:193-208.

Brodal, P. (1980) The cortical projection to the nucleus reticularis tegmenti pontis in the rhesus monkey. .Exp.Brain Res. *38*:19-27.

Brodal, P. (1980) The projection from the nucleus reticularis tegmenti pontis to the cerebellum in the rhesus monkey. .Exp.Brain Res. *38*:29-36.

Brodal, A. and K. Kawamura (1980) Olivocerebellar projection: a review. .Adv.Anat.Embryol.Cell.Biol. *64*:IVIII, 1-140.

Brodal, A., F. Walberg, K.J. Berkley, and A. Pelt (1980) Anatomical demonstration of branching olivocerebellar fibres by means of a double retrograde labelling technique. .Neuroscience. *5*:2193-2202.

Brodal, P. and A. Brodal (1981) The olivocerebellar projection in the monkey. Experimental studies with the method of retrograde tracing of horseradish peroxidase. .J.Comp.Neurol. *201*:375-393.

Brodal, P. (1982) Further observations on the cerebellar projections from the pontine nuclei and the nucleus reticularis tegmenti pontis in the rhesus monkey. .J.Comp.Neurol. *204*:44-55.

Brodal, P. and A. Brodal (1982) Further observations on the olivocerebellar projection in the monkey. .Exp.Brain Res. *45*:71-83.

Brodal, P., E. Dietrichs, J.G. Bjaalie, T. Nordby, and F. Walberg (1983) Is lectin-coupled horseradish peroxidase taken up and transported by undamaged as well as by damaged fibers in the central nervous system? Brain Res. *278*:1-9.

Brodal, A. and P. Brodal (1985) Observations on the secondary vestibulocerebellar projections in the macaque monkey. Exp.Brain Res. *58*:62-74.

Brodal, P., E. Dietrichs, and F. Walberg (1986) Do pontocerebellar mossy fibres give off collaterals to the cerebellar nuclei? An experimental study in the cat with implantation of crystalline HRP-WGA. .Neurosci.Res. *4*:12-24.

Brodal, P., J.G. Bjaalie, and J.E. Aas (1991) Organization of cingulo-ponto-cerebellar connections in the cat. Anat.Embryol.Berl. *184*:245-254.

Brodal, P. and J.G. Bjaalie (1992) Organization of the pontine nuclei. .Neurosci.Res. *13*:83-118.

Brodmann, K. (1909) Vergleichende Lokaliastionslehre der Grosshirnrinde in ihren Prinzipien dargestellt auf Grund des Zellenbaues. Narth: Leipzig.

Brown, J.T., V. Chan Palay, and S.L. Palay (1977) A study of afferent input to the inferior olivary complex in the rat by retrograde axonal transport of horseradish peroxidase. .J.Comp.Neurol. *176*:1-22.

Brown, P.A. (1980) The inferior olivary connections to the cerebellum in the rat studied by retrograde axonal transport of horseradish peroxidase. Brain Res.Bull. *5*:267-275.

Bruce, C.J., M.E. Goldberg, M.C. Bushnell, and G.B. Stanton (1985) Primate frontal eye fields. II. Physiological and anatomical correlates of electrically evoked eye movements. .J.Neurophysiol. *54*:714-734.

Brudzynski, S.M. and G.J. Mogenson (1984) The role of the nucleus reticularis tegmenti pontis in locomotion: a lesion study in the rat. .Brain Res.Bull. *12*:513-520.

Buisseret Delmas, C. (1988) Sagittal organization of the olivocerebellonuclear pathway in the rat. II. Connections with the nucleus interpositus. Neurosci.Res. *5*:494-512.

Buisseret Delmas, C. (1988) Sagittal organization of the olivocerebellonuclear pathway in the rat. I. Connections with the nucleus fastigii and the nucleus vestibularis lateralis. Neurosci.Res. *5*:475-493.

Buisseret Delmas, C. and P. Angaut (1988) The cerebellar nucleocortical projections in the rat. A retrograde labelling study using horseradish peroxidase combined to a lectin. Neurosci.Lett. *84*:255-260.

Buisseret Delmas, C. and P. Angaut (1989) Anatomical mapping of the cerebellar nucleocortical projections in the rat: a retrograde labeling study. J.Comp.Neurol. *288*:297-310.

Buisseret Delmas, C. and P. Angaut (1993) The cerebellar olivo-corticonuclear connections in the rat. .Prog.Neurobiol. *40*:63-87.

Buisseret Delmas, C., N. Yatim, P. Buisseret, and P. Angaut (1993) The X zone and CX subzone of the cerebellum in the rat. .Neurosci.Res. *16*:195-207.

Bukowska, D. (1995) Cerebellovestibular projection from the posterior lobe cortex in the rabbit: an experimental study with the retrograde HRP method. II. Zonal organization. Acta.Neurobiol.Exp.Warsz. *55*:35-47.

Bunt, A.H., A.E. Hendrickson, -J.S. Lund, R.D. Lund, and A.F. Fuchs (1975) Monkey retinal ganglion cells: morphometric analysis and tracing of axonal projections, with a consideration of the peroxidase technique. .J.Comp.Neurol. *164*:265-285.

Burne, R.A., M.A. Eriksson, J.A. Saint Cyr, and D.J. Woodward (1978) The organization of the pontine projection to lateral cerebellar areas in the rat: dual zones in the pons. .Brain Res. *139*:340-347.

Burne, R.A., G.A. Mihailoff, and D.J. Woodward (1978) Visual corticopontine input to the paraflocculus: a combined autoradiographic and horseradish peroxidase study. .Brain Res. *143*:139-146.

Burne, R.A., S.A. Azizi, G.A. Mihailoff, and D.J. Woodward (1981) The tectopontine projection the the rat with comments on visual pathways to the basilar pons. .J.Comp.Neurol. *202*:287-307.

Burne, R.A. and D.J. Woodward (1983) Visual cortical projections to the paraflocculus in the rat. An electrophysiologic study. .Exp.Brain Res. *49*:55-67.

Buttner, U. and W. Waespe (1984) Purkinje cell activity in the primate flocculus during optokinetic stimulation, smooth pursuit eye movements and vestibuo-ocular reflex suppression. Exp. Br. Res. 55(1):97-104.

Buttner-Ennever J. A., B. Cohen, A. K. Horn, and H. Reisline (1996) Efferent pathways of the NOT in the monkey and their role in eye movements. J. Comp. Neurol. *373*: 90-107.

Cakal, S. R. (1911) Histologie du systeme nerveux de l'homme et des vertebres. Maloine: Paris.

Campbell, N.C. and D.M. Armstrong (1983) Topographical localization in the olivocerebellar projection in the rat: an autoradiographic study. .Brain Res. *275*:235-249.

Campbell, N.C. and D.M. Armstrong (1983) The olivocerebellar projection in the rat: an autoradiographic study. .Brain Res. *275*:215-233.

Campbell, N.C. and D.M. Armstrong (1985) Origin in the medial accessory olive of climbing fibres to the x and lateral c1 zones of the cat cerebellum: a combined electrophysiological/WGA-HRP investigation. Exp.Brain Res. *58*:520-531.

Carleton, S.C. and M.B. Carpenter (1983) Afferent and efferent connections of the medial, inferior and lateral vestibular nuclei in the cat and monkey. Brain Res. *278*:29-51.

Carpenter, M.B. and R.J. Cowie (1985) Connections and oculomotor projections of the superior vestibular nucleus and cell group 'y'. Brain Res. *336*:265-287.

Chesire, R.M., J.T. Cheng, and P. Teitelbaum (1983) The inhibition of movement by morphine or haloperidol depends on an intact nucleus reticularis tegmenti pontis. .Physiol.Behav. *30*:809-818.

Chesire, R.M., J.T. Cheng, and P. Teitelbaum (1984) Reversal of akinesia and release of festination by morphine or GABA applied focally to the nucleus reticularis tegmenti pontis. .Behav.Neurosci. *98*:739-742.

Chubb, M.C. and A.F. Fuchs (1982) Contribution of y group of vestibular nuclei and dentate nucleus of cerebellum to generation of vertical smooth eye movements. .J.Neurophysiol. *48*:75-99.

Cohen, J.L., F. Robinson, J. May, and M. Glickstein (1981) Corticopontine projections of the lateral suprasylvian cortex: de-emphasis of the central visual field. .Brain Res. *219*:239-248.

Clarke, R. H. and V. Horsley (1905) On the intrinsic fibers of the cerebellum, its nuclei, and its efferent tract. Brain 28: 13-29.

Colby, C.L., J.R. Duhamel, and M.E. Goldberg (1993) The analysis of visual space by the lateral intraparietal area of the monkey: the role of extraretinal signals. .Prog.Brain Res. *95*:307-316.

Conde, F. (1988) Cerebellar projections to the red nucleus of the cat. Behav.Brain Res. *28*:65-68.

Coulter, J. D. and E. G. Jones (1977) Differentail distribution of corticospinal projections from individual cyto-architectonic fields in the monkey. Brain Res. 129:335-340.

Courville, J. (1966) Somatotopical organization of the projection from the nucleus interpositus anterior of the cerebellum to the red nucleus. An experimental study in the cat with silver impregnation methods. .Exp.Brain Res. *2*:191-215.

Courville, J. and C.W. Cooper (1970) The cerebellar nuclei of macaca mulatta: a morphological study. .J.Comp.Neurol. *140*:241-254.

Courville, J., N. Diakiw, and A. Brodal (1973) Cerebellar corticonuclear projection in the cat. The paramedian lobule. An experimental study with silver methods. .Brain Res. *50*:25-45.

Courville, J., N. Diakiw, and A. Brodal (1973) Cerebellar corticonuclear projection in the cat. The paramedian lobule. An experimental study with silver methods. .Brain Res. *50*:25-45.

Courville, J. and S. Otabe (1974) The rubro-olivary projection in the macaque: an experimental study with silver impregnation methods. .J.Comp.Neurol. *158*:479-494.

Courville, J., F. Faraco Cantin, and N. Diakiw (1974) A functionally important feature of the distribution of the olivo-cerebellar climbing fibers. .Can.J.Physiol.Pharmacol. *52*:1212-1217.

Courville, J. (1975) Distribution of olivocerebellar fibers demonstrated by a radioautographic tracing method. .Brain Res. *95*:253-263.

Courville, J. and N. Diakiw (1976) Cerebellar corticonuclear projection in the cat. The vermis of the anterior and posterior lobes. .Brain Res. *110*:1-20.

Courville, J., J.R. Augustine, and P. Martel (1977) Projections from the inferior olive to the cerebellar nuclei in the cat demonstrated by retrograde transport of horseradish peroxidase. .Brain Res. *130*:405-419.

Courville, J. and F. Faraco Cantin (1978) On the origin of the climbing fibers of the cerebellum. An experimental study in the cat with an autoradiographic tracing method. .Neuroscience. *3*:797-809.

Courville, J., F. Faraco Cantin, and A. Legendre (1983) Detailed organization of cerebello-olivary projections in the cat. An autoradiographic study. .Arch.Ital.Biol. *121*:219-236.

Courville, J., F. Faraco Cantin, and L. Marcon (1983) Projections from the reticular formation of the medulla, the spinal trigeminal and lateral reticular nuclei to the inferior olive. .Neuroscience. *9*:129-139.

Crandall, W.F. and E.L. Keller (1985) Visual and oculomotor signals in nucleus reticularis tegmenti pontis in alert monkey. .J.Neurophysiol. *54*:1326-1345.

Daniel, H., J.M. Billard, P. Angaut, and C. Batini (1987) The interposito-rubrospinal system. Anatomical tracing of a motor control pathway in the rat. Neurosci.Res. *5*:87-112.

De Zeeuw, C.I., J.C. Holstege, T.J. Ruigrok, and J. Voogd (1989) Ultrastructural study of the GABAergic, cerebellar, and mesodiencephalic innervation of the cat medial accessory olive: anterograde tracing combined with immunocytochemistry. .J.Comp.Neurol. *284*:12-35.

De Zeeuw, C.I., T.J. Ruigrok, J.C. Holstege, H.G. Jansen, and J. Voogd (1990) Intracellular labeling of neurons in the medial accessory olive of the cat: II. Ultrastructure of dendritic spines and their GABAergic innervation. .J.Comp.Neurol. *300*:478-494.

De Zeeuw, C.I., N.M. Gerrits, J. Voogd, C.S. Leonard, and J.I. Simpson (1994) The rostral dorsal cap and ventrolateral outgrowth of the rabbit inferior olive receive a GABAergic input from dorsal group Y and the ventral dentate nucleus. .J.Comp.Neurol. *341*:420-432.

De Zeeuw, C.I., D.R. Wylie, P.L. DiGiorgi, and J.I. Simpson (1994) Projections of individual Purkinje cells of identified zones in the flocculus to the vestibular and cerebellar nuclei in the rabbit. J.Comp.Neurol. *349*:428-447.

Deniau, J.M., H. Kita, and S.T. Kitai (1992) Patterns of termination of cerebellar and basal ganglia efferents in the rat thalamus. Strictly segregated and partly overlapping projections. Neurosci.Lett. *144*:202-206.

Desimone, R. and L.G. Ungerleider (1986) Multiple visual areas in the caudal superior temporal sulcus of the macaque. .J.Comp.Neurol. *248*:164-189.

Dietrichs, E. and F. Walberg (1979) The cerebellar corticonuclear and nucleocortical projections in the cat as studied with anterograde and retrograde transport of horseradish peroxidase. I. The paramedian lobule. .Anat.Embryol.Berl. *158*:13-39.

Dietrichs, E. and F. Walberg (1979) The cerebellar corticonuclear and nucleocortical projections in the cat as studied with anterograde and retrograde transport of horseradish peroxidase. I. The paramedian lobule. .Anat.Embryol.Berl. *158*:13-39.

Dietrichs, E. and F. Walberg (1980) The cerebellar corticonuclear and nucleocortical projections in the cat as studied with anterograde and retrograde transport of horseradish peroxidase. II. Lobulus simplex, crus I and II. Anat.Embryol.Berl. *161*:83-103.

Dietrichs, E. and F. Walberg (1980) The cerebellar corticonuclear and nucleocortical projections in the cat as studied with anterograde and retrograde transport of horseradish peroxidase. II. Lobulus simplex, crus I and II. Anat.Embryol.Berl. *161*:83-103.

Dietrichs, E. and F. Walberg (1981) The cerebellar nucleo-olivary projection in the cat. Anat.Embryol.Berl. *162*:51-67.

Dietrichs, E. and F. Walberg (1981) The cerebellar nucleo-olivary projection in the cat. Anat.Embryol.Berl. *162*:51-67.

Dietrichs, E. (1981) The cerebellar corticonuclear and nucleocortical projections in the cat as studied with anterograde and retrograde transport of horseradish peroxidase. III. The anterior lobe. .Anat.Embryol.Berl. *162*:223-247.

Dietrichs, E. (1981) The cerebellar corticonuclear and nucleocortical projections in the cat as studied with anterograde and retrograde transport of horseradish peroxidase. IV. The paraflocculus. .Exp.Brain Res. *44*:235-242.

Dietrichs, E. (1981) The cerebellar corticonuclear and nucleocortical projections in the cat as studied with anterograde and retrograde transport of horseradish peroxidase. IV. The paraflocculus. Exp.Brain Res. *44*:235-242.

Dietrichs, E. (1981) The cerebellar corticonuclear and nucleocortical projections in the cat as studied with anterograde and retrograde transport of horseradish peroxidase. III. The anterior lobe. Anat.Embryol.Berl. *162*:223-247.

Dietrichs, E., F. Walberg, and T. Nordby (1981) On retro- and anterograde transport of horseradish peroxidase in the pontocerebellar fibers as studied with the Mesulam TMB technique. Brain Res. *204*:179-183.

Dietrichs, E., F. Walberg, and T. Nordby (1981) On retro- and anterograde transport of horseradish peroxidase in the pontocerebellar fibers as studied with the Mesulam TMB technique. Brain Res. *204*:179-183.

Dietrichs, E. (1983) The cerebellar corticonuclear and nucleocortical projections in the cat as studied with anterograde and retrograde transport of horseradish peroxidase. V. The posterior lobe vermis and the flocculo-nodular lobe. Anat.Embryol.Berl. *167*:449-462.

Dietrichs, E., J.G. Bjaalie, and P. Brodal (1983) Do pontocerebellar fibers send collaterals to the cerebellar nuclei? .Brain Res. *259*:127-131.

Dietrichs, E., Z.H. Zheng, and F. Walberg (1983) The cerebellar corticovestibular projection in the cat as studied with retrograde transport of horseradish peroxidase. Anat.Embryol.Berl. *166*:369-383.

Dietrichs, E. and F. Walberg (1985) The cerebellar nucleo-olivary and olivo-cerebellar nuclear projections in the cat as studied with anterograde and retrograde transport in the same animal after implantation of crystalline WGA-HRP. II. The fastigial nucleus. Anat.Embryol.Berl. *173*:253-261.

Dietrichs, E., F. Walberg, and T. Nordby (1985) The cerebellar nucleo-olivary and olivo-cerebellar nuclear projections in the cat as studied with anterograde and retrograde transport in the same animal after implantation of crystalline WGA-HRP. I. The dentate nucleus. .Neurosci.Res. *3*:52-70.

Dietrichs, E. and F. Walberg (1986) The cerebellar nucleo-olivary and olivocerebellar nuclear projections in the cat as studied with anterograde and retrograde transport in the same animal

after implantation of crystalline WGA-HRP. III. The interposed nuclei. Brain Res. *373*:373-383.

Dietrichs, E. and F. Walberg (1987) Cerebellar nuclear afferents--where do they originate? A re-evaluation of the projections from some lower brain stem nuclei. Anat.Embryol.Berl. *177*:165-172.

Dietrichs, E. and F. Walberg (1990) The olivocerebellar projection to lobules I and II. Arch.Ital.Biol. *128*:171-182.

Dom, R., S. King, and G.F. Martin (1973) Evidence for two direct cerebello-olivary connections. .Brain Res. *57*:498-501.

Dow, R. S. (1936) The fiber connections of the posterior parts of the cerebellum in the rat and cat. J. Comp. Neurol. 63:527-538.

Drager, U.C. and D.H. Hubel (1975) Responses to visual stimulation and relationship between visual, auditory, and somatosensory inputs in mouse superior colliculus. .J.Neurophysiol. *38*:690-713.

Drager, U. C. and D. H. Hubel (1975) Topography of visual and somatosensory projections to mouse superior colliculus. J. Neurophys. 39:91-101.

Drager, U.C. and D.H. Hubel (1976) Topography of visual and somatosensory projections to mouse superior colliculus. .J.Neurophysiol. *39*:91-101.

Dursteler, M.R., C. Blakemore, and L.J. Garey (1977) Uptake of horseradish peroxidase by geniculo-cortical axons in the golden hamster: analysis by computer reconstruction. .Exp.Brain Res. *29*:487-500.

Dursteler, M. R. and R. H. Wurtz (1988) Pursuit and optokinetic deficits following chemical lesions of cortical areas MT and MST. J. Neurophysiol. 60(3):940-65.

Eccles, J. C. (1967) Circuits in the cerebellar control of movement. Proc. Natl. Acad. Sci. U.S.A. *58*: 336-343.

Edwards, S., Ginsburgh, C. Henkel, C. and B. Stein (1979) Sources of subcortical projections to the superior colliculus in the cat. J. Comp. Neurol. 184:309-330.

Eisenman, L.M. and C.R. Noback (1980) The ponto-cerebellar projection in the rat: differential projections to sublobules of the uvula. Exp.Brain Res. *38*:11-17.

Eisenman, L.M. (1981) Olivocerebellar projections to the pyramis and copula pyramidis in the rat: differential projections to parasagittal zones. J.Comp.Neurol. *199*:65-76.

Eisenman, L.M., D.D. Sieger, and G.J. Blatt (1983) The olivocerebellar projection to the uvula in the mouse. J.Comp.Neurol. *221*:53-59.

Eisenman, L.M. (1984) Organization of the olivocerebellar projection to the uvula in the rat. Brain Behav.Evol. *24*:1-12.

Ekerot, C.F. and B. Larson (1979) The dorsal spino-olivocerebellar system in the cat. II. Somatotopical organization. .Exp.Brain Res. *36*:219-232.

Ekerot, C.F. and B. Larson (1979) The dorsal spino-olivocerebellar system in the cat. I. Functional organization and termination in the anterior lobe. .Exp.Brain Res. *36*:201-217.

Ekerot, C.F. and B. Larson (1980) Termination in overlapping sagittal zones in cerebellar anterior lobe of mossy and climbing fiber paths activated from dorsal funiculus. .Exp.Brain Res. *38*:163-172.

Ekerot, C.F. and B. Larson (1982) Branching of olivary axons to innervate pairs of sagittal zones in the cerebellar anterior lobe of the cat. .Exp.Brain Res. *48*:185-198.

Ekerot, C.F., M. Garwicz, and J. Schouenborg (1991) Topography and nociceptive receptive fields of climbing fibres projecting to the cerebellar anterior lobe in the cat. J.Physiol.Lond. *441*:257-274.

Epema, A.H., N.M. Gerrits, and J. Voogd (1990) Secondary vestibulocerebellar projections to the flocculus and uvulo-nodular lobule of the rabbit: a study using HRP and double fluorescent tracer techniques. Exp.Brain Res. *80*:72-82.

Erickson, R.G. and P. Thier (1991) A neuronal correlate of spatial stability during periods of self-induced visual motion. .Exp.Brain Res. *86*:608-616.

Erickson, R.G. and P. Thier (1992) Responses of direction-selective neurons in monkey cortex to self-induced visual motion. .Ann.N.Y.Acad.Sci. *656*:766-774.

Evarts, E.V. and W.T. Thach (1969) Motor mechanisms of the CNS: cerebrocerebellar interrelations. .Annu.Rev.Physiol. *31*:451-498.

Fahimi, H.D. and V. Herzog (1973) A colorimetric method for measurement of the (peroxidase-mediated) oxidation of 3,3'-diaminobenzidine. .J.Histochem.Cytochem. *21*:499-502.

Faugier Grimaud, S. and J. Ventre (1989) Anatomic connections of inferior parietal cortex (area 7) with subcortical structures related to vestibulo-ocular function in a monkey (Macaca fascicularis). .J.Comp.Neurol. *280*:1-14.

Felleman, D.J. and J.H. Kaas (1984) Receptive-field properties of neurons in middle temporal visual area (MT) of owl monkeys. .J.Neurophysiol. *52*:488-513.

Flourens, P. (1823) Arch. Gen. Med. 321-370 [translated by E. Clarke and E. O'Malley (1968) in: *The Human Brain and Spinal Cord*, pp. 656-661, University of California]

Flumerfelt, B.A., S. Otabe, and J. Courville (1973) Distinct projections to the red nucleus from the dentate and interposed nuclei in the monkey. .Brain Res. *50*:408-414.

Frankfurter, A., J.T. Weber, G.J. Royce, N.L. Strominger, and J.K. Harting (1976) An autoradiographic analysis of the tecto-olivary projection in primates. .Brain Res. *118*:245-257.

Frankfurter, A., J.T. Weber, and J.K. Harting (1977) Brain stem projections to lobule VII of the posterior vermis in the squirrel monkey: as demonstrated by the retrograde axonal transport of tritiated horseradish peroxidase. Brain Res. *124*:135-139.

Fries, W. and K. Albus (1980) Responses of pontine nuclei cells to electrical stimulation of the lateral and suprasylvian gyrus in the cat. .Brain Res. *188*:255-260.

Fries, W. (1990) Pontine projection from striate and prestriate visual cortex in the macaque monkey: an anterograde study. .Vis.Neurosci. *4*:205-216.

Fuchs, A.F., M.J. Mustari, F.R. Robinson, and C.R. Kaneko (1992) Visual signals in the nucleus of the optic tract and their brain stem destinations. .Ann.N.Y.Acad.Sci. *656*:266-276.

Fuchs, A.F. and M.J. Mustari (1993) The optokinetic response in primates and its possible neuronal substrate. .Rev.Oculomot.Res. *5*:343-369.

Fuchs, A.F., F.R. Robinson, and A. Straube (1993) Role of the caudal fastigial nucleus in saccade generation. I. Neuronal discharge pattern. .J.Neurophysiol. *70*:1723-1740.

Fuchs, A.F., F.R. Robinson, and A. Straube (1994) Participation of the caudal fastigial nucleus in smooth-pursuit eye movements. I. Neuronal activity. .J.Neurophysiol. *72*:2714-2728.

Fujikado, T. and H. Noda (1987) Saccadic eye movements evoked by microstimulation of lobule VII of the cerebellar vermis of macaque monkeys. J. Physiol. Lond. *394*: 573-94.

Fukushima, K., B. W. Peterson, Y. Uchino, J. D. Coulter and V. J. Wilson (1977) Direct fastigiospinal fibres in the cat. Br. Res. *126*: 538 - 542.

Galletti, C., M.G. Maioli, S. Squatrito, and P.P. Battaglini (1982) Corticopontine projections from the visual area of the superior temporal sulcus in the macaque monkey. .Arch.Ital.Biol. *120*:411-417.

Gamlin, P.D., J.W. Gnadt, and L.E. Mays (1989) Abducens internuclear neurons carry an inappropriate signal for ocular convergence. J.Neurophysiol. *62*:70-81.

Gamlin, P.D. and L.E. Mays (1992) Dynamic properties of medial rectus motoneurons during vergence eye movements. J.Neurophysiol. *67*:64-74.

Gamlin, P.D., Y. Zhang, R.A. Clendaniel, and L.E. Mays (1994) Behavior of identified Edinger-Westphal neurons during ocular accommodation. J.Neurophysiol. *72*:2368-2382.

Gamlin, P.D. and R.J. Clarke (1995) Single-unit activity in the primate nucleus reticularis tegmenti pontis related to vergence and ocular accommodation. .J.Neurophysiol. *73*:2115-2119.

Gamlin, P. D. R. and Zhang, H. Y. (1996) Effects of muscimol blockade of the posterior fastigial nucleus on vergence and oculau accommodation in the primate. Abs. Society for Neuroscience *22*: 2034.

Gamlin, P.D., K. Yoon, and H. Zhang (1996) The role of cerebro-ponto-cerebellar pathways in the control of vergence eye movements. .Eye. *10*:167-171.

Gardner, E.P. and A.F. Fuchs (1975) Single-unit responses to natural vestibular stimuli and eye movements in deep cerebellar nuclei of the alert rhesus monkey. .J.Neurophysiol. *38*:627-649.

Garwicz, M. and C.F. Ekerot (1994) Topographical organization of the cerebellar cortical projection to nucleus interpositus anterior in the cat. .J.Physiol.Lond. *474*:245-260.

Gayer, N.S. and R.L. Faull (1988) Connections of the paraflocculus of the cerebellum with the superior colliculus in the rat brain. Brain Res. *449*:253-270.

Gellman, R., J.C. Houk, and A.R. Gibson (1983) Somatosensory properties of the inferior olive of the cat. .J.Comp.Neurol. *215*:228-243.

Gellman, R., A.R. Gibson, and J.C. Houk (1985) Inferior olivary neurons in the awake cat: detection of contact and passive body displacement. .J.Neurophysiol. *54*:40-60.

Gerfen, C.R., D.D. O'Leary, and W.M. Cowan (1982) A note on the transneuronal transport of wheat germ agglutinin-conjugated horseradish peroxidase in the avian and rodent visual systems. .Exp.Brain Res. *48*:443-448.

Gerrits, N.M. and J. Voogd (1982) The climbing fiber projection to the flocculus and adjacent paraflocculus in the cat. .Neuroscience. *7*:2971-2991.

Gerrits, N.M., A.H. Epema, and J. Voogd (1984) The mossy fiber projection of the nucleus reticularis tegmenti pontis to the flocculus and adjacent ventral paraflocculus in the cat. Neuroscience. *11*:627-644.

Gerrits, N.M. and J. Voogd (1986) The nucleus reticularis tegmenti pontis and the adjacent rostral paramedian reticular formation: differential projections to the cerebellum and the caudal brain stem. Exp.Brain Res. *62*:29-45.

Gerrits, N.M. and J. Voogd (1987) The projection of the nucleus reticularis tegmenti pontis and adjacent regions of the pontine nuclei to the central cerebellar nuclei in the cat. .J.Comp.Neurol. *258*:52-69.

Gerrits, N.M., A.H. Epema, A. van Linge, and E. Dalm (1989) The primary vestibulocerebellar projection in the rabbit: absence of primary afferents in the flocculus. Neurosci.Lett. *105*:27-33.

Ghez, C. (1975) Input-output relations of the red nucleus in the cat. Br. Res. *98*: 93-308.

Ghez, C. and K. Kubota (1977) Activity of red nucleus neurons associated with a skilled forelimb movement in the cat. Br. Res. *131*: 383-8.
Gibson, A., M. Glickstein, and J.F. Stein (1977) The projection from visual pontine nucleus neurones to the cerebellum in cats [proceedings]. .J.Physiol.Lond. *272*:88P

Gibson, A., J. Baker, G. Mower, and M. Glickstein (1978) Corticopontine cells in area 18 of the cat. .J.Neurophysiol. *41*:484-495.

Gibson, A.R., D.I. Hansma, J.C. Houk, and F.R. Robinson (1984) A sensitive low artifact TMB procedure for the demonstration of WGA-HRP in the CNS. .Brain Res. *298*:235-241.

Gibson, A.R., J.C. Houk, and N.J. Kohlerman (1985) Magnocellular red nucleus activity during different types of limb movement in the macaque monkey. .J.Physiol.Lond. *358*:527-549.

Gibson, A.R., J.C. Houk, and N.J. Kohlerman (1985) Relation between red nucleus discharge and movement parameters in trained macaque monkeys. .J.Physiol.Lond. *358*:551-570.

Gibson, A.R., F.R. Robinson, J. Alam, and J.C. Houk (1987) Somatotopic alignment between climbing fiber input and nuclear output of the cat intermediate cerebellum. J.Comp.Neurol. *260*:362-377.

Gibson, A.R., K.M. Horn, J.F. Stein, and P.L. van Kan (1996) Activity of interpositus neurons during a visually guided reach. .Can.J.Physiol.Pharmacol. *74*:499-512.

Glickstein, M. and D. Whitteridge (1976) Degeneration of layer III pyramidal cells in area 18 following destruction of callosal input. .Brain Res. *104*:148-151.

Glickstein, M., J.L. Cohen, B. Dixon, A. Gibson, M. Hollins, E. Labossiere, and F. Robinson (1980) Corticopontine visual projections in macaque monkeys. .J.Comp.Neurol. *190*:209-229.

Glickstein, M., J.G. May, and B.E. Mercier (1985) Corticopontine projection in the macaque: the distribution of labelled cortical cells after large injections of horseradish peroxidase in the pontine nuclei. .J.Comp.Neurol. *235*:343-359.

Glickstein, M., J. May, and B. Mercier (1990) Visual corticopontine and tectopontine projections in the macaque. .Arch.Ital.Biol. *128*:273-293.

Glickstein, M., N. Gerrits, I. Kralj Hans, B. Mercier, J. Stein, and J. Voogd (1994) Visual pontocerebellar projections in the macaque. .J.Comp.Neurol. *349*:51-72.

Glickstein, M. and J. Voogd (1995) Lodewijk Bolk and the comparative anatomy of the cerebellum. .Trends.Neurosci. *18*:206-210.

Gonatas, N.K., C. Harper, T. Mizutani, and J.O. Gonatas (1979) Superior sensitivity of conjugates of horseradish peroxidase with wheat germ agglutinin for studies of retrograde axonal transport. .J.Histochem.Cytochem. *27*:728-734.

Gonzalo Ruiz, A., G.R. Leichnetz, and D.J. Smith (1988) Origin of cerebellar projections to the region of the oculomotor complex, medial pontine reticular formation, and superior colliculus in New World monkeys: a retrograde horseradish peroxidase study. J.Comp.Neurol. *268*:508-526.

Gonzalo Ruiz, A. and G.R. Leichnetz (1990) Connections of the caudal cerebellar interpositus complex in a new world monkey (Cebus apella). Brain Res.Bull. *25*:919-927.

Gonzalo Ruiz, A. and G.R. Leichnetz (1990) Afferents of the caudal fastigial nucleus in a New World monkey (Cebus apella). .Exp.Brain Res. *80*:600-608.

Gould, B.B. (1979) The organization of afferents to the cerebellar cortex in the cat: projections from the deep cerebellar nuclei. J.Comp.Neurol. *184*:27-42.

Gravel, C. and R. Hawkes (1990) Parasagittal organization of the rat cerebellar cortex: direct comparison of Purkinje cell compartments and the organization of the spinocerebellar projection. J.Comp.Neurol. *291*:79-102.

Graybiel, A.M., H.J. Nauta, R.J. Lasek, and W.J. Nauta (1973) A cerebello-olivary pathway in the cat: an experimental study using autoradiographic tracing technics. .Brain Res. *58*:205-211.

Grob, P., J. BG-95ner Ennever, W. Lang, K. Akert, and A. Fah (1982) A comparison of the retrograde tracer properties of [125I] wheat germ agglutinin (WGA) with HRP after injection into the corpus callosum. .Brain Res. *236*:193-198.

Groenewegen, H.J., A.J. Boesten, and J. Voogd (1975) The dorsal column nuclear projections to the nucleus ventralis posterior lateralis thalami and the inferior olive in the cat: an autoradiographic study. .J.Comp.Neurol. *162*:505-517.

Groenewegen, H.J. and J. Voogd (1975) Projections from the gracile and internal cuneate nuclei to the inferior olive in the cat as demonstrated by autoradiography. .Acta.Morphol.Neerl.Scand. *13*:232-234.

Groenewegen, H.J. and J. Voogd (1976) Olivocerebellar climbing fiber projections in the cat. An autoradiographic and degeneration study [proceedings]. .Acta.Morphol.Neerl.Scand. *14*:247-249.

Groenewegen, H.J. and J. Voogd (1977) The parasagittal zonation within the olivocerebellar projection. I. Climbing fiber distribution in the vermis of cat cerebellum. .J.Comp.Neurol. *174*:417-488.

Groenewegen, H.J., J. Voogd, and S.L. Freedman (1979) The parasagittal zonation within the olivocerebellar projection. II. Climbing fiber distribution in the intermediate and hemispheric parts of cat cerebellum. J.Comp.Neurol. *183*:551-601.

Grottel, K., R. Zimny, and K. Kowalski (1988) The pontocerebellar efferents from the pontine reticular tegmental nucleus in the rabbit: differential projections to the paramedian sublobules as revealed with tracing of retrograde axonal transport of horseradish peroxidase. J.Hirnforsch. *29*:203-216.

Halperin, J.J. and J.H. LaVail (1975) A study of the dynamics of retrograde transport and accumulation of horseradish peroxidase in injured neurons. .Brain Res. *100*:253-269.

Haines, D.E. (1976) Cerebellar corticonuclear and corticovestibular fibers of the anterior lobe vermis in a prosimian primate (Galago senegalensis). .J.Comp.Neurol. *170*:67-95.

Haines, D.E., J.L. Culberson, and G.F. Martin (1976) Laterality and topography of cerebellar cortical efferents in the opossum (Didelphis marsupialis virginiana). Brain Res. *106*:152-158.

Haines, D.E. (1977) Cerebellar corticonuclear and corticovestibular fibers of the flocculonodular lobe in a prosimian primate (Galago senegalensis). .J.Comp.Neurol. *174*:607-630.

Haines, D.E. and R.H. Whitworth (1978) Cerebellar cortical efferent fibers of the paraflocculus of tree shrew (Tupaia glis). .J.Comp.Neurol. *182*:137-150.

Haines, D.E. and J.A. Rubertone (1979) Cerebellar corticonuclear fibers of the dorsal culminate lobule (anterior lobe--lobule V) in a prosimian primate, Galago senegalensis. .J.Comp.Neurol. *186*:321-341.

Haines, D.E. and S.L. Koletar (1979) Topography of cerebellar corticonuclear fibers of the albino rat. Vermis of anterior and posterior lobes. .Brain Behav.Evol. *16*:271-292.

Haines, D.E. and J.C. Pearson (1979) Cerebellar corticonuclear - nucleocortical topography: a study of the tree shrew (Tupaia) paraflocculus. .J.Comp.Neurol. *187*:745-758.

Haines, D.E. and G.W. Patrick (1981) Cerebellar corticonuclear fibers of the paramedian lobule of tree shrew (Tupaia glis) with comments on zones. J.Comp.Neurol. *201*:99-119.

Haines, D.E. (1981) Zones in the cerebellar cortex. Their organization and potential relevance to cerebellar stimulation. J.Neurosurg. *55*:254-264.

Haines, D. E., Patick, G. W. and Satrulee, P. (1982) Organisation of cerebellar corticonuclear fiber systems. In: The Cerebellum: New Vistas. Edited by: Chan-Palay, V. Springer-Verlag, Berlin, Heidelberg.

Haines, D.E. (1988) Evidence of intracerebellar collateralization of nucleocortical cell processes in a prosimian primate (Galago): a fluorescence retrograde study. J.Comp.Neurol. *275*:441-451.

Haines, D.E. and E. Dietrichs (1991) Evidence of an x zone in lobule V of the squirrel monkey (Saimiri sciureus) cerebellum: the distribution of corticonuclear fibers. Anat.Embryol.Berl. *184*:255-268.

Hammer, K.H. and F. Klingberg (1991) Disturbance of brightness discrimination and active avoidance learning after lesions of nucleus reticularis tegmenti pontis (NRTP) of rats are related to impairment of goal-directed behaviour. .Biomed.Biochim.Acta. *50*:169-174.

Hamori, J. and J. Takacs (1989) Two types of GABA-containing axon terminals in cerebellar glomeruli of cat: an immunogold-EM study. .Exp.Brain Res. *74*:471-479.

Haroian, A.J., L.C. Massopust, and P.A. Young (1981) Cerebellothalamic projections in the rat: an autoradiographic and degeneration study. J.Comp.Neurol. *197*:217-236.

Haroian, A.J. (1982) Cerebello-olivary projections in the rat: an autoradiographic study. Brain Res. *235*:125-130.

Harting, J.K. (1977) Descending pathways from the superior collicullus: an autoradiographic analysis in the rhesus monkey (Macaca mulatta). .J.Comp.Neurol. *173*:583-612.

Hawkes, R., M. colonnier, and N. Leclerc (1985) Monoclonal antibodies reveal sagittal banding in the rodent cerebellar cortex. .Brain Res. *333*:359-365.

Hawkes, R. and N. Leclerc (1986) Immunocytochemical demonstration of topographic ordering of Purkinje cell axon terminals in the fastigial nuclei of the rat. .J.Comp.Neurol. *244*:481-491.

Hawkes, R. and N. Leclerc (1989) Purkinje cell axon collateral distributions reflect the chemical compartmentation of the rat cerebellar cortex. .Brain Res. *476*:279-290.

Hawkes, R. and K. Herrup (1995) Aldolase C/zebrin II and the regionalization of the cerebellum. .J.Mol.Neurosci. *6*:147-158.

Hedreen, J. C. and S. McGrath (1977) Observations on labelling of cell bodies, axons and terminals after injection of horseradish peroxidase into the rat brain. J. Comp. Neurol. *176*:225-246.

Hepp, K., V. Henn, and J. Jaeger (1982) Eye movement related neurons in the cerebellar nuclei of the alert monkey. .Exp.Brain Res. *45*:253-264.

Herrick, C. J. (1924) Origin and evolution of the cerebellum. Arch. Neurol. Psych. 11:621-652.

Herzog, V. and H.D. Fahimi (1973) A new sensitive colorimetric assay for peroxidase using 3,3'-diaminobenzidine as hydrogen donor. .Anal.Biochem. *55*:554-562.

Hess, D.T. and J. Voogd (1986) Chemoarchitectonic zonation of the monkey cerebellum. .Brain Res. *369*:383-387.

Hirai, T., S. Onodera, and K. Kawamura (1982) Cerebellotectal projections studied in cats with horseradish peroxidase or tritiated amino acids axonal transport. Exp.Brain Res. *48*:1-12.

Hoddevik, G.H., A. Brodal, and F. Walberg (1976) The olivocerebellar projection in the cat studied with the method of retrograde axonal transport of horseradish peroxidase. III. The projection to the vermal visual area. J.Comp.Neurol. *169*:155-170.

Hoddevik, G.H. (1977) The pontine projection to the flocculonodular lobe and the paraflocculus studied by means of retrograde axonal transport of horseradish peroxidase in the rabbit. Exp.Brain Res. *30*:511-526.

Hoddevik, G.H. and A. Brodal (1977) The olivocerebellar projection studied with the method of retrograde axonal transport of horseradish peroxidase. V. The projections to the flocculonodular lobe and the paraflocculus in the rabbit. .J.Comp.Neurol. *176*:269-280.

Hoddevik, G.H., A. Brodal, K. Kawamura, and T. Hashikawa (1977) The pontine projection to the cerebellar vermal visual area studied by means of the retrograde axonal transport of horseradish peroxidase. .Brain Res. *123*:209-227.

Hoddevik, G.H. (1978) The projection from nucleus reticularis tegmenti pontis onto the cerebellum in the cat. A study using the methods of anterograde degeneration and retrograde axonal transport of horseradish peroxidase. .Anat.Embryol.Berl. *153*:227-242.

Hoddevik, G.H. and F. Walberg (1979) The pontine projection onto longitudinal zones of the paramedian lobule in the cat. .Exp.Brain Res. *34*:233-240.

Hoddevik, G.H., E. Dietrichs, and F. Walberg (1991) Afferent connections to the abducent nucleus in the cat. Arch.Ital.Biol. *129*:63-72.

Hohman, L. B. (1929) The efferent connections of the cerebellar cortex; investigations based upon experimental extirpations in the cat. Res. Publ. Assoc. Res. Nerv. Ment. Dis. 6:445-60.

Houk, J. C. and Gibson, A. R. (1987) Sensorimotor processing through the cerebellum. In: New Concepts in Cerebellar Neurobiology. Alan Liss, Inc. pgs 387-416.

Houk, J.C., A.R. Gibson, C.F. Harvey, P.R. Kennedy, and P.L. van Kan (1988) Activity of primate magnocellular red nucleus related to hand and finger movements. .Behav.Brain Res. *28*:201-206.

Hrycyshyn, A.W., H. Ghazi, and B.A. Flumerfelt (1989) Axonal branching of the olivocerebellar projection in the rat: a double-labeling study. J.Comp.Neurol. *284*:48-59.

Ikeda, Y., H. Noda, and S. Sugita (1989) Olivocerebellar and cerebelloolivary connections of the oculomotor region of the fastigial nucleus in the macaque monkey. J.Comp.Neurol. *284*:463-488.

Ilg, U.J. and K.P. Hoffmann (1991) Responses of monkey nucleus of the optic tract neurons during pursuit and fixation. .Neurosci.Res. *12*:101-110.

Itaya, S.K. and G.W. van Hoesen (1982) WGA-HRP as a transneuronal marker in the visual pathways of monkey and rat. .Brain Res. *236*:199-204.

Ito, M., I. Orlov, and M. Yamamoto (1982) Topographical representation of vestibulo-ocular reflexes in rabbit cerebellar flocculus. Neuroscience. *7*:1657-1664.

Jansen, J and A. Brodal (1940) Experimental studies on the intrinsic fibres of the cerebellum. II. The cortico-nuclear projection. J. Comp. Neurol. 73:267-321.

Jansen, J and A. Brodal (1942) Experimental studie on the intrinsic fibres of the cerebellum. The cortico-nuclear projection in the rabbit and the monkey (macaca rhesus). Skr. Norsk. Vidensk, Akad. I. Math. Nat. Kl. 11(3): 1-50.

Jones, E.G. and R.Y. Leavitt (1974) Retrograde axonal transport and the demonstration of non-specific projections to the cerebral cortex and striatum from thalamic intralaminar nuclei in the rat, cat and monkey. .J.Comp.Neurol. *154*:349-377.

Jones, E.G. (1975) Possible determinants of the degree of retrograde neuronal labeling with horseradish peroxidase. .Brain Res. *85*:249-253.

Jones, E.G. and S.P. Wise (1977) Size, laminar and columnar distribution of efferent cells in the sensory-motor cortex of monkeys. .J.Comp.Neurol. *175*:391-438.

Jones, E.G. and B.K. Hartman (1978) Recent advances in neuroanatomical methodology. .Annu.Rev.Neurosci. *1*:215-296.

Judge, S. J. Optically-induced changes in tonic vergence and AC/A ratio in normal monkeys and monkeys with lesions of the flocculus and ventral paraflocculus. Exp. Br. Res. 66(1): 1-9.

Kalil, K. (1979) Projections of the cerebellar and dorsal column nuclei upon the inferior olive in the rhesus monkey: an autoradiographic study. J.Comp.Neurol. *188*:43-62.

Kalil, K. (1981) Projections of the cerebellar and dorsal column nuclei upon the thalamus of the rhesus monkey. .J.Comp.Neurol. *195*:25-50.

Kanda, K., Y. Sato, K. Ikarashi, and T. Kawasaki (1989) Zonal organization of climbing fiber projections to the uvula in the cat. J.Comp.Neurol. *279*:138-148.

Kassel, J. (1980) Superior colliculus projections to tactile areas of rat cerebellar hemispheres. Brain Res. *202*:291-305.

Katayama, S. and N. Nisimaru (1988) Parasagittal zonal pattern of olivo-nodular projections in rabbit cerebellum. Neurosci.Res. *5*:424-438.

Kato, N., S. Kawaguchi, and H. Miyata (1988) Cerebro-cerebellar projections from the lateral suprasylvian visual area in the cat. J.Physiol.Lond. *395*:473-485.

Kawamura, K. and A. Brodal (1973) The tectopontine projection in the cat: an experimental anatomical study with comments on pathweays for teleceptive impulses to the cerebellum. .J.Comp.Neurol. *149*:371-390.

Kawamura, K. and M. Chiba (1979) Cortical neurons projecting to the pontine nuclei in the cat. An experimental study with the horseradish peroxidase technique. .Exp.Brain Res. *35*:269-285.

Kawamura, K. and T. Hashikawa (1979) Olivocerebellar projections in the cat studied by means of anterograde axonal transport of labelled amino acids as tracers. .Neuroscience. *4*:1615-1633.

Kawamura, K. and T. Hashikawa (1981) Projections from the pontine nuclei proper and reticular tegmental nucleus onto the cerebellar cortex in the cat. An autoradiographic study. J.Comp.Neurol. *201*:395-413.

Kawamura, S., S. Hattori, S. Higo, and T. Matsuyama (1982) The cerebellar projections to the superior colliculus and pretectum in the cat: an autoradiographic and horseradish peroxidase study. .Neuroscience. *7*:1673-1689.

Kawano, K., A. Takemura, Y. Inoue, T. Kitama, Y. Kobayashi, and M.J. Mustari (1996) Visual inputs to cerebellar ventral paraflocculus during ocular following responses. .Prog.Brain Res. *112*:415-422.

Keller, E.L. and W.F. Crandall (1981) Neural activity in the nucleus reticularis tegmenti pontis in the monkey related to eye movements and visual stimulation. .Ann.N.Y.Acad.Sci. *374*:249-261.

Keller, E.L. and W.F. Crandall (1983) Neuronal responses to optokinetic stimuli in pontine nuclei of behaving monkey. .J.Neurophysiol. *49*:169-187.

Keller, E.L., D.P. Slakey, and W.F. Crandall (1983) Microstimulation of the primate cerebellar vermis during saccadic eye movements. .Brain Res. *288*:131-143.

Kennedy, P.R., A.R. Gibson, and J.C. Houk (1986) Functional and anatomic differentiation between parvicellular and magnocellular regions of red nucleus in the monkey. .Brain Res. *364*:124-136.

Killackey, H. P. and R. S. Erzurumulu (1981) Trigeminal projections to the superior colliculus of the rat. J. Comp. Neurol. 201:221-242.

King, J.S., J.A. Andrezik, W.M. Falls, and G.F. Martin (1976) The synaptic organization of the cerebello-olivary circuit. .Exp.Brain Res. *26*:159-170.

Kitai, S.T., J.D. Kocsis, and T. Kiyohara (1976) Electrophysiological properties of nucleus reticularis tegmenti pontis cells: antidromic and synaptic activation. .Exp.Brain Res. *24*:295-309.

Klimoff, J. (1897) On the conduction paths of the cerebellum. Experimental-anatomical observations (in Russian). Dissertation, Imperial University of Kazan.

Klimoff, J. (1899) Ueber die Leitungsbahnen des Kleinhirns. Arch. Anat. Physiol. Anat. Abth. 11-27.

Klinkhachorn, P.S., D.E. Haines, and J.L. Culberson (1984) Cerebellar cortical efferent fibers in the North American opossum, Didelphis virginiana. II. The posterior vermis. J.Comp.Neurol. *227*:439-451.

Kolston, J., R. Apps, and J.R. Trott (1995) A combined retrograde tracer and GABA-immunocytochemical study of the projection from nucleus interpositus posterior to the posterior lobe C2 zone of the cat cerebellum. Eur.J.Neurosci. *7*:926-933.

Komatsu, H. and R.H. Wurtz (1988) Relation of cortical areas MT and MST to pursuit eye movements. I. Localization and visual properties of neurons. .J.Neurophysiol. *60*:580-603.

Krauzlis, R.J. and S.G. Lisberger (1994) Simple spike responses of gaze velocity Purkinje cells in the floccular lobe of the monkey during the onset and offset of pursuit eye movements. J.Neurophysiol. *72*:2045-2050.

Krauzlis, R. J. (1994) The visual drive for smooth eye movements. in: The visual detection of motion. Academic Press. pgs 437-473.

Krishnan, N. and M. Singer (1973) Penetration of peroxidase into peripheral nerve fibers. .Am.J.Anat. *136*:1-14.

Kristensson, K. and Y. Olsson (1971) Uptake and retrograde axonal transport of peroxidase in hypoglossal neurons. Electron microscopical localization in the neuronal perikaryon. .Acta.Neuropathol.Berl. *19*:1-9.

Kristensson, K., Y. Olsson, and J. Sjostrand (1971) Axonal uptake and retrograde transport of exogenous proteins in the hypoglossal nerve. .Brain Res. *32*:399-406.

Kurimoto, Y., S. Kawaguchi, and M. Murata (1995) Cerebellotectal projection in the rat: anterograde and retrograde WGA-HRP study of individual cerebellar nuclei. Neurosci.Res. *22*:57-71.

Kuypers, H. G. (1960) Central cortical projections to motor and somatosensory cell groups. An experiment of study in the Rhesus monkey. Brain 83: 161-184.

Kuypers, H. G. (1982) A new look at the organization of the motor system. Prog. Br. Res. *57*: 381-403.

Kyuho, S. and R. Matsuzaki (1991) Topographical organization of the tecto-olivo-cerebellar projection in the cat. Neuroscience *41*: 227-241.

Lafleur, J., J. Lean,de, and L.J. Poirier (1974) Physiopathology of the cerebellum in the monkey. I. Origin of cerebellar afferent nervous fibers from the spinal cord and brain stem. .J.Neurol.Sci. *22*:471-490.

Lamarre, Y., L. Busby, and G. Spidalieri (1983) Fast ballistic arm movements triggered by visual, auditory and somesthetic stimuli in the monkey. I. Activity of precentral cortical neurons. J. Neurophysiol. *50*: 1343-58.

Langer, T., A.F. Fuchs, M.C. Chubb, C.A. Scudder, and S.G. Lisberger (1985) Floccular efferents in the rhesus macaque as revealed by autoradiography and horseradish peroxidase. .J.Comp.Neurol. *235*:26-37.

Langer, T., A.F. Fuchs, C.A. Scudder, and M.C. Chubb (1985) Afferents to the flocculus of the cerebellum in the rhesus macaque as revealed by retrograde transport of horseradish peroxidase. .J.Comp.Neurol. *235*:1-25.

Larsell, O (1935) The development and morphology of the cerebellum in the opposum. Part II. Later deveopment and the adult. J. Comp. Neurol. 64:275-302.

Larsell, O. (1953) The cerebellum of the cat and monkey. J. Comp. Neurol. 99:135-199.

Larsell, O. (1970) The comparative anatomy and histology of the cerebellum from monotremes through apes. Jansen, J. (ed.) University of Minnesota Press, Minneapolis.

LaVail, J.H. and M.M. LaVail (1972) Retrograde axonal transport in the central nervous system. .Science. *176*:1416-1417.

LaVail, J.H. and M.M. LaVail (1974) The retrograde intraaxonal transport of horseradish peroxidase in the chick visual system: a light and electron microscopic study. .J.Comp.Neurol. *157*:303-357.

LaVail, J.H., K.R. Winston, and A. Tish (1973) A method based on retrograde intraaxonal transport of protein for identification of cell bodies of origin of axons terminating within the CNS. .Brain Res. *58*:470-477.

LaVail, M.M. and J.H. LaVail (1975) Retrograde intraaxonal transport of horseradish peroxidase in retinal ganglion cells of the chick. .Brain Res. *85*:273-280.

Le Taillanter, M. and J. Lannou (1988) Responses of nucleus reticularis tegmenti pontis neurons to vestibular stimulation in the rat. .Exp.Brain Res. *69*:417-423.

Leclerc, N., L. Dore, A. Parent, and R. Hawkes (1990) The compartmentalization of the monkey and rat cerebellar cortex: zebrin I and cytochrome oxidase. .Brain Res. *506*:70-78.

Lee, H.S., R.J. Kosinski, and G.A. Mihailoff (1989) Collateral branches of cerebellopontine axons reach the thalamus, superior colliculus, or inferior olive: a double-fluorescence and combined fluorescence-horseradish peroxidase study in the rat. Neuroscience. *28*:725-734.

Legg, C.R., B. Mercier, and M. Glickstein (1989) Corticopontine projection in the rat: the distribution of labelled cortical cells after large injections of horseradish peroxidase in the pontine nuclei. .J.Comp.Neurol. *286*:427-441.

Leichnetz, G.R., D.J. Smith, and R.F. Spencer (1984) Cortical projections to the paramedian tegmental and basilar pons in the monkey. .J.Comp.Neurol. *228*:388-408.

Leichnetz, G.R. (1989) Inferior frontal eye field projections to the pursuit-related dorsolateral pontine nucleus and middle temporal area (MT) in the monkey. .Vis.Neurosci. *3*:171-180.

Leventhal, A.G., R.W. Rodieck, and B. Dreher (1981) Retinal ganglion cell classes in the Old World monkey: morphology and central projections. .Science. *213*:1139-1142.

Lisberger, S.G. and A.F. Fuchs (1978) Role of primate flocculus during rapid behavioral modification of vestibuloocular reflex. II. Mossy fiber firing patterns during horizontal head rotation and eye movement. .J.Neurophysiol. *41*:764-777.

Lisberger, S.G. and A.F. Fuchs (1978) Role of primate flocculus during rapid behavioral modification of vestibuloocular reflex. I. Purkinje cell activity during visually guided

horizontal smooth-pursuit eye movements and passive head rotation. .J.Neurophysiol. *41*:733-763.

Lisberger, S.G., F.A. Miles, and D.S. Zee (1984) Signals used to compute errors in monkey vestibuloocular reflex: possible role of flocculus. J.Neurophysiol. *52*:1140-1153.

Lisberger, S.G. (1994) Neural basis for motor learning in the vestibuloocular reflex of primates. III. Computational and behavioral analysis of the sites of learning. J.Neurophysiol. *72*:974-998.

Lisberger, S.G., T.A. Pavelko, H.M. Bronte Stewart, and L.S. Stone (1994) Neural basis for motor learning in the vestibuloocular reflex of primates. II. Changes in the responses of horizontal gaze velocity Purkinje cells in the cerebellar flocculus and ventral paraflocculus. J.Neurophysiol. *72*:954-973.

Lisberger, S.G., T.A. Pavelko, and D.M. Broussard (1994) Neural basis for motor learning in the vestibuloocular reflex of primates. I. Changes in the responses of brain stem neurons. J.Neurophysiol. *72*:928-953.

Lisberger, S.G., T.A. Pavelko, and D.M. Broussard (1994) Responses during eye movements of brain stem neurons that receive monosynaptic inhibition from the flocculus and ventral paraflocculus in monkeys. J.Neurophysiol. *72*:909-927.

Lou, J.S. and J.R. Bloedel (1986) The responses of simultaneously recorded Purkinje cells to the perturbations of the step cycle in the walking ferret: a study using a new analytical method--the real-time postsynaptic response (RTPR). .Brain Res. *365*:340-344.

Lynch, G., C. Gall, P. Mensah, and C.W. Cotman (1974) Horseradish peroxidase histochemistry: a new method for tracing efferent projections in the central nervous system. .Brain Res. *65*:373-380.

MacAvoy, M.G., J.P. Gottlieb, and C.J. Bruce (1991) Smooth-pursuit eye movement representation in the primate frontal eye field. .Cereb.Cortex. *1*:95-102.

Maciewicz, R.J., C.R. Kaneko, S.M. Highstein, and R. Baker (1975) Morphophysiological identification of interneurons in the oculomotor nucleus that project to the abducens nucleus in the cat. .Brain Res. *96*:60-65.

Maciewicz, R.J., C.R. Kaneko, S.M. Highstein, and K. Eagen (1977) Vestibular and medullary brain stem afferents to the abducens nucleus in the cat. .Brain Res. *123*:229-240.

MacKay, W.A. (1988) Cerebellar nuclear activity in relation to simple movements. .Exp.Brain Res. *71*:47-58.

Maekawa, K. and J.I. Simpson (1972) Climbing fiber activation of Purkinje cells in the flocculus by impulses transferred through the visual pathway. .Brain Res. *39*:245-251.

Maekawa, K. and J.L. Simpson (1973) Climbing fiber responses evoked in vestibulocerebellum of rabbit from visual system. .J.Neurophysiol. *36*:649-666.

Maioli, M.G., R. Domeniconi, S. Squatrito, and E. Riva Sanseverino (1992) Projections from cortical visual areas of the superior temporal sulcus to the superior colliculus, in macaque monkeys. .Arch.Ital.Biol. *130*:157-166.

Marple Horvat, D.E. and J.F. Stein (1990) Neuronal activity in the lateral cerebellum of trained monkeys, related to visual stimuli or to eye movements. J.Physiol.Lond. *428*:595-614.

Martin, G.F., R. Dom, J.S. King, M. RoBards, and C.R. Watson (1975) The inferior olivary nucleus of the opossum (Didelphis marsupialis virginiana), its organization and connections. .J.Comp.Neurol. *160*:507-533.

Martin, G.F., C.K. Henkel, and J.S. King (1976) Cerebello-olivary fibers: their origin, course and distribution in the North American opossum. .Exp.Brain Res. *24*:219-236.

Massion, J. (1967) The mammalian red nucleus. .Physiol.Rev. *47*:383-436.

Massion, J. and L. Rispal Padel (1972) Spatial organization of the cerebello-thalamo-cortical pathway. Brain Res. *40*:61-65.

Matsushita, M. and M. Ikeda (1970) Olivary projections to the cerebellar nuclei in the cat. .Exp.Brain Res. *10*:488-500.

Matsushita, M. and M. Ikeda (1976) Projections from the lateral reticular nucleus to the cerebellar cortex and nuclei in the cat. Exp.Brain Res. *24*:403-421.

Matsushita, M. and Y. Hosoya (1978) The location of spinal projection neurons in the cerebellar nuclei (cerebellospinal tract neurons) of the cat. A study with the horseradish-peroxidase technique. Br. Res. *142*: 237-248.

Matsushita, M. and H. Yaginuma (1990) Afferents to the cerebellar nuclei from the cervical enlargement in the rat, as demonstrated with the Phaseolus vulgaris leucoagglutinin method. Neurosci.Lett. *113*:253-259.

Matsushita, M. and H. Yaginuma (1995) Projections from the central cervical nucleus to the cerebellar nuclei in the rat, studied by anterograde axonal tracing. J.Comp.Neurol. *353*:234-246.

Maunsell, J.H. and D.C. van Essen (1983) Functional properties of neurons in middle temporal visual area of the macaque monkey. I. Selectivity for stimulus direction, speed, and orientation. .J.Neurophysiol. *49*:1127-1147.

Maunsell, J.H. and D.C. van Essen (1983) The connections of the middle temporal visual area (MT) and their relationship to a cortical hierarchy in the macaque monkey. .J.Neurosci. *3*:2563-2586.

Maunsell, J.H. and D.C. van Essen (1983) Functional properties of neurons in middle temporal visual area of the macaque monkey. II. Binocular interactions and sensitivity to binocular disparity. .J.Neurophysiol. *49*:1148-1167.

May, J.G. and R.A. Andersen (1986) Different patterns of corticopontine projections from separate cortical fields within the inferior parietal lobule and dorsal prelunate gyrus of the macaque. .Exp.Brain Res. *63*:265-278.

May, P.J. and W.C. Hall (1986) The cerebellotectal pathway in the grey squirrel. Exp.Brain Res. *65*:200-212.

May, P.J., H. Baker, P.P. Vidal, R.F. Spencer, and R. Baker (1987) Morphology and distribution of serotoninergic and oculomotor internuclear neurons in the cat midbrain. .J.Comp.Neurol. *266*:150-170.

May, J.G., E.L. Keller, and D.A. Suzuki (1988) Smooth-pursuit eye movement deficits with chemical lesions in the dorsolateral pontine nucleus of the monkey. .J.Neurophysiol. *59*:952-977.

May, P.J., R. Hartwich Young, J. Nelson, D.L. Sparks, and J.D. Porter (1990) Cerebellotectal pathways in the macaque: implications for collicular generation of saccades. .Neuroscience. *36*:305-324.

May, P.J., J.D. Porter, and P.D. Gamlin (1992) Interconnections between the primate cerebellum and midbrain near-response regions. .J.Comp.Neurol. *315*:98-116.

Mays, L.E., J.D. Porter, P.D. Gamlin, and C.A. Tello (1986) Neural control of vergence eye movements: neurons encoding vergence velocity. J.Neurophysiol. *56*:1007-1021.

McCrea, R.A., G.A. Bishop, and S.T. Kitai (1977) Electrophysiological and horseradish peroxidase studies of precerebellar afferents to the nucleus interpositus anterior. II. Mossy fiber system. Brain Res. *122*:215-228.

McCrea, R.A., G.A. Bishop, and S.T. Kitai (1978) Morphological and electrophysiological characteristics of projection neurons in the nucleus interpositus of the cat cerebellum. .J.Comp.Neurol. *181*:397-419.

McCurdy, M.L., D.I. Hansma, J.C. Houk, and A.R. Gibson (1987) Selective projections from the cat red nucleus to digit motor neurons [published erratum appears in J Comp Neurol 1988 Jul 15; 273(3):445]. .J.Comp.Neurol. *265*:367-379.

McIlwain, J. T. (1983) Representation of the visual streak in visuotopic maps of the cat's superior colliculus: influence of the mapping variable. Vision Res. 23(5):507-516.

Mercier, B.E., C.R. Legg, and M. Glickstein (1990) Basal ganglia and cerebellum receive different somatosensory information in rats. .Proc.Natl.Acad.Sci.U.S.A. *87*:4388-4392.

Mihailoff, G.A., R.A. Burne, and D.J. Woodward (1978) Projections of the sensorimotor cortex to the basilar pontine nuclei in the rat: an autoradiographic study. .Brain Res. *145*:347-354.

Mihailoff, G.A., R.A. Burne, S.A. Azizi, G. Norell, and D.J. Woodward (1981) The pontocerebellar system in the rat: an HRP study. II. Hemispheral components. J.Comp.Neurol. *197*:559-577.

Mihailoff, G.A. (1993) Cerebellar nuclear projections from the basilar pontine nuclei and nucleus reticularis tegmenti pontis as demonstrated with PHA-L tracing in the rat. J.Comp.Neurol. *330*:130-146.

Miles, T.S., J.P. Lund, and J. Courville (1978) The fine topography of climbing fiber projections to the paramedian lobule of the cerebellum in the cat. Exp.Neurol. *60*:151-167.

Miles, F. A., Fuller, J. H., Braitman, D. J. and B. M. Dow (1980) Long-term adaptive changes in primate vestibulo-ocular reflex. III Electrophysiological observations in flocculus of normal monkeys. J. Neurophysiol. 43:1437-76.

Miles, F. A. and S. G. Lisberger (1981) The "error" signals subserving adaptive gain control in the primate vestibulo-ocular reflex. Ann. N. Y. Acad. Sci. 374:513-25.

Miller, R.A. and N.L. Strominger (1973) Efferent connections of the red nucleus in the brainstem and spinal cord of the Rhesus monkey. .J.Comp.Neurol. *152*:327-345.

Mizuno, N., A. Konishi, K. Itoh, N. Iwahori, and Y. Nakamura (1980) Identification of axon terminals of the cerebello-olivary fibers in the cat: an electron microscope study using the anterograde horseradish peroxidase method. .Neurosci.Lett. *20*:11-14.

Mower, G., A. Gibson, and M. Glickstein (1979) Tectopontine pathway in the cat: laminar distribution of cells of origin and visual properties of target cells in dorsolateral pontine nucleus. .J.Neurophysiol. *42*:1-15.

Mower, G., A. Gibson, F. Robinson, J. Stein, and M. Glickstein (1980) Visual pontocerebellar projections in the cat. .J.Neurophysiol. *43*:355-366.

Mugnaini, E. (1983) The length of cerebellar parallel fibers in chicken and rhesus monkey. .J.Comp.Neurol. *220*:7-15.

Mustari, M.J., A.F. Fuchs, T.P. Langer, C. Kaneko, and J. Wallman (1988) The role of the primate lateral terminal nucleus in visuomotor behavior. .Prog.Brain Res. *75*:121-128.

Mustari, M.J., A.F. Fuchs, and J. Wallman (1988) Response properties of dorsolateral pontine units during smooth pursuit in the rhesus macaque. .J.Neurophysiol. *60*:664-686.

Mustari, M.J. and A.F. Fuchs (1989) Response properties of single units in the lateral terminal nucleus of the accessory optic system in the behaving primate. .J.Neurophysiol. *61*:1207-1220.

Mustari, M.J. and A.F. Fuchs (1990) Discharge patterns of neurons in the pretectal nucleus of the optic tract (NOT) in the behaving primate. .J.Neurophysiol. *64*:77-90.

Mustari, M.J., A.F. Fuchs, C.R. Kaneko, and F.R. Robinson (1994) Anatomical connections of the primate pretectal nucleus of the optic tract. .J.Comp.Neurol. *349*:111-128.

Nagao, S. (1992) Different roles of flocculus and ventral paraflocculus for oculomotor control in the primate. Neuroreport. *3*:13-16.

Nauta, H.J., M.B. Pritz, and R.J. Lasek (1974) Afferents to the rat caudoputamen studied with horseradish peroxidase. An evaluation of a retrograde neuroanatomical research method. .Brain Res. *67*:219-238.

Newsome, W.T., R.H. Wurtz, M.R. Dursteler, and A. Mikami (1985) Deficits in visual motion processing following ibotenic acid lesions of the middle temporal visual area of the macaque monkey. .J.Neurosci. *5*:825-840.

Newsome, W.T., R.H. Wurtz, M.R. Dursteler, and A. Mikami (1985) Punctate chemical lesions of striate cortex in the macaque monkey: effect on visually guided saccades. .Exp.Brain Res. *58*:392-399.

Nikundiwe, A.M., J.G. Bjaalie, and P. Brodal (1994) Lamellar organization of pontocerebellar neuronal populations. A multi-tracer and 3-D computer reconstruction study in the cat. .Eur.J.Neurosci. *6*:173-186.

Noda, H. and D.A. Suzuki (1979) The role of the flocculus of the monkey in saccadic eye movements. .J.Physiol.Lond. *294*:317-334.

Noda, H. and A. Mikami (1986) Discharges of neurons in the dorsal parafloccullus of monkeys during eye movements and visual stimulation. J.Neurophysiol. *56*:1129-1146.

Noda, H. and T. Fujikado (1987) Topography of the oculomotor area of the cerebellar vermis in macaques as determined by microstimulation. J. Neurophysiol. *58(2):* 359-78.

Noda, H., S. Murakami, J. Yamada, J. Tamada, Y. Tamaki, and T. Aso (1988) Saccadic eye movements evoked by microstimulation of the fastigial nucleus of macaque monkeys. .J.Neurophysiol. *60*:1036-1052.

Noda, H., S. Sugita, and Y. Ikeda (1990) Afferent and efferent connections of the oculomotor region of the fastigial nucleus in the macaque monkey. .J.Comp.Neurol. *302*:330-348.

Noda, H. (1991) Cerebellar control of saccadic eye movements: its neural mechanisms and pathways. Jpn. J. Physiol. *41(3):* 351-68.

Nyby, O. and J. Jansen (1951) An experimental investigation of the cortico-pontine projection in Macaca Mulata. Skr. Nor. Vidensk. Aakad. Oslo. I Mat. Naturvidensk. Kl.3:1-47.

Madigan, J. C. and M. B. Carpenter (1971) Cerebellum of Rhesus Monkey. Atlas of lobules, laminae, and folia, in sections. University Park Press, Baltimore, London, Tokyo.

Ohtsuka, K. and H. Noda (1990) Direction-selective saccadic-burst neurons in the fastigial oculomotor region of the macaque. .Exp.Brain Res. *81*:659-662.

Ohtsuka, K. and H. Noda (1991) Saccadic burst neurons in the oculomotor region of the fastigial nucleus of macaque monkeys. .J.Neurophysiol. *65*:1422-1434.

Ohtsuka, K. and H. Noda (1995) Disharge properties of Purkinje cells in the oculomotor vermis during visually guided saccades in the macaque monkey. J. Neurophysiol. 74(5): 1828-40.

Olszewski, J. and D. Baxter (1954) Cytoarchitecture of the human brain stem. Karger: Basel.

Orioli, P.J. and P.L. Strick (1989) Cerebellar connections with the motor cortex and the arcuate premotor area: an analysis employing retrograde transneuronal transport of WGA-HRP. .J.Comp.Neurol. *288*:612-626.

Oscarsson, O. (1969) Termination and functional organization of the dorsal spino-olivocerebellar path. .J.Physiol.Lond. *200*:129-149.

Oscarsson, O. and B. Sjolund (1977) The ventral spino-olivocerebellar system in the cat. I. Identification of five paths and their termination in the cerebellar anterior lobe. Exp.Brain Res. *28*:469-486.

Ostrowska, A., R. Zimny, L. Zguczynski, and E. Sikora (1991) The neurons of origin of non-cortical afferent connections to the oculomotor nucleus. A retrograde labeling study in the rabbit. Arch.Ital.Biol. *129*:239-258.

Oyster, C.W. and H.B. Barlow (1967) Direction-selective units in rabbit retina: distribution of preferred directions. .Science. *155*:841-842.

Oyster, C.W. (1968) The analysis of image motion by the rabbit retina. .J.Physiol.Lond. *199*:613-635.

Oyster, C.W., J.I. Simpson, E.S. Takahashi, and R.E. Soodak (1980) Retinal ganglion cells projecting to the rabbit accessory optic system. .J.Comp.Neurol. *190*:49-61.

Paallysaho, J., S. Sugita, and H. Noda (1990) Cerebellar corticonuclear and nucleocortical projections in the vermis of posterior lobe of the rat as studied with anterograde and retrograde transport of WGA-HRP. Neurosci.Res.N.Y. *8*:158-178.

Paallysaho, J., S. Sugita, and H. Noda (1991) Brainstem mossy fiber projections to lobules VIa, VIb,c, VII and VIII of the cerebellar vermis in the rat. Neurosci.Res. *12*:217-231.

Paton, J.F., A. La Noce, R.M. Sykes, L. Sebastiani, P. Bagnoli, B. Ghelarducci, and D.J. Bradley (1991) Efferent connections of lobule IX of the posterior cerebellar cortex in the rabbit--some functional considerations. J.Auton.Nerv.Syst. *36*:209-224.

Payne, J.N. (1983) The cerebellar nucleo-cortical projection in the rat studied by the retrograde fluorescent double-labelling method. .Brain Res. *271*:141-144.

Perry, V.H. and A. Cowey (1984) Retinal ganglion cells that project to the superior colliculus and pretectum in the macaque monkey. .Neuroscience. *12*:1125-1137.

Perry, V.H., R. Oehler, and A. Cowey (1984) Retinal ganglion cells that project to the dorsal lateral geniculate nucleus in the macaque monkey. .Neuroscience. *12*:1101-1123.

Peschanski, M. and H.J. Ralston (1985) Light and electron microscopic evidence of transneuronal labeling with WGA-HRP to trace somatosensory pathways to the thalamus. .J.Comp.Neurol. *236*:29-41.

Plioplys, A.V., J. Thibault, and R. Hawkes (1985) Selective staining of a subset of Purkinje cells in the human cerebellum with monoclonal antibody mabQ113. .J.Neurol.Sci. *70*:245-256.

Ralston, D.D. (1994) Cerebellar terminations in the red nucleus of Macaca fascicularis: an electron-microscopic study utilizing the anterograde transport of WGA:HRP. Somatosens.Mot.Res. *11*:101-107.

Rhoades, R. W. (1981) Organisation of somastosensory input to the deep collicular laminae in hamster. Behav. Br. Res. 3:201-222.

Ritchie, L. (1976) Effects of cerebellar lesions on saccadic eye movements. .J.Neurophysiol. *39*:1246-1256.

Robertson, L.T. and S.A. Elias (1988) Representations of the body surface by climbing fiber responses in the dorsal paraflocculus of the cat. Brain Res. *452*:97-104.

Robinson, D.A. and A.F. Fuchs (1969) Eye movements evoked by stimulation of frontal eye fields. .J.Neurophysiol. *32*:637-648.

Robinson, D.A. (1972) Eye movements evoked by collicular stimulation in the alert monkey. .Vision.Res. *12*:1795-1808.

Robinson, F.R., J.L. Cohen, J. May, A.K. Sestokas, and M. Glickstein (1984) Cerebellar targets of visual pontine cells in the cat. .J.Comp.Neurol. *223*:471-482.

Robinson, F.R., J.C. Houk, and A.R. Gibson (1987) Limb specific connections of the cat magnocellular red nucleus [published erratum appears in J Comp Neurol 1987 May 22;259(4): 622]. .J.Comp.Neurol. *257*:553-577.

Robinson, F.R., A. Straube, and A.F. Fuchs (1993) Role of the caudal fastigial nucleus in saccade generation. II. Effects of muscimol inactivation. .J.Neurophysiol. *70*:1741-1758.

Robinson, F.R., Fuchs, A.F., Straube, A. and S. Watanbe (1996) The role of the interpositus nucleus in saccades is different from the role of the fastigial nucleus. Abs. Society for Neuroscience *22*:1200.

Roldan, M. and F. Reinoso Suarez (1981) Cerebellar projections to the superior colliculus in the cat. J.Neurosci. *1*:827-834.

Ron, S. and D.A. Robinson (1973) Eye movements evoked by cerebellar stimulation in the alert monkey. .J.Neurophysiol. *36*:1004-1022.

Rosene, D.L. and M.M. Mesulam (1978) Fixation variables in horseradish peroxidase neurohistochemistry. I. The effect of fixation time and perfusion procedures upon enzyme activity. .J.Histochem.Cytochem. *26*:28-39.

Rosina, A., L. Provini, M. Bentivoglio, and H.G. Kuypers (1980) Ponto-neocerebellar axonal branching as revealed by double fluorescent retrograde labeling technique. .Brain Res. *195*:461-466.

Rosina, A. and L. Provini (1982) Longitudinal and topographical organization of the olivary projection to the cat ansiform lobule. Neuroscience. *7*:2657-2676.

Rosina, A. and L. Provini (1983) Somatotopy of climbing fiber branching to the cerebellar cortex in cat. Brain Res. *289*:45-63.

Rosina, A. and L. Provini (1984) Pontocerebellar system linking the two hemispheres by intracerebellar branching. .Brain Res. *296*:365-369.

Rosina, A. and L. Provini (1987) Spatial distribution of axon collaterals of single inferior olive neurons. .J.Comp.Neurol. *256*:317-328.

Rosina, A., Marcotti, W., Morara, S. and Provini, L. (1996) Differentiated cortico-nuclear projections from forelimb-areas in cerebellar C1-C3 compartments. Abs. Society for Neuroscience *22*: 1629.

Rubertone, J.A. and D.E. Haines (1981) Secondary vestibulocerebellar projections to flocculonodular lobe in a prosimian primate, Galago senegalensis. J.Comp.Neurol. *200*:255-272.

Ruegg, D. and M. Wiesendanger (1975) Corticofugal effects from sensorimotor area I and somatosensory area II on neurones of the pontine nuclei in the cat. .J.Physiol.Lond. *247*:745-757.

Ruigrok, T.J. and J. Voogd (1990) Cerebellar nucleo-olivary projections in the rat: an anterograde tracing study with Phaseolus vulgaris-leucoagglutinin (PHA-L). .J.Comp.Neurol. *298*:315-333.

Ruigrok, T.J., R.J. Osse, and J. Voogd (1992) Organization of inferior olivary projections to the flocculus and ventral paraflocculus of the rat cerebellum. .J.Comp.Neurol. *316*:129-150.

Rushmer, D.S., W.J. Roberts, and G.K. Augter (1976) Climbing fiber responses of cerebellar Purkinje cells to passive movement of the cat forepaw. .Brain Res. *106*:1-20.

Saint Cyr, J.A. and J. Courville (1979) Projection from the vestibular nuclei to the inferior olive in the cat: an autoradiographic and horseradish peroxidase study. Brain Res. *165*:189-200.

Sato, Y., T. Kawasaki, and K. Ikarashi (1982) Zonal organization of the floccular Purkinje cells projecting to the vestibular nucleus in cats. .Brain Res. *232*:1-15.

Sato, Y., T. Kawasaki, and K. Ikarashi (1983) Afferent projections from the brainstem to the three floccular zones in cats. I. Climbing fiber projections. Brain Res. *272*:27-36.

Sato, Y. and N.H. Barmack (1985) Zonal organization of olivocerebellar projections to the uvula in rabbits. .Brain Res. *359*:281-291.

Sato, Y., K. Kanda, K. Ikarashi, and T. Kawasaki (1989) Differential mossy fiber projections to the dorsal and ventral uvula in the cat. J.Comp.Neurol. *279*:149-164.

Sato, H. and H. Noda (1992) Posterior vermal Purkinje cells in macaques respond during saccades, smooth pursuit and/or optokinetic stimulation. Neurosci. Res. 12(5): 583-95.

Schell, G.R. and P.L. Strick (1984) The origin of thalamic inputs to the arcuate premotor and supplementary motor areas. .J.Neurosci. *4*:539-560.

Schiller, P.H., S.D. True, and J.L. Conway (1980) Deficits in eye movements following frontal eye-field and superior colliculus ablations. .J.Neurophysiol. *44*:1175-1189.

Schiller, P.H., J.H. Sandell, and J.H. Maunsell (1987) The effect of frontal eye field and superior colliculus lesions on saccadic latencies in the rhesus monkey. .J.Neurophysiol. *57*:1033-1049.

Schmahmann, J.D. and D.N. Pandya (1989) Anatomical investigation of projections to the basis pontis from posterior parietal association cortices in rhesus monkey. .J.Comp.Neurol. *289*:53-73.

Schnyder, H. and H. Kunzle (1983) Differential labeling in neuronal tracing with wheat germ agglutinin. .Neurosci.Lett. *35*:115-120.

Segraves, M.A., M.E. Goldberg, S.Y. Deng, C.J. Bruce, L.G. Ungerleider, and M. Mishkin (1987) The role of striate cortex in the guidance of eye movements in the monkey. .J.Neurosci. *7*:3040-3058.

Sherlock, D.A. and G. Raisman (1975) A comparison of anterograde and retrograde axonal transport of horseradish peroxidase in the connections of the mammillary nuclei in the rat. .Brain Res. *85*:321-324.

Shidara, M. and K. Kawano (1993) Role of Purkinje cells in the ventral paraflocculus in short-latency ocular following responses. Exp.Brain Res. *93*:185-195.

Shinoda, Y., Y. Sugiuchi and T. Futami (1993) Organization of excitatory inputs from the cerebral cortex to the cerebellar dentate nucleus. Can. J. Neurol. Sci. 20(3): S19-28.

Shojaku, H., T.J. Grudt, and N.H. Barmack (1990) Vestibular and visual signals in the ventral paraflocculus of the cerebellum in rabbits. Neurosci.Lett. *108*:99-104.

Singer, W., H. Hollander and H. Vanegas (1977) Decreased peroxidase labelling of lateral geniculate neurons following deafferentation. Br. Res. *120*: 133-137.

Sousa Pinto, A. and A. Brodal (1969) Demonstration of a somatotopical pattern in the cortico-olivary projection in the cat. An experimental-anatomical study. .Exp.Brain Res. *8*:364-386.

Sparrow, J.R. and J.A. Kiernan (1979) Uptake and retrograde transport of proteins by regenerating axons. .Acta.Neuropathol.Berl. *47*:39-47.

Staines, W.A., H. Kimura, H.C. Fibiger, and E.G. McGeer (1980) Peroxidase-labeled lectin as a neuroanatomical tracer: evaluation in a CNS pathway. .Brain Res. *197*:485-490.

Stanton, G.B. (1980) Topographical organization of ascending cerebellar projections from the dentate and interposed nuclei in Macaca mulatta: an anterograde degeneration study. J.Comp.Neurol. *190*:699-731.

Stanton, G.B., M.E. Goldberg, and C.J. Bruce (1988) Frontal eye field efferents in the macaque monkey: II. Topography of terminal fields in midbrain and pons. .J.Comp.Neurol. *271*:493-506.

Stanton, G.B., M.E. Goldberg, and C.J. Bruce (1988) Frontal eye field efferents in the macaque monkey: I. Subcortical pathways and topography of striatal and thalamic terminal fields. .J.Comp.Neurol. *271*:473-492.

Stanton, G.B., C.J. Bruce, and M.E. Goldberg (1995) Topography of projections to posterior cortical areas from the macaque frontal eye fields. .J.Comp.Neurol. *353*:291-305.

Stein, J.F. and M. Glickstein (1992) Role of the cerebellum in visual guidance of movement. .Physiol.Rev. *72*:967-1017.

Stone, L.S. and S.G. Lisberger (1986) Detection of tracking errors by visual climbing fiber inputs to monkey cerebellar flocculus during pursuit eye movements. .Neurosci.Lett. *72*:163-168.

Stone, L. S. and S. G. Lisberger (1987) Synergistic action of complex and simple spikes in the monkey flocculus in the control of smooth-pursuit eye movement. In: The Olivocerebellar System in Motor Control. pgs 299-313. Ed. by Strata, P. Springer-Verlag, Berlin.

Stone, L.S. and S.G. Lisberger (1990) Visual responses of Purkinje cells in the cerebellar flocculus during smooth-pursuit eye movements in monkeys. II. Complex spikes. .J.Neurophysiol. *63*:1262-1275.

Strick, P.L. (1976) Activity of ventrolateral thalamic neurons during arm movement. .J.Neurophysiol. *39*:1032-1044.

Strick, P.L. (1985) How do the basal ganglia and cerebellum gain access to the cortical motor areas? Behav.Brain Res. *18*:107-123.

Strominger, N.L., T.C. Truscott, R.A. Miller, and G.J. Royce (1979) An autoradiographic study of the rubroolivary tract in the rhesus monkey. .J.Comp.Neurol. *183*:33-45.

Strominger, N.L., L.R. Nelson, and R.N. Strominger (1985) Banding of rubro-olivary terminations in the principal inferior olivary nucleus of the chimpanzee. .Brain Res. *343*:185-187.

Stryker, M.P. and P.H. Schiller (1975) Eye and head movements evoked by electrical stimulation of monkey superior colliculus. .Exp.Brain Res. *23*:103-112.

Sugimoto, T., N. Mizuno, S. Nomura, and Y. Nakamura (1980) Fastigio-olivary fibers in the cat as revealed by the autoradiographic tracing method. .Brain Res. *199*:443-446.

Sugimoto, T., N. Mizuno, and K. Itoh (1981) An autoradiographic study on the terminal distribution of cerebellothalamic fibers in the cat. Brain Res. *215*:29-47.

Sugimoto, T., N. Mizuno, and K. Uchida (1982) Distribution of cerebellar fiber terminals in the midbrain visuomotor areas: an autoradiographic study in the cat. Brain Res. *238*:353-370.

Sugita, S., J. Paallysaho, and H. Noda (1989) Topographical organization of the olivocerebellar projection upon the posterior vermis in the rat. Neurosci.Res. *7*:87-102.

Suzuki, D.A. and E.L. Keller (1984) Visual signals in the dorsolateral pontine nucleus of the alert monkey: their relationship to smooth-pursuit eye movements. .Exp.Brain Res. *53*:473-478.

Suzuki, D.A. and E.L. Keller (1988) The role of the posterior vermis of monkey cerebellum in smooth-pursuit eye movement control. II. Target velocity-related Purkinje cell activity. .J.Neurophysiol. *59*:19-40.

Suzuki, D.A. and E.L. Keller (1988) The role of the posterior vermis of monkey cerebellum in smooth-pursuit eye movement control. I. Eye and head movement-related activity. .J.Neurophysiol. *59*:1-18.

Suzuki, D.A., J.G. May, E.L. Keller, and R.D. Yee (1990) Visual motion response properties of neurons in dorsolateral pontine nucleus of alert monkey. .J.Neurophysiol. *63*:37-59.

Suzuki, H. and M. Azuma (1983) Topographic studies on visual neurons in the dorsolateral prefrontal cortex of the monkey. .Exp.Brain Res. *53*:47-58.

Swenson, R.S. and A.J. Castro (1983) The afferent connections of the inferior olivary complex in rats: a study using the retrograde transport of horseradish peroxidase. .Am.J.Anat. *166*:329-341.

Swenson, R.S. and A.J. Castro (1983) The afferent connections of the inferior olivary complex in rats. An anterograde study using autoradiographic and axonal degeneration techniques. .Neuroscience. *8*:259-275.

Tabuchi, T., T. Umetani, and T. Yamadori (1989) Corticonuclear and corticovestibular projections from the uvula in the albino rat: differential projections from sublobuli of the uvula. Brain Res. *492*:176-186.

Takahashi, O., T. Satoda, R. Matsushima, M. Uemura Sumi, and N. Mizuno (1987) Distribution of cerebellar neurons projecting directly to the spinal cord: an HRP study in the Japanese monkey and the cat. J.Hirnforsch. *28*:105-113.

Takeda, T. and K. Maekawa (1989) Olivary branching projections to the flocculus, nodulus and uvula in the rabbit. II. Retrograde double labeling study with fluorescent dyes. Exp.Brain Res. *76*:323-332.

Takeda, T. and K. Maekawa (1989) Olivary branching projections to the flocculus, nodulus and uvula in the rabbit. I. An electrophysiological study. Exp.Brain Res. *74*:47-62.

Takeda, T. and K. Maekawa (1989) Olivary branching projections to the flocculus, nodulus and uvula in the rabbit. II. Retrograde double labeling study with fluorescent dyes. .Exp.Brain Res. *76*:323-332.

Tan, J., N.M. Gerrits, R. Nanhoe, J.I. Simpson, and J. Voogd (1995) Zonal organization of the climbing fiber projection to the flocculus and nodulus of the rabbit: a combined axonal tracing and acetylcholinesterase histochemical study. J.Comp.Neurol. *356*:23-50.

Tan, J., J.I. Simpson, and J. Voogd (1995) Anatomical compartments in the white matter of the rabbit flocculus. .J.Comp.Neurol. *356*:1-22.

Tanaka, K., Y. Sugita, M. Moriya, and H. Saito (1993) Analysis of object motion in the ventral part of the medial superior temporal area of the macaque visual cortex. .J.Neurophysiol. *69*:128-142.

Thach, W.T. (1968) Discharge of Purkinje and cerebellar nuclear neurons during rapidly alternating arm movements in the monkey. .J.Neurophysiol. *31*:785-797.

Thach, W.T. (1970) Discharge of cerebellar neurons related to two maintained postures and two prompt movements. II. Purkinje cell output and input. .J.Neurophysiol. *33*:537-547.

Thach, W.T. (1972) Cerebellar output: properties, synthesis and uses. .Brain Res. *40*:89-102.

Thach, W.T. (1975) Timing of activity in cerebellar dentate nucleus and cerebral motor cortex during prompt volitional movement. .Brain Res. *88*:233-241.

Thach, W.T. (1978) Correlation of neural discharge with pattern and force of muscular activity, joint position, and direction of intended next movement in motor cortex and cerebellum. .J.Neurophysiol. *41*:654-676.

Thach, W.T. and E.G. Jones (1979) The cerebellar dentatothalamic connection: terminal field, lamellae, rods and somatotopy. .Brain Res. *169*:168-172.

Thach, W.T., H.P. Goodkin, and J.G. Keating (1992) The cerebellum and the adaptive coordination of movement. .Annu.Rev.Neurosci. *15*:403-442.

Thach, W.T., J.G. Perry, S.A. Kane, and H.P. Goodkin (1993) Cerebellar nuclei: rapid alternating movement, motor somatotopy, and a mechanism for the control of muscle synergy. .Rev.Neurol.Paris. *149*:607-628.

Thielert, C.D. and P. Thier (1993) Patterns of projections from the pontine nuclei and the nucleus reticularis tegmenti pontis to the posterior vermis in the rhesus monkey: a study using retrograde tracers. .J.Comp.Neurol. *337*:113-126.

Thier, P. and W. Koehler (1987) Morphology, number, and distribution of putative GABA-ergic neurons in the basilar pontine gray of the monkey. .J.Comp.Neurol. *265*:311-322.

Thier, P., W. Koehler, and U.W. Buettner (1988) Neuronal activity in the dorsolateral pontine nucleus of the alert monkey modulated by visual stimuli and eye movements. .Exp.Brain Res. *70*:496-512.

Thier, P., W. Koehler, and U.W. Buettner (1989) Investigation of the dorsolateral basilar pontine grey of the alert monkey. .Brain Behav.Evol. *33*:75-79.

Thier, P., A. Bachor, J. Faiss, J. Dichgans, and E. Koenig (1991) Selective impairment of smooth-pursuit eye movements due to an ischemic lesion of the basal pons. .Ann.Neurol. *29*:443-448.

Thier, P., Dicke, P. W., Barash, S. and Ilg, U. (1996) Demonstration of saccade-related single-unit activity in the dorsolateral pontine nucleus (dlpn) of the Rhesus monkey. Abs. Society for Neuroscience *22*:1458

Thunnissen, I.E., A.H. Epema, and N.M. Gerrits (1989) Secondary vestibulocerebellar mossy fiber projection to the caudal vermis in the rabbit. J.Comp.Neurol. *290*:262-277.

Tolbert, D.L., L.C. Massopust, M.G. Murphy, and P.A. Young (1976) The anatomical organization of the cerebello-olivary projection in the cat. J.Comp.Neurol. *170*:525-544.

Tolbert, D.L., H. Bantli, and J.R. Bloedel (1977) The intracerebellar nucleocortical projection in a primate. .Exp.Brain Res. *30*:425-434.

Tolbert, D.L., H. Bantli, and J.R. Bloedel (1978) Multiple branching of cerebellar efferent projections in cats. Exp.Brain Res. *31*:305-316.

Tolbert, D.L., H. Bantli, and J.R. Bloedel (1978) Organizational features of the cat and monkey cerebellar nucleocortical projection. J.Comp.Neurol. *182*:39-56.

Tolbert, D.L. and H. Bantli (1979) An HRP and autoradiographic study of cerebellar corticonuclear-nucleocortical reciprocity in the monkey. .Exp.Brain Res. *36*:563-571.

Tolbert, D.L. and H. Bantli (1980) Uptake and transport of 3H-GABA (gamma-aminobutyric acid) injected into the cat dentate nucleus. .Exp.Neurol. *70*:525-538.

Tolbert, D.L. (1982) The cerebellar nucleocortical pathway. In: The Cerebellum: New Vistas Edited by: Chan-Palay, V. Springer-Verlag, Berlin, Heidelberg. pgs 296-317.

Torigoe, Y., R.H. Blanks, and W. Precht (1986) Anatomical studies on the nucleus reticularis tegmenti pontis in the pigmented rat. II. Subcortical afferents demonstrated by the retrograde transport of horseradish peroxidase. J.Comp.Neurol. *243*:88-105.

Trott, J. R. (1987) The olivocerebellar input to the medial and lateral halves of the c1 and c3 zones of the cat anterior lobe. In: *The Olivocerebellar System in Motor Control*, Strata, P. (ed). Springer-Verlag, Berlin.

Trott, J.R. and D.M. Armstrong (1987) The cerebellar corticonuclear projection from lobule Vb/c of the cat anterior lobe: a combined electrophysiological and autoradiographic study. II. Projections from the vermis. .Exp.Brain Res. *68*:339-354.

Trott, J.R. and D.M. Armstrong (1987) The cerebellar corticonuclear projection from lobule Vb/c of the cat anterior lobe: a combined electrophysiological and autoradiographic study. I. Projections from the intermediate region. Exp.Brain Res. *66*:318-338.

Trott, J.R., R. Apps, and D.M. Armstrong (1990) Topographical organisation within the cerebellar nucleocortical projection to the paravermal cortex of lobule Vb/c in the cat. .Exp.Brain Res. *80*:415-428.

Trott, J.R. and R. Apps (1993) Zonal organization within the projection from the inferior olive to the rostral paramedian lobule of the cat cerebellum. Eur.J.Neurosci. *5*:162-173.

Tusa, R.J. and L.G. Ungerleider (1988) Fiber pathways of cortical areas mediating smooth pursuit eye movements in monkeys. .Ann.Neurol. *23*:174-183.

Uchida, K., N. Mizuno, T. Sugimoto, K. Itoh, and M. Kudo (1983) Direct projections from the cerebellar nuclei to the superior colliculus in the rabbit: an HRP study. J.Comp.Neurol. *216*:319-326.

Uchizono, K. (1969) Analysis of interneurons based on their synaptic organization in the cerebellar cortex of the cat. .Arch.Histol.Jpn. *30*:329-351.

Umetani, T. (1989) Topographic organization of the corticonuclear fibers from the tuber vermis and paramedian lobule in the albino rat. Brain Behav.Evol. *33*:334-341.

Umetani, T. (1989) Topographic organization of the cerebello-olivary projection in the albino rat: an autoradiographic orthograde tracing study. Kobe.J.Med.Sci. *35*:65-91.

Umetani, T. (1992) Efferent projections from the flocculus in the albino rat as revealed by an autoradiographic orthograde tracing method. Brain Res. *586*:91-103.

Umetani, T. (1993) Topographic organization of the corticonuclear projections from the paraflocculus in the albino rat: an autoradiographic orthograde tracing study. Brain Behav.Evol. *42*:128-136.

Umetani, T., T. Tabuchi, and R. Ichimura (1986) Cerebellar corticonuclear and corticovestibular fibers from the posterior lobe of the albino rat, with comments on zones. Brain Behav.Evol. *29*:54-67.

Umetani, T. and T. Tabuchi (1988) Topographic organization of the corticonuclear and corticovestibular projections from the pyramis and copula pyramidis in the albino rat. An autoradiographic orthograde tracing study. Brain Behav.Evol. *32*:160-168.

Ungerleider, L.G. and M. Mishkin (1979) The striate projection zone in the superior temporal sulcus of Macaca mulatta: location and topographic organization. .J.Comp.Neurol. *188*:347-366.

Ungerleider, L.G., R. Desimone, T.W. Galkin, and M. Mishkin (1984) Subcortical projections of area MT in the macaque. .J.Comp.Neurol. *223*:368-386.

Ungerleider, L.G. and R. Desimone (1986) Projections to the superior temporal sulcus from the central and peripheral field representations of V1 and V2. .J.Comp.Neurol. *248*:147-163.

Ungerleider, L.G. and R. Desimone (1986) Cortical connections of visual area MT in the macaque. .J.Comp.Neurol. *248*:190-222.

Van der Steen, J., J.I. Simpson, and J. Tan (1994) Functional and anatomic organization of three-dimensional eye movements in rabbit cerebellar flocculus. .J.Neurophysiol. *72*:31-46.

van der Want, J.J., N.M. Gerrits, and J. Voogd (1987) Autoradiography of mossy fiber terminals in the fastigial nucleus of the cat. .J.Comp.Neurol. *258*:70-80.

van der Want, J.J. and J. Voogd (1987) Ultrastructural identification and localization of climbing fiber terminals in the fastigial nucleus of the cat. .J.Comp.Neurol. *258*:81-90.

van der Want, J.J., L. Wiklund, M. Guegan, T. Ruigrok, and J. Voogd (1989) Anterograde tracing of the rat olivocerebellar system with Phaseolus vulgaris leucoagglutinin (PHA-L). Demonstration of climbing fiber collateral innervation of the cerebellar nuclei. J.Comp.Neurol. *288*:1-18.

van der Want, J.J., L. Wiklund, M. Guegan, T. Ruigrok, and J. Voogd (1989) Anterograde tracing of the rat olivocerebellar system with Phaseolus vulgaris leucoagglutinin (PHA-L). Demonstration of climbing fiber collateral innervation of the cerebellar nuclei. .J.Comp.Neurol. *288*:1-18.

van Kan, P.L., A.R. Gibson, and J.C. Houk (1993) Movement-related inputs to intermediate cerebellum of the monkey [published erratum appears in J Neurophysiol 1993 Mar;69(3): following table of contents]. .J.Neurophysiol. *69*:74-94.

van Kan, P.L., J.C. Houk, and A.R. Gibson (1993) Output organization of intermediate cerebellum of the monkey. J.Neurophysiol. *69*:57-73.

van Kan, P.L., K.M. Horn, and A.R. Gibson (1994) The importance of hand use to discharge of interpositus neurones of the monkey [published erratum appears in J Physiol (Lond) 1994 Dec 15;481(Pt 3):811]. .J.Physiol.Lond. *480*:171-190.

Vanegas, H., H. Hollander, and H. Distel (1978) Early stages of uptake and transport of horseradish-peroxidase by cortical structures, and its use for the study of local neurons and their processes. .J.Comp.Neurol. *177*:193-211.

Vilis, T. and J. Hore (1981) Characteristics of saccadic dysmetria in monkeys during reversible lesions of medial cerebellar nuclei. .J.Neurophysiol. *46*:828-838.

Vilis, T. and J. Hore (1981) Characteristics of nystagmus produced by reversible lesions of the medial cerebellar nuclei in the alert monkey. .Acta.Otolaryngol.Stockh. *91*:267-274.

Voogd, J. (1967) Comparative aspects of the structure and fibre connexions of the mammalian cerebellum. .Prog.Brain Res. *25*:94-134.

Voogd, J. (1969) The importance of fibre connections in the comparative anatomy of the mammalian cerebellum. In: Llinas, R. (ed.) Neurobiology of cerebellar evolution and development. AMA-ERF, Chicago, p.493.

Voogd, J. and F. Bigare (1980) Topographical distribution of olivary and corticonuclear fibres in the cerebellum. A review. In: The Inferior Olivary Nucleus: Anatomy and Physiology. Eds: Courville, J., de Montigny, C. and Y. Lamarre. Raven Press New York.

Wakefield, C. and N. Shonnard (1979) Observations of HRP labeling following injection through a chronically implanted cannula--a method to avoid diffusion of HRP into injured fibers. .Brain Res. *168*:221-226.

Walberg, F., A. Brodal, and G.H. Hoddevik (1976) A note on the method of retrograde transport of horseradish peroxidase as a tool in studies of afferent cerebellar connections, particularly those from the inferior olive; with comments on the orthograde transport in Purkinje cell axons. .Exp.Brain Res. *24*:383-401.

Walberg, F. and A. Brodal (1979) The longitudinal zonal pattern in the paramedian lobule of the cat's cerebellum: an analysis based on a correlation of recent HRP data with results of studies with other methods. .J.Comp.Neurol. *187*:581-588.

Walberg, F., N. Kotchabhakdi, and G.H. Hoddevik (1979) The olivocerebellar projections to the flocculus and paraflocculus in the cat, compared to those in the rabbit. A study using horseradish peroxidase as a tracer. .Brain Res. *161*:389-398.

Walberg, F., T. Nordby, and E. Dietrichs (1980) A note on the anterograde transport of horseradish peroxidase within the olivocerebellar fibres. .Exp.Brain Res. *40*:233-236.

Walberg, F., T. Nordby, K.P. Hoffmann, and H. Hollander (1981) Olivary afferents from the pretectal nuclei in the cat. .Anat.Embryol.Berl. *161*:291-304.

Walberg, F. and T. Nordby (1981) A re-examination of the rubro-olivary tract in the cat, using horseradish peroxidase as a retrograde and an anterograde neuronal tracer. .Neuroscience. *6*:2379-2391.

Walberg, F., E. Dietrichs, and T. Nordby (1986) The origin and termination of the dentatorubral fibres in the cat as studied with retrograde and anterograde transport of peroxidase labelled lectin. Exp.Brain Res. *63*:294-300.

Walberg, F. and E. Dietrichs (1986) Is there a reciprocal connection between the red nucleus and the interposed cerebellar nuclei? Conclusions based on observations of anterograde and retrograde transport of peroxidase-labelled lectin in the same animal. .Brain Res. *397*:73-85.

Walberg, F., T. Nordby, and E. Dietrichs (1987) The olivonodular projection: a re-examination based on folial cerebellar implants. Neurosci.Lett. *81*:82-88.

Walberg, F. and E. Dietrichs (1988) The interconnection between the vestibular nuclei and the nodulus: a study of reciprocity. Brain Res. *449*:47-53.

Ware, C. B. and E. J. Mufson (1979) Spinal cord projections from the medial cerebellar nucleus in the tree shrew (Tupaia Glis). Br. Res. *171*:383-400.

Watanabe, E. (1984) Neuronal events correlated with long-term adaptation of the horizontal vestibulo-ocular reflex in the primate flocculus. Br. Res. 297(1):169-74.

Watanabe, E. (1985) Role of the primate flocculus in adaptation of the vestibulo-ocular reflex. Neurosci. Res. 3(1):20-38.

Watt, C.B. and G.A. Mihailoff (1983) The cerebellopontine system in the rat. I. Autoradiographic studies. J.Comp.Neurol. *215*:312-330.

Weiss, C., J.C. Houk, and A.R. Gibson (1990) Inhibition of sensory responses of cat inferior olive neurons produced by stimulation of red nucleus. .J.Neurophysiol. *64*:1170-1185.

West, R. A. and Strick, P. L. Organizational features of the dentato-thalamo-cortical projection. Abs. Society for Neuroscience *22*: 1631.

Wharton, S.M. and J.N. Payne (1985) Axonal branching in parasagittal zones of the rat olivocerebellar projection: a retrograde fluorescent double-labelling study. Exp.Brain Res. *58*:183-189.

Whitworth, R.H., Jr., D.E. Haines, and G.W. Patrick (1983) The inferior olive of a prosimian primate, Galago senegalensis. II. Olivocerebellar projections to the vestibulocerebellum. J.Comp.Neurol. *219*:228-240.

Whitworth, R.H., Jr., D.E. Haines, and G.W. Patrick (1984) Olivocerebellar projections to paramedian lobule in tree shrew (Tupaia glis): a horseradish peroxidase study. Brain Res. *305*:271-282.

Whitworth, R.H., Jr. and D.E. Haines (1986) The inferior olive of Saimiri sciureus: olivocerebellar projections to the anterior lobe. Brain Res. *372*:55-71.

Wiklund, L., G. Toggenburger, and M. Cuenod (1984) Selective retrograde labelling of the rat olivocerebellar climbing fiber system with D-[3H]aspartate. .Neuroscience. *13*:441-468.

Wiklund, L., F. Rossi, P. Strata, and J.J. van der Want (1990) The rat olivocerebellar system visualized in detail with anterograde PHA-L tracing technique, and sprouting of climbing fibers demonstrated after subtotal olivary lesions. Eur.J.Morphol. *28*:256-267.

Wilson, V. J., Y. Uckino, R. A. Mauriz, A. Susswein and K. Fukushima (1978) Properties and connections of cat fastigiospinal neurons. Exp. Br. Res. *32*:1-17.

Wurtz, R.H. and M.E. Goldberg (1972) The role of the superior colliculus in visually-evoked eye movements. .Bibl.Ophthalmol. *82*:149-158.

Wurtz, R. H., and J. E. Albano (1980) Visuo-motor function of the primate superior colliculus. Ann. Rev. Neurosci. 3: 189-226.

Yamamoto, M. (1979) Topographical representation in rabbit cerebellar flocculus for various afferent inputs from the brainstem investigated by means of retrograde axonal transport of horseradish peroxidase. Neurosci.Lett. *12*:29-34.

Yamada, J. and H. Noda (1987) Afferent and efferent connections of the oculomotor cerebellar vermis in the macaque monkey. .J.Comp.Neurol. *265*:224-241.

Yamada, T., D.A. Suzuki, and R.D. Yee (1996) Smooth pursuitlike eye movements evoked by microstimulation in macaque nucleus reticularis tegmenti pontis. .J.Neurophysiol. *76*:3313-3324.

Yatim, N., C. Buisseret Delmas, P. Buisseret, C. Compoint, and P. Angaut (1995) Nucleus medialis-nucleus interpositus interface: its olivary and cerebellocortical projections in the rat. .J.Comp.Neurol. *363*:1-14.

Yuen, H., R.M. Dom, and G.F. Martin (1974) Cerebellopontine projections in the American opossum. A study of their origin, distribution and overlap with fibers from the cerebral cortex. .J.Comp.Neurol. *154*:257-285.

Zee, D.S., Yamazaki, A., Butler, P.H. and G. Gucer (1981) Effects of ablation of flocculus and paraflocculus on eye movements in primate. J. Neurophysiol. *46*:878-899.

Zhang, Y., P.D. Gamlin, and L.E. Mays (1991) Antidromic identification of midbrain near response cells projecting to the oculomotor nucleus. .Exp.Brain Res. *84*:525-528.

Zhang, Y., L.E. Mays, and P.D. Gamlin (1992) Characteristics of near response cells projecting to the oculomotor nucleus. .J.Neurophysiol. *67*:944-960.

Zhang, H. Y. and Gamlin, P. D. R. (1994) Sensorimotor characteristics of far response neurons in the cerebellum of Rhesus monkey. Abs. Association for Research in Vision and Opthalmology.

Zhang, H. Y. and Gamlin, P. D. R. (1996) Single unit activity within the posterior fastigial nucleus during vergence and accommodation in the alert primate. Abs. Society for Neuroscience *22*: 2034.

Zimny, R., K. Grottel, D. Jakielska, and A. Ostrowska (1989) Topographic and zonal pattern of olivocerebellar projection to the paramedian lobule in the rabbit: an experimental study with an HRP retrograde tracing method. Neurosci.Res. *7*:173-198.